Human-Urban Radiation Exchange Simulation Model

by

Sookuk Park
B.A., Kyungpook National University, 1995
M.L.A., Kyungpook National University, 1997
M.Sc., University of Guelph, 2003

A Dissertation Submitted in Partial Fulfillment
of the Requirements for the Degree of

DOCTOR OF PHILOSOPHY

in the Department of Geography

Supervisory Committee

Human-Urban Radiation Exchange Simulation Model

by

Sookuk Park
B.A., Kyungpook National University, 1995
M.L.A., Kyungpook National University, 1997
M.Sc., University of Guelph, Canada, 2003

Supervisory Committee

Dr. Stanton E. Tuller, Department of Geography
Supervisor

Dr. Larry McCann, Department of Geography
Departmental Member

Dr. Ian J. Walker, Department of Geography
Departmental Member

Dr. Andrew Weaver, School of Earth and Ocean Sciences
Outside Member

Abstract

Supervisory Committee

Dr. Stanton E. Tuller, Department of Geography
Supervisor

Dr. Larry McCann, Department of Geography
Departmental Member

Dr. Ian J. Walker, Department of Geography
Departmental Member

Dr. Andrew Weaver, School of Earth and Ocean Sciences
Outside Member

The purpose of this study is to develop an improved human radiation exchange model for use by planners and researchers. Although applicable for all environments, emphasis will be on urban areas.

All processes of radiation exchange between the human body surface and surrounding environments were investigated through human body area factors (effective radiation area factor, f_{eff}, and projected area factor, f_p), existing human thermal exchange models and three-dimensional (3D) computer simulation models with collected microclimatic data.

For new body area factors, a sample of standing contemporary Canadian adults in normal-weight (male: 31 persons, female: 40) and over-weight (male: 48, female: 20) body mass index (BMI) categories were analyzed. A 3D mean body model was created for each category. Only very small differences in f_{eff} and f_p were found between genders and BMI categories. Differences in f_{eff} and f_p values between this study and previous studies were very large, up to 0.101 and 0.173, respectively.

Another common body posture, walking, was also studied for the normal-weight male and female BMI categories. 3D computer walking body models at four stride positions were created. The directionless f_p values for walking posture had minor differences between genders and positions in a stride. However, the differences of mean directional f_p values between azimuth angles were great enough (up to 0.072) to create important differences in modeled radiation receipt. When both standing and walking postures are considered, the mean f_{eff} value of standing (0.826) and walking (0.846), 0.836, could be used. However, f_p

values should be selected carefully because differences between directional and directionless f_p values were large enough that they could influence the estimated level of human thermal sensation.

A new human radiation exchange model was developed using the new body area factors and compared with five existing models and one method (Burt, COMFA, MENEX, OUT_SET* and RayMan models and the six-directional method) using collected microclimatic data observed in Guelph, Ontario, Canada. Most differences between models came from absorbed solar radiation, especially absorbed direct beam solar radiation because of differences in f_p^* ($=f_p \times f_{eff}$) and f_{eff} or some missing components (f_{eff} or view factors). The lowest differences between the new model and the RayMan model alter the net all-wave radiation estimate up to 29 Wm^{-2}, which can be significant in the human thermal exchange model.

For 3D computer estimation, a new human-urban radiation exchange simulation model was developed combining the new human radiation exchange model and improved urban area factors (i.e., albedos and view factors of sunny and shaded building, ground and vegetation surfaces). The results of the new computer model were compared with microclimatic data collected in Nanaimo, B.C., Canada and Changwon, Republic of Korea as well as with two other 3D computer simulation programs, RayMan Pro and ENVI-met 3.1. The differences between the collected data and the new model were very small. Their correlation was very strong, over 0.99 for total radiation. RayMan Pro and ENVI-met 3.1 programs had larger differences, and their correlations with measured data were weaker than the new model's. Accurate meteorological and urban setting data should be obtained for better results.

The new model will give planners and researchers a simple tool to estimate accurate radiation effects in complex urban areas.

Table of Contents

List of Tables

List of Figures

List of Symbols

Symbol	Name	Unit
A	slope angle	°
a_b	albedo (reflectivity) of a person's body surface	
a_{cl}	albedo of clothing	
a_g	albedo of the ground surface	
a_o	mean albedo of ground-based, solid objects projecting into the sky hemisphere, especially building surfaces	
a_{veg}	albedo of vegetation (tree) surface	
A_{eff}	effective radiation area	m^2
A_D	total body surface area	m^2
A_{Du}	total body surface area calculated using DuBois and DuBois (1916) formula	m^2
A_{3DS}	total body surface area obtained from 3DS Max computer software program	m^2
A_P	projected body surface area	m^2
allheight	sum of ground and obstruction heights at the observation point (x, y)	
allheight1	sum of ground and obstruction heights at other points ($x1$, $y1$)	
B	the Bowen ratio	
d	sun-earth distance	
$\bar{d}$	mean sun-earth distance during the year	
D	distance between the observation point and the building surface perpendicular to the point	m
e_a	vapour pressure of the air	hPa
eleangle	an angle of height difference between (x, y) and ($x1$, $y1$)	
F	angle factor	
F_d	the diffuse angular function depending on the solar elevation angle	
f_{eff}	effective radiation area factor ($=A_{eff}/A_D$)	
f_{eff_ADu}	effective radiation area factor computed using A_{Du}	
f_p	projected area factor per unit of effective radiation body area ($=A_p/A_{eff}$)	
f_p^*	projected area factor per unit of total body area ($=A_p/A_D=f_p \times f_{eff}$)	
G_0	global solar radiation	Wm^{-2}
h	a height above sea level	m
H	building height	m
J	Julian day (1 to 365 or 366 in the year)	
k	radius vector, the correction for solar constant by the variation of sun-earth distance (r) from its mean value ($\bar{r}$) during the year, e.g., shortest at very early January (k =1.034) and longest at very early July (k =0.967)	
$K\downarrow$	total incoming solar radiation from the sky hemisphere incident on the (human body) surface	Wm^{-2}
$K\uparrow$	total solar radiation from the ground hemisphere incident on the (human body) surface	Wm^{-2}
K_b	incoming direct beam solar radiation on a horizontal surface	Wm^{-2}

K_b^+	direct beam solar radiation incident on the human body surface perpendicular to the sun's rays	Wm^{-2}
K_b^*	absorbed direct beam solar radiation on the human body surface	Wm^{-2}
K_{bg_slope}	direct beam solar radiation incident on the ground surface	Wm^{-2}
K_{bo}	the solar constant (1367 Wm^{-2})	Wm^{-2}
K_{bo_slope}	direct beam solar radiation incident on a building surface	Wm^{-2}
K_{bveg_slope}	direct beam solar radiation incident on a vegetation (tree) surface	Wm^{-2}
K_d	diffuse beam solar radiation from the sky on the horizontal ground surface	Wm^{-2}
K_d^+	diffuse beam solar radiation incident on the human body surface	Wm^{-2}
K_d^*	diffuse beam solar radiation from the sky absorbed on the body surface	Wm^{-2}
K_{d0}	diffuse beam solar radiation from the sky on the horizontal ground surface in a cloudless sky condition	Wm^{-2}
K_{d8}	diffuse beam solar radiation from the sky on the horizontal ground surface in an overcast sky condition	Wm^{-2}
K_{d_aniso}	anisotropically diffused solar radiation around the sun	Wm^{-2}
K_{d_iso}	isotropically diffused solar radiation in the sky	Wm^{-2}
K_{d_slope}	diffuse beam solar radiation incident on slopes (building, tree or ground surface)	Wm^{-2}
K_{dg_slope}	diffuse beam solar radiation incident on the ground surface	Wm^{-2}
K_{do_slope}	diffuse beam solar radiation incident on a building surface	Wm^{-2}
K_{dveg_slope}	diffuse beam solar radiation incident on a vegetation (tree) surface	Wm^{-2}
K_r	total reflected solar radiation by objects and ground ($=K_{ro}+K_{rg}$)	Wm^{-2}
K_r^+	total solar radiation reflected by objects and ground incident on the human body surface ($=K_{ro}^+ + K_{rveg}^+ + K_{rg}^+$)	Wm^{-2}
K_r^*	total solar radiation reflected by objects and ground absorbed on the human body surface	Wm^{-2}
K_{rg}	solar radiation reflected by the ground	Wm^{-2}
K_{rg}^+	solar radiation reflected by the ground incident on the human body surface	Wm^{-2}
K_{ro}	solar radiation reflected by objects in the sky hemisphere (buildings, trees and other structures)	Wm^{-2}
K_{ro}^+	solar radiation reflected by buildings in the sky hemisphere incident on the human body surface	Wm^{-2}
K_{rveg}^+ ($=K_{rveg}$)	solar radiation reflected by trees in the sky hemisphere incident on the human body surface	Wm^{-2}
L	net longwave radiation on the human body surface ($=L^*-L_b$)	Wm^{-2}
L^+	longwave radiation incident on the human body surface	Wm^{-2}
L^* ($=L_{abs}$)	longwave radiation absorbed by the human body surface from the surrounding environment	Wm^{-2}
$L\downarrow$	total incoming longwave radiation from the sky hemisphere incident on the human body surface	Wm^{-2}
$L\uparrow$	total longwave radiation from the ground hemisphere incident on the human body surface	Wm^{-2}
L_a	incoming longwave radiation from the sky to the horizontal ground surface	Wm^{-2}
L_a^+	longwave radiation coming from the sky incident on the human body surface	Wm^{-2}
L_b	longwave radiation emitted from the human body surface	Wm^{-2}

L_{env}	longwave radiation from an averaged surface temperature (T_{mrt}) of the surrounding environments	Wm^{-2}
L_g	longwave radiation emitted from the horizontal ground surface	Wm^{-2}
L_g^+	longwave radiation coming from the ground surface incident on the human body surface	Wm^{-2}
L_o	longwave radiation coming from objects in the sky hemisphere to the horizontal ground surface	Wm^{-2}
L_o^+	longwave radiation coming from building surfaces incident on the human body surface	Wm^{-2}
L_{veg}^+ ($=L_{veg}$)	longwave radiation coming from vegetation (tree) surfaces incident on the human body surface	Wm^{-2}
LT	local time (mean time zone time)	minutes
m	relative optical air mass	
n	the number of annuli of a fisheye lens photograph	
$n_{1/4}$	number of observations over one-quarter of the entire spherical surface area	
$n_{1/2}$	number of observations over one half of the entire spherical surface area	
N	degree of cloudiness in octas [cloudless (N=0) and overcast (N=8)]	
P	local atmospheric air pressure	hPa
P_0	normal air pressure at sea level (1013 hPa)	hPa
Q	net all-wave radiation on the human body surface ($=R^*+L$)	Wm^{-2}
Q_s	soil heat flux density	Wm^{-2}
Q^*	absorbed total radiation on the human body surface	Wm^{-2}
r	radius from the center of fisheye lens projection to the top of a building	
R	radius of a fisheye lens photograph	
R	total incoming solar radiation on a horizontal surface	Wm^{-2}
R^+	solar (shortwave) radiation incident on the human body surface	Wm^{-2}
R^*	absorbed solar (shortwave) radiation on the human body surface	Wm^{-2}
$RealL$	real longitude of the observation point	°
RH	relative humidity (1.0=100 %)	decimal
t	transmissivity for direct beam solar radiation of objects between the observation point and the sun [obstructed by building=0, open sky=1 and obstructed by tree=0.15 (spruce) to 0.75 (willow) dependent of canopy density, from Brown and Gillespie (1995)]	
t_r	direct beam transmittance under cloudless skies [$= \exp(-0.8662 \cdot \gamma \cdot T_L \cdot m)$]	
t_{veg}	a transmission factor of vegetation	
T_a	air temperature	K
T_b	human skin temperature	K
T_g	ground surface temperature	K
T_L	the Linke turbidity factor that is used to characterize the degree of transparency of the atmosphere and represents the number of clean dry atmospheres necessary to produce the observed attenuation	
T_{mrt}	mean radiant temperature	°C
T_o	building surface temperature	K
T_{rd}	the diffuse transmission function at zenith (the center of the sky, sun elevation=90°) depending on the turbidity	
T_{sk}	skin temperature	K

T_{veg}	vegetation (tree) surface temperature	K
TimeZoneL	central longitude of time zone of the observation point	°
TLT	true local time	minutes
v	wind speed	ms^{-1}
w	reduction by water vapour absorption of incoming direct beam solar radiation	
W	building width	m
x	the x-axis location of the observation point	
$x1$	the x-axis locations of other points	
y	the y-axis location of the observation point	
$y1$	the y-axis locations of other points	
z	zenith angle of the sun	°
Z	equation of time which ranges from -14 to +16 minutes	minutes
Z_{sl}	an angle between the perpendicular to the slope and the sun	°
ψ_g	ground view factor	decimal
ψ_o	obstruction (building) view factor	decimal
ψ_{sky}	sky view factor (1.0=100 %)	decimal
ψ_{veg}	vegetation (trees) view factor	decimal
$\psi_{veg\ in\ sky}$	vegetation (trees) view factor in the sky which means the sky is located behind the vegetation (trees) not buildings. This view factor is used to compute transmitted solar radiation through the canopy of the vegetation, especially trees.	decimal
$\psi_{w\text{-}sky}$	view factor of sky (or ground) seen from the building/vegetation surfaces	decimal
α	(solar) azimuth angle	°
α_{sl}	azimuth angle of the slope	°
α_i	the angular width (°) of wall in the i-th annulus of fisheye lens photograph	°
β	(solar) altitude angle corrected from the original (solar) altitude (β_0) by the atmospheric refraction component ($\Delta\beta$) or building/tree's elevation angle	°
β_0	original solar altitude angle	°
$\Delta\beta$	atmospheric refraction component	°
ε_a	emissivity of air (0.97 to 0.99)	
ε_b	emissivity of the human body surface	
ε_o	emissivity of building surfaces	
ε_{sky}	sky emissivity	
ε_{veg}	emissivity of vegetation (tree) surfaces	
σ	Stefan-Boltzmann constant (=$5.67\cdot10^{-8}$ $Wm^{-2}K^{-4}$)	$Wm^{-2}K^{-4}$
ζ	latitude of the observation point	
ζ_r	attenuation coefficient due to molecular scattering	
ζ_d	attenuation coefficient due to turbidity	
λ	solar wavelength	μm
τ	turbidity coefficient for incoming direct beam solar radiation	
η	dependence of K_d on solar altitude	
γ	integrated optical thickness of the terrestrial atmosphere free of clouds, water vapour and aerosols	

δ	declination of the sun (solar zenith angle above the equator at noon on the day of observation) which varies between -23.44° at the winter solstice via 0° at the equinox to 23.44° at the summer solstice	°
ω	solar hour angle (angle between the hour circle through the sun at the time of observation and the local meridian) which is 0 at true solar noon, positive in the afternoon and negative in the morning	°

Acknowledgments

First of all, I would like to express my deepest sense of gratitude to my supervisor Dr. Stanton E. Tuller for his patient guidance, support and excellent advice throughout this study. I appreciate his vast, deep knowledge and his assistance in writing papers. I would like to thank the other members of my committee, Dr. Larry McCann, Dr. Andrew Weaver and Dr. Ian J. Walker, for the assistance and encouragement they provided. I would like to thank Dr. Chris de Freitas at the University of Auckland, New Zealand to serve as my external examiner.

I would also like thank my family for the support they provided me through my entire life. In particular, I must acknowledge my wife Gigi and my daughter Amy. Most drawings were created by my wife, and I cannot imagine how I could finish data collection without my wife and daughter's help. Without their love, encouragement and assistance, I would not have finished this study. My parents, Taekyu Park and Gapsun Kim, and my parents-in-law, Byunghong An and Junghee Kim, are my precious supporters. I always appreciate their love, support and encouragement. Also, I believe my grandmother looks after me continuously.

I thank my colleagues and graduate secretary Darlene for their assistance. They helped me to go through my PhD program without big concerns. I also thank UVic librarians for giving me Canadian Community Health Survey data, Saanich Commonwealth Place recreation centre for allowing me to collect human body data and Victorians who participated in the data collection.

Lastly, I appreciate my former supervisor of the master program at University of Guelph, Dr. Robert D. Brown, for his first introducing the study area of human thermal comfort to me. This inspired me to have a big question in my research life and made me continue my study to solve the question.

Thank all UVic Geography people very much.

Introduction

The human body exchanges energy with both the atmosphere and surrounding solid environment. A major way people are affecting their environment is through alteration of the landscape, especially urban development. We are currently in a period of very rapid urban (re)development. Urban areas now have more than half of the world's population, and this will reach nearly 60 % by 2030 (UNHSP 2008). The building sector is responsible for 30–40 % of global energy use (UNEP 2007) and, at a global level, accounts for about 30 % of greenhouse gas emissions (UNEP 2010). Moreover, 75 % of the world's energy consumption and 80 % of its greenhouse gas emissions occur in cities (UNEP 2008). Urban and landscape planning policies can have a significant influence on alteration of the thermal environment for urban dwellers. Healthy, comfortable lives of our increasing urban population will be favoured by urban and landscape planning policies and evaluations that consider human thermal exchange, comfort and stress. The extreme case of thermally malfunctioning urban areas is human mortality caused by heat stress (e.g., Nakai et al. 1999; Smoyer et al. 2000; Dessai 2002; Davis et al. 2003; Tan et al. 2007) and cold stress (e.g., Díaz et al. 2005; Raatikka et al. 2007).

The human thermal exchange (human energy balance) model includes metabolism, solar (shortwave) and terrestrial (longwave) radiation exchanges, conductive, convective and evaporative heat exchanges. The sum of these energy exchanges indicates the level of physiological thermal comfort. If net energy exchange is greater than zero, a person will eventually feel warm or hot. Conversely, a person will feel cool or cold. The first case is called heat stress and the second is cold stress. However, human thermal comfort is not only a result of physiological influences but also psychological influences that are affected by different climate zones, physiological acclimatization and cultural differences (Nikolopoulou and Steemers 2003). Therefore, a human thermal comfort analysis should start with a human thermal exchange model which is based on physiological aspects and then the thermal comfort zones should be adjusted dependent on peoples' acclimatization and cultural differences.

The basic equation of human thermal exchange is:

$$M + R^* + L^* - L_b + C + E + C_r + E_r + H = S \quad (1)$$

where M is metabolic heat production, R^* is absorbed solar radiation, L^* is absorbed longwave radiation, L_b is emitted longwave radiation from a human outer surface area, C is sensible heat loss or gain on the outer body surface, E is latent heat loss on the outer body surface, C_r is sensible heat loss or gain by respiration, E_r is latent heat loss by respiration, H is heat loss or gain via conduction with solid surfaces, and S is net heat storage (Fig. 1a).

In most applications of human thermal exchange modeling, input variables are: air temperature, humidity, wind speed, sun's azimuth and altitude angles and quantities of incoming solar irradiance (direct beam, diffuse beam and reflected solar) and incoming longwave radiation from the surrounding environment. Human factors are usually parameters. These include activity levels, body area factors (effective radiation area factor, f_{eff}, and projected area factor, f_p, dependent on body postures) and clothing factors (area factor, insulation and permeability). The other parameters are urban factors: properties of buildings, vegetation including trees and ground surfaces which include locations, sizes, orientations, materials, albedos and emissivities.

Street level convective and evaporative heat exchanges are very complex and difficult to estimate accurately given micro spatiotemporal variations in wind speed, air temperature and humidity in multifaceted urban outdoor areas. Several researchers have tried to produce wind maps in large urban areas. However, the focus was not on street level wind in large areas but on the roof-top level, a single urban canyon, meso-scale (regional) or night time [i.e., MetPhoMod (the METeorology and atmospheric PHOtochemistry mesoscale MODel, http://www.giub.unibe.ch/klimet/metphomod/), MUKLIMO 3 (the three-dimensional Microscale Urban CLImate Model, Sievers 1990), KLAM_21 (nocturnal drainage wind simulation model, Sievers 2005)].

Radiation exchange is one of the most effective climatic influences in the human thermal exchange model. Radiation can be divided into solar (R) and longwave (L) radiation. Solar radiation can also be separated into direct beam solar radiation (K_b), diffuse beam solar radiation from the open sky (K_d) and solar radiation reflected from buildings (K_{ro}), trees (K_{rveg}) and ground (K_{rg}) surfaces. Longwave radiation can be divided into incoming longwave radiation from the open sky (L_a), from building surfaces (L_o), from tree surfaces (L_{veg}) and from the ground surface (L_g) and emitted longwave radiation from the human body surface (L_b) (Fig. 1b). K_b is the largest daytime radiation component. It is more than 800 Wm^{-2}

on a horizontal surface on clear summer days in mid-latitude areas like Victoria and Vancouver, B.C., Canada, and decreases to 0 Wm^{-2} at night.

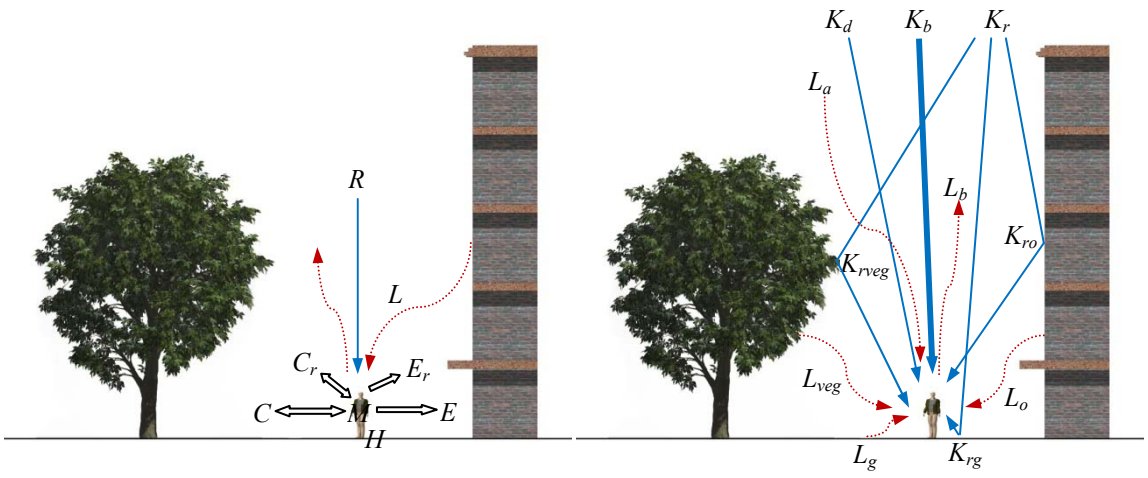

Fig. 1 Energy transfers between a human body and its surrounding environment: (a) human thermal exchange model (human energy balance model) and (b) radiation exchange model

Modeling of radiation exchange between the human body and its surrounding urban environment requires both human area factors and urban area factors (Fig. 2). The human area factors are body area factors and clothing area factors. The urban area factors are sky view factor (ψ_{sky}); view factors of sunny and shaded surfaces of buildings, vegetation and ground; and albedos and emissivities of buildings, vegetation and ground surfaces. In previous studies, several constraints exist. In human body area factors (see Sections 1.1 and 2.1), (1) significant differences in effective radiation area factors (11 %) and projected area factors (5 %) exist, e.g., between Fanger (1972) and Kubaha et al. (2004). (2) There are no complete studies of body area factors for walking posture which is a common posture in outdoor areas. Most studies focused on body area factors for sitting and standing postures. The well-known physiological equivalent temperature (PET, Höppe 1993, 1999) and universal thermal climate index (UTCI, http://www.utci.org) target a walking adult model, but no appropriate body area factors for walking posture can be found yet. (3) No body area factors exist for contemporary adults. The renowned Fanger (1972) study modelled 1970's college students (10 males and 10 females) and recent studies, Tanabe et al. (2000) and Kubaha et al. (2004), used computer body models.

In urban area factors (see Section 4.1), (1) albedos available for urban materials are too broad, e.g., albedo of brick as 0.2-0.5 (Brown and Gillespie 1995). (2) Most radiation exchange models did not separate the view factors of vegetation surfaces (trees) from those of building surfaces in the sky hemisphere. Vegetation usually has much lower surface temperature and lower surface albedo than most building surface materials. Vegetation can create more temperate urban thermal environments than those affected by building surfaces. (3) View factors of sunny/shaded isothermal urban surfaces are not analyzed separately in most existing models. These separated view factors will affect the simulation of reflected solar radiation and emitted longwave radiation because sunny and shaded surfaces will have different albedos and surface temperatures. (4) Accuracy problems exist in three-dimensional computer models, e.g., ENVI-met and RayMan. RayMan underestimates mean radiant temperature (T_{mrt}) at low sun altitudes (Thorsson et al. 2007), and ENVI-met overestimates T_{mrt} in the morning and underestimates during the afternoon and night-time (Ali-Toudert 2005).

The constraints noted above make radiation exchange analysis in human thermal exchange models difficult. More details on these constraints in existing studies are explained in each chapter.

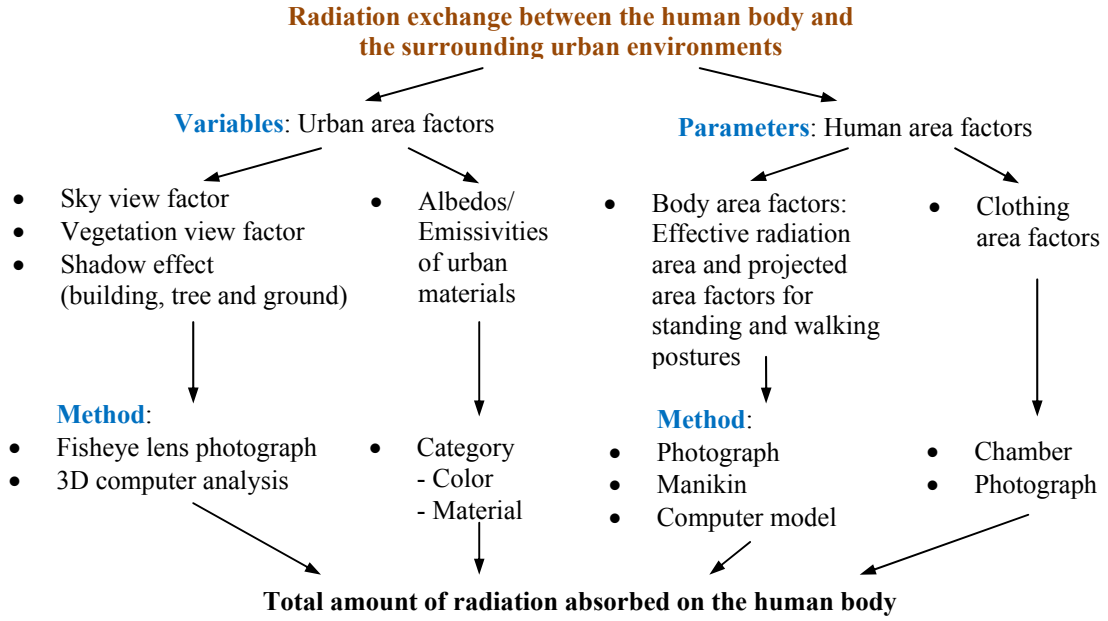

Fig. 2 Human-urban radiation exchange concept

Purpose and objectives:

This study will explore all processes included in the human radiation exchange model through human body area factors (Chapters 1 & 2), existing theoretical methods (Chapter 3) and three-dimensional (3D) computer simulation modeling (Chapter 4). The goal of this study is to develop an improved method for urban/landscape planners and researchers to use as a tool in human radiation exchange and thermal sensation analyses in outdoor urban environments.

The objectives of this study are: (1) to define human body area factors appropriate for contemporary adult body shapes for radiation analysis, (2) to investigate solar and longwave radiation portions of existing human thermal exchange models and develop a more accurate, easy-to-use human radiation exchange model, (3) to test existing urban area parameters and formulas with measured data and produce a reasonably accurate urban radiation exchange process model that is easy to apply in planning and (4) to develop a combined new 3D human-urban radiation exchange computer simulation model for outdoor urban areas and test its applications in case studies.

Chapters 1 and 2 will cover the study of human body area factors, and the new human radiation exchange model will be discussed in the Chapter 3. Chapter 4 will explain urban factors and a new human-urban radiation exchange simulation model. The first two chapters were submitted to the International Journal of Biometeorology on October 29th, 2009 and published online on November 16th, 2010 (DOI: 10.1007/s00484-010-0385-2). Also, the results of Chapter 1 were presented at the 18th International Congress of Biometeorology 22-26 September 2008 in Tokyo, Japan. Combined results of Chapters 1 and 2 were presented at the 51st Annual Conference of the Western Division, Canadian Association of Geographers 5-7 March 2009 in Nanaimo. For readers' better understanding, more information was added in the discussion sections in Chapters 1 and 2 than is in the published paper. The results of Chapter 3; comparing existing human radiation exchange models; were presented at the 7th International Conference on Urban Climate (ICUC-7) 29 June-3 July 2009 in Yokohama, Japan. The paper was selected by the International Association for Urban Climate (IAUC) Awards Committee as the winner of the ICUC-7 (2009) William P. Lowry Graduate Student Prize given to the author of the best graduate student paper in urban biometeorology/bioclimatology. It was published in the 34th Urban Climate News, December 2009 (www.urban-climate.org). An expanded paper was submitted to Theoretical and Applied Climatology on

May 31st, 2010 and published online on January (DOI: 10.1007/s00704-010-0388-2). More results were also added in Chapter 3.

Bioclimatic maps, which have important information for urban/landscape planning, can be produced based on the results of human thermal exchange models (e.g., in Germany, see http://www.staedtebauliche-klimafibel.de/Climate_Booklet/kap_2/kap_2-6.htm). However, the existing methods are difficult for planners to understand and many models are not easy to use because of scientific terminology, undefined input data and their methods and limitations. The significance of this study is that models to estimate all processes of human radiation exchange are intensively investigated. Problems and weakness of existing methods are presented and improvements given. Therefore, easy-to-use but reasonably accurate methods for human radiation exchange analysis in the dynamic outdoor urban environment will be suggested. The body model will allow more adequate and accurate estimation required in urban/landscape planning and human health studies such as the effects of increasing heat stress created by rapid urbanization and global warming.

References

Ali-Toudert F (2005) Dependence of Outdoor Thermal Comfort on Street Design in Hot and Dry Climate. Berichte des Meteorologischen Institutes der Universität Freiburg Nr. 15, http://www.freidok.uni-freiburg.de/volltexte/2078

Brown RD, Gillespie TJ (1995) Microclimatic Landscape Design: Creating Thermal Comfort and Energy Efficiency. John Wiley & Sons Inc., New York

Davis RE, Knappenberger PC, Novicoff WM, Michaels PJ (2003) Decadal changes in summer mortality in U.S. cities. International Journal of Biometeorology 47(3): 166-175

Dessai S (2002) Heat stress and mortality in Lisbon Part 1. model construction and validation. International Journal of Biometeorology 47(1): 6-12

Díaz J, García R, López C, Linares C, Tobías A, Prieto L (2005) Mortality impact of extreme winter temperatures. International Journal of Biometeorology 49(3): 179-183

Fanger PO (1972) Thermal Comfort: Analysis and Applications in Environmental Engineering. McGraw-Hill, New York

Höppe PR (1993) Heat balance modeling. Experientia 49: 741-746. doi: 10.1007/BF01923542

Höppe PR (1999) The physiological equivalent temperature – a universal index for the biometeorological assessment of the thermal environment. International Journal of Biometeorology 43: 71-75. doi: 10.1007/s004840050118

Kubaha K, Fiala D, Toftum J, Taki AH (2004) Human projected area factors for detailed direct and diffuse solar radiation analysis. International Journal of Biometeorology 49: 113-129. doi: 10.1007/s00484-004-0214-6

Nakai S, Itoh T, Morimoto T (1999) Deaths from heat-stroke in Japan: 1968~1994. International Journal of Biometeorology 43(3): 124-127

Nikolopoulou M, Steemers K (2003) Thermal comfort and psychological adaptation as a guide for designing urban spaces. Energy and Buildings 35: 95-101

Raatikka V, Rytkönen M, Näyhä S, Hassi J (2007) Prevalence of cold-related complaints, symptoms and injuries in the general population: the FINRISK 2002 cold substudy. International Journal of Biometeorology 51(5): 441-448

Sievers U (1990) Dreidimensionale Simulationen in Stadtgebieten. In: Umweltmeteorologie, Sitzung des Hauptausschusses II am 7. und 8. Juni in Lahnstein. Schriftenreihe Band 15, Kommission Reinhaltung der Luft im VDI und DIN, Düsseldorf

Sievers U (2005) Das Kaltluft-Abfluss-Modell KLAM_21. Theoretische Grundlagen, Anwendungen und Handhabung des PC-Modells. Berichte des Deutschen Wetterdienstes 227

Smoyer KE, Rainham DGC, Hewko JN (2000) Heat-stress-related mortality in five cities in Southern Ontario: 1980-1996. International Journal of Biometeorology 44(4): 190-197

Tan J, Zheng Y, Song G, Kalkstein LS, Kalkstein AJ, Tang X (2007) Heat wave impacts on mortality in Shanghai, 1998 and 2003. International Journal of Biometeorology 51(3): 193-200

Tanabe S, Narita C, Ozeki Y, Konishi M (2000) Effective radiation area of human body calculated by a numerical simulation. Energy and Buildings 32: 205-215. doi: 10.1016/S0378-7788(00)00045-1

Thorsson S, Lindberg F, Eliasson I, Holmer B (2007) Different methods for estimating the mean radiant temperature in an outdoor urban setting. International Journal of Climatology 27: 1983-1993 doi: 10.1002/joc.1537

UNEP (2007) Global Environment Outlook GEO4 Environment for Development. United Nations Environment Programme ISBN: 978-92-807-2836-1

UNEP (2008) United Nations Environment Programme Publication: Kick the Habit-a UN Guide to Climate Neutrality. UNEMG, UNEP/GRID-Arendal ISBN: 978-92-807-2926-9

UNEP (2010) Guidelines on Education Policy for Sustainable Built Environments. United Nations Environment Programme ISBN: 978-92-807-3095-1

UNHSP (2008) State of the World's Cities 2008/2009-Harmonious Cities. United Nations Human Settlements Programme ISBN: 978-92-1-132010-7

Chapter 1. Human Body Area Factors for Radiation Exchange Analysis I: Standing Posture

Abstract

Human body area factors, effective radiation area factors (f_{eff}) and projected area factors (f_p), of unclothed Caucasians' standing posture used in estimating human radiation exchange with the surrounding environment were determined from a sample of adults in Canada. Both normal-weight (male, n=31; female, n=40) and over-weight (male, n=48; female, n=20) body mass index (BMI) categories were analyzed using several computer software programs. A three-dimensional (3D) mean body model was created for each category. To calculate f_{eff}, measurements at every 10° azimuth and altitude angle were a good compromise between time and accuracy. There was only a 0.005 difference with measurements taken every 5°. Only very small differences in f_{eff} and f_p were found between gender (male or female) and body type (normal- or over-weight). For example, differences in f_{eff} were less than 0.009. The mean f_{eff} value was 0.826. Differences between values presented in available studies are much larger. Differences in f_p values between this study and previous studies were up to 0.173. Effects of body area factors on modeled human radiation exchange vary with the magnitude of incoming solar and longwave radiation and are, therefore, climate dependent. For example, the 0.1 f_{eff} and 0.006 to 0.012 f_p differences between this study and those of Fanger created a 21 to 26 Wm^{-2} difference in body net all-wave radiation in warm and hot daytime, summer situations. The f_{eff} difference would create a 35 to 45 Wm^{-2} difference in night time absorbed longwave radiation. These differences may be large enough to influence the estimated level of human thermal sensation.

1.1 Introduction

Human receipt and emission of radiation are affected by body shape, posture and clothing. Body shape and posture control the body surface area exposed to direct beam solar or other point-source radiation (projected area, A_p) and the total area exposed to the surrounding radiant environment rather than to other body parts (effective radiation area, A_{eff}). Often, factors that represent proportions of the body surface area are utilized. The projected area factor is A_p/A_{eff} (f_p) or A_p/A_D (f_p^*) and the effective radiation area factor (f_{eff}) is A_{eff}/A_D where A_D is total body surface area. The effect of clothing can be considered by utilizing clothing area factors dependent on various clothing types and ensembles employing information found in sources such as McCullough et al. (1985, 1989), ASHRAE (2001) and ISO9920 (2007). A number of human thermal exchange models have employed f_{eff} and f_p based on the works of Underwood and Ward (1966) and Fanger (1972). The results of these 2 studies were determined by photographing a limited sample of standing and sitting people from a variety of angles in an indoor setting. Steinman et al. (1988) modified Fanger's model making it applicable to the complex enclosures found in modern architecture using mean f_p values. Jones et al. (1998) applied the photographic method to a mannequin in clothed and unclothed standing postures. They studied both the whole body and individual body parts. Tanabe et al. (2000) and Kubaha et al. (2004) used three-dimensional (3D), computerized human body models in unclothed sitting and standing postures.

Human body shape in developed countries is changing. There is increasing concern about implications of the trend toward more over-weight people. The mean contemporary Canadian adult population is already considered to belong to the over-weight body mass index (BMI) category (Table 1.1).

Studies that have investigated the effects of gender (male or female) and body type (under-, normal-, over-weight or obese) on body area factors have usually relied on small samples. Results are not wholly consistent between studies. Bandow and Bohnenkamp (1935) used an electrical capacity technique and found that f_{eff} slightly decreased with increasing body size for males but increased for females. However, Guibert and Taylor (1952) noted these results suffered from problems of accuracy and consistency (9 % difference in f_{eff} when the measurement was repeated). Guibert and Taylor (1952) showed 3 % and 1 % decreases of f_{eff} from medium to heavy and light standing male body types, respectively.

However, they studied only one male subject in each light, medium and heavy body type category (Table 1.2). Horikoshi et al. (1990) also tested only three male subjects and found a 1 % difference in f_{eff} between two under-weight subjects and no difference in f_{eff} between under-weight and over-weight subjects. Underwood and Ward (1966) used 25 male and 25 female subjects 14–59 years old and found less than 1.0 % difference in f_p^* between gender and less than 2.5 % between body sizes (largest and smallest A_D subjects). Though they compared f_p^* between genders and body sizes, they did not compare f_p^* between different body types. They also measured at only five different azimuth angles (0, 45, 90, 135 and 180°) and four different altitude angles (0, 30, 63 and 90°). Fanger (1972) reported no gender- and body type-related differences in f_{eff} and no gender-, body type- and clothing-related differences in f_p. His 10 male and 10 female college students belonged to only one body type category, the normal-weight BMI class, so his results did not confirm similarity or difference of body area factors (f_{eff} and f_p) between various body types. Therefore, it can be said that similarity or variation of body area factors among the combination of gender and body type has not yet been clearly proved.

The purpose of this chapter is to investigate the relevant body area factors, f_{eff} and f_p, of a larger sample of contemporary Caucasian male and female adults than employed in the studies cited above (Table 1.2). Results will be compared with those reported in previous studies. Some effects of variation in body area factors on modeled human radiation exchange will be noted.

Table 1.1 The mean height, weight and Body Mass Index (BMI) of Canadian adults

		CHS (1978) (Age: 20–70+)	CHHS (1992) (Age: 18–70+)	CCHS (2004) (Age: 19–70+)
Male	Height (m)	1.726	1.756	1.745
	Weight (kg)	76.2	79.5	82.9
	BMI[a]	25.6	25.8	27.2
Female	Height (m)	1.590	1.624	1.613
	Weight (kg)	62.8	65.6	69.4
	BMI	24.8	24.9	26.7

[a] BMI=weight(kg)/height(m)^2; BMI class: under-weight (<18.5), normal-weight (18.5–24.9), over-weight (25.0–29.9), obese class 1 (30.0–34.9), obese class 2 (35.0–39.9), obese class 3 (≥ 40.0)

Table 1.2 Studies comparing gender and body type

Studies	Gender	Body type[a]	# of subjects	BMI	BMI Class	Ponderal Index[b]
This study	Male	NW_M	31	23.0	normal-weight	2.13-2.39
		OW_M	48	26.9	over-weight	2.34-2.53
	Female	NW_F	40	22.0	normal-weight	2.18-2.44
		OW_F	20	27.2	over-weight	2.39-2.60
Guibert and Taylor (1952)	Male	Medium	1	24.3	normal-weight	2.38
		Heavy	1	30.4	obese class 1	2.57
		Light	1	17.4	under-weight	2.09
Fanger (1972)	Male		10		normal-weight	2.17-2.35
	Female		10		normal-weight	2.22-2.32
Underwood and Ward (1966)	Male		25	no data		
	Female		25			
Horikoshi et al. (1990)	Male	Medium	2	18.2	under-weight	2.2
		Heavy	1	25.1	over-weight	2.5

[a] NW_M: normal-weight male, NW_F: normal-weight female, OW_M: over-weight male, OW_F: over-weight female

[b] Ponderal Index: measure of a person's fatness/leanness calculated as a relationship between weight and height ($kg^{0.33}/m$)

1.2 Analytical basic theory

According to the reciprocity theorem (Fanger 1972),

$$A_1 F_{A_1-A_2} = A_2 F_{A_2-A_1} \tag{1.1}$$

A_1 is the effective radiation area of the human body surface (A_{eff}), $F_{A_1-A_2}$ is the angle factor between the person and the surrounding sphere (A_2), $A_2 = 4\pi r^2$ is the spherical surface area and $F_{A_2-A_1}$ is the angle factor between the sphere and the person.

For a small part of the spherical surface area, dA_2,

$$dF_{A_1-dA_2} = dF_{A_1-cos\beta_2 dA_2} \tag{1.2}$$

$$A_1 dF_{A_1-COS\beta_2 dA_2} = cos\beta_2 dA_2 F_{cos\beta_2 dA_2-A_1} \quad \text{(ASHRAE 1997)} \tag{1.3}$$

Therefore, the angle factor between A_1 and A_2 would be (Oguro et al. 2001)

$$F_{A_1-A_2} = \int_{A_2} dF_{A_1-dA_2} = \int_{A_2} dF_{A_1-cos\beta_2 dA_2} = \int_{A_2} \left(\frac{F_{cos\beta_2 dA_2-A_1}}{A_1}\right) cos\beta_2 dA_2 \tag{1.4}$$

From the definition of angle factor (ASHRAE 1997),

$$F_{cos\beta_2 dA_2 - A_1} = \int_{A_1} \frac{cos\beta_1 cos\beta_2 dA_1}{\pi r^2} \tag{1.5}$$

β_1 and β_2 are incident angles between central points of dA_1 and dA_2. If the size of the body part dA_1 and the portion dA_2 are very small compared to the distance r between dA_1 and dA_2, it can be considered that $cos\beta_2 \approx 1.0$. Then Eq. 1.5 can be written as,

$$F_{cos\beta_2 dA_2 - A_1} = \int_{A_1} \frac{cos\beta_1 dA_1}{\pi r^2} = \frac{A_P}{\pi r^2} \tag{1.6}$$

$$A_P = \int_{A_1} cos\beta_1 dA_1 \tag{1.7}$$

By substituting Eq. 1.6 into Eq. 1.4,

$$F_{A_1 - A_2} = \frac{1}{\pi} \int_{A_2} \frac{f_P}{r^2} cos\,\beta_2 dA_2 = \frac{1}{\pi} \sum_{i=1}^{n} \frac{f_{Pi}}{r^2} cos\beta_2 dA_2 \quad \text{(Kubaha et al. 2003)} \tag{1.8}$$

$$f_P = \frac{A_P}{A_1} = \frac{A_P}{A_{eff}} \tag{1.9}$$

n is the number of equal areas dA_2 comprising the entire spherical surface area.

As the angle factor $F_{A_1 - A_2}$ should be 1.0, the effective radiation area of the body A_1 (=A_{eff}) can be estimated by combining Eq. 1.9 and Eq. 1.8,

$$A_{eff} = \frac{1}{\pi} \int_{A_2} \frac{A_P}{r^2} cos\,\beta_2 dA_2 = \frac{1}{\pi} \sum_{i=1}^{n} \frac{A_{Pi}}{r^2} cos\beta_2 dA_2 \tag{1.10}$$

Because A_P data may be measured from only ¼ of the entire spherical surface area (α: 0–180°, β: 0–90°), A_{eff} can be calculated with,

$$A_{eff} = 4 \times \frac{1}{\pi} \sum_{i=1}^{n_{1/4}} \frac{A_{Pi}}{r^2} cos\beta_2 dA_2 \tag{1.11}$$

when A_P data are collected at a variety of α and β angle increments in ¼ of the spherical surface area.

The f_{eff} values are found using:

$$f_{eff} = \frac{A_{eff}}{A_D} \tag{1.12}$$

1.3 Methods

1.3.1 Subjects

The mean BMI of contemporary Caucasian adults in Canada is in the over-weight category (CCHS 2004). However, the mean has been changing over time and varies with location/region. Therefore, body data were collected for a sample of both normal- (male, n=31; female, n=40) and over-weight (male, n=48; female, n=20) adults (age 18–65 years) at Saanich Commonwealth Place recreation centre, Victoria, B.C., Canada (Table 1.3). This study was approved by the University of Victoria ethics committee (Protocol Number: 06-172). The participant consent form and survey poster are attached in Appendix A. The mean BMI of four body type categories of this study, 24.8, was at the border between the normal-weight and over-weight categories (Table 1.3).

All subjects wore swim suits (male: triangle or box style, female: one piece or bikini style). They were asked to stand and walk naturally yielding a sample of natural adult postures. All participants were well aware of their age and height, so these data were collected using a survey. Heights (m) were confirmed using photometric comparison with several reference heights. Weights (kg) for all subjects were measured with a digital electronic scale manufactured by Taylor (http://www.taylorusa.com) and calibrated with several reference weights. Photos of each person were taken one each from the front and side with Sony Cybershot 3.2 and Nikon Coolpix 8700 cameras (Fig. 1.1a). The photos were taken at the median height of the torso (chest and abdomen), 1.2 m, instead of using the weighting height of the human body, 1.1 m, because the torso has the largest surface area among all body parts. The distance was 10 m to reduce image distortion. Subjects' individual basic data and the relationships between these are given in Fig. 1.2. There was virtually no correlation between age and the other three variables (height, weight and BMI) and between height and BMI. The highest correlation was between normal-weight females' weight and BMI (r^2=0.65).

The normal-weight male and female models were analyzed using four different angle increments; 5°, 10°, 15° and 30°; to assess the effects of the number of observations on estimated A_{eff} and f_{eff}. $n_{1/4}$ is 36×18=648 (per 5°), 18×9=162 (per 10°), 12×6=72 (per 15°) and 6×3=18 (per 30°), respectively. The ¼

spherical surface area was taken at the mid-point of the angle measurement, e.g., for every 5° at azimuth (α): 2.5, 7.5, 12.5·····167.5, 172.5, 177.5°; altitude (β): 2.5, 7.5, 12.5·····77.5, 82.5, 87.5°.

Table 1.3 Subjects' mean basic body data categorized by Body Mass Index (BMI) class

Category	# of persons	Height (m)		Weight (kg)		BMI		Total body surface area (m^2)	
		Mean	Standard Deviation	Mean	Standard Deviation	Mean	Standard Deviation	Mean	
								A_{3DS}[a]	A_{Du}[b]
NW_M	31	1.81	0.06	75.6	6.5	23.0	1.4	1.95	1.96
NW_F	40	1.69	0.05	62.5	6.4	22.0	1.8	1.65	1.71
OW_M	48	1.81	0.05	88.0	5.8	26.9	1.4	2.07	2.08
OW_F	20	1.66	0.05	75.2	6.4	27.2	1.6	1.71	1.84
Mean of four categories		1.74		75.3		24.8		1.85	1.90

[a] A_{3DS} obtained from 3DS Max computer software program

[b] DuBois and DuBois's (1916) formula $A_{Du} = 0.007184 \cdot (H \times 100)^{0.725} \cdot W^{0.425}$ (m^2), H: height (m), W: weight (kg)

1.3.2 Data processing

Before analyzing collected data, image distortion was tested with reference images in AutoCad 2002 (Autodesk®, http://www.autodesk.com). It was found that there was no centroid distortion (i.e., between two same size objects, an object located on the centre is bigger than an object located on the edge in photographs). Only horizontal/vertical rotation correction was required. The digital body shape images were imported into AutoCad 2002 after rotation correction using ACDSee Pro. 1.5 (ACDSee®, http://www.acdsee.com). Edge-of-body lines were digitized. Heights and widths of important body parts (m) as well as the angles between them (°) were measured (Table 1.4). The mean values of body parts were used to make front and side body frames (Fig. 1.1b). Four three-dimensional (3D), computerized body models (normal- and over-weight male and female models) were created in Poser 6 & 7 (SmithMicro®, http://www.smithmicro.com) using the frames (Figs. 1.1c & d). The two male models consisted of 62,298 small surface elements and female models 194,206 as the female models were created in the advanced version, Poser 7. This would yield greater micro-details for females. However, this study is concerned with more general body images. Therefore, additional micro-details are not important. See Figs. 1.1c and d.

The 3D models were imported into AutoCad and rotated regularly by azimuth (α), $0° \leq \alpha \leq 180°$, and altitude (β), $0° \leq \beta \leq 90°$ (Fig. 1.3). Rotated images were exported to Photoshop 7.0 (Adobe®, http://www.adobe.com). To keep the same scale for exporting the images, the same scale value in the zoom

function was used during the entire process in each category in the AutoCad program. The pixel values (1 pixel ≈ 0.056 cm^2) in Photoshop were converted to the real A_p values. Total body surface area (A_D) was calculated using the DuBois and DuBois (1916) formula (A_{Du}) and 3DS Max 9 computer software (A_{3DS}; Autodesk®, http://www.autodesk.com).

.

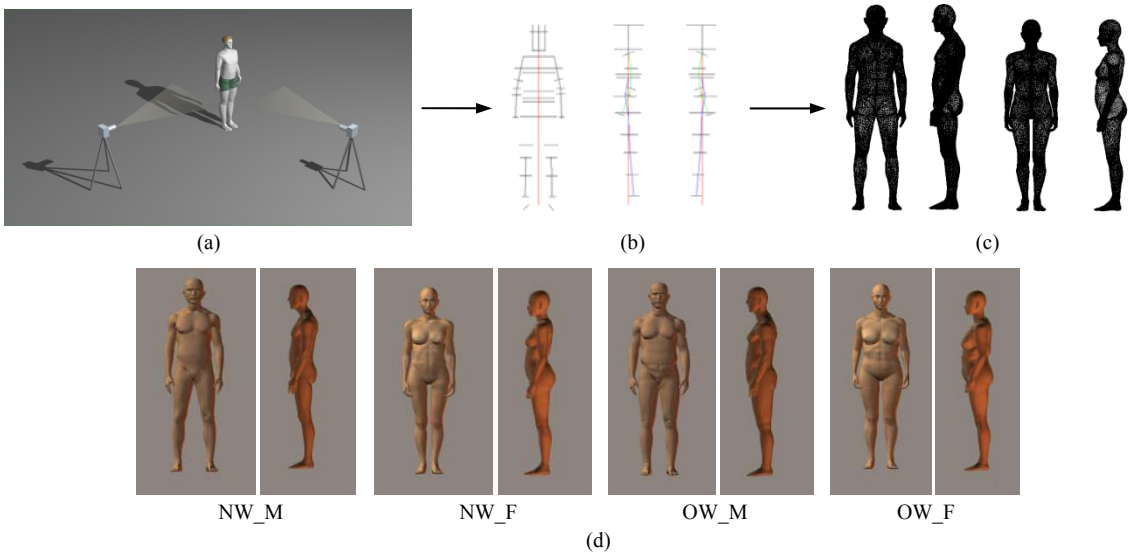

Fig. 1.1 The process for creating three-dimensional (3D) computer body models: (a) taking pictures, created in Vectorworks 2008 (Nemetschek Vectorworks®, http://www.nemetschek.net), (b) creating body frames, (c) building 3D computer models, (d) front and side views of 3D computer models in Poser

Fig. 1.2 Description and comparison of subjects' body variables among age, height, weight and Body Mass Index (BMI). NW and OW are normal-weight and over-weight, respectively

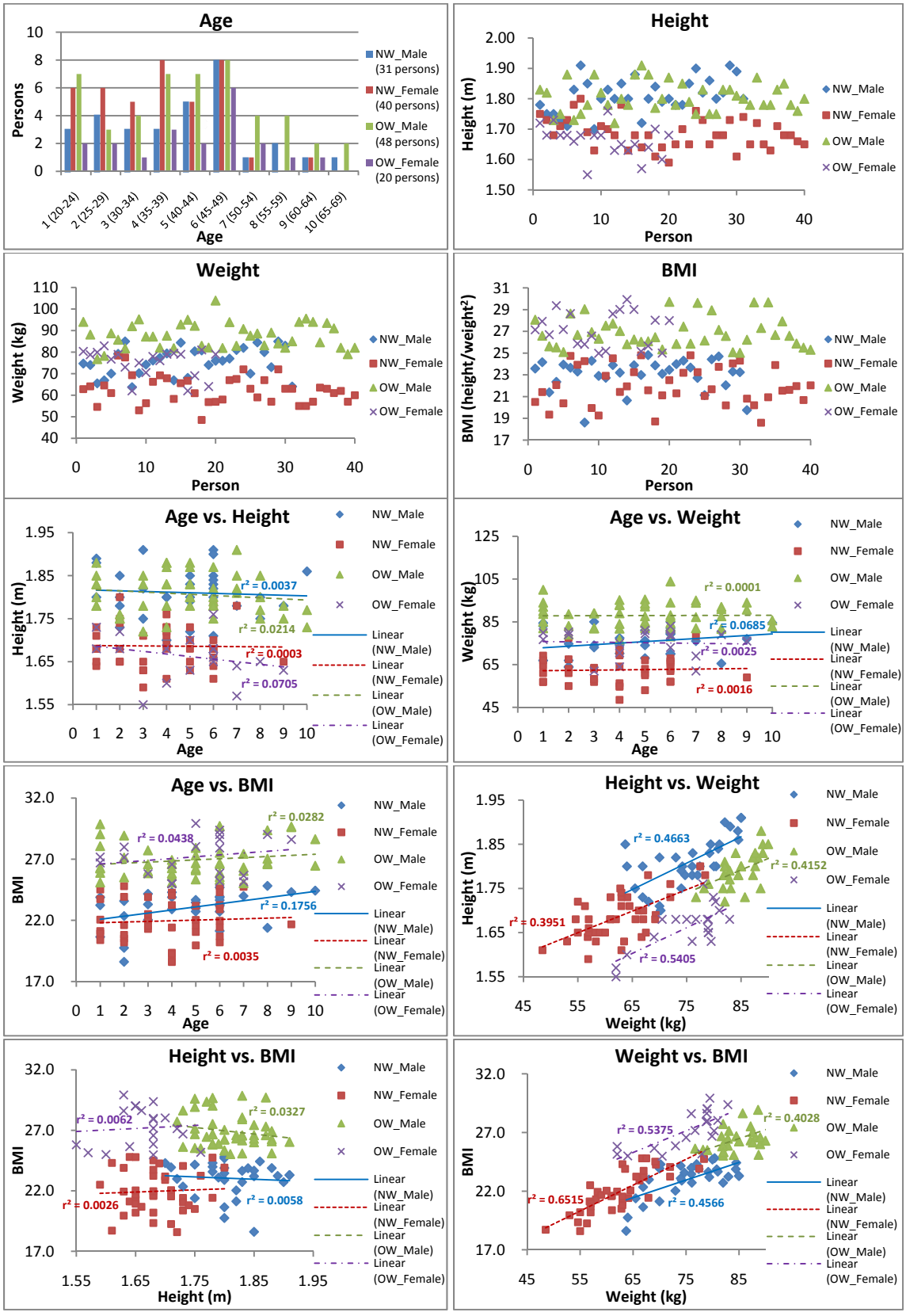

Table 1.4 Mean measured body part data. Dimensions are meters, and angles are degrees. NW and OW are normal- and over-weight, and M and F are male and female

Front	NW_M	NW_F	OW_M	OW_F	**Left_Side**	NW_M	NW_F	OW_M	OW_F
Head_length	0.259	0.235	0.240	0.228	Length_Head_Chin	0.246	0.235	0.244	0.228
Head_width	0.175		0.169	0.160	Neck	0.120	0.105	0.136	0.118
Neck	0.123	0.113	0.134	0.118	Height_Chin_Neck	0.045	0.036	0.041	0.036
Height_Neck	1.552	1.415	1.521	1.399	Chest		0.223		
Shoulder	0.309	0.282	0.321	0.263	Length_Neck_Chest		0.141		
Height_Shoulder	1.492	1.364	1.472	1.364	Angle_Neck_Chest		180		
Between arms	0.479	0.433	0.504	0.460	Breast_side	0.259	0.242	0.281	0.277
Height_Between arms	1.376	1.253	1.357	1.249	Length_Neck_Breast	0.203	0.212	0.204	0.224
Chest	0.335	0.308	0.366	0.334	Angle_Neck_Breast	180	186	183	189
Height_Chest	1.328	1.250	1.335	1.241	Length_Breast_Waist	0.228	0.157	0.211	0.141
Breast		0.300	0.347	0.333	Angle_Breast_Waist	188	185	212	187
Height_Breast		1.173	1.291	1.155	below Breast	0.237		0.268	
Waist	0.301	0.269	0.325	0.304	Length_Breast_below Breast	0.040		0.033	
Height_Waist	1.144	1.050	1.132	1.044	Angle_Breast_below Breast	180		176	
Abdomen	0.322		0.349		Waist	0.236	0.202	0.262	0.246
Height_Abdomen	1.073		1.058		Length_Waist_Hip	0.169	0.191	0.174	0.176
Upper pelvis	0.317		0.337		Angle_Waist_Hip	170	170	171	168
Height_Upper pelvis	1.035		1.022		Hip	0.260	0.245	0.294	0.281
Hip	0.367	0.348	0.382	0.383	Upper Arm	0.135	0.126	0.161	0.144
Height_Hip	0.890	0.867	0.891	0.883	Elbow	0.091	0.078	0.099	0.087
Upper arm (Right arm)	0.088	0.080	0.096		Lower Arm	0.094	0.079	0.101	0.088
Elbow	0.079	0.078	0.089	0.086	Wrist	0.060	0.053	0.058	0.052
Lower arm	0.089	0.077	0.089	0.080	Length_Neck_Upper Arm	0.149	0.119	0.132	0.117
Wrist	0.053	0.047	0.058	0.054	Angle_Neck_Upper Arm	169	172	171	171
Length_Shoulder_Elbow	0.329	0.321	0.352	0.330	Length_Upper Arm_Elbow	0.202	0.217	0.225	0.207
Length_Elbow_Wrist	0.290	0.243	0.265	0.233	Angle_Upper Arm_Elbow	181	181	184	183
Angle_Shoulder_Elbow[a]	191	189	193	195	Length_Elbow_Wrist	0.284	0.255	0.279	0.250
Angle_Elbow_Wrist	182	185	184	185	Angle_Elbow_Wrist	199	199	200	200
Thigh (Right leg)		0.159		0.195	Thigh		0.195		0.198
Height_Thigh		0.742		0.730	Knee	0.131	0.119	0.138	0.126
Knee	0.112	0.111	0.118	0.122	Lower Leg	0.121	0.115	0.130	0.122
Height_Knee	0.480	0.424	0.474	0.426	Ankle	0.107	0.104	0.118	0.107
Length_Hip_Knee	0.412	0.443	0.427	0.460	Length_Hip_Thigh		0.098		0.111
Angle_Hip_Knee	185	182	192	189	Angle_Hip_Thigh		190		188
Lower leg	0.116	0.113	0.123	0.123	Length_Hip_Knee	0.403	0.383	0.420	0.389
Ankle	0.070	0.065	0.070	0.067	Angle_Hip_Knee	177	178	177	177
Length_Knee_Ankle	0.401	0.375	0.401	0.375	Length_Knee_Ankle	0.436	0.406	0.442	0.405
Angle_Knee_Ankle	181	177	182	182	Angle_Knee_Ankle	175	178	177	178
					Height_Ankle	0.090	0.072	0.080	0.073

[a] Angle : N=0°, E=90°, S=180° and W=270° (clockwise)

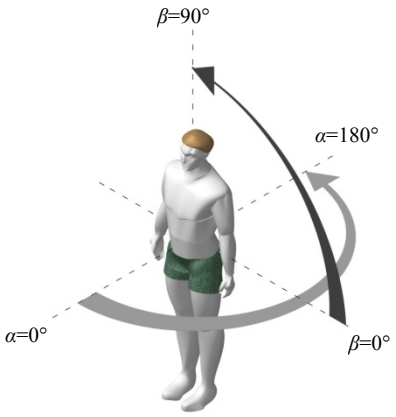

Fig. 1.3 Quarter sphere [azimuth angle ($0° \leq \alpha \leq 180°$) and altitude angle ($0° \leq \beta \leq 90°$)] for determining projected area factors (f_p) of standing posture since the body shape is symmetrical in the posture (created in Vectorworks 2008)

1.4 Results

1.4.1 Observation pattern

Systematically measured A_p values are used to find A_{eff} and f_{eff}, but how often should the A_p values be measured? Values measured in four different degree increments (every 5, 10, 15 and 30°) were compared. The more frequent the measurements, the more detailed the representation of the human body and the more accurate the determination of A_p and A_{eff}. The number of per 5° measurements, 648, was almost 4 times the number of per 10° measurements, 162, but the differences in f_{eff} were small, about 0.0055 (Table 1.5). Per 15° and 30° measurements created greater differences, 0.016 and 0.067, respectively. Therefore, further analysis employed measurements taken every 10°. This interval is recommended as providing a good balance between accuracy and work load.

1.4.2 Total body surface area (A_D, m^2)

Two methods were used for determining A_D: the DuBois and DuBois (1916) formula (A_{Du}) and 3DS Max 9.0 software (A_{3DS}). The DuBois and DuBois (1916) formula overestimated A_D in both male and female models compared with the 3DS Max method. The overestimation was less than 1 % in male models but reached 7.4 % in female models (Table 1.6). Also, the overestimation in over-weight models was almost twice that in normal-weight models.

DuBois and DuBois (1916) noted their formula could produce maximum ±5 % errors. Many other researchers have also found some errors in the formula and modified it (Boyd 1935, Gehan and George 1970, Haycock et al. 1978, EPA 1985, Mosteller 1987, Mattar 1989, Shuter and Aslani 2000, Livingston and Lee 2001 and Tikuisis et al. 2001 and, in Asia, Fujimoto et al. 1968, Kurazumi et al. 1994 and Yu et al. 2003). Recently, 3D scanning technology was adopted in this field. Tikuisis et al. (2001) studied 641 American and European adults' A_D and Yu et al. (2003) sampled 3951 Chinese adults' A_D using the advanced technology. The formula estimates of Tikuisis et al. (2001) were closest to A_{3DS} for both normal- and over-weight males, within 0.3 % of our A_{3DS} (Table 1.6). The formula results of Yu et al. (2003) were

closest for both normal-weight, 0.9 %, and over-weight, 4.1 %, females. How the difference of A_D affects f_{eff} will be explained in section 1.4.4. The measured values of A_{3DS} were used as A_D in this study.

In summary, the Tikuisis et al. (2001) and DuBois and DuBois (1916) formulas yielded males' A_D values close to the results of this study determined via 3D model analysis. The Yu et al. (2003) formula results were closest to the results of this study for females.

Table 1.5 Comparison of effective radiation area factors (f_{eff}) dependent on measuring angles. NW_M and _F are normal-weight male and female

Gender	Measuring Angle	per 5°	per 10°	per 15°	per 30°
	# of Measurements	648	162	72	18
NW_M	A_{eff}[a] (m^2)	1.6284	1.6176	1.5970	1.4981
	f_{eff} (A_{eff}/A_{3DS}[b])	0.8351	0.8295	0.8190	0.7683
	f_{eff} difference[c]		**-0.0055**	**-0.0161**	**-0.0668**
NW_F	A_{eff} (m^2)	1.3679	1.3589	1.3413	1.2556
	f_{eff} (A_{eff}/A_{3DS})	0.8290	0.8236	0.8129	0.7610
	f_{eff} difference		**-0.0054**	**-0.0161**	**-0.0680**
Mean	f_{eff} (A_{eff}/A_{3DS})	**0.8320**	**0.8266**	**0.8160**	**0.7646**
	f_{eff} difference		**-0.0054**	**-0.0160**	**-0.0674**

[a] A_{eff}: effective radiation area

[b] A_{3DS}: total body surface area obtained from 3DS Max 9.0

[c] f_{eff} differences from per 5°

Table 1.6 Comparison of total human body surface area estimated via different methods. All formulas yield body surface area in m^2. NW and OW are normal- and over-weight, and M and F are male and female

	Models	Subjects					Difference from A_{3DS} (%)				
	Formula	NW_M	OW_M	NW_F	OW_F	Mean	NW_M	OW_M	NW_F	OW_F	Absolute Mean
	H: height (cm)	181.1	180.7	168.6	166.3	174.2					
	W: weight (kg)	75.6	88.0	62.5	75.2	75.31					
***A_{3DS}* (m^2)**		**1.950**	**2.070**	**1.650**	**1.710**	**1.85**					
DuBois and DuBois (1916) (A_{Du})	$0.007184 \cdot H^{0.725} \cdot W^{0.425}$	**1.957**	**2.084**	**1.715**	**1.836**	**1.90**	**-0.4**	**-0.7**	**-3.9**	**-7.4**	**3.1**
Boyd (1935)	$0.0178 \cdot H^{0.5} \cdot W^{0.484}$	1.943	2.089	1.711	1.858	1.90	0.4	-0.9	-3.7	-8.6	3.4
Gehan and George (1970)	$0.0235 \cdot H^{0.42246} \cdot W^{0.51456}$	1.956	2.113	1.722	1.883	1.92	-0.3	-2.1	-4.4	-10.1	4.2
Haycock et al. (1978)	$0.024265 \cdot H^{0.3964} \cdot W^{0.5378}$	1.950	2.115	1.712	1.881	1.91	0.0	-2.2	-3.8	-10.0	4.0
EPA (1985)	$0.0239 \cdot H^{0.417} \cdot W^{0.517}$	1.954	2.112	1.720	1.882	1.92	-0.2	-2.0	-4.2	-10.0	4.1
Mosteller (1987)	$[(H \cdot W)/3600]^{0.5}$	1.949	2.101	1.711	1.864	1.91	0.0	-1.5	-3.7	-9.0	3.6
Mattar (1989)	$(H + W - 60)/100$	1.966	2.087	1.711	1.815	1.89	-0.8	-0.8	-3.7	-6.1	2.9
Shuter and Aslani (2000)	$0.00949 \cdot H^{0.655} \cdot W^{0.441}$	1.925	2.056	1.690	1.817	1.87	1.3	0.7	-2.4	-6.3	2.7
Livingston and Scott (2001)	$0.1173 \cdot W^{0.6466}$	1.922	2.121	1.700	1.917	1.91	1.4	-2.4	-3.1	-12.1	4.8
Fujimoto et al. (1968)	$0.008883 \cdot H^{0.663} \cdot W^{0.444}$	1.903	2.033	1.669	1.795	1.85	2.4	1.8	-1.1	-5.0	2.6
Kurazumi et al. (1994)	$0.0100315 \cdot H^{0.693} \cdot W^{0.383}$	1.929	2.042	1.708	1.816	1.87	1.1	1.3	-3.5	-6.2	3.0
Tikuisis et al. (2001)	$0.01281 \cdot H^{0.60} \cdot W^{0.44}$ for men, $0.01474 \cdot H^{0.55} \cdot W^{0.47}$ for women	**1.944**	**2.076**	1.727	1.870	1.90	**0.3**	**-0.3**	-4.7	-9.3	3.7
Yu et al. (2003)	$0.015925(H \cdot W)^{0.5}$	1.863	2.008	**1.635**	**1.781**	1.82	4.5	3.0	**0.9**	**-4.1**	3.1

1.4.3 Projected area factor

Projected area factor can be presented in two ways. The first expresses projected area as a proportion of body effective radiation area, $f_p = A_p / A_{eff}$. This is then used in a formula to find the mean radiant temperature (T_{mrt}) in PMV (Predicted Mean Vote, Fanger 1972) and PET (Physiological Equivalent Temperature, Höppe 1993 and 1999). The second is the proportion of total body surface area, $f_p^* = A_p / A_D = A_p / A_{eff} \times A_{eff} / A_D = f_p \times f_{eff}$. This is used for calculating quantities of absorbed direct beam solar radiation or other point source radiation (e.g., infrared heater) per unit area of the entire body surface. Both f_p and f_p^* are used to input the effect of direct beam solar radiation or other point source radiation into human thermal exchange models.

The projected area factor (f_p) difference between normal-weight males and females reversed around 60–90° azimuth (α) angle (Fig. 1.4). Female f_p values were up to 0.017 greater before α = 60–90°, and male f_p values were up to 0.014 greater after. Females' breasts and males' more open stance between the two legs seem to create this phenomenon. The comparison of f_p values was expanded to all four body type models (Fig. 1.5). The maximum difference is between the normal-weight male and female categories, 0.017. The maximum difference between other combinations was 0.015. Fanger (1972) reported only a very small male–female difference in f_p. The results of this study produce the same conclusion: f_p is nearly independent of gender.

Depending on the application, we can consider two extremes of human body orientation. The first is the directionless orientation used when people are facing a variety of different directions. Body orientation is essentially random. This mode is also used in general modeling studies when we do not know the actual body orientation. The second is the directional orientation used when people face a known, consistent direction.

Directionless f_p values of the four body types were very close (Table 1.7). When altitude angle (β) was up to 65°, the maximum difference was only up to 0.002. When β was 75° and 85°, more differences occurred between normal- and over-weight female models, 0.005 and 0.01 respectively. Therefore, the mean f_p values can be used to represent the contemporary Caucasian adult population in Canada. They can also be computed using a polynomial equation suitable for modeling applications (the formula for Mean of Standing posture in Fig. 1.6) with maximum error of 0.002 at β angles between 5^o and 85^o.

If the exact direction of standing people is known, more precise estimation of f_p can be obtained from Fig. 1.6. The maximum directional difference in f_p averaged from all body type models occurs between the front and side views of the body taken from a low β angle perpendicular to the body surface. In this study with α (azimuth) and β angles measured in 10° increments beginning at 5°, the maximum difference was 0.128 between α=5° and α=95° when β=5°. The differences decreased with increasing β angles.

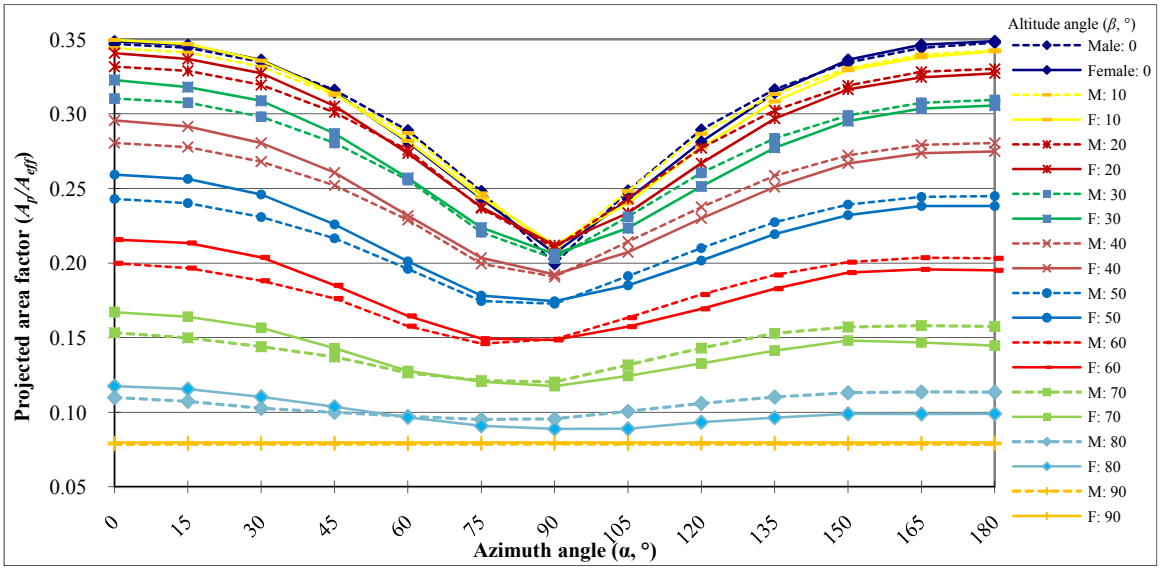

Fig. 1.4 Comparison of projected area factors (f_p) of normal-weight male and female models (standing posture)

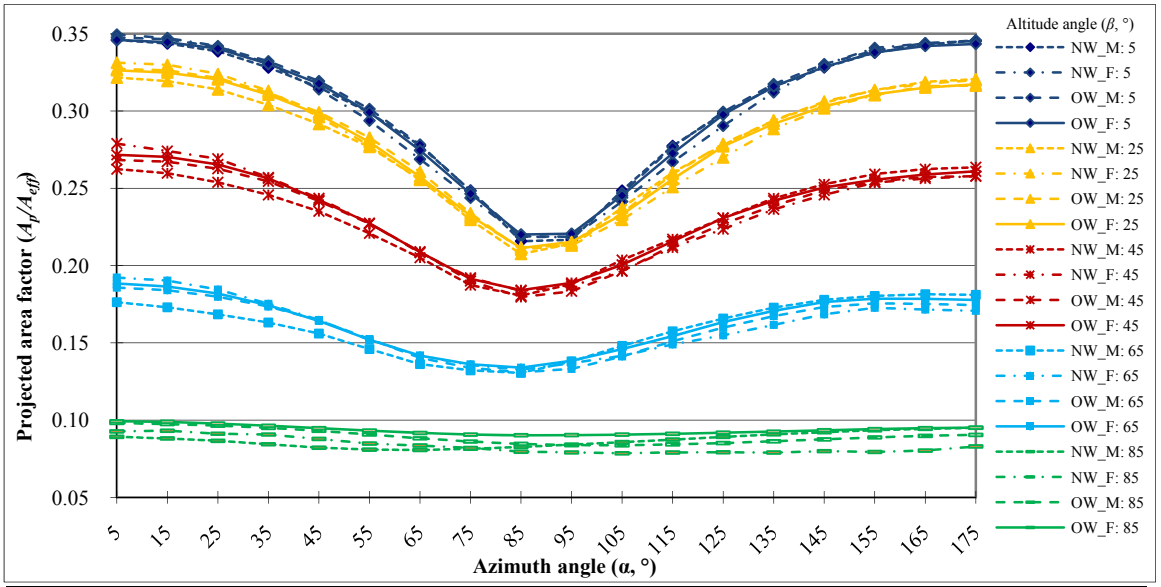

Difference	NW_M-NW_F	NW_M-OW_M	NW_M-OW_F	NW_F-OW_M	NW_F-OW_F	OW_M-OW_F
Max.	0.017	0.011	0.014	0.011	0.015	0.007

Fig. 1.5 Comparison of projected area factors (f_p) of normal- and over-weight male and female models (standing posture)

Table 1.7 Directionless projected area factors (f_p) of normal- and over-weight male and female models

Category		Altitude angle (β, °)										
		0	5	15	25	35	45	55	65	75	85	90
NW_M		0.303	0.302	0.296	0.282	0.261	0.233	0.199	0.161	0.123	0.087	0.079
NW_F		0.302	0.301	0.295	0.283	0.262	0.234	0.201	0.161	0.120	0.084	0.080
OW_M			0.303	0.297	0.284	0.263	0.232	0.199	0.161	0.122	0.089	
OW_F			0.301	0.296	0.282	0.262	0.235	0.202	0.163	0.125	0.094	
	Male mean		0.303	0.297	0.283	0.262	0.232	0.199	0.161	0.122	0.088	
	Female mean		0.301	0.295	0.282	0.262	0.235	0.201	0.162	0.123	0.089	
	Overall mean	**0.302**	**0.302**	**0.296**	**0.283**	**0.262**	**0.233**	**0.200**	**0.162**	**0.123**	**0.088**	**0.079**

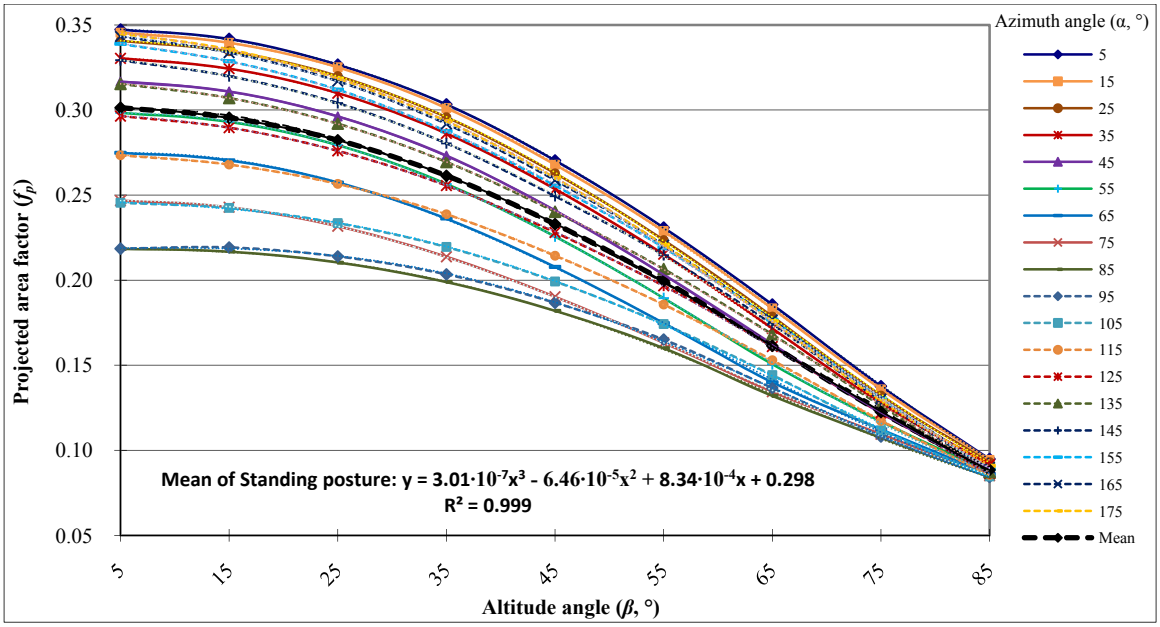

5°: $y = 3.20 \cdot 10^{-7} x^3 - 7.40 \cdot 10^{-5} x^2 + 1.05 \cdot 10^{-3} x + 0.343$	15°: $y = 3.39 \cdot 10^{-7} x^3 - 7.60 \cdot 10^{-5} x^2 + 1.10 \cdot 10^{-3} x + 0.341$
25°: $y = 3.67 \cdot 10^{-7} x^3 - 7.84 \cdot 10^{-5} x^2 + 1.14 \cdot 10^{-3} x + 0.336$	35°: $y = 3.96 \cdot 10^{-7} x^3 - 8.02 \cdot 10^{-5} x^2 + 1.19 \cdot 10^{-3} x + 0.325$
45°: $y = 4.31 \cdot 10^{-7} x^3 - 8.18 \cdot 10^{-5} x^2 + 1.21 \cdot 10^{-3} x + 0.311$	55°: $y = 4.69 \cdot 10^{-7} x^3 - 8.35 \cdot 10^{-5} x^2 + 1.29 \cdot 10^{-3} x + 0.293$
65°: $y = 4.57 \cdot 10^{-7} x^3 - 7.83 \cdot 10^{-5} x^2 + 1.19 \cdot 10^{-3} x + 0.270$	75°: $y = 3.27 \cdot 10^{-7} x^3 - 5.92 \cdot 10^{-5} x^2 + 7.96 \cdot 10^{-4} x + 0.244$
85°: $y = 2.15 \cdot 10^{-7} x^3 - 4.79 \cdot 10^{-5} x^2 + 9.79 \cdot 10^{-4} x + 0.214$	95°: $y = 2.11 \cdot 10^{-7} x^3 - 5.04 \cdot 10^{-5} x^2 + 1.24 \cdot 10^{-3} x + 0.213$
105°: $y = 1.94 \cdot 10^{-7} x^3 - 4.76 \cdot 10^{-5} x^2 + 7.75 \cdot 10^{-4} x + 0.242$	115°: $y = 2.09 \cdot 10^{-7} x^3 - 5.02 \cdot 10^{-5} x^2 + 5.61 \cdot 10^{-4} x + 0.271$
125°: $y = 2.17 \cdot 10^{-7} x^3 - 5.25 \cdot 10^{-5} x^2 + 4.31 \cdot 10^{-4} x + 0.295$	135°: $y = 2.08 \cdot 10^{-7} x^3 - 5.27 \cdot 10^{-5} x^2 + 2.92 \cdot 10^{-4} x + 0.315$
145°: $y = 2.06 \cdot 10^{-7} x^3 - 5.37 \cdot 10^{-5} x^2 + 2.35 \cdot 10^{-4} x + 0.329$	155°: $y = 2.20 \cdot 10^{-7} x^3 - 5.61 \cdot 10^{-5} x^2 + 2.33 \cdot 10^{-4} x + 0.338$
165°: $y = 2.89 \cdot 10^{-7} x^3 - 6.57 \cdot 10^{-5} x^2 + 5.22 \cdot 10^{-4} x + 0.341$	175°: $y = 3.35 \cdot 10^{-7} x^3 - 7.17 \cdot 10^{-5} x^2 + 6.96 \cdot 10^{-4} x + 0.342$

Fig. 1.6 Directional projected area factors (f_p) dependent on solar altitude angles (β) of the mean male and female body type models and best fit equations for azimuth angles (α) between 5° and 175°

The directional projected area factors of this study were compared with those of Underwood and Ward (1966), Jones et al. (1998), Fanger (1972), Tanabe et al. (2000) and Kubaha et al. (2004). The f_p^*

values in Jones et al. (1998) and Underwood and Ward (1966) are from the ratio A_p/A_D instead of A_p/A_{eff} so their f_p^* values are expected to be lower than their unknown f_p values because A_D is larger than A_{eff}. For this comparison, adjusted f_p^* values of normal-weight males in this study were used because Jones et al. and Underwood and Ward results came from males only. The greatest difference between this study and Jones et al. (1998) occurred at α=180° and β=0°, 0.173, and with Underwood and Ward (1966) at α=0° & 180° and β=0°, 0.149 (Fig. 1.7).

The mean directional f_p value of all four body type models combined was compared with the results of Fanger (1972), Tanabe et al. (2000) and Kubaha et al. (2004). The differences with Fanger's (1972) values were up to 0.02 at the medium altitude angle (β=45°) and from the oblique back azimuth angle, α=135° (Fig. 1.8). Values reported by Kubaha et al. (2004) were up to 0.022 different at the lowest altitude angle (β=15°) and the lowest azimuth angle (α=15°). The maximum difference with Tanabe et al.'s (2000) values was only 0.008. An interesting result was that the greater differences with Fanger and Tanabe et al. occurred more at the higher azimuth angles (from side to back: 90°≤α≤180°) when β is increasing and with Kubaha et al. more at the lower azimuth angles (α<90°) when β is increasing. Probably, the location of arms and hands and the stance width affect these phenomena. The 3D computer body models of Kubaha et al. and this study had more relaxed and more front-located arms and hands as well as a wider stance compared with thigh-side located hands and closer legs of the Fanger and Tanabe et al. models.

The directionless f_p values of the four studies are compared in Fig. 1.9a. The greatest differences between this study and the others were: 0.012 at β=45° with Fanger, 0.011 at β=90° with Tanabe et al. and 0.01 at β=75° with Kubaha et al. All differences are small. However, differences in directionless f_p^* values are greater than those of f_p. The differences between this study and those of Fanger and Tanabe et al. increased if f_p is multiplied by each study's different f_{eff} value (Fig. 1.9b). The maximum differences increased to 0.033 at β=40° with Fanger and to 0.025 at β=0° and 45° with Tanabe et al. Differences with Kubaha et al. remained the same. Differences with the frequently used Fanger's values are nearly constant at β angles less than 60°, around 0.03. The effects of these differences on radiation exchange will be shown later in the discussion.

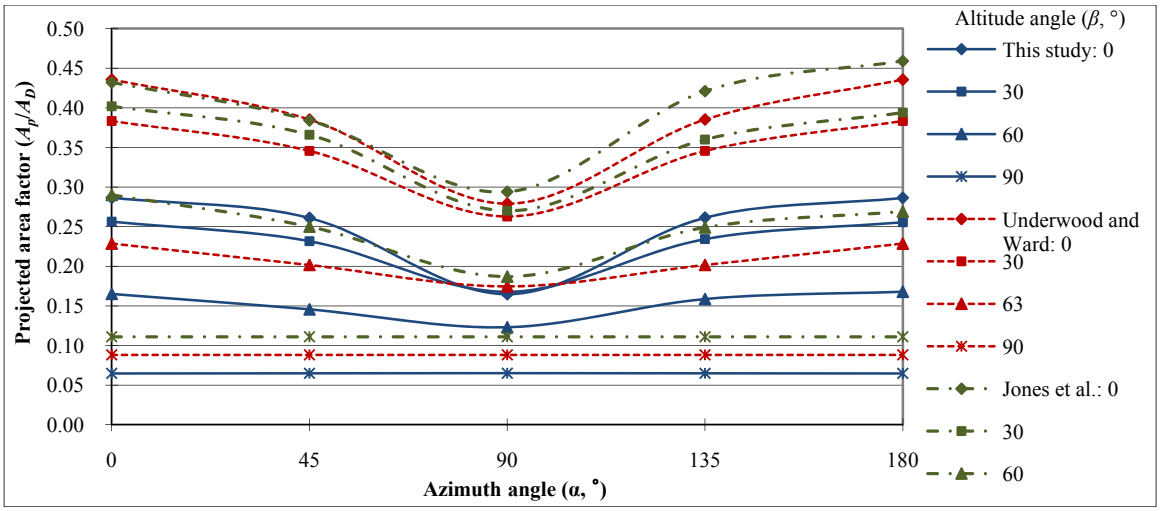

Fig. 1.7 Comparison of directional projected area factors (f_p^*) of normal-weight males between Underwood and Ward (1966), Jones et al. (1998) and this study

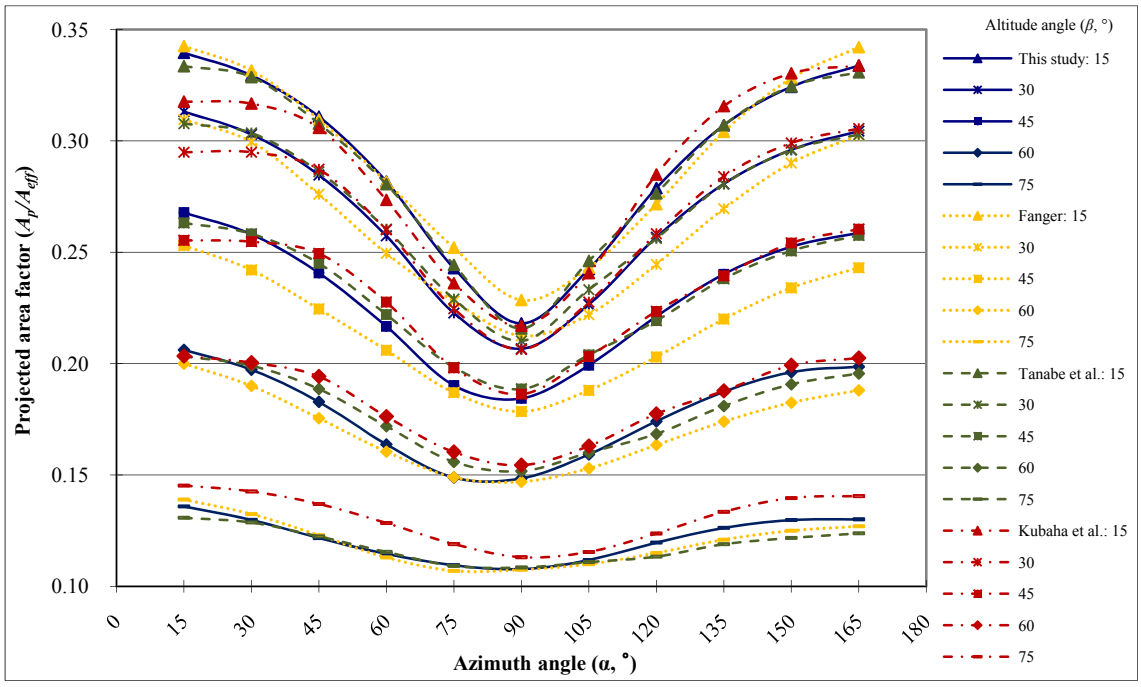

Fig. 1.8 Comparison of directional projected area factors (f_p) of standing posture between Fanger (1972), Tanabe et al. (2000), Kubaha et al. (2004) and this study

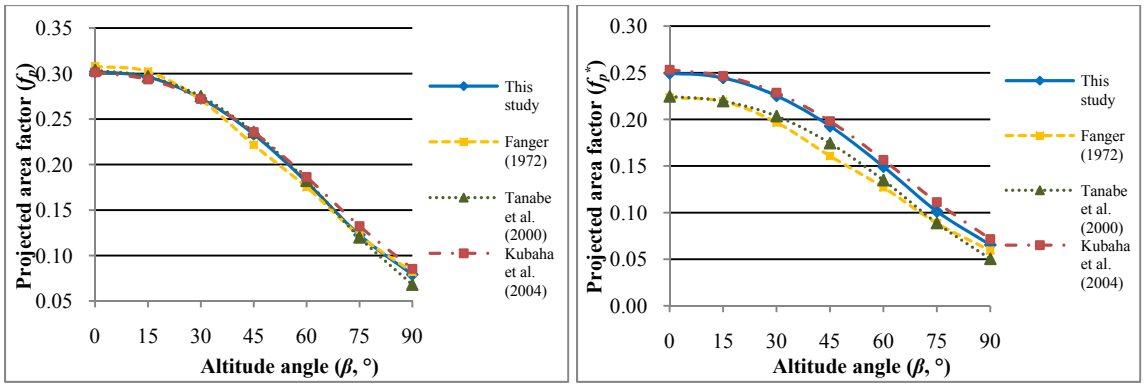

(a) (b)

Fig. 1.9 Comparison of directionless (a) projected area factors (f_p) and (b) projected area factors (f_p^*) between Fanger (1972), Tanabe et al. (2000), Kubaha et al. (2004) and this study

1.4.4 Effective radiation area factor (f_{eff})

Effective radiation area factor (f_{eff}) is the result of effective radiation area (A_{eff}) divided by total body surface area (A_D). It is used to estimate quantities of absorbed diffuse beam and reflected solar and longwave radiation on the human body surface. Total body surface areas (A_D) used to compute f_{eff} were obtained from 3D computer body models in 3DS Max 9 (male: 2.01 m^2, female: 1.68 m^2). The mean f_{eff} value was 0.826 which means 82.6 % of total human body surface area exchanges radiation with its surrounding environment. The maximum difference between all four body type models was only 0.009 (Table 1.8). Therefore, f_{eff} was not related to gender or body type for our sample of people.

f_{eff_ADu} values using A_{Du} were compared with f_{eff} values (Table 1.8). The differences of f_{eff_ADu} and f_{eff} values of male models were only up to 0.005, but in female models the differences were much greater. f_{eff_ADu} was 0.032 less in the normal-weight female model and 0.057 less in the over-weight female model. The reason is A_{Du} values of normal- and over-weight female models were 3.9 % and 7.4 % more than A_{3DS} values, respectively, much more than the 0.4 % and 0.7 % for males.

The mean height, 1.74 m, (male: 1.81 m, female: 1.675 m) of this study was similar to subjects' heights in previous studies (Table 1.9). The mean A_D value of the four body type categories, 1.845 m^2, was close to Kubaha et al.'s (2004) and Guibert and Taylor's (1952) studies but much greater than those of Fanger (1972) and Tanabe et al. (2000) (Table 1.9). The f_{eff} value of this study, 0.826, lies closest to that of

Miyazaki et al. (1995). The absolute range between Kubaha et al.'s (2004) value, 0.84, and Fanger's (1972) widely used value, 0.725, is over 0.11.

Table 1.8 Comparison of effective radiation area factors (f_{eff}) of Body Mass Index (BMI) categories

Category	A_{eff} (m²)	A_D		f_{eff}	f_{eff_ADu}	***Diff. of*** f_{eff} **-** f_{eff_ADu}
		A_{3DS} (m²)	A_{Du} (m²)			
NW_M	1.618	1.95	1.96	**0.830**	**0.827**	**0.003**
OW_M	1.700	2.07	2.08	**0.821**	**0.816**	**0.005**
NW_F	1.359	1.65	1.71	**0.824**	**0.792**	**0.032**
OW_F	1.419	1.71	1.84	**0.830**	**0.773**	**0.057**
Mean	1.524	1.845	1.898	**0.826**	**0.802**	**0.024**

Table 1.9 Comparison of standing posture effective radiation area factors (f_{eff}) with previous studies

Description	Height (m)	Total body surface area (A_D, m²)	Effective radiation area factor (f_{eff})	Subjects
This study	1.74 (male: 1.81, female: 1.67)	1.845 (male: 2.01, female: 1.68)	0.826	79 males 60 females
Kubaha et al. (2004)	1.75	1.83	0.84	Male 3D model
Tanabe et al. (2000)	1.75	1.72	0.74	Male 3D model
Miyazaki et al. (1995)	1.71	1.58	0.83	.
Horikoshi et al. (1990)	1.70	1.69	0.80	3 males
Fanger (1972)	1.72 (male: 1.78, female: 1.66)	1.74 (male: 1.86, female: 1.61)	0.725	10 males 10 females
Underwood and Ward (1966)	.	Male: 1.80 Female: 1.59	.	25 males 25 females
Guibert and Taylor (1952)	1.72	1.84	0.78	3 males

1.5 Discussion

The projected area factor (f_p^* or f_p) is used to calculate incident direct beam solar radiation. f_{eff} is used for calculating incident diffuse beam solar radiation, solar radiation received after reflecting from the surrounding environment and both emitted and incident longwave radiation.

A comparison using this study's and Fanger's (1972) widely used f_{eff} and f_p^* values illustrates some of the human radiation exchange effects of differences in the body area factors. Incoming solar radiation was multiplied by an assumed absorptivity of a human body surface, 0.7 (70 %), and longwave radiation by an assumed absorptivity (emissivity) of 0.97.

Absorbed longwave radiation was the most sensitive radiation stream (Fig. 1.10a). The least was absorbed direct beam solar radiation on the human body surface (K_b^*) which depends on solar altitude. It is most sensitive to variations in incoming direct beam solar radiation on the human body surface (K_b^+) at around β=40°, and after β=50° the slopes of the linear regression lines decline rapidly (Fig. 1.10b).

Gagge et al. (1969) found mean skin temperature (T_{sk}) was between 27 °C and 36.5 °C under steady state conditions. Within this range of T_{sk}, differences in longwave radiation emitted from the body surface (L_b) between this study and Fanger (1972) were in a very narrow range, 6 Wm^{-2} (45–51 Wm^{-2}) (Fig. 1.10c). With an assumed mean T_{sk} of 31 °C, the L_b difference created by the 0.1 f_{eff} difference between this study and Fanger was 47 Wm^{-2}.

Slopes of the linear regression lines are created by a combination of f_{eff} and f_p^* differences and the assumed absorptivity of the body for the radiation type. Incoming longwave radiation (L) and diffuse beam and reflected solar radiation on the human body surface ($K_d^+ + K_r^+$) are affected only by f_{eff} which has a greater difference (0.1) than f_p^* (0.02–0.03). Hence, the slopes were greater for longwave and diffuse beam and reflected solar radiation than for direct beam solar radiation. The assumed body absorptivity for longwave radiation (0.97) is greater than that for solar radiation (0.70). This is the sole cause of the difference in sensitivity between L and $K_d^+ + K_r^+$.

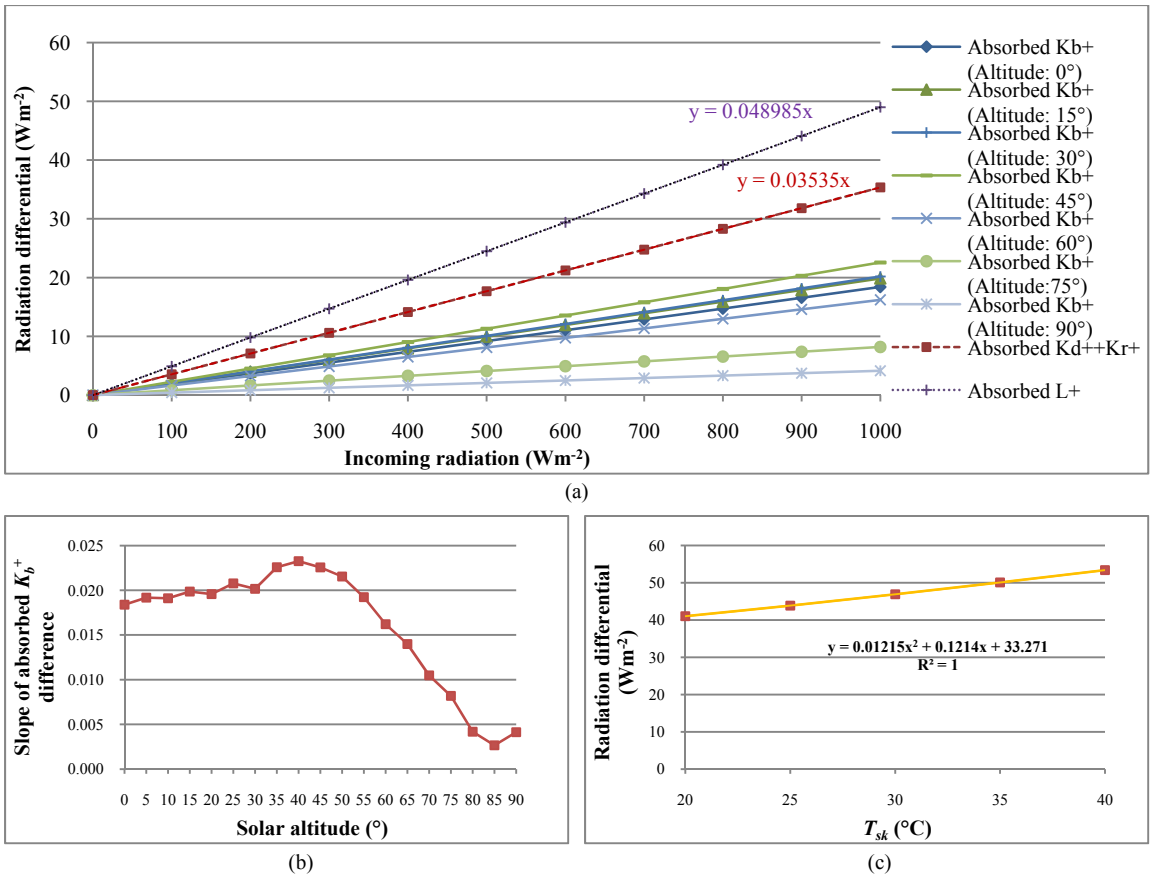

Fig. 1.10 Effects on modeled absorbed and emitted radiation on a body surface created by differences in body area factors between this study and Fanger (1972). (a) Differences in absorbed K_b^+ (direct beam) by solar altitude, K_d^+ (diffuse beam) + K_r^+ (reflected solar radiation) and L^+ (longwave radiation) dependent on amounts of incoming radiation (b) Slope of absorbed K_b^+ difference by solar altitude (c) Differences in L_b (longwave radiation emitted from the human body surface) at different T_{sk} (mean skin temperatures)

Effects of the differences in f_{eff} and f_p^* values between this study and Fanger (1972) on human radiation exchange are illustrated using input data from a selection of Canadian urban sites. T_{sk} was assumed to be 31°C for calculating L_b from Gagge et al. (1969). The absorbed solar radiation (R^*) and net-longwave radiation (L) were computed with Eqs. 1.13 & 1.14:

$$R^* = \left\{f_p \cdot f_{eff} \cdot {K_b}^+ + \frac{1}{2} f_{eff}({K_d}^+ + {K_r}^+)\right\}(1-\alpha_b)$$

$$= \left\{{f_p}^* \cdot {K_b}^+ + \frac{1}{2} f_{eff}({K_d}^+ + {K_r}^+)\right\}(1-\alpha_b) \quad (\mathrm{Wm^{-2}}) \tag{1.13}$$

$$L = \frac{1}{2} \cdot 0.97 \cdot f_{eff}\left(L_a + L_o + L_g\right) - f_{eff} L_b \quad (\mathrm{Wm^{-2}}) \tag{1.14}$$

when we apply f_p^*, K_b^+ is direct beam solar radiation incident on the human body surface perpendicular to the sun's rays. K_d^+ and K_r^+ are diffuse beam and solar radiation reflected by obstructions in the sky

hemisphere incident on the human body surface. a_b is solar radiation albedo of a person's body surface (0.3). L_a and L_o are longwave radiation coming from the sky and vertical objects (buildings and trees) in the sky hemisphere to a horizontal surface. L_g is longwave radiation emitted from the horizontal ground surface. L_b is emitted longwave radiation from a human body surface.

The simulations are:

1) A typical clear summer day at noon (Aug. 30, 2007) in downtown Victoria, B.C. (latitude and longitude: 48º25'N, 123º19'W, solar altitude angle (β): 51.2°, sky view factor (ψ_{sky}): 0.61 (Fig. 1.11a), air temperature (T_a): 24.5 °C, relative humidity (RH): 45 %, wind speed (v): <1.5 ms^{-1}). The differences of f_{eff} (0.1) and f_p^* (0.031) between Fanger (1972) and this study created a 20.9 Wm^{-2} difference in net radiation on a standing person (Table 1.10).

2) A hot clear summer day at noon (Aug. 5, 2008) in downtown Nanaimo, B.C. (latitude and longitude: 49º10'N, 123º56'W, β: 57.9°, ψ_{sky}: 0.43 (Fig. 1.11b), T_a: 31.1 °C, RH: 45 %, v: <1.2 ms^{-1}). The differences of f_{eff} (0.1) and f_p^* (0.024) created a gap of 26.5 Wm^{-2} in net radiation.

3) A typical clear summer day (Aug. 10, 2002) at the University of Guelph, Ontario (latitude and longitude: 43º32'N, 80º14'W, β: 60.9°, ψ_{sky}: 0.88 (Fig. 1.11c), T_a: 29.9 °C, RH: 38.7 %, v: calm). The differences of f_{eff} (0.1) and f_p^* (0.022) made a gap of 24.6 Wm^{-2} in net radiation.

4) Effects of differences in effective radiation area factors on human absorbed longwave radiation at night were simulated for a variety of mean radiant temperatures. The mean radiant temperature (T_{mrt}) of the surrounding environment was assumed to be the ambient T_a and incoming longwave radiation was evenly distributed over the entire surrounding environment. An environmental emissivity of 0.97 was used. The differences were 35–45 Wm^{-2} when T_a was 10–30 °C (Table 1.11).

The small differences in projected area factors used in these examples, 0.022–0.031, limited the effect on direct beam solar radiation to about 13–18 Wm^{-2} with the assumed human albedo of 0.30 (Table 1.10). High pavement and building wall temperatures create a high amount of incoming longwave radiation in the summer urban environments (i.e., simulations 1-3). This, combined with the 0.1 difference in effective radiation area factor and the high absorptivity/emissivity of the human body yielded human absorbed and emitted longwave radiation values much greater than those of solar radiation. The combination of the greater f_p^* and f_{eff} created about 70 Wm^{-2} more total absorbed radiation and about 21–26

Wm^{-2} more net radiation on the simulated human body. If the amounts of net radiation are changed to mean radiant temperature (T_{mrt}) using the radiative heat transfer coefficient of 4.7 $Wm^{-2}K^{-1}$ which is nearly constant for typical indoor temperatures (ASHRAE 2001), the differences in body area factors will create a difference in T_{mrt} of around 5 K.

At night, only longwave radiation and f_{eff} are the active radiation type and body area factor. Differences in absorbed longwave radiation created by a difference in f_{eff} increase with environmental longwave radiation. The simulated differences ranged from 35 to 45 Wm^{-2} as we move from a cool to very warm environment (Table 1.11).

The relationship between measured T_{mrt} and a human biometeorological thermal index, physiological equivalent temperature (PET), can be found (Matzarakis et al. 2007):

$$PET = 0.5191 \times T_{mrt} + 6.7986 \qquad (r^2 = 0.7569) \qquad (1.15)$$

A change of 5.0 K in T_{mrt} makes a 2.6 °C difference in PET which is about half a level of thermal perception and physiological stress (Table 1.12). Therefore, it can be noted that the differences of body area factors (f_p and f_{eff}) can have a significant influence in human thermal exchange modeling.

(a) (b) (c)

Fig. 1.11 Fisheye lens photographs. (a) Victoria, B.C., ψ_{sky}=0.61 (b) Nanaimo, B.C., ψ_{sky}=0.43 (c) Guelph, Ontario, ψ_{sky}=0.88. Sky view factor (ψ_{sky}) was analyzed using BMSky-view (Gál et al. 2007)

Table 1.10 Daytime differences in computed human radiation between body area factors of Fanger (1972) and this study

	Location		Body area factor		Incoming radiation (Wm^{-2})			Net radiation (Wm^{-2})					T_{mrt} Difference[a] (K)
			f_{eff}	f_p	K_b^+	$K_d^+ + K_r^+$	L_{env}	K_b^*	$K_d^* + K_r^*$	L_{abs}	L_b	Total	
Daytime	Victoria, B.C.	This study	0.826	0.217	657	192	886	105.8	55.5	354.9	388.0	128.2	
		Fanger	0.725	0.205	657	192	886	87.7	48.7	311.5	340.6	107.4	
		Difference	f_p^*:	0.031				18.1	6.8	43.4	47.4	**20.8**	**4.4**
	Nanaimo, B.C.	This study	0.826	0.187	707	325	985	90.2	94.0	394.6	388.0	190.8	
		Fanger	0.725	0.18	707	325	985	76.2	82.5	346.4	340.6	164.5	
		Difference	f_p^*:	0.024				14.0	11.5	48.3	47.4	**26.3**	**5.6**
	Guelph, Ontario	This study	0.826	0.173	759	340	957	86.1	98.3	383.4	388.0	179.7	
		Fanger	0.725	0.167	759	340	957	72.9	86.3	336.5	340.6	155.1	
		Difference	f_p^*:	0.022				13.1	12.0	46.9	47.4	**24.6**	**5.2**

[a] T_{mrt} differences were calculated using the radiative heat transfer coefficient, 4.7 $Wm^{-2}K^{-1}$ (ASHRAE 2001)

Table 1.11 Examples of computed absorbed radiation differences at night between effective radiation area factors of Fanger (1972) and this study

T_a (°C)	L_{env} [a] (T_{mrt}=T_a) (Wm^{-2})	L_{abs}		L_{abs} differences (Wm^{-2})	T_{mrt} differences (K)
		This study (Wm^{-2})	Fanger (Wm^{-2})		
10	352.8	282.7	248.1	34.6	7.4
20	405.3	324.8	285.1	39.7	8.4
30	463.6	371.4	326.0	45.4	9.7

[a] an environmental emissivity of 0.97 was used

Table 1.12 Levels of thermal perception and physiological stress of predicted mean vote (PMV) and physiological equivalent temperature (PET) (Matzarakis et al. 1999)

PMV	PET (°C)	Thermal perception	Grade of physiological stress
		very cold	extreme cold stress
-3.5	4		
		cold	strong cold stress
-2.5	8		
		cool	moderate cold stress
-1.5	13		
		slightly cool	slight cold stress
-0.5	18		
		neutral(comfortable)	no thermal stress
0.5	23		
		slightly warm	slight heat stress
1.5	29		
		warm	moderate heat stress
2.5	35		
		hot	strong heat stress
3.5	41		
		very hot	extreme heat stress

1.6 Conclusions

Body surface areas, effective radiation area factors (f_{eff}) and projected area factors (f_p^* and f_p) were determined for a sample of 139 adults. The sample included men and women in the normal- and over-weight body mass index (BMI) categories. Participants were those engaged in recreation center activities. Although the sample included people with an over-weight BMI, the results of this study should be viewed as applicable to active adults who seek adequate exercise.

Mean total body surface area of the adult subjects was greater than that presented in most other studies. One reason is the inclusion of over-weight subjects. BMI has been increasing over time. CCHS (2004) revealed the mean Canadian male and female adult BMI is now in the over-weight category. The inclusion of over-weight subjects allowed the sample to better represent the contemporary Canadian adult population than is the case of idealized figures or samples of younger people used in previous studies. The trend toward greater BMI is not confined to Canada but is becoming a major health concern in developed countries around the world.

Body surface area and radiation area factors were determined by computer analysis of body images taken from a number of regularly spaced azimuth and altitude angles. Measurements every 10° are recommended as a good compromise between accuracy and data processing time.

Differences in f_p and f_{eff} between the four body types were relatively small. For most general modeling studies, a single value can be used regardless of gender or BMI category without seriously affecting the projected results.

Differences between values presented in the wide variety of available studies are much greater than those found for body type. Hence, differences come more from methods employed than from the human figures from which the body area factors were determined. The results of this study, in general, tend to be closer to those of studies using similar methods.

Human energy balance models have usually used body area factors of sitting and standing postures. However, in many outdoor situations and some indoor activities walking posture is more common. Chapter 2 of this study will show the results of body area factors for walking posture.

References

ASHRAE (1997) Thermal Comfort. In: ASHRAE handbook - Fundamentals, Chapter 8. American Society of Heating, Refrigerating and Air-conditioning Engineers, Inc., Atlanta

ASHRAE (2001) Thermal Comfort. In: ASHRAE handbook - Fundamentals, Chapter 8. American Society of Heating, Refrigerating and Air-conditioning Engineers, Inc., Atlanta

Bandow F, Bohnenkamp H (1935) Über die Bestimmung der Strahlungsfläche des Menschen aus seiner elektrischen Kapazität. Pflüger's Archivfür die gesamte Physiologie 236: 427-434

Boyd E (1935) The Growth of the Surface Area of the Human Body. University of Minnesota Press, Minneapolis

CCHS (2004) Canadian Community Health Survey, Nutrition: General Health Component, Cycle 2.2. Statistics Canada. http://www.hc-sc.gc.ca/fn-an/surveill/nutrition/commun/index-eng.php

CHHS (1992) Canadian Heart Health Survey, 1986-1992. Health Canada. http://hdl.handle.net/10573/42050

CHS (1978) Canada Health Survey. Statistics Canada. http://www.statcan.gc.ca/cgi-bin/imdb/p2SV.pl?Function=getSurvey&SDDS=3217&lang=en&db=imdb&adm=8&dis=2

DuBois D, DuBois EF (1916) A formula to estimate the approximate surface area if height and weight be known. Archives of Internal Medicine 17: 863-871

EPA (US Environmental Protection Agency) (1985) Development of Statistical Distributions or Ranges of Standard Factors used in Exposure Assessments. EPA/600/8-85-010. Office of Health and Environmental Assessment, Washington (DC)

Fanger PO (1972) Thermal Comfort: Analysis and Applications in Environmental Engineering. McGraw-Hill, New York

Fujimoto S, Watanabe T, Sakamoto A, Yukawa K, Morimoto K (1968) Studies on the physical surface area of Japanese, Part 18. Calculation formulas in three stages over all ages. Japanese Journal of Hygiene 23: 443–450

Gagge AP, Stolwijk JAJ, Nishi Y (1969) The prediction of thermal comfort when thermal equilibrium is maintained by sweating. ASHRAE Transactions 75, Part 2: 108-123

Gál T, Rzepa M, Gromek B, Unger J (2007) Comparison between sky view factor values computed by two different methods in an urban environment. Acta Climatologica et Chorologica, Universitatis Szegediensis, Tomus 40-41: 17-26

Gehan EA, George SL (1970) Estimation of human body surface area from height and weight. Cancer Chemotherapy Representative 54: 225-235

Guibert A, Taylor C (1952) Radiation area of the human body. Journal of Applied Physiology 5: 24-37

Haycock GB, Schwartz GJ, Wisotsky DH (1978) Geometric method for measuring body surface area: a height-weight formula validated in infants, children, and adults. Journal of Pediatrics 93: 62-66. doi: 10.1016/S0022-3476(78)80601-5

Höppe PR (1993) Heat balance modeling. Experientia 49: 741-746. doi: 10.1007/BF01923542

Höppe PR (1999) The physiological equivalent temperature – a universal index for the biometeorological assessment of the thermal environment. International Journal of Biometeorology 43: 71-75. doi: 10.1007/s004840050118

Horikoshi T, Tsuchikawa T, Kobayashi Y, Miwa E, Kurazumi Y, Hirayama K (1990) The effective radiation area and angle factor between man and a rectangular plane near him. ASHRAE Transactions 96: 60-66

ISO9920 (2007) ISO 9920: Ergonomics of the Thermal Environment: Estimation of Thermal Insulation and Water Vapour Resistance of a Clothing Ensemble. ISO, Geneva

Jones BW, Hong S, McCullough EA (1998) Detailed projected area data for the human body. ASHRAE Transactions 104: 1327-1339

Kubaha K, Fiala D, Lomas KJ (2003) Predicting human geometry-related factors for detailed radiation analysis in indoor spaces. Building Simulation, Eindhoven, Netherlands, August 11-14

Kubaha K, Fiala D, Toftum J, Taki AH (2004) Human projected area factors for detailed direct and diffuse solar radiation analysis. International Journal of Biometeorology 49: 113-129. doi: 10.1007/s00484-004-0214-6

Kurazumi Y, Horikoshi T, Tsuchikawa T, Matsubara N (1994) The body surface area of Japanese. Japanese Journal of Biometeorology 31: 5–29

Livingston EH, Lee S (2001) Body surface area prediction in normalweight and obese patients. American Journal of Physiology: Endocrinology and Metabolism 281: 586-591

Mattar JA (1989) A simple calculation to estimate body surface area in adults and its correction with the Dubois formula. Critical Care Medicine 17: 846-847

Matzarakis A, Mayer H, Iziomon MG (1999) Applications of a universal thermal index: physiological equivalent temperature. International Journal of Biometeorology 43: 76-84. doi: 10.1007/s004840 050119

Matzarakis A, Rutz F, Mayer H (2007) Modelling radiation fluxes in simple and complex environments-application of the RayMan model. International Journal of Biometeorology 51: 323-334. doi: 10.1007/s00484-006-0061-8

McCullough EA, Jones BW, Huck J (1985) A comprehensive data base for estimating clothing insulation. ASHRAE Transactions 91: 29-47

McCullough EA, Jones BW, Tamura T (1989) A data base for determining the evaporative resistance of clothing. ASHRAE Transactions 94: 316-328

Miyazaki Y, Saito M, Seshimo Y (1995) A study of evaluation of non-uniform environments by human body model. Journal of Human and Living Environment 2: 92-100

Mosteller RD (1987) Simplified calculation of body surface area. New England Journal of Medicine 317: 1098-1098

Oguro M, Arens E, Zhang H, Tsuzuki K, Katayama T (2001) Measurement of Projected Area Factors for Thermal Radiation Analysis on Each Part of the Human Body. Center for the Built Environment, University of California, Berkeley

Shuter B, Aslani A (2000) Body surface area: Du Bois and Du Bois revisited. European Journal of Applied Physiology 82: 250-254. doi: 10.1007/s004210050679

Steinman M, Kalisperis LM, Summers LH (1988) Angle factor determination from a person to inclined surfaces. ASHRAE Transactions 94: 1809-1823

Tanabe S, Narita C, Ozeki Y, Konishi M (2000) Effective radiation area of human body calculated by a numerical simulation. Energy and Buildings 32: 205-215. doi: 10.1016/S0378-7788(00)00045-1

Tikuisis P, Meunier P, Jubenville CE (2001) Human body surface area: measurement and prediction using three dimensional body scans. European Journal of Applied Physiology 85: 264-271. doi: 10.1007/s004210100484

Underwood CR, Ward EJ (1966) The solar radiation area of man. Ergonomics 9: 155-168. doi**:** 10.1080/00140136608964361

Yu CY, Lo YH, Chiou WK (2003) The 3D scanner for measuring body surface area: a simplified calculation in the Chinese adult. Applied Ergonomics 34: 273-278. doi: 10.1016/S0003-6870(03)00007-3

Chapter 2. Human Body Area Factors for Radiation Exchange Analysis II: Walking Posture

Abstract

Human body area factors, effective radiation area factors (f_{eff}) and projected area factors (f_p), for walking posture were studied using a sample of contemporary normal-weight Canadian Caucasian adults (male, n=31; female, n=40). Three-dimensional (3D) computer walking body models at four stride positions were created with measured angle values of walking people's upper body, arms and legs.

The directionless (mean of all walking directions) f_p differences among the stride positions and the directional f_p differences between normal-weight male (NW_M) and normal-weight female (NW_F) models were small, only up to 0.026. Therefore, directionless walking posture f_p differences between genders and positions in a stride were minor. However, the differences of mean directional f_p values of the positions dependent on azimuth angles from both models were large enough (up to 0.072) to create important differences in modeled radiation receipt.

f_{eff} in the NW_M model varies from 0.821 to 0.848 depending on the stride position (mean: 0.836) and for NW_F from 0.835 to 0.868 (mean: 0.856). The representative f_{eff} for walking posture was 0.846. When both standing and walking postures are considered, the mean f_{eff} value of standing (0.826) and walking (0.846), 0.836, could be used. However, f_p values should be selected carefully because differences between directional and directionless f_p values were large enough that they could influence the estimated level of human thermal sensation.

2.1 Introduction

Currently available body models consider only sitting and standing postures. In outdoor areas and many indoor situations, walking is another common posture. Physiological equivalent temperature (PET, Höppe 1993 and 1999) and universal thermal climate index (UTCI, http://www.utci.org) are based on an adult's walking posture. However, only one study, Ward and Underwood (1967), modeled one position of a walking stride among three male subjects using a photographic method, but measured angle variation was too limited, and the results seem unrealistically high. Also, they did not define the effective radiation area factor (f_{eff}). Roller and Goldman (1968) measured a projected area factor ($f_p^* = A_p/A_D$, comparable with $f_p = A_p/A_{eff}$ where A_p, A_{eff} and A_D are projected, effective radiation and total body surface areas) of 0.24 at only one solar altitude, 60°, which was 0.02 greater than standing posture. Steadman (1979 and 1984) assumed 0.85 as a walking subject's f_{eff} for the bare parts of the body and presented a formula for estimating f_p as a function of altitude angle adding 0.02 to Fanger's (1972) standing posture mean f_p values. de Freitas et al. (1985) modeled moving people (runners), but they estimated runners' f_{eff} as 0.82 from Fanger's (1972) f_p values and f_p^* values from Taylor's (1956) formula. Their estimate of f_{eff} has not been tested, and Taylor's formula is not for a moving body posture but for a cylindrical standing posture (Pugh and Chrenko 1966).

This chapter presents the relevant body area factors for walking posture of contemporary Caucasian adults in Canada for use in modeling human radiation exchange. This is the first detailed investigation of walking posture to include the complete stride cycle. The results will be compared with standing posture from Chapter 1.

2.2 Methods

Videos of 31 normal-weight, walking males and 40 females wearing swim suits were taken one each from the front and side with Sony DCR-TRV22 and Canon ZR45 video cameras (Fig. 2.1a) and processed following the procedures outlined in Chapter 1 for standing posture.

Four images within a complete walking stride, the 1/4, 2/4, 3/4 and 4/4 positions, were extracted from the videos using Adobe Premiere Pro 1.5. Angles among upper body, arms and legs were measured in AutoCad 2002. The mean angles were used to construct walking body models in Poser 7 (Fig. 2.1b). The

1/4 starting position of a stride had the right arm and left leg located in front of the torso. The opposite walking positions (e.g., 1/4 position with the left arm and right leg in front) were assumed to have the same A_p and f_p values at the opposite azimuth angles. Angles of 2/4 and 4/4_Front used mean values of 1/4 and 3/4_Front because their positions were transitional between the latter two (Table 2.1).

Underwood and Ward's (1966) and Fanger's (1972) photographic methods were combined with 3D computer simulation modeling to compute the body area factors. The 3D models were rotated within 0°≤ azimuth angle (α) ≤180° and -90°≤ altitude angle (β) ≤90° in 10° increments and the 324 images exported to Photoshop to determine A_p and f_p values (Fig. 2.2). These values are the same for any two opposite directions (e.g., f_p when α=40° and β=30° is equal to f_p when α=220° and β=-30°) so that the total f_p value from the whole sphere will be equal to twice the total f_p value from half a sphere for asymmetrical walking posture (Fig. 2.2). Also, for direct beam solar radiation analysis, f_p values from a quarter sphere of lower altitude angles (0°≤ α ≤180° and -90°≤ β ≤0°) were f_p values of the oppositely located quarter sphere of upper altitude angles (180°≤ α ≤360° and 0°≤ β ≤90°) because direct beam solar radiation comes only from the upper half sphere (the sky hemisphere).

Fig. 2.1 Walking posture analysis procedure: (a) recording videos, (b) walking postures at 1/4, 2/4, 3/4 and 4/4 positions of a stride from 3D normal-weight male and female models

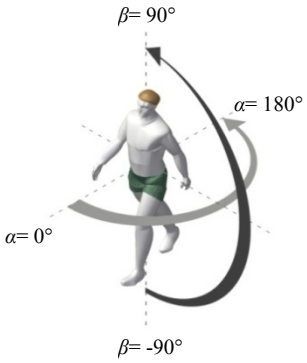

Fig. 2.2 Half a sphere [azimuth angle (0°≤α≤180°) and altitude angle (-90°≤β≤90°)] for determining projected area factors (f_p) of walking posture. The body shape is asymmetrical in this posture (created in Vectorworks 2008)

f_{eff} values for each of the four stride positions of the male and female models were analyzed through Eqs. 2.1–2.3.

$$A_{eff} = \frac{1}{\pi}\int_{A_2}\frac{A_P}{r^2}cos\,\beta_2 dA_2 = \frac{1}{\pi}\sum_{i=1}^{n}\frac{A_{Pi}}{r^2}cos\beta_2 dA_2 \tag{2.1}$$

where A_{eff} is the effective radiation area. A_p is the projected area. r is the distance between a human body and a surrounding sphere. $cos\beta_2$ is the incident angle between a human body and a small surface of a surrounding sphere dA_2. n is the number of equal areas of dA_2 comprising the entire spherical surface area.

Because A_p data were measured only from half a spherical surface area (α: 0–180°, β: -90–90°) for walking posture, A_{eff} can be calculated with,

$$A_{eff} = 2 \times \frac{1}{\pi}\sum_{i=1}^{n_{1/2}}\frac{A_{Pi}}{r^2}cos\beta_2 dA_2 \tag{2.2}$$

where A_p data were collected at every 10° of α and β in half a spherical surface. $n_{1/2}$ is 18×18=324. The half sphere should be divided by equal angles of α (5, 15, 25···155, 165, 175°) and β (-85, -75, -65···65, 75, 85°).

The f_{eff} values were found using:

$$f_{eff} = \frac{A_{eff}}{A_D} \tag{2.3}$$

where A_D is total body surface area.

2.3 Results

The mean of the walking stride duration of the NW_M and NW_F models was 0.6 seconds, NW_M: 0.62 [standard deviation (S.D.) = 0.07] and NW_F: 0.57 (S.D. = 0.05) seconds. Detailed angle information of four positions of a stride is shown in Table 2.1.

Table 2.1 Angles of body parts dependent on positions of a stride. Angles start from a vertical line through the center of the body from top to bottom. Plus angles indicate the body part points to the right in the image. Minus angles indicate the body part points to the left in the image

Model	Position	Image	Angle (°)								
			neck -hip	left shoulder -elbow	left elbow-waist	right shoulder -elbow	right elbow-waist	left hip-knee	left knee-ankle	right hip-knee	right knee-ankle
NW_M	1/4_Side		3	14	-2	-6	-42	-26	-16	16	26
	2/4_Side			9	-6	3	-31	-21	-1	7	46
	3/4_Side			-2	-21	4	-18	-8	6	-16	46
	4/4_Side			-11	-41	8	-9	7	13	-26	1
	1/4_Front			12	7	-10	-6				
	3/4_Front			10	6	-10	-6				
NW_F	1/4_Side		14	12	0	-10	-45	-27	-16	15	28
	2/4_Side			8	0	-7	-40	-24	-6	10	42
	3/4_Side			0	-14	-2	-18	-8	5	-17	48
	4/4_Side			-9	-33	6	-6	7	12	-29	4
	1/4_Front			8	5	-9	-9				
	3/4_Front			8	9	-8	-10				

2.3.1 Projected area factor

The NW_M and NW_F models had very similar f_p values (Fig. 2.3). The maximum difference between them was only 0.025 at the 2/4 position when α=195° and β=25°. The difference was close to the maximum difference between the genders for standing posture, 0.017. NW_M had slightly higher f_p values than NW_F's when α was around 180° (back of the body). The opposite results happened when α was close to 0° (front of the body). This seems to be created by female's breasts and males' wider arm angles from the torso (Table 2.1). This phenomenon is very similar in standing posture.

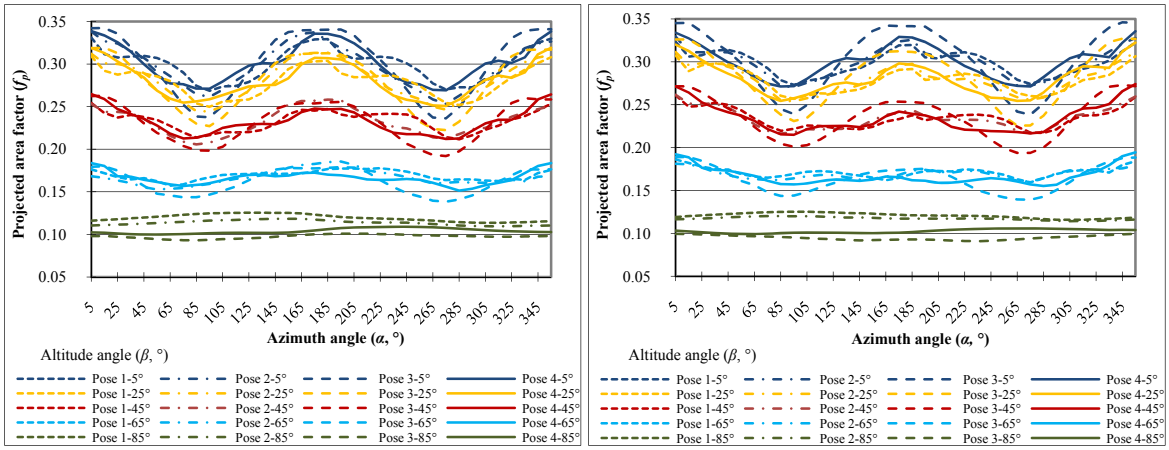

Fig. 2.3 Projected area factors of walking posture: (a) the normal-weight male model, (b) the normal-weight female model. (Pose 1, 2, 3 & 4: 1/4, 2/4, 3/4 & 4/4 positions in a walking stride)

Directionless f_p values can be used for simple modeling when walking direction cannot be defined or is not important. Table 2.2 shows the directionless f_p values from positions of a stride of both male and female models dependent on altitude angles (β). Both male and female models had very small differences between stride positions, up to 0.007, until β=65°. The greatest difference between the positions, 0.026, occurred at β=85° for NW_F. At β=85° (the overhead view where f_p is small), variation in the horizontal projection of the legs and arms has the greatest relative effect. However, the differences of mean directionless f_p values between the two gender models were only up to 0.002. It can be concluded here that directionless f_p values for walking posture are independent of gender and positions in a walking stride at most β angles.

For specific purposes where the walking direction is known, exact directional f_p values averaged from all stride positions dependent on β angles can be found or calculated with the formulas in Fig. 2.4. The formulas can estimate directional f_p values with a difference of less than 0.002 with measured f_p values. The maximum f_p difference among α angles was 0.072 between α=5° (=185°) and α=95° (=275°) when β=5°, and the differences decreased with increasing β angles.

The previous studies for walking posture, Ward and Underwood (1967) and Steadman (1979 and 1984), were compared with this study after converting f_p (= A_p/A_{eff}) to f_p^* (= $A_p/A_D = f_p \times f_{eff}$) because Ward and Underwood (1967) used total body surface area (A_D) to find projected area factors f_p^* for direct beam solar radiation analysis and did not define f_{eff}. Usually, f_p is used to estimate mean radiant temperature (T_{mrt}) in predicted mean vote (PMV, Fanger 1972) and physiological equivalent temperature (PET, Höppe 1993 and 1999). f_p^* is employed to calculate the quantity of absorbed direct beam solar radiation on a unit area of the total body surface (units: Wm^{-2}). The purpose of the use of f_p and f_p^* is the same, to input the effect of direct beam solar radiation or other point source radiation into human thermal exchange models. Either one of these values can be used depending on the purpose. For easy comparison, directionless f_p^* values of standing posture from Chapter 1 are also included. Steadman's (1984) f_p formula (=0.380–0.0032β, 0.106≤ f_p ≤0.318, 25°≤ β ≤85°) for walking posture slightly overestimated current study values by up to 0.017, which was expected because he used Fanger's (1972) standing posture mean f_p values (Fig. 2.5). However, Ward and Underwood's (1967) values compared to ours were up to 0.207 higher for walking posture. The differences are substantial for direct beam solar radiation analysis because a 0.02 f_p^* difference creates a 14 Wm^{-2} difference in absorbed direct beam solar radiation on the human body surface for standing posture (see Table 1.10 in Chapter 1).

Table 2.2 Directionless projected area factors (f_p) of normal-weight male (NW_M) and female (NW_F) models

Category	Position of a stride	Altitude angle (β, °)								
		5	15	25	35	45	55	65	75	85
NW_M	1/4	0.300	0.293	0.280	0.259	0.233	0.202	0.169	0.141	0.119
	2/4	0.298	0.296	0.282	0.260	0.233	0.201	0.167	0.135	0.114
	3/4	0.300	0.293	0.279	0.258	0.231	0.199	0.162	0.126	0.098
	4/4	0.302	0.295	0.281	0.260	0.233	0.201	0.166	0.133	0.104
	Mean	0.300	0.294	0.281	0.259	0.233	0.201	0.166	0.134	0.109
NW_F	1/4	0.298	0.292	0.279	0.260	0.234	0.204	0.171	0.142	0.121
	2/4	0.299	0.293	0.280	0.260	0.234	0.203	0.169	0.139	0.117
	3/4	0.302	0.296	0.282	0.261	0.234	0.201	0.164	0.125	0.095
	4/4	0.301	0.294	0.281	0.261	0.234	0.203	0.167	0.132	0.103
	Mean	0.300	0.294	0.281	0.261	0.234	0.203	0.168	0.135	0.109
	Mean	**0.300**	**0.294**	**0.280**	**0.260**	**0.233**	**0.202**	**0.167**	**0.134**	**0.109**

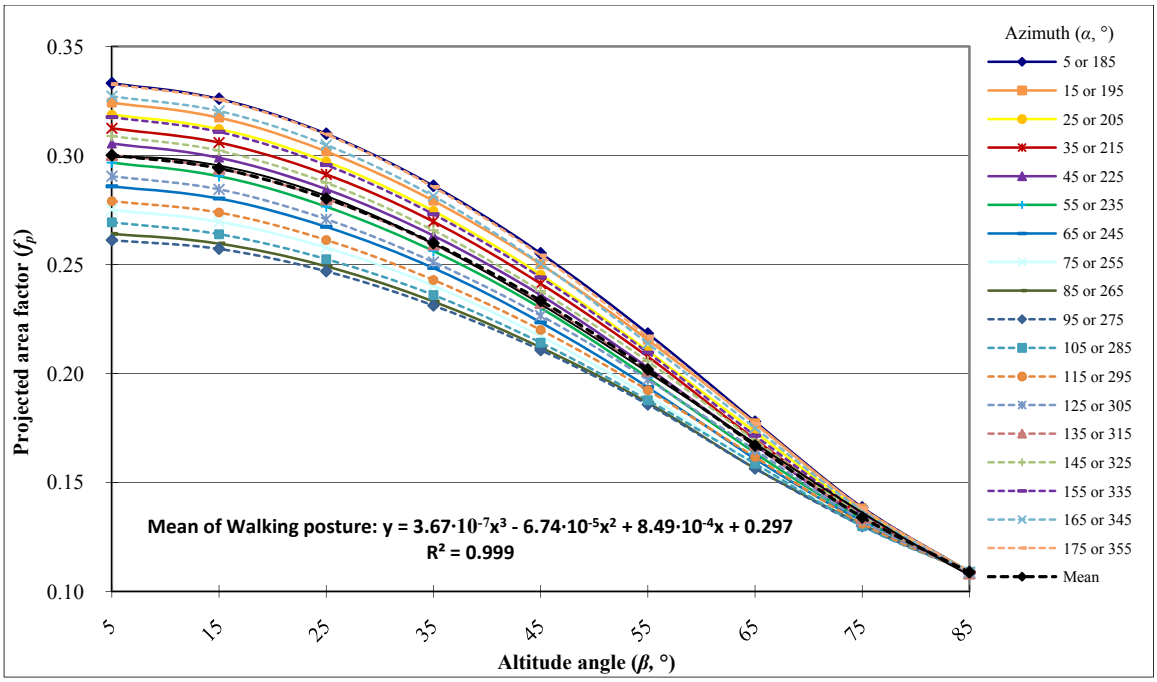

5 or 185°: $y = 4.21\cdot10^{-7}x^3 - 7.79\cdot10^{-5}x^2 + 9.73\cdot10^{-4}x + 0.329$	15 or 195°: $y = 3.68\cdot10^{-7}x^3 - 7.04\cdot10^{-5}x^2 + 8.20\cdot10^{-4}x + 0.321$
25 or 205°: $y = 4.04\cdot10^{-7}x^3 - 7.40\cdot10^{-5}x^2 + 9.31\cdot10^{-4}x + 0.315$	35 or 215°: $y = 4.08\cdot10^{-7}x^3 - 7.40\cdot10^{-5}x^2 + 9.77\cdot10^{-4}x + 0.308$
45 or 225°: $y = 4.01\cdot10^{-7}x^3 - 7.16\cdot10^{-5}x^2 + 9.11\cdot10^{-4}x + 0.301$	55 or 235°: $y = 3.93\cdot10^{-7}x^3 - 6.95\cdot10^{-5}x^2 + 8.90\cdot10^{-4}x + 0.293$
65 or 245°: $y = 3.68\cdot10^{-7}x^3 - 6.56\cdot10^{-5}x^2 + 8.65\cdot10^{-4}x + 0.282$	75 or 255°: $y = 3.31\cdot10^{-7}x^3 - 6.01\cdot10^{-5}x^2 + 7.90\cdot10^{-4}x + 0.272$
85 or 265°: $y = 2.99\cdot10^{-7}x^3 - 5.59\cdot10^{-5}x^2 + 7.99\cdot10^{-4}x + 0.260$	95 or 275°: $y = 2.89\cdot10^{-7}x^3 - 5.48\cdot10^{-5}x^2 + 8.06\cdot10^{-4}x + 0.258$
105 or 285°: $y = 2.90\cdot10^{-7}x^3 - 5.46\cdot10^{-5}x^2 + 6.78\cdot10^{-4}x + 0.266$	115 or 295°: $y = 3.05\cdot10^{-7}x^3 - 5.73\cdot10^{-5}x^2 + 6.81\cdot10^{-4}x + 0.276$
125 or 305°: $y = 3.17\cdot10^{-7}x^3 - 5.95\cdot10^{-5}x^2 + 6.44\cdot10^{-4}x + 0.288$	135 or 315°: $y = 3.52\cdot10^{-7}x^3 - 6.51\cdot10^{-5}x^2 + 7.50\cdot10^{-4}x + 0.297$
145 or 325°: $y = 3.72\cdot10^{-7}x^3 - 6.83\cdot10^{-5}x^2 + 7.83\cdot10^{-4}x + 0.306$	155 or 335°: $y = 4.07\cdot10^{-7}x^3 - 7.40\cdot10^{-5}x^2 + 9.21\cdot10^{-4}x + 0.314$
165 or 345°: $y = 4.40\cdot10^{-7}x^3 - 7.95\cdot10^{-5}x^2 + 1.04\cdot10^{-3}x + 0.323$	175 or 355°: $y = 4.40\cdot10^{-7}x^3 - 8.00\cdot10^{-5}x^2 + 1.02\cdot10^{-3}x + 0.328$

Fig. 2.4 Directional projected area factors (f_p) of walking posture dependent on both azimuth (α) and altitude (β) angles

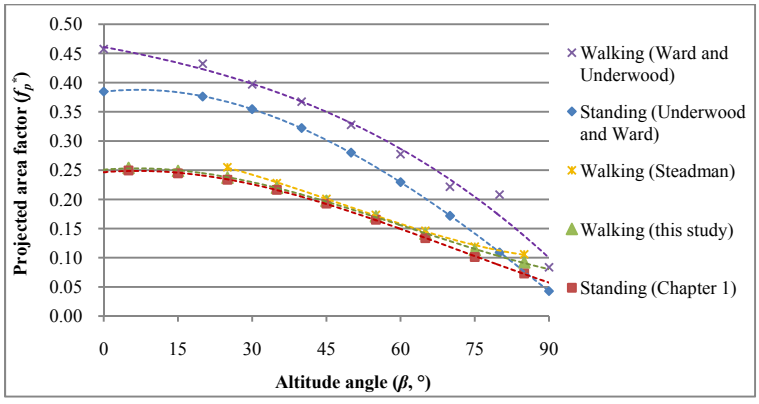

Fig. 2.5 Comparison of the mean directionless projected area factors (f_p^*) of normal-weight male and female models with those of previous studies

2.3.2 Effective radiation area factor (f_{eff})

In the NW_M model, there was a 0.027 difference in f_{eff} between the four positions of a walking stride (Table 2.3). The greatest f_{eff} value was 0.848 at the 1/4 position where the arms were spread farthest from the torso and legs were farthest apart (Table 2.1). The lowest was 0.821 at the 3/4 position when the legs were close together and arms were near the torso. The NW_F model had more variation, 0.033. The greatest f_{eff} was 0.868 at the 1/4 position, and the lowest was 0.835 at the 3/4 position. The representative f_{eff} of walking posture was 0.846 which was about 0.02 higher than f_{eff} of standing posture, 0.826, (see Chapter 1). These walking posture values (Table 2.3) are close to the 0.85 and 0.82 assumed by Steadman (1979) for walking subjects and de Freitas et al. (1985) for runners, respectively.

The greatest f_{eff} which occurred at the 1/4 position of the stride was only 0.018 higher than the f_{eff} of standing posture in NW_M, but for NW_F it was 0.044 higher. Moreover, the NW_F had higher f_{eff} values in all stride positions than for standing posture, but f_{eff} of the 3/4 position in NW_M was 0.009 lower than for standing posture. In standing posture, NW_M had a much wider stance between the legs than NW_F (Fig. 2.6a). Even though the 3/4 position in NW_M has more body movement, the legs are located closer than the wide open stance in standing posture (Fig. 2.6).

Table 2.3 Effective radiation area factors (f_{eff}) of walking posture of normal-weight male (NW_M) and female (NW_F) models

BMI Category	Position of a stride	A_{eff} (m^2)	f_{eff}
NW_M	1/4	1.654	0.848
	2/4	1.632	0.837
	3/4	1.602	0.821
	4/4	1.632	0.837
	Mean	1.630	0.836
NW_F	1/4	1.432	0.868
	2/4	1.425	0.864
	3/4	1.379	0.835
	4/4	1.416	0.858
	Mean	1.414	0.856
Mean		1.521	**0.846**

Fig. 2.6 3D normal-weight male (left) and normal-weight female (right) computer models for (a) standing posture from Chapter 1 and (b) 3/4 position of walking posture

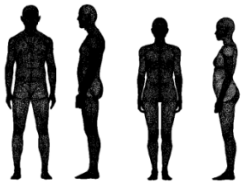

(a)

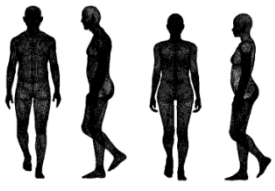

(b)

2.4 Discussion

The mean f_p values of the 1/4 through 4/4 stride positions for walking posture are compared with those for standing posture (Fig. 2.7). The f_p values of walking posture have less variation between front/back (α=0° and 180°) and side (α=90°) α angles with increasing β angles than those of standing posture. Also, the actual directional f_p differences between α angles of walking posture were lower, maximum difference 0.072, than those of standing posture, maximum difference 0.128 (Fig. 2.8). More open walking body posture reduced the f_p differences dependent on α angles. These directional f_p differences would create absorbed direct beam solar radiation differences up to 16 Wm^{-2} in walking posture and up to 29 Wm^{-2} in standing posture in both low and moderate solar altitude angle simulations (β=25°, K_b^+=350 Wm^{-2} and β=55°, K_b^+=700 Wm^{-2}), where K_b^+ is incident direct beam solar radiation on the human body surface and 0.7 (70 %) is assumed as the absorptivity of the human body surface for solar radiation.

If walking direction is not important or unknown and percentages of standing and walking people are unknown (e.g., square, plaza or open field), directionless f_p values for direct beam solar radiation analysis can be estimated from a formula for combined standing and walking postures (Fig. 2.9). If walking direction is known (e.g., corridors in subway stations and buildings, along sidewalks or park trails), directional f_p values for walking posture can be found in Fig. 2.4.

f_{eff} values for both standing and walking postures are listed in Table 2.4. However, the f_{eff} difference from averaged standing and walking postures (0.836) to standing posture (0.826) and walking posture (0.846) was only 0.01 which is not significant in radiation analysis. Therefore, the mean f_{eff} value, 0.836, can usually be used in most applications.

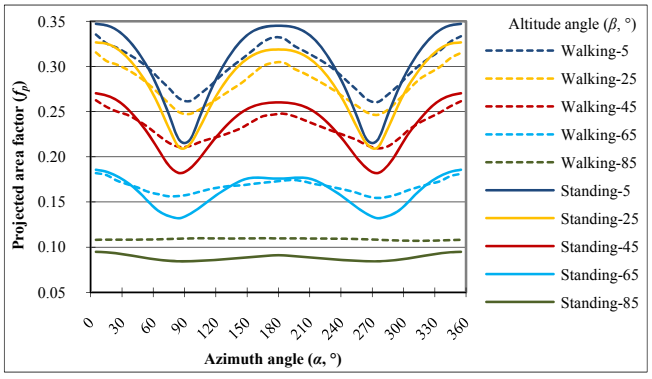

Fig. 2.7 Comparison of directional projected area factors (f_p) of standing and walking postures for a selection of altitude angles (β) between 5° and 85°

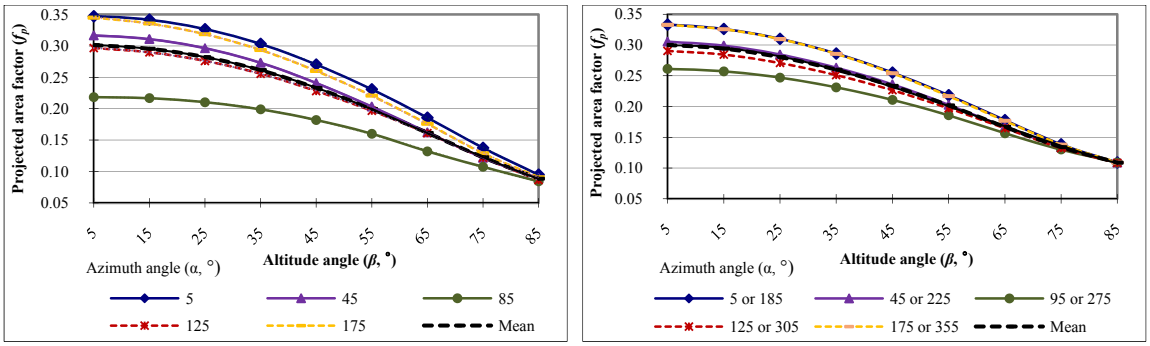

(a) (b)

Fig. 2.8 Directional projected area factors (f_p) dependent on altitude angles (β) for (a) standing posture and (b) walking posture

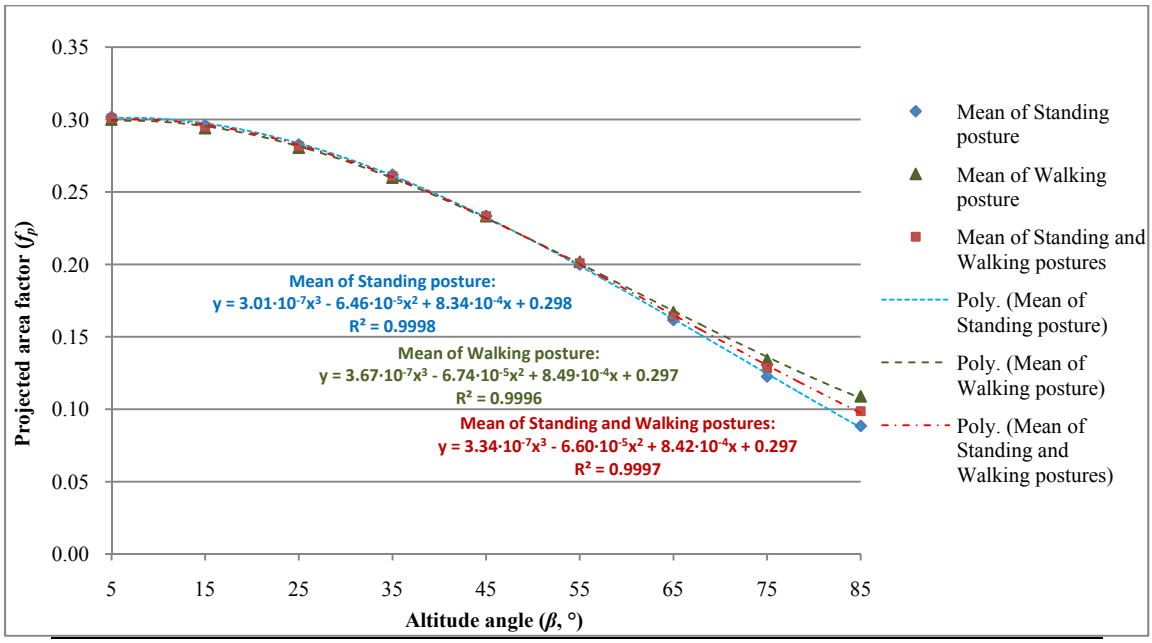

Posture	Altitude angle (β, °)								
	5	15	25	35	45	55	65	75	85
Standing	0.302	0.296	0.283	0.262	0.233	0.200	0.162	0.123	0.088
Walking	0.300	0.294	0.281	0.260	0.233	0.202	0.167	0.134	0.109
Standing and Walking	0.301	0.295	0.282	0.261	0.233	0.201	0.164	0.128	0.099

Fig. 2.9 Directionless projected area factors (f_p) of standing and walking postures and best-fit polynomial equations

Posture	A_{eff} (m²)	f_{eff}
Standing	1.489	0.826
Walking	1.521	0.846
Standing and Walking	1.505	0.836

Table 2.4 Effective body surface areas (A_{eff}) and effective radiation area factors (f_{eff}) of standing and walking postures of normal-weight models

Directionless f_p values for walking posture from half a sphere ($0 \leq \alpha \leq 360$, $0 \leq \beta \leq 90$) and a quarter sphere ($0 \leq \alpha \leq 180$, $0 \leq \beta \leq 90$) are compared in Table 2.5. Theoretically, standing posture is symmetrical, so f_p values from a quarter sphere would be analyzed to find total f_p values from an entire sphere. Walking posture is asymmetrical, so f_p values from half a sphere should be analyzed. However, the differences in walking posture directionless f_p values between the two ways were negligible, only up to 0.001. Therefore, analysis for directionless f_p values within a quarter sphere ($0 \leq \alpha \leq 180$, $0 \leq \beta \leq 90$) can be adequate to find the total f_p values from an entire sphere even though the walking body postures are not symmetrical.

Table 2.5 Comparison of directionless projected area factors (f_p) from half a sphere and a quarter sphere (walking posture)

Sphere	Angle range (°)	Altitude angle (β, °)								
		5	15	25	35	45	55	65	75	85
Half (1/2)	$0 \leq \alpha \leq 360$ $0 \leq \beta \leq 90$	0.300	0.294	0.280	0.260	0.233	0.202	0.167	0.134	0.109
Quarter (1/4)	$0 \leq \alpha \leq 180$ $0 \leq \beta \leq 90$	0.301	0.294	0.280	0.260	0.233	0.202	0.167	0.134	0.109
	difference	0.001	0.000	0.000	0.000	0.000	0.000	0.000	0.000	0.000

2.5 Conclusions

One common body posture in outdoor/indoor areas, walking, was studied with normal-weight male (NW_M) and female (NW_F) three-dimensional (3D) computer body models created with contemporary Canadian Caucasian adult body data. Four positions of a stride were extracted from video files.

Directionless f_p values for walking posture had minor differences between genders and positions in a stride. The directional f_p differences between NW_M and NW_F models were also small, up to 0.025. However, directional f_p values had larger differences between α angles. The maximum difference, 0.072, was between the front and side of the body. Large differences occurred at low β angles that are closest to perpendicular to the vertical body surface, and differences decrease with increasing β angles.

The representative combined male and female f_{eff} value for walking posture was 0.846. f_{eff} values between standing (0.826) and walking (0.846) postures were not too different. The mean f_{eff} (0.836) could be applied in most general modeling studies where applications to a variety of people both standing and walking are of interest. Standing posture has been used in many applications where walking posture is more appropriate. The small difference in f_{eff} suggests this has not caused any major errors or invalid conclusions. However, f_p values should be selected carefully because differences between directional and directionless f_p values were large at some α angles.

The new body area factors, f_{eff} and f_p, for standing and walking postures were analyzed in Chapter 1 & 2. The results can be used in a variety of human thermal exchange studies and expand their applicability to a wide range of activities. These new results will be compared with diverse body area factors used in the radiation components of existing human thermal exchange models in Chapter 3.

References

de Freitas CR, Dawson NJ, Young AA, Mackey WJ (1985) Microclimate and heat stress of runners in mass participation events. Journal of Climate and Applied Meteorology 24: 184-191. doi: 10.1175/1520-0450(1985)024<0184:MAHSOR>2.0.CO;2

Fanger PO (1972) Thermal Comfort: Analysis and Applications in Environmental Engineering. McGraw-Hill, New York

Höppe PR (1993) Heat balance modeling. Experientia 49: 741-746. doi: 10.1007/BF01923542

Höppe PR (1999) The physiological equivalent temperature – a universal index for the biometeorological assessment of the thermal environment. International Journal of Biometeorology 43: 71-75. doi: 10.1007/s004840050118

Pugh LGCE, Chrenko FA (1966) The effective area of the human body with respect to direct solar radiation. Ergonomics 9: 63-67 doi: 10.1080/00140136608964343

Roller WL, Goldman RF (1968) Prediction of solar heat load on man. Journal of Applied Physiology 24: 717-721

Steadman RG (1979) The assessment of sultriness. Part II: Effects of wind, extra radiation and barometric pressure on apparent temperature. Journal of Applied Meteorology 18: 874-885. doi: 10.1175/1520-0450 (1979)018<0874:TAOSPI>2.0.CO;2

Steadman RG (1984) A universal scale of apparent temperature. Journal of Climate and Applied Meteorology 23: 1674-1687

Taylor PF (1956) Middle East Trials: Meteorological Observations (July-August, 1955). Rep. No. 67, Clothing and Stores Experimental Establishment, Directorate of Physiological and Biological Research, Minister of Supply, U.K.

Underwood CR, Ward EJ (1966) The solar radiation area of man. Ergonomics 9: 155-168. doi**:** 10.1080/00140136608964361

Ward EJ, Underwood CR (1967) Effect of posture on the solar radiation area of man. Ergonomics 10: 399-409. doi**:**10.1080/00140136708930887

Chapter 3. Comparison of Human Radiation Exchange Models in Outdoor Areas

Abstract

Results from the radiation components of seven different human thermal exchange models/methods are compared. These include the Burt, COMFA, MENEX, OUT_SET* and RayMan models, the six-directional method and the new Park and Tuller model employing projected area factors (f_p) and effective radiation area factors (f_{eff}) determined from a sample of normal- and over-weight Canadian Caucasian adults. Input data include solar and longwave radiation measured during a clear summer day in southern Ontario.

Variations between models came from differences in f_p and f_{eff} and different estimates of longwave radiation from the open sky. The ranges between models for absorbed solar, net longwave and net all-wave radiation were 164, 31 and 187 Wm^{-2}, respectively. Most differences between models came from absorbed solar radiation because of differences in f_p^* ($=f_p \times f_{eff}$) and f_{eff} or some variations in components included in the radiation equations.

The 6 directional method of absorbed solar and net longwave radiation should both be multiplied by f_{eff}. The MENEX model needs f_{eff} added to its net longwave radiation equation for the proper results of net longwave radiation, requires more precise values of f_p^* for absorbed direct beam solar radiation and needs to multiply absorbed diffuse and reflected solar radiation by f_{eff} and 1/2. The Burt model also needs more accurate f_p^*. The OUT_SET* model should use only 1/2 of the horizontal surface diffuse and reflected solar radiation to account for the view factor of the vertical body surface. It also needs better values of f_p^*. The RayMan model uses Fanger's f_p^* and f_{eff} values. The f_{eff} value is almost 0.11 lower than that of the Park and Tuller model. This difference changes the net all-wave radiation estimate up to 29 Wm^{-2}, which can be significant in human thermal exchange analysis. Therefore, proper f_p and f_{eff} values should be used for accurate estimation of radiation on the human body surface.

3.1 Introduction

Urban outdoor environments have a very important and different climatic variable, solar radiation, compared with indoor environments. Insolation effectively raises the apparent temperature nearly 14 °C under calm conditions and 7 °C in a strong wind (Steadman 1971). Each increase of direct beam solar radiation of around 200 Wm^{-2} increases predicted mean vote (PMV, Fanger 1972) by one sensation scale unit (Hodder and Parsons 2007).

A number of human thermal exchange models have been developed which include all important modes of energy exchange. Some of those capable of use in outdoor urban environments are the Burt model (Burt 1979, modified by Tuller 1990), COMFA (COMfort FormulA; Brown and Gillespie 1986, 1995), MENEX (Man-ENvironment heat Exchange; Blazejczyk 1994, 2004, 2005), RayMan (Matzarakis et al. 2000, 2007, 2010) and OUT-SET* (Pickup and de Dear 2000). The Sultriness model (Steadman 1979, 1984), CS (Cold Stress) and HS (Heat Stress) models (Auliciems and Kalma 1979) and STEBIDEX (Skin Temperature Energy Balance Index) and HEBIDEX (Heat Budget Index) models (de Freitas 1985) were excluded in this study. The Sultriness model uses the same standing posture mean projected area factors (f_p) from Fanger (1972) as does RayMan. The solar radiation estimation method of the CS and HS models from Breckenridge and Goldman (1972) was compared previously by Blazejczyk et al. (1993). The STEBIDEX and HEBIDEX models' body posture is sitting on the sand, which is different from the standing and walking postures that are the focus of this thesis.

Early versions of different methods for estimating solar radiation absorbed on the human body surface were reviewed by Blazejczyk et al. (1993) using Krys and Brown's (1990) cylindrical body type equation which is a solar radiation component of the COMFA model.

Four different approaches have been used to analyse the effects of human body shape on human solar and longwave radiation exchange. The first is experimental results from a photographic method such as used in the PMV and RayMan models. The second is experimental results from a standing person's shadow patterns on the ground surface used in the Burt model or a mannequin as an analogue of the human body used in the MENEX model. The third assumes the human body is a cylinder used in the COMFA (Kenny et al. 2008) and OUT_SET* (Spagnolo and de Dear 2003) models. The COMFA model uses a

directionless cylinder, and the OUT_SET* model uses Underwood and Ward's (1966) elliptical cylinder (major axis facing the sun). The last is a cube combined with six-direction measured radiation data (upward, downward, east, west, south and north) (VDI 1998, Huang et al. 2005, Ali-Toudert et al. 2005, Matzarakis et al. 2007, Oliveira and Andrade 2007, Thorsson et al. 2007). Huang et al. (2005) used weighting factors of 0.238 for each of the four cardinal directions and 0.024 for up- and downward. Other researchers adopted the weighting factors from VDI (1998): 0.22 for each cardinal direction and 0.06 for up- and downward based on the directionless mean projected area factors of Fanger (1972).

The four different concepts of the human body shape can create large differences among models in the body area factors used in radiation analysis. The important body area factors are the effective radiation area factor (f_{eff}) and projected area factor (f_p). Body shape and posture control the area exposed to direct beam solar radiation (projected area, A_p) and the total body surface area exposed to the surrounding radiant environment rather than to other body parts (effective radiation area, A_{eff}). f_p (= A_p / A_{eff}) and f_p^* (= A_p / A_D = $f_p \times f_{eff}$, where A_D is the total body surface area) are used in the calculation of direct beam solar radiation. f_p is used in a formula for calculating the mean radiant temperature (T_{mrt}) in PMV and RayMan, and f_p^* is used in the Burt, COMFA, MENEX and OUT_SET* models. f_{eff} (= A_{eff} / A_D) is employed to estimate all solar and longwave exchanges.

In this chapter, results from the radiation components of five existing human thermal exchange models (Burt, COMFA, MENEX, OUT_SET* and RayMan models) along with the six-directional method (VDI 1998) and a new human radiation exchange model, Park and Tuller model, are compared. The latter model employs mean body area factors (f_{eff} and f_p) of standing and walking postures determined from a sample of 139 normal- and over-weight Caucasian adults (see Chapter 1 and 2). Emphasis is on the effect of differences in human body area factors.

3.2 Materials and Methods

3.2.1 Radiation models

Net all-wave radiation on the human body surface (Q) is the sum of absorbed total solar (shortwave) radiation (R^*) and net longwave (terrestrial) radiation (L) on the surface:

$$Q = R^* + L \quad (\mathrm{Wm^{-2}}) \tag{3.1}$$

3.2.1.1 Absorbed solar radiation

The units of all radiation streams and used in all models in this study are $\mathrm{Wm^{-2}}$.

3.2.1.1.1 Park and Tuller model

$$R^* = {K_b}^* + {K_d}^* + {K_r}^*$$

$$= \left\{ f_p f_{eff} \frac{K_b}{sin\beta}\, t + \frac{1}{2} f_{eff} \left[K_d \psi_{sky} + (K_b cos Z_{sl} t + K_d \psi_{w\_sky}) \alpha_o + (K_b t + K_d \psi_{sky} + K_{ro}) \alpha_g \right] \right\} (1 - \alpha_b)$$

$$= \left\{ {f_p}^* \frac{K_b}{sin\beta}\, t + \frac{1}{2} f_{eff} \left[K_d \psi_{sky} + K_{ro} + K_{rg} \right] \right\} (1 - \alpha_b) \quad (\mathrm{Wm^{-2}}) \tag{3.2}$$

This equation was created from a basic solar radiation equation of Park (2003) with view factor and angular concepts. K_b, K_d and K_r are direct beam, diffuse beam and reflected solar radiation incident on the horizontal surface. Superscript * indicates the corresponding radiation absorbed on the body surface. K_r is sum of solar radiation reflected by objects in the sky hemisphere (K_{ro}) and by the ground surface (K_{rg}). a_o, a_g and a_b are albedos of objects in the sky hemisphere, the ground surface and the body surface, respectively. ${f_p}^*$ is $f_p \times f_{eff}$. f_p can be calculated with a formula, $f_p = 3.34 \cdot 10^{-7}\beta^3 - 6.60 \cdot 10^{-5}\beta^2 + 8.42 \cdot 10^{-4}\beta + 0.297$, from Fig. 2.9 in Chapter 2 for the mean of directionless standing and walking postures. The formula yields f_p within 0.002 of measured f_p values. t is transmissivity for K_b of objects between the specific object of interest and the sun. β is solar altitude (°). Z_{sl} is the angle between the perpendicular to the object surface and the sun (°). ψ_{sky} is sky view factor. ψ_{w_sky} is the view factor of open sky seen from the object surface. The mean value of f_{eff} for standing and walking postures from the sample of Caucasian male and female adults in Canada, 0.836, was used in this model (see Chapter 2).

3.2.1.1.2 RayMan model

The equation is assumed to be same as the Park and Tuller model's except for values of f_p and f_{eff}. f_p can be calculated with the formula, $f_p = 0.308\cos\left[\beta\left(0.998 - \frac{\beta^2}{50000}\right)\right]$ (Jendritzky et al. 1990), which was derived from Fanger's (1972) directionless f_p values for standing posture. The formula results are within 0.004 of Fanger's (1972) measured data. Fanger's f_{eff} result for standing posture, 0.725, is used in this model (Matzarakis et al. 2010).

3.2.1.1.3 MENEX model

$$R^* = \left[f_p{}^* K_b + (K_d + K_r)(0.0018 + 0.0462 \ln \beta)\right](1 - \alpha_b) \tag{3.3}$$

This model does not use an f_{eff}. $f_p{}^*$ can be calculated from:

$$\text{if } \beta \leq 5°, \qquad f_p{}^* = 1.4e^{(-0.51+0.368\cdot\beta)}$$

$$\text{if } \beta > 5°, \qquad f_p{}^* = \frac{26.34}{\beta} - 0.329 \tag{3.4}$$

3.2.1.1.4 OUT_SET* model

$$R^* = \left\{f_p{}^* \frac{K_b}{sin\beta} + f_{eff}\left[K_d + (K_b + K_d)\alpha_g\right]\right\}(1 - \alpha_b) \tag{3.5}$$

$f_p{}^*$ can be estimated from an equation of Underwood and Ward's (1966) elliptical cylinder model (orientation: major axis facing the sun):

$$f_p{}^* = (0.42cos\beta + 0.043sin\beta) \tag{3.6}$$

f_{eff} is 0.75 (Jendritzky and Nübler 1981). This model does not have the ½ function in estimating the K_d and K_r components. The ½ function accounts for the fact that a unit area of the vertical body surface is exposed to only ½ of the upper and lower hemispheres. Therefore, the unit area receives only ½ of the measured diffuse beam and reflected radiation on/from a horizontal surface.

3.2.1.1.5 Burt model

$$R^* = (K_b{}^+ + K_d{}^+ + K_r{}^+)(1 - \alpha_{cl}) = \left\{f_p{}^* K_b + \frac{1}{2} f_{eff}\left[K_d + (K_b + K_d)\alpha_g\right]\right\}(1 - \alpha_b) \tag{3.7}$$

f_{eff} is 0.725 from Fanger (1972). The f_p^* equation is originally from Terjung and Louie (1971):

$$f_p^* = 4.278 \exp(-0.0512\ \beta) \tag{3.8}$$

3.2.1.1.6 COMFA model

$$R^* = [f_p^* K_b t + \frac{1}{2} f_{eff}\left[K_d \psi_{sky} + (K_b cos Z_{sl} t + K_d \psi_{w\_sky})\alpha_o + (K_b t + K_d \psi_{sky} + K_{ro})\alpha_g\right](1 - \alpha_b) \tag{3.9}$$

This model did not originally use half the quantity of diffuse beam and reflected solar radiation. This was included by Kenny et al. (2008). f_{eff} is 0.78 for medium body build erect (standing) posture from Kerslake (1972) (originally from Guibert and Taylor 1952). f_p^* is estimated from a formula:

$$f_p^* = \frac{1/tan\beta}{\pi} \tag{3.10}$$

3.2.1.2 Net longwave radiation

All models except the COMFA and Park and Tuller models assume an unobstructed upper (sky) hemisphere, which means ψ_{sky} is 1.0 (100 %). Therefore, there is no longwave radiation emitted from vertical obstructions such as buildings and trees (L_o). All models were modified to include this term by incorporating the components of ψ_{sky} and 1– ψ_{sky} in the model comparison.

3.2.1.2.1 Park and Tuller model

$$\begin{aligned} L = {} & \frac{1}{2} f_{eff} \varepsilon_b \left[\varepsilon_{sky} \sigma (T_a + 273)^4 \psi_{sky} + \varepsilon_o \sigma (T_o + 273)^4 \left(1 - \psi_{sky}\right) + \varepsilon_g \sigma (T_g + 273)^4\right] \\ & - f_{eff} \varepsilon_b \sigma (273 + T_b)^4 \\ = {} & \frac{1}{2} f_{eff} \varepsilon_b (L_a + L_o + L_g) - f_{eff} L_b \ \ (\mathrm{Wm^{-2}}) \end{aligned} \tag{3.11}$$

This equation was created from a basic longwave equation of Park (2003). T and ε are temperature (°C) and emissivity, respectively. Subscripts a, o, g and b indicate ambient air, obstruction surface in the sky hemisphere, the ground surface and the human body surface, respectively. σ is the Stefan-Boltzmann constant (5.67×10^{-8} $\mathrm{Wm^{-2}K^{-4}}$). f_{eff} is 0.836.

3.2.1.2.2 MENEX model

$$L = \frac{1}{2}\varepsilon_b\left[\varepsilon_a\sigma(T_a+273)^4\,(0.82-0.25\cdot 10^{-0.094\cdot e_a})\psi_{sky} + \varepsilon_o\sigma(T_o+273)^4\left(1-\psi_{sky}\right)\right.$$
$$\left. + \varepsilon_g\sigma(T_g+273)^4\right] - \varepsilon_b\sigma(273+T_b)^4$$
$$= \frac{1}{2}\varepsilon_b\left[\varepsilon_a\cdot\sigma\cdot(T_a+273)^4\,(0.82-0.25\cdot 10^{-0.094\cdot e_a})\psi_{sky} + L_o + L_g\right] - L_b \quad (3.12)$$

$$e_a = RH \times \exp\left(18.956 - \frac{4030.18}{T_a+235}\right) \quad (3.13)$$

This model adopted the equation of sky emissivity $\left[\varepsilon_{sky} = \varepsilon_a\left(0.82-0.25\cdot 10^{-0.094\cdot e_a}\right)\right]$ from Geiger (1965). e_a, vapour pressure of the air (hPa), is calculated with Antoine's equation (Parsons 1993). *RH* is relative humidity (decimal). This model does not use an f_{eff}. 0.97 is used for ε_a.

3.2.1.2.3 RayMan model

This model uses the same Geiger (1965) sky emissivity equation as the MENEX model (Matzarakis et al. 2010). However, to facilitate the comparison of the effects of Fanger's (1972) f_{eff} value with those used in other models, the longwave radiation formula applied in this paper is assumed to be the same as Park and Tuller's except the value of f_{eff} is 0.725.

3.2.1.2.4 OUT_SET* model

$$L = \frac{1}{2}f_{eff}\varepsilon_b\left\{\sigma[0.7+5.95\times 10^{-5}e_a\exp\left(\frac{1500}{T_a+273}\right)](T_a+273)^4\psi_{sky} + \varepsilon_o\sigma(T_o+273)^4\left(1-\psi_{sky}\right)\right.$$
$$\left. + \varepsilon_g\sigma(T_g+273)^4\right\} - f_{eff}\varepsilon_b\sigma(273+T_b)^4$$
$$= \frac{1}{2}f_{eff}\varepsilon_b\left\{\sigma[0.7+5.95\times 10^{-5}e_a\exp\left(\frac{1500}{T_a+273}\right)](T_a+273)^4\psi_{sky} + L_o + L_g\right\} - f_{eff}L_b \quad (3.14)$$

The equation for calculating sky emissivity $\left[\varepsilon_{sky} = 0.7+5.95\times 10^{-5}e_a\exp\left(\frac{1500}{T_a+273}\right)\right]$ is from Idso (1981). f_{eff} is 0.75.

3.2.1.2.5 Burt model

$$L = \frac{1}{2} f_{eff} \varepsilon_b \left[\varepsilon_a \sigma (T_a + 273)^4 \left(0.55 + 0.065 e_a^{\frac{1}{2}}\right) \psi_{sky} + \varepsilon_o \sigma (T_o + 273)^4 \left(1 - \psi_{sky}\right) + \varepsilon_g \sigma (T_g + 273)^4 \right] - f_{eff} \varepsilon_b \sigma (273 + T_b)^4$$

$$= \frac{1}{2} f_{eff} \varepsilon_b \left[\varepsilon_a \sigma (T_a + 273)^4 \left(0.55 + 0.065 e_a^{\frac{1}{2}}\right) \psi_{sky} + L_o + L_g \right] - f_{eff} L_b \quad (3.15)$$

The equation for calculating sky emissivity $\left[\varepsilon_{sky} = \varepsilon_a \left(0.55 + 0.065 e_a^{\frac{1}{2}}\right)\right]$ is originally from Brunt (1932) and evaluated by Iziomon et al. (2003) converting the units of e_a from millimetres of mercury (mmHg) to hectopascals (hPa). f_{eff} is 0.725. ε_a in this model is 0.99.

3.2.1.2.6 COMFA model

$$L = \frac{1}{2} f_{eff} \varepsilon_b \left\{ (1.2 \varepsilon_a \sigma (T_a + 273)^4 - 171) \psi_{sky} + \varepsilon_o \sigma (T_o + 273)^4 \left(1 - \psi_{sky}\right) + \varepsilon_g \sigma \left(T_g + 273\right)^4 \right\} - f_{eff} \varepsilon_b \sigma (273 + T_b)^4$$

$$= \frac{1}{2} f_{eff} \varepsilon_b \left\{ (1.2 \varepsilon_a \sigma (T_a + 273)^4 - 171) \psi_{sky} + L_o + L_g \right\} - f_{eff} L_b \quad (3.16)$$

The regression equation for estimating longwave radiation from the clear sky as a function of air temperature is from Swinbank (1963). f_{eff} is 0.78. ε_a is 0.98.

3.2.2 Radiation data

To compare the existing radiation models, clear summer data from August 10, 2002 were used: data were collected in the morning (0730–0900 hours), around noon (1130–1300 hours) and in the afternoon (1530–1700 hours). The research site was Winegard Walk at the University of Guelph, Guelph, Ontario, Canada (Fig. 3.1). The latitude and longitude of the site are 43º 32´ N, 80º 14´ W. The mean ground elevation is 345 m above sea level. For this study, only the data observed at sunny locations were used as reference data for the radiation analysis: 4 locations (number 1, 8, 9 and 11) in the morning, all 13 locations around noon and 8 locations (number 1, 3, 5, 8, 9, 10, 11 and 13) in the afternoon (Fig. 3.2 and Table 3.1). A Kipp & Zonen CNR1 net-radiometer was used to collect both shortwave and longwave radiation. This instrument

has two CM 3 pyranometers and two CG 3 pyrgeometers, one of each mounted to face in opposite directions (e.g., up- and downward). Each pyranometer has a 180° field of view, and both of them will cover the entire sphere. Each pyrgeometer's field of view is only 150°, so both of them will cover 300° not the entire sphere. However, the differences of collected longwave radiation that can be created by the limited field of view are negligible, e.g., 5.4 Wm^{-2} when total incoming longwave radiation from an entire hemisphere is 400 Wm^{-2} if the entire hemisphere is assumed to be isothermal. Radiation data were collected from six directions (up- and downward and the four cardinal directions) for 1 min for each two directions at the height of 1.2 m and saved every 5 s on a 21x datalogger, made by Campbell Scientific Corporation. To collect air temperature, a Mannix Model CMM880 digital thermo-hygrometer was used. Humidity data were measured at the nearby Guelph Turfgrass Institute. For more detail, see Park (2003). The Guelph data were used in Park (2003), but they are employed for a different purpose in this study.

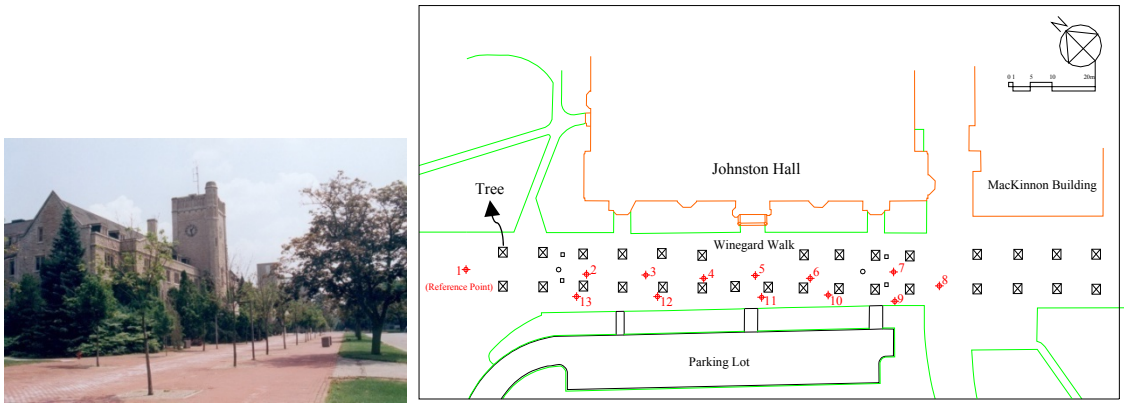

Fig. 3.1 View of Winegard Walk and the 13 observation locations

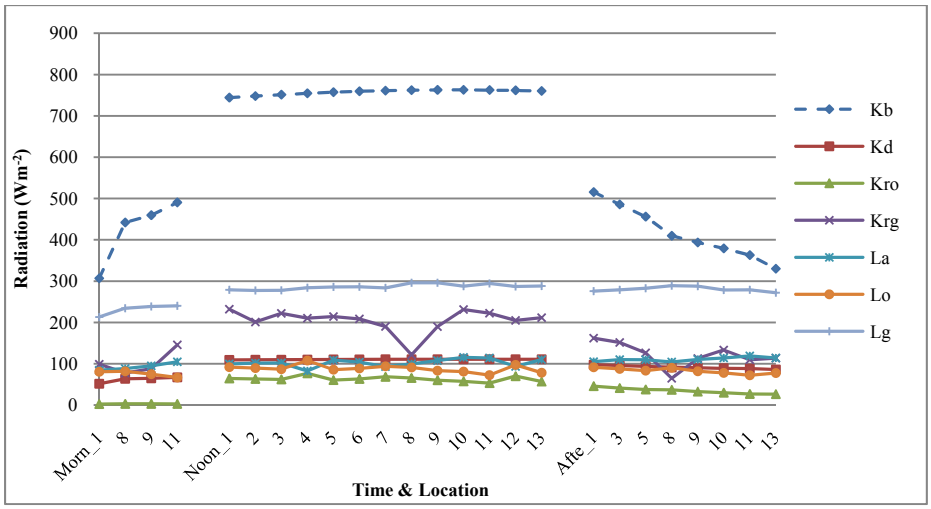

Fig. 3.2 Observed incoming solar and longwave radiation incident on a horizontal surface

Table 3.1 Collected climatic and radiation data on August 10, 2002 in Guelph, Ontario

Time	Site	Sky view factor (ψ_{sky})	Air Temp. (T_a, °C)	Relative Humidity (RH)	Solar altitude (β, °)	Radiation (Wm^{-2})						
						K_b	K_d	K_{ro}	K_{rg}	L_a	L_o	L_g
Morning	1	0.60	19.6	0.891	23.0	306.7	51.5	2.5[a]	98.8	84.3	80.4	213.2
	8	0.60	21.3	0.741	31.7	441.8	63.4	3.0[a]	77.7	88.3	81.7	234.4
	9	0.64	21.7	0.721	32.8	459.6	64.8	3.0[a]	87.9	95.1	74.9	238.8
	11	0.68	22.6	0.680	34.9	490.4	67.1	2.9[a]	145.8	104.6	66.9	240.0
Noon	1	0.60	29.5	0.413	60.1	744.1	109.3	64.5	232.1	99.6	91.9	278.7
	2	0.61	29.4	0.408	60.6	747.8	109.6	63.3	201.2	101.4	89.4	277.4
	3	0.62	28.9	0.404	60.9	751.2	109.8	62.1	221.9	102.1	86.7	277.8
	4	0.53	28.5	0.398	61.3	754.5	110.1	76.8	210.2	82.6	107.6	283.9
	5	0.63	30.6	0.393	61.6	757.2	110.3	60.5	214.3	108.9	85.7	285.9
	6	0.62	29.9	0.387	61.9	759.4	110.5	63.3	208.6	103.8	88.7	286.2
	7	0.59	28.1	0.382	62.0	761.0	110.6	68.4	190.2	93.2	93.9	283.5
	8	0.60	29.3	0.377	62.3	762.1	110.8	65.6	121.9	99.7	91.0	296.0
	9	0.64	29.7	0.371	62.3	762.7	110.8	60.1	190.0	107.7	83.4	296.1
	10	0.66	31.3	0.366	62.4	762.9	110.9	57.3	231.3	115.6	80.9	287.8
	11	0.68	28.8	0.360	62.3	762.4	110.9	53.3	222.4	113.9	72.6	294.5
	12	0.58	29.1	0.354	62.3	761.6	110.9	70.0	204.8	93.5	97.3	287.2
	13	0.66	29.1	0.349	62.1	760.2	110.9	57.0	211.7	109.9	78.4	288.0
Afternoon	1	0.60	29.2	0.362	41.7	515.5	97.6	45.7	162.0	104.9	91.5	275.8
	3	0.62	29.7	0.365	39.6	485.6	95.9	41.3	151.4	110.0	87.6	279.0
	5	0.63	28.6	0.368	37.7	456.0	94.1	37.8	126.4	109.8	83.4	282.8
	8	0.60	28.7	0.374	34.7	409.7	91.2	36.8	64.9	104.3	90.3	289.0
	9	0.64	28.4	0.376	33.6	393.4	90.2	32.5	112.8	110.4	82.0	287.8
	10	0.66	28.4	0.377	32.8	379.1	89.3	30.0	133.5	113.9	77.9	278.6
	11	0.68	28.4	0.379	31.7	362.9	88.3	26.9	109.6	118.8	72.3	279.0
	13	0.66	28.3	0.383	29.7	329.9	86.1	26.4	113.4	113.8	77.6	272.0

[a] the low values of K_{ro} in the morning resulted from no reflection of direct beam solar radiation by the building surface which was shaded.

To simply compare the models, the effect of clothing was not included in the calculation. The albedos of the body surface (a_b), objects in the sky hemisphere (a_o) and ground (a_g) and emissivity of the body surface (ε_b) were set to 0.3, 0.2, 0.3 and 0.97, respectively. These values were frequently used in previous modeling studies. The same values of incoming direct beam (K_b), diffuse beam (K_d), reflected (K_r) by objects (buildings, trees and other structures) in the sky hemisphere (K_{ro}) and by the ground (K_{rg}) solar radiation, and longwave radiation coming from objects in the sky hemisphere (L_o) and ground (L_g) derived from the measured data were directly used in all radiation models (Table 3.1 and Fig. 3.2). The Park and Tuller, RayMan and six-directional models employed measured longwave radiation from the sky (L_a). L_a values computed from air temperature and humidity via Eqs. 3.12 through 3.16 were used in the other four models. Gagge et al. (1969) found human skin temperature (T_b) was between 27 °C and 36.5 °C in steady-state conditions. Within this range of T_b, the greatest difference in longwave radiation emitted by the body surface (L_b) between the greatest and lowest f_{eff} compared in this study, 0.836 from the Park and Tuller

model and 0.725 from Fanger (1972), was only 6 Wm^{-2}. Thus, a T_b of 31 °C was assumed for all simulations.

The amounts of solar and longwave radiation mentioned above were calculated from radiation data collected on a horizontal surface. They were not the quantities of radiation on a body surface perpendicular to the sun's rays. The Burt and COMFA models used f_p^* values developed on the basic concept of shadow areas of a standing person on the horizontal ground surface (Terjung and Louie 1971, Fig. 3.3a). In contrast, the OUT_SET*, RayMan and Park and Tuller models took the perpendicular to the sun's rays surface area concept (Fig. 3.3b). The perpendicular concept models should be multiplied by 1 / cos(90-β) = 1 / sinβ to facilitate direct application of direct beam solar radiation measured on a horizontal surface. β is solar altitude (elevation).

All models except the Park and Tuller and COMFA models are for unobstructed horizons. They do not have components for the open sky view factor (ψ_{sky}) and reflected solar radiation from objects in the sky hemisphere (K_{ro}). Therefore, fixed values of diffuse beam solar radiation and reflected solar radiation from objects in the sky hemisphere were used in the solar radiation calculation of all models:

$$K_d \rightarrow K_d \psi_{sky} \tag{3.17}$$

$$(K_b + K_d)\alpha_g \rightarrow [K_b cosZ_{sl} t + K_d \psi_{w\_sky}]\alpha_o + (K_b t + K_d \psi_{sky} + K_{ro})\alpha_g = K_{ro} + K_{rg} = K_r \tag{3.18}$$

The quantities of absorbed solar and net longwave radiation on the body surface area were compared among the models. The differences among them would be caused by their different adopted concepts of body shapes which resulted in various body area factors. They also use different methods of determining longwave radiation from the clear sky.

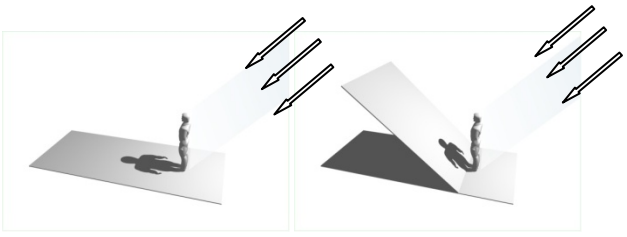

(a) (b)

Fig. 3.3 Two different approaches to obtain projected areas: (a) shadow area on the horizontal ground surface (Burt and COMFA models), (b) shadow area on the surface perpendicular to sun's rays (RayMan, OUT_SET* and Park and Tuller model) (created using VectorWorks 2008)

3.3 Results and Discussion

3.3.1 Comparison of projected area factors (f_p^*)

Variations in the key factor in the analysis of direct beam solar radiation among models, f_p^*, are presented in Fig. 3.4. The horizontal shadow areas used in the Burt, COMFA and MENEX models were multiplied by sinβ to convert them to surface areas perpendicular to the sun's rays, equivalent to the projected area factors used in the other models.

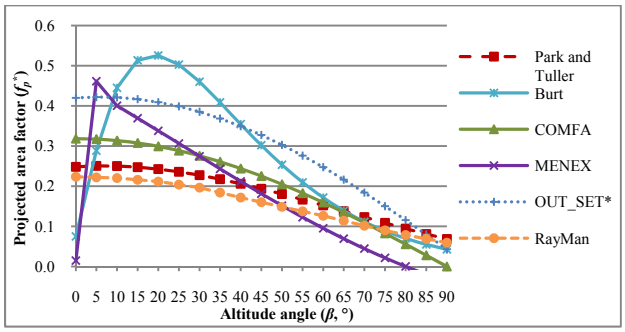

(a)

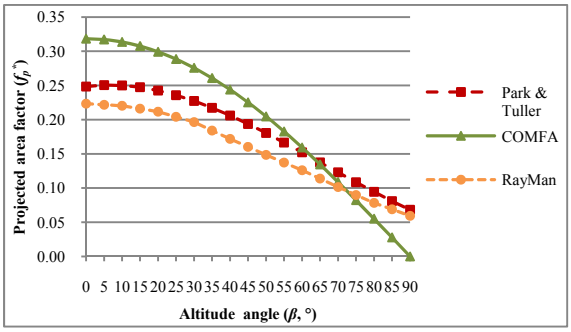

(b)

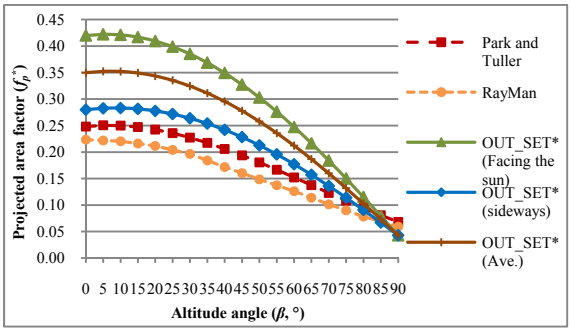

(c)

Fig. 3.4 Various comparisons of projected area factors (f_p^*): (a) Comparison of projected area factors (f_p^*), (b) comparison of f_p^* of Park and Tuller, RayMan and COMFA models and (c) comparison of f_p^* of Park and Tuller, RayMan and OUT_SET*

The differences in f_p^* between the Park and Tuller model and Fanger's result used in the RayMan model are small, around 0.03 when β is less than 65°, and decrease as β approaches 90° (Fig. 3.4a). Next closest results to the Park and Tuller model were from the COMFA model which used a cylindrical body model. The maximum difference between them was 0.07 at β=0°. The difference decreased continually until β=63° and increased again up to 0.068 at β=90° (Fig. 3.4b). The OUT_SET* model used the results of Underwood and Ward's (1966) photographic method, but only considered the anterior/posterior of the body facing the sun, not the body sides (see Kerslake 1972). This overestimated f_p^* compared with a body

exposed to the sun from a variety of directions. This creates more differences with the other photographic methods such as the Park and Tuller and RayMan models (Fig. 3.4c). The MENEX and Burt models had the highest values at β=5° and 20°, respectively, and crossing points with the Park and Tuller model around β=42° and 65°. Differences between f_p^* are greatest at low solar altitudes (Fig. 3.4a).

3.3.2 Absorbed radiation comparison

All five radiation estimating models and the six-directional method were compared with the Park and Tuller model in absorbed solar, net longwave and net all-wave radiation because the Park and Tuller model was recently developed from a larger sample of people than previous studies (Chapters 1 & 2) and its results were close to the median of a group of models whose results were relatively close, i.e., six-directional method, COMFA, RayMan and Park and Tuller (Fig. 3.6a and c).

3.3.2.1 Absorbed direct beam solar radiation (K_b^*)

In this study, β was 23.0–35.9° in the morning (0734–0845 hours), 60.1–62.4° around noon (1133–1244 hours) and 41.7–29.7° in the afternoon (1533–1642 hours).

Four of the six models (Park and Tuller, RayMan, COMFA and MENEX) form a group where values of absorbed direct beam solar radiation (K_b^*) are all relatively close, within 50 Wm^{-2} (Fig. 3.5). The Burt and OUT_SET* model results were above those of this model group. The Burt model deviated in the morning and afternoon and the OUT_SET* model at all times of the day. This mirrors the patterns of the projected area factor f_p^*. The OUT_SET* model had a relatively high f_p^* value compared with most other models at all solar altitudes less than 80^o.The Terjung and Louie (1971) method used in the Burt model had the highest f_p^* values of all models. This occurred at solar altitudes around 20^o. Thus, the Burt model deviates from other models in f_p^* and K_b^* at times and observation sites with solar altitudes near this value (Figs. 3.4 and 3.5). Its estimated K_b^* was up to 151 Wm^{-2} greater than that of the Park and Tuller model in the morning. The MENEX model was within the group in the morning and afternoon except for station 1 in

the morning (Morn_1) and had a difference of only around 30 Wm^{-2} with the group's median around noon (Fig. 3.5).

The closest results with the Park and Tuller model's were those of the RayMan model which had values that were 15–20 Wm^{-2} lower in the morning and afternoon and 16 Wm^{-2} lower around noon (Fig. 3.5). COMFA model results were very close to those of the Park and Tuller model around noon, within 1–4 Wm^{-2}.

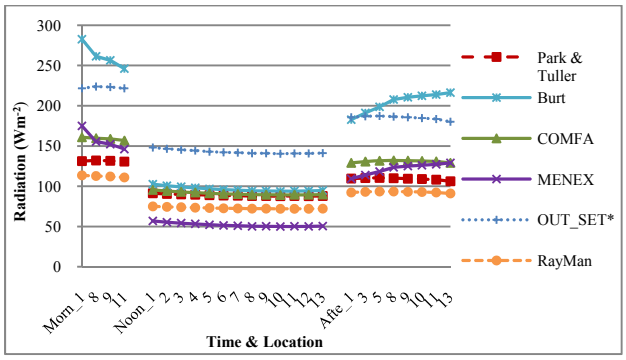

Fig. 3.5 Comparison of absorbed direct beam solar radiation on the body surface in the morning, around noon and in the afternoon

3.3.2.2 Absorbed total solar radiation (R^*)

The OUT_SET* model had the greatest quantity of absorbed total solar radiation among all models for the day as a whole (Fig. 3.6a). It has a relatively high projected area factor and absorbed direct beam solar radiation as noted above. It is one of the models where diffuse beam and reflected solar radiation measured on a horizontal surface were not reduced by one half, producing greater quantities of these two radiation streams than most of the other models.

The MENEX model also had relatively high values of absorbed total solar radiation throughout the day (Fig. 3.6a). Its estimated absorbed direct beam solar radiation is close to that of most other models during the morning and afternoon and the lowest of all models at noon (Fig. 3.5). However, it differs from most other models in the lack of the ½ function correction for diffuse sources of radiation on/from a horizontal surface used as input in this study. It also does not apply an effective radiation area factor (f_{eff}) to these diffuse sources of radiation. These two factors combine to give the MENEX model the greatest diffuse beam and reflected solar radiation absorbed on the human body surface (Fig. 3.6d). The current

version of MENEX has reduced the importance of diffuse radiation (http://www.igipz.pan.pl/geoekoklimat/blaz/MENEX_2005 .pdf).

The COMFA model had the closest values to the Park and Tuller model around noon, about 4 Wm^{-2} differences. It had 14–27 Wm^{-2} more absorbed total solar radiation in the morning and afternoon. The Burt model also had close values to those of the Park and Tuller model around noon but had high values in the morning and afternoon close to those of the MENEX model because of its high f_p^* values. The six-directional method continually yielded 8–44 Wm^{-2} more than the Park and Tuller model's values. The RayMan model has a similar f_p (= A_p / A_{eff}) as the Park and Tuller model, but f_{eff} of the Park and Tuller model is 0.836 which is much higher than RayMan's 0.725. Therefore, the RayMan f_p^* (= $A_p / A_D = f_p \times f_{eff}$) values were around 0.03 lower all day than the Park and Tuller model's. The lower RayMan f_p^* and f_{eff} values created somewhat lower absorbed direct beam, diffuse beam and reflected solar radiation than the Park and Tuller model's (Fig. 3.6d). Therefore, its absorbed total solar radiation was 23–30 Wm^{-2} lower.

3.3.2.3 Net longwave radiation (*L*)

The range between model estimates of net longwave radiation was not large, 31 Wm^{-2} between the OUT_SET* and Park and Tuller models in the morning and 23 Wm^{-2} between the MENEX and Park and Tuller models around noon and in the afternoon (Fig. 3.6b). The effective radiation area factor (f_{eff}) values and methods determining incoming longwave radiation from the open sky were the variables creating differences between models in this study. Differences in employed f_{eff} affect both the gain of absorbed and the loss of emitted longwave radiation. One offsets the other. The difference in net longwave radiation between models with unequal f_{eff} values will depend on the difference between incoming and emitted longwave radiation. The differences between these two radiation streams were not great in the very warm, sunny and summer conditions during our observations. The maximum daily mean difference in open sky longwave radiation (L_a) between models was only 19 Wm^{-2} (Fig. 3.7). These two factors combined to limit the magnitude of net longwave radiation differences between models.

Computed open sky incoming longwave radiation exceeded the measured value for all models that employed the computed values, OUT_SET*, COMFA, Burt and MENEX (Fig. 3.6b). The OUT_SET*

model's method gave the greatest values. This combined with its relatively low f_{eff} (0.75) which limited the magnitude of the negative net longwave radiation gave it the greatest values during the morning. A high f_{eff} (1.0) and relatively high computed incoming sky longwave radiation gave the MENEX model the highest values during mid-day and the afternoon. The Park and Tuller model used the lower measured open sky longwave radiation values. Its relatively high f_{eff} accentuated the magnitude of its negative net longwave radiation, and it had the lowest net longwave radiation throughout the day (Fig. 3.6b). The values of the Park and Tuller and RayMan models were nearly identical near noon and in the afternoon.

3.3.2.4 Net all-wave radiation (*Q*)

Most of the variations in net all-wave radiation between models resulted from absorbed solar radiation. The greatest difference overall between the Park and Tuller model and the other models in net all-wave radiation was with the OUT_SET* model (Fig. 3.6c). The mean difference over the entire day was +146 Wm^{-2}, composed of the OUT_SET* model's 128 and 18 Wm^{-2} greater absorbed total solar and net longwave radiation, respectively (Figs. 3.6a, b). The second greatest difference was a 122 Wm^{-2} greater mean for the MENEX model. MENEX and OUT_SET* were the two models with the greatest absorbed total solar radiation for the day as a whole. The MENEX model also had the greatest net longwave radiation. The six-directional method had 36 Wm^{-2} greater net all-wave radiation than the Park and Tuller model, 29 and 7 Wm^{-2} more absorbed total solar and net longwave radiation, respectively.

The COMFA model had close results with the Park and Tuller model around noon. This model had more differences at the lower solar altitude (39, 10 and 27 Wm^{-2} in the morning, noon and afternoon). The RayMan model had the opposite phenomenon to the COMFA model. Its net all-wave radiation difference with the Park and Tuller model was relatively constant throughout the day (15, 27 and 23 Wm^{-2} lower in the morning, noon and afternoon with more differences coming at the higher solar altitude). The Burt model had the closest results with the Park and Tuller model around noon, but much larger differences in the morning (+147 Wm^{-2}) and afternoon (+94 Wm^{-2}) due to the greater gaps in absorbed direct beam solar radiation. Mean differences by time presented above between the Park and Tuller model and the other models are shown in Fig. 3.6d.

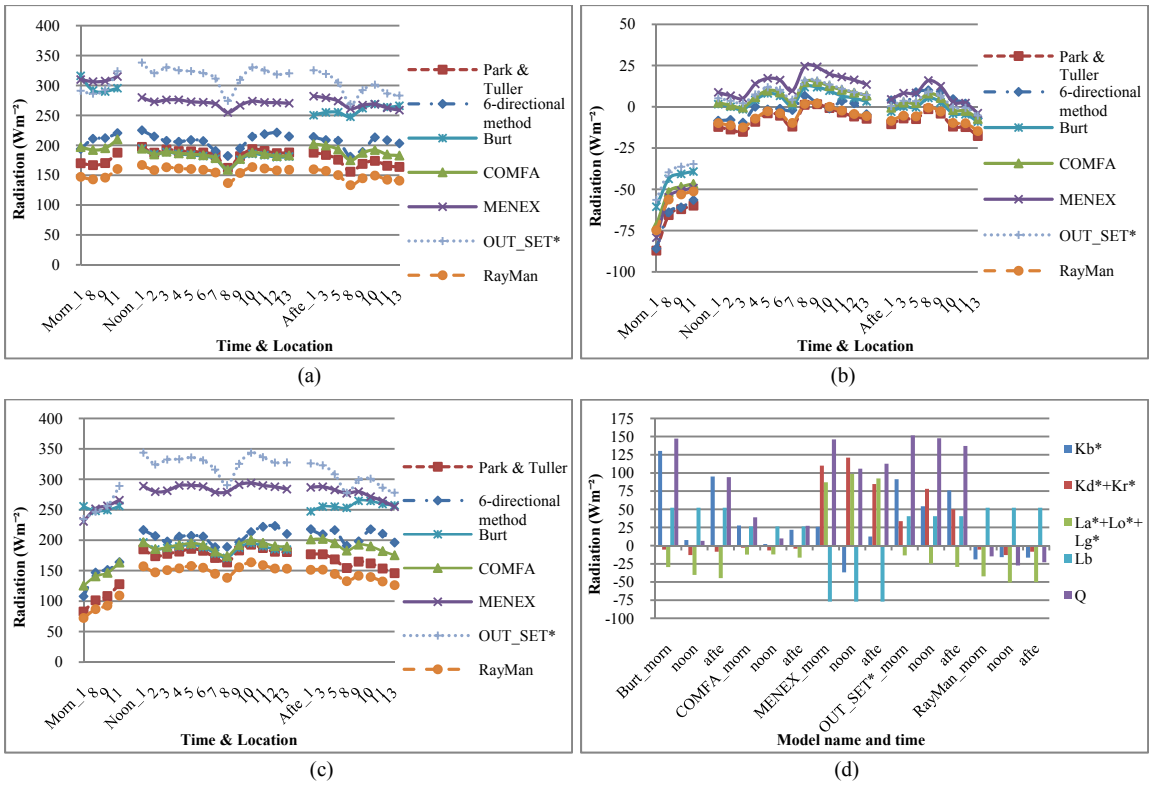

Fig. 3.6 Comparison of (a) absorbed total solar radiation, (b) net longwave radiation, (c) net all-wave radiation and (d) differences in absorbed and emitted radiation between the Park and Tuller model and the other models

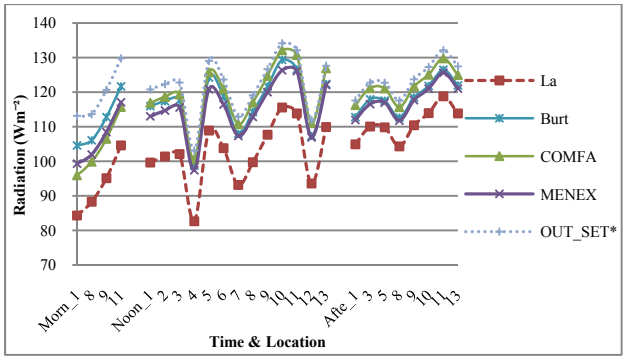

Fig. 3.7 Comparison between measured incoming longwave radiation from the open sky to the horizontal ground surface (L_a) and computed L_a results from the Burt, COMFA, MENEX and OUT_SET* models

3.3.3 Correlation among the models

Pearson's product–moment correlation coefficients between models were determined for absorbed total solar, net longwave and net all-wave radiation (Table 3.2). The inputs were the 25 time–site values from each model.

Time and site differences in longwave radiation were determined by the variations in measured quantities of longwave radiation, air temperature and humidity depending on the model. The major control of differences in the computed open sky incoming longwave radiation was air temperature. The time–site correlation between air temperature and the measured amount of incoming longwave radiation from the upper hemisphere was 0.963. Hence, the time–site variations in longwave radiation were similar for all models producing very significant correlations in human body net longwave radiation, all over 0.95 and many over 0.99 (Table 3.2a).

Table 3.2 The correlation among the models: (a) absorbed total shortwave (top half) and net longwave radiation (bottom half) (b) net all-wave radiation [*correlation coefficient (*r*) is significant at the 0.01 level (2-tailed)]

Shortwave / Longwave	Park and Tuller model	6-directional method	COMFA model	MENEX model	Burt model	RayMan model	OUT_SET* model
Park and Tuller model		0.652*	0.320	0.105	-0.537	0.996*	0.994*
6-directional method	0.983*		0.587*	0.344	-0.011	0.683*	0.684*
COMFA model	0.996*	0.967*		0.742*	0.621*	0.401	0.400
MENEX model	0.995*	0.966*	1*		0.593*	0.161	0.126
Burt model	0.993*	0.959*	0.999*	0.999*		-0.459	-0.466
RayMan model	1*	0.983*	0.996*	0.995*	0.993*		0.997*
OUT_SET* model	0.993*	0.958*	0.999*	0.999*	1*	0.993*	

(a)

Net all-wave radiation	Park and Tuller model	6-directional method	COMFA model	MENEX model	Burt model	RayMan model	OUT_SET* model
Park and Tuller model	1						
6-directional method	0.911*	1					
COMFA model	0.957*	0.948*	1				
MENEX model	0.951*	0.836*	0.912*	1			
Burt model	-0.593*	-0.326	-0.336	-0.583*	1		
RayMan model	0.999*	0.919*	0.964*	0.947*	-0.569*	1	
OUT_SET* model	0.953*	0.825*	0.889*	0.928*	-0.641*	0.947*	1

(b)

Correlations for absorbed total solar radiation were determined mainly by variation patterns of the projected area factor (f_p^*) with solar altitude. Models whose graphs of f_p^* with solar altitude have similar shape through the range of solar altitudes encountered in the field observations (23^o to 63^o) will have high correlation coefficients (Fig. 3.4 and Table 3.2a). Those whose shapes differ will have low correlations.

Correlation coefficients between the Park and Tuller, RayMan and OUT_SET* models were all very significant (over 0.994). The Burt and MENEX models whose curves have unique shapes have the lowest correlations with other models.

The correlations for net all-wave radiation were also very significant among the Park and Tuller, RayMan and OUT_SET* models even though all models except the Burt model had correlations over 0.90 (Table 3.2b). Only these three models had high correlations for both absorbed total solar and net longwave radiation. The strongest correlation was between the Park and Tuller and RayMan models, r=0.999, as expected. The correlations between the Park and Tuller and OUT_SET* models and between the RayMan and OUT_SET* models were r=0.953 and r=0.947, respectively (Table 3.2b).

3.3.4 Comparison of revised radiation models

In this section, four revised models (6-directional method*f_{eff}, OUT_SET*1/2, MENEX*f_{eff}, MENEX*f_{eff}*1/2 models) were compared with the Park and Tuller model. The COMFA, Burt and RayMan models were excluded in this comparison. The Burt model made very large errors due to its f_p^* values at low solar altitudes although the model has all required radiation components in its formulas (i.e., use of f_{eff} in absorbed solar and net longwave radiation and the 1/2 function in K_d and K_r components). The COMFA and RayMan models had results close to the Park and Tuller model because of close values of f_p^* and the only difference among them was f_{eff} (RayMan: 0.725, COMFA: 0.78 and Park and Tuller: 0.836).

The six-directional method was modified to six-directional method*f_{eff} by multiplying by the Park and Tuller's f_{eff}, 0.836. For the OUT_SET*1/2 model, the second part (K_d and K_r components) of its R^* equation (Eqs. 3.5 and 3.6) was multiplied by 1/2 like the other models' R^* equations to account for the vertical body surface's view factor for diffuse radiation incident on or coming from a horizontal surface (Eq. 3.19).

$$R^* = \left\{(0.42cos\beta + 0.043sin\beta)\frac{K_b}{sin\theta} + \mathbf{\frac{1}{2}} f_{eff}\left[K_d + (K_b + K_d)\alpha_g\right]\right\}(1 - \alpha_b) \qquad (3.19)$$

The MENEX model did not multiply its horizontal surface diffuse and reflected solar radiation by 1/2 and did not apply an f_{eff} value to its K_d, K_r and L components. However, the components of the model's

equations are derived from experimental studies, so two revised models were made because the two missing components listed above could be included already in its original equations. Eqs. 3.20 and 3.21 add Park and Tuller's f_{eff} to MENEX's R^* for β>5° and L equations (Eqs. 3.3, 3.4 and 3.12). Eqs. 3.22 and 3.23 are the revised model including both 1/2 and f_{eff} in its R^* for β>5° and f_{eff} in L equations.

$$\text{if } \beta > 5°, \qquad R^* = \left[K_b\left(\frac{26.34}{\beta} - 0.329\right) + \boldsymbol{f_{eff}}(K_b + K_r)(0.0018 + 0.0462 \ln \beta)\right](1-\alpha_b) \quad (3.20)$$

$$L = \frac{1}{2}\varepsilon_b \boldsymbol{f_{eff}}\left[\varepsilon_a \cdot \sigma \cdot (T_a + 273)^4 \,(0.82 - 0.25 \cdot 10^{-0.094 \cdot e_a})\psi_{sky} + L_o + L_g\right] - \boldsymbol{f_{eff}} L_b \quad (3.21)$$

$$\text{if } \beta > 5°, \qquad R^* = \left[K_b\left(\frac{26.34}{\beta} - 0.329\right) + \boldsymbol{\frac{1}{2} f_{eff}}(K_b + K_r)(0.0018 + 0.0462 \ln \beta)\right](1-\alpha_b) \quad (3.22)$$

$$L = \frac{1}{2}\varepsilon_b \boldsymbol{f_{eff}}\left[\varepsilon_a \cdot \sigma \cdot (T_a + 273)^4 \,(0.82 - 0.25 \cdot 10^{-0.094 \cdot e_a})\psi_{sky} + L_o + L_g\right] - \boldsymbol{f_{eff}} L_b \quad (3.23)$$

Both revised models have the same L components, so only MENEX*f_{eff} was used in the L comparison.

Most differences between these revised models and the Park and Tuller model were created by absorbed solar radiation (Fig. 3.8a, d). In net longwave radiation, the differences were less than 21 Wm^{-2} except for the OUT_SET* model (Fig. 3.8b, d), so the differences shown in the absorbed solar radiation comparison created most of the differences in net all-wave radiation (Fig. 3.8c, d).

The six-directional method*f_{eff} had very close results to those of the Park and Tuller model throughout the day. The maximum net all-wave radiation difference was 23 Wm^{-2} in the afternoon, but the absolute average differences for the day as a whole were only 10, 9 and 10 Wm^{-2} in absorbed solar, net longwave and net all-wave radiation, respectively.

The 1/2 function in OUT_SET*1/2 reduced the original differences around 38 (30 %), 88 (67 %) and 56 Wm^{-2} (45 %) in the morning, noon and afternoon, respectively. The OUT_SET*1/2 model shows its 1/2 function for K_d and K_r can reduce differences with the Park and Tuller model by about 1/2 during the daytime. However, the model still needs reduced f_p^* values to decrease the other half of the differences.

The effect of f_{eff} in the MENEX*f_{eff} model reduced the original R^* differences in the morning, noon and afternoon by an average 10, 38 and 16 %, respectively. The MENEX*f_{eff} *1/2 model had closer R^* values to the Park and Tuller model than did the MENEX*f_{eff} model reducing the differences 36, 136

and 57 % at the same times as above, but it still made a large overestimation in R^* at lower solar altitudes. In the L comparison, this revised model reduced the differences a little at noon (11 %) and in the afternoon (7 %) but made a large reduction in the morning (114 %). The two models show clearly that the original MENEX model creates a large overestimation of absorbed K_d^+ and K_r^+. Also, its higher f_p^* values at lower solar altitudes produce higher absorbed K_b^+ values in the morning and afternoon. Therefore, in net all-wave radiation the differences made by MENEX*f_{eff} and MENEX*f_{eff}*1/2 models were similar to those of the absorbed solar radiation. The MENEX model seems to need better f_p^* values, f_{eff} for its L equation and f_{eff} and 1/2 multiplication to the K_d and K_r components of R^*.

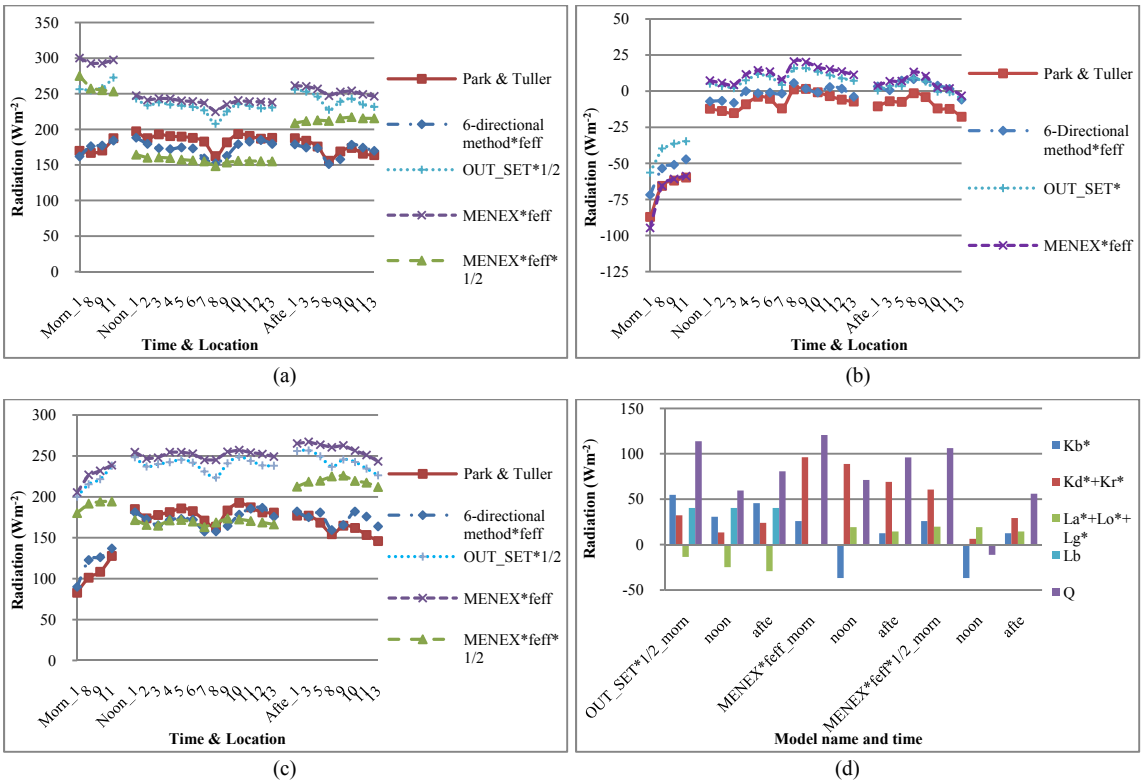

Fig. 3.8 Revised radiation comparison: (a) absorbed total solar radiation, (b) net longwave radiation, (c) net all-wave radiation and (d) differences of absorbed and emitted radiation between the Park and Tuller model and the revised models

3.4 Conclusions

The radiation components of five existing human thermal exchange models (Burt, COMFA, MENEX, OUT_SET* and RayMan models), one experimental model [six-directional method from VDI (1998)] and the new Park and Tuller model were compared.

Results of all models were referenced against those of the Park and Tuller model. This is not to suggest this model is the most appropriate for all applications. It is the one that employs the most recently derived human body radiation area factors. Also, it addresses the body shape and size of the current-day adult population. It puts the comparisons in the time perspective. Direct comparison with this model eases the identification of differences that might arise when using older, widely employed or more recent methods. The Park and Tuller radiation area factors were developed from a larger sample of actual adults and used up-to-date video and computer technology compared with most of the older methods. However, it has not undergone the testing of extensive applications experienced by the older methods.

Absolute net longwave radiation differences between models were not large (maximum difference, 31 Wm^{-2}). Although effective radiation area factors (f_{eff}) had a wide range from 0.725 to 1.0, the magnitude of the differences between human body absorbed and emitted longwave radiation was relatively small. This and the limited range between incoming longwave radiation from the sky used in the models (measured and computed) limited the magnitude of model differences in net longwave radiation. The situation can be different at other times and in other environments, e.g., very cold or hot radiant environments where environmental radiant temperature differs markedly from human surface/clothing temperature. In these types of environments, inappropriate f_{eff} values can lead to large errors in estimated human net longwave radiation.

All four methods of computing incoming longwave radiation from the clear sky overestimated the measured value. The Idso (1981) method used in the OUT_SET* model yielded the highest value followed by the Swinbank (1963) equation (COMFA), Brunt (1932) method (Burt model) and that found in Geiger (1965) used by MENEX. However, the differences between computation methods were small, 7.5 Wm^{-2} for the day as a whole. The variation between the mean from all four computation methods and measured open sky longwave radiation was 14 Wm^{-2}. Measured longwave radiation data are seldom available and

estimates must be made for many applied climate studies. In most cases, the differences we found between measured and computed open sky longwave radiation and between those estimated by different formulas will not have a major impact on human net all-wave radiation or total thermal exchange evaluations.

A key variable in model absorbed solar radiation differences is the projected area factor (f_p^*). The empirical MENEX and Burt models' factors had a great deal of variation with solar altitude compared with the other models whose curves have a much lower slope (Fig. 3.4). Absorbed direct beam solar radiation estimated using these two models is more sensitive to variations in solar altitude. Moreover, the Burt model has a crossing point of its f_p^* line with Park and Tuller model's f_p^* line near the noon solar altitude in this study so that the model had results close to those of the Park and Tuller model at noon. However, the model can produce very different noon results at other seasons and latitudes that have different solar altitudes.

The OUT_SET* model's elliptical cylinder body model has higher f_p^* values than most of the other models at solar altitudes less than 80^o. The major axis of the ellipse facing the sun maximizes the projected area factor compared with models that incorporate the sun's rays intersecting all sides of the body. For example, OUT_SET*'s f_p^* is between 0.07 and 0.10 greater than that of the non-elliptical cylinder used in the COMFA model (Fig. 3.4). This creates relatively high absorbed direct beam and total solar radiation (Figs. 3.5 and 3.6).

The RayMan model has f_p^* values very similar to those of the Park and Tuller model, 0.035–0.025 lower, which produced about 27 Wm^{-2} lower absorbed total solar radiation during the daytime.

Both effective radiation area factor and whether or not diffuse sources of radiation measured on or from a horizontal surface are reduced by one half to account for a unit area of the vertical body surface's exposure to only half the entire horizontal surface were important controls of model differences in estimated absorbed diffuse beam and reflected-from-the-ground solar radiation. The MENEX model had the highest total of absorbed diffuse beam and reflected solar radiation simply because of its implied 1.0 f_{eff} and no ½ function (Fig 3.6d). The ½ function is quantitatively more important than most differences in f_{eff}. Next highest was the OUT_SET* model which had a relatively low f_{eff} value of 0.75 but did not have the ½ function.

To modify each model for radiation estimates similar to Park and Tuller's, the six-directional method should include f_{eff} such as Park and Tuller's 0.836 in both absorbed solar and net longwave

radiation equations. The revised method will provide a close estimate all day. The MENEX model needs f_{eff} in its net longwave radiation equation, requires more precise values of f_p^* for absorbed direct beam solar radiation and needs to multiply the absorbed diffuse and reflected solar radiation by f_{eff} and 1/2. The Burt model also needs new, more accurate values of f_p^*. The OUT_SET* model should use 1/2 of the values of absorbed diffuse and reflected solar radiation and also needs better values of f_p^*. The RayMan model uses Fanger's f_p and f_{eff} values, and the f_{eff} value is almost 0.11 (11 %) lower than Park and Tuller's. This makes the model underestimate net all-wave radiation, and its differences can be important in estimating human thermal exchange (see section 1.5 in Chapter 1).

Human radiation exchange has widespread application and can aid in the planning of more comfortable and healthy environments for people. Several human radiation exchange models are available employing a variety of different assumptions. This study has compared a selection of these models. Several radiation streams were derived from measured data and were the same for all models. Therefore, model differences were created by the input of longwave radiation from the clear sky, human body projected area factor (f_p) and effective radiation area factor (f_{eff}) used in each model and the presence or absence of the 1/2 function for reflected and diffuse beam solar radiation. Values of these human radiation area factors were determined via different methods including using samples of people or mannequins of different age, size and shape or objects such as cylinders. Model differences in human net all-wave radiation were up to about 150 Wm^{-2} which can have an important effect on thermal sensation.

It is suggested that those estimating human radiation exchange study a variety of models and take care to select algorithms and human radiation area factors that are most applicable to the subjects of their study. We also encourage more direct comparison of available models in a variety of different environments. These types of studies will help those wishing to estimate human radiation exchange select appropriate models and methods.

The next chapter will show a new three-dimensional human-urban radiation exchange computer simulation model combining newly found urban area factors with the human radiation exchange model.

References

Ali-Toudert F, Djenane M, Bensalem R, Mayer H (2005) Outdoor thermal comfort in the old desert city of Beni-Isguen, Algeria. Climate Research 28: 243-256. doi: 10.3354/cr028243

Auliciems A, Kalma JD (1979) A climatic classification of human thermal stress in Australia. Journal of Applied Meteorology 18: 616-626

Blazejczyk K, Nilsson H, Holmér I (1993) Solar heat load on man: Review of different methods of estimation. International Journal of Biometeorology 37: 125-132

Blazejczyk K (1994) New climatological-and-physiological model of the human heat balance outdoor (MENEX) and its applications in bioclimatological studies in different scales. In: Blazejczyk K, Krawczyk B (eds) Bioclimatic Research of the Human Heat Balance. Polish Academy of Sciences, Institute of Geography and Spatial Organization, Warsaw, 27-58

Blazejczyk K (2004) Assessment of radiation balance in man in various meteorological and geographical conditions. Geographia Polonica 77: 63-76

Blazejczyk K (2005) MENEX_2005-The Updated Version of Man-Environment Heat Exchange Model. http://www.igipz.pan.pl/geoekoklimat/blaz/MENEX_2005.pdf

Breckenridge VR, Goldman RF (1972) Human solar heat load. ASHRAE Transactions 1: 110-119

Brown RD, Gillespie TJ (1986) Estimating outdoor thermal comfort using a cylindrical radiation thermometer and an energy budget model. International Journal of Biometeorology 30: 43-52. doi: 10.1007/BF02192058

Brown RD, Gillespie TJ (1995) Microclimatic Landscape Design: Creating Thermal Comfort and Energy Efficiency. Wiley, New York

Brunt D (1932) Notes on radiation in the atmosphere. Quarterly Journal of the Royal Meteorological Society 58: 389-420. doi: 10.1002/qj.49705824704

Burt JE (1979) A Model of Human Thermal Comfort and Associated Comfort Patterns for the United States. C. W. Thornthwaite Associates, Centerton, NJ

de Freitas CR (1985) Assessment of human bioclimate based on thermal response. International Journal of Biometeorology 29(2): 97-119

Fanger PO (1972) Thermal Comfort: Analysis and Applications in Environmental Engineering. McGraw-Hill, New York

Gagge AP, Stolwijk JAJ, Nishi Y (1969) The prediction of thermal comfort when thermal equilibrium is maintained by sweating. ASHRAE Transactions 75, Part 2: 108-123

Geiger R (1965) The Climate Near The Ground. Harvard University Press, Cambridge, Massachusetts

Guibert A, Taylor CL (1952) Radiation area of the human body. Journal of Applied Physiology 5: 24-37

Hodder SG, Parsons K (2007) The effects of solar radiation on thermal comfort. International Journal of Biometeorology 51: 233-250. doi: 10.1007/s00484-006-0050-y

Huang H, Ooka R, Kato S (2005) Urban thermal environment measurements and numerical simulation for an actual complex urban area covering a large district heating and cooling system in summer. Atmospheric Environment 39: 6362-6375. doi: 10.1016/j.atmosenv.2005.07.018

Idso SB (1981) A set of equations for full spectrum and 8- to 14 μm and 10.5- to 12.5 μm thermal radiation from cloudless skies. Water Resources Research 17: 295-304. doi:10.1029/WR017i002p00295

Iziomon MG, Mayer H, Matzarakis A (2003) Downward atmospheric longwave irradiance under clear and cloudy skies: Measurement and parameterization. Journal of Atmospheric and Solar-Terrestrial Physics 65: 1107-1116. doi:10.1016/j.jastp.2003.07.007

Jendritzky G, Nübler W (1981) A model analyzing the urban thermal environment in physiologically significant terms. Archives for Meteorology, Geophysics, and Bioclimatology, Series B, 29: 313-326

Jendritzky G, Menz H, Schirmer H, Schmidt-Kessen W (1990) Methodik zur raumbezogenen Bewertung der thermischen Komponente im Bioklima des Menschen (Fortgeschriebenes Klima-Michel-Modell). Beitr Akad Raumforsch Landesplan, No. 114

Kenny NA, Warland JS, Brown RD, Gillespie TG (2008) Estimating the radiation absorbed by a human. International Journal of Biometeorology 52: 491-503. doi: 10.1007/s00484-008-0145-8

Kerslake DM (1972) The Stress of Hot Environments. Cambridge University Press, Cambridge, ISBN 0-521-08343-5

Krys SA, Brown RD (1990) Radiation absorbed by a vertical cylinder in complex outdoor environments under clear sky conditions. International Journal of Biometeorology 34: 69-75

Matzarakis A, Rutz F, Mayer H (2000) Estimation and calculation of the mean radiant temperature within urban structures. In: de Dear RJ, Kalma JD, Oke TR, Auliciems A (eds.) Biometeorology and Urban Climatology at the Turn of the Millennium. ICB-ICUC'99, Sydney, WCASP-50, WMO/TD No. 1026, 273-278

Matzarakis A, Rutz F, Mayer H (2007) Modelling radiation fluxes in simple and complex environments-application of the RayMan model. International Journal of Biometeorology 51: 323-334. doi: 10.1007/s00484-006-0061-8

Matzarakis A, Rutz F, Mayer H (2010) Modelling radiation fluxes in simple and complex environments: basics of the RayMan model. International Journal of Biometeorology 54: 131-139. doi: 10.1007/s00484-009-0261-0

Oliveira S, Andrade H (2007) An initial assessment of the bioclimatic comfort in an outdoor public space in Lisbon. International Journal of Biometeorology 52: 69-84. doi: 10.1007/s00484-007-0100-0

Park S (2003) Estimating Radiation Received by a Person in the Landscape. MSc thesis, University of Guelph, Ontario

Parsons K (1993) Human Thermal Environments: The Effects of Hot, Moderate and Cold Environments on Human Health, Comfort and Performance-the Principles and the Practice. Taylor & Francis, London

Pickup J, de Dear R (2000) An outdoor thermal comfort index (OUT-SET*) – Part I - the model and its assumptions. In: de Dear RJ, Kalma JD, Oke TR, Auliciems A (eds) Biometeorology and Urban Climatology at the Turn of the Millennium. ICB-ICUC'99, Sydney, WCASP-50, WMO/TD No. 1026, 279-283

Spagnolo J, de Dear R (2003) A field study of thermal comfort in outdoor and semi-outdoor environments in subtropical Sydney Australia. Building and Environment 38: 721-738. doi:10.1016/S0360-1323(02)00209-3

Steadman RG (1971) Indices of windchill of clothed persons. Journal of Applied Meteorology 10: 674-683. doi: 10.1175/1520-0450(1971)010<0674:IOWOCP>2.0.CO;2

Steadman RG (1979) The assessment of Sultriness. Part II: Effects of wind, extra radiation and barometric pressure on apparent temperature. Journal of Applied Meteorology 18: 874-885

Steadman RG (1984) A universal scale of apparent temperature. Journal of Climate and Applied Meteorology 23: 1674-1687

Swinbank WC (1963) Long-wave radiation from clear skies. Quarterly Journal of the Royal Meteorological Society 89: 339-348. doi: 10.1002/qj.49708938105

Terjung WH, Louie S (1971) Potential solar radiation climates of man. Annals of the Association of American Geographers 61: 481-500. doi: 10.1111/j.1467-8306.1971.tb00801.x

Thorsson S, Lindberg F, Eliasson I, Holmer B (2007) Different methods for estimating the mean radiant temperature in an outdoor urban setting. International Journal of Climatology 27: 1983-1993. doi: 10.1002/joc.1537

Tuller SE (1990) Standard seasons. International Journal of Biometeorology 34: 181-188. doi: 10.1007/BF01048718

Underwood CR, Ward EJ (1966) The solar radiation area of man. Ergonomics 9: 155-168. doi**:** 10.1080/00140136608964361

VDI (1998) 3787, Part 2: Environmental Meteorology-Methods for the Human Biometeorological Evaluation of Climate and Air Quality for Urban and Regional Planning at Regional Level Part 1: Climate. Beuth, Berlin

Chapter 4. New Human-Urban Radiation Exchange Simulation Model

Abstract

A new human-urban radiation exchange simulation model was developed using newly found urban area factors (view factors and surface albedos and temperatures) in downtown Nanaimo, B.C., Canada with human area factors of contemporary Canadian adults. Data collection was conducted at two sites, Nanaimo, B.C., Canada and Changwon, Republic of Korea. The collected data were compared with the results of the new model and two other three-dimensional radiation programs, RayMan Pro and ENVI-met 3.1.

The differences of total all-wave radiation between collected data and the new model results were very small: mean 15 Wm^{-2} (19 Wm^{-2} at only sunny locations). Their squared correlation (r^2) was very strong, over 0.995, for solar radiation coming from the sky hemisphere ($K\downarrow$) and a little weaker for longwave radiation. The RayMan Pro and ENVI-met 3.1 programs had greater differences, mean 44 Wm^{-2} (71 Wm^{-2}) and 320 Wm^{-2} (372 Wm^{-2}) respectively. Their r^2 values were weaker than the new model's, 0.990 and 0.935 in $K\downarrow$ respectively.

In the results of the new model, total absorbed longwave radiation by the human body (L^*) was much higher than total absorbed solar radiation (R^*). Mean L^* and R^* were around 400 and 155 Wm^{-2} at the sunny locations. Shadows at a specific small location can make a moderate difference in L^* in urban areas if the shaded area with its lower surface temperature covers a large proportion of the urban surfaces, 31.4 Wm^{-2} in L^* between the sunny and shaded locations. However, the shadow effect on total absorbed radiation in the daytime was dominantly controlled by R^*, i.e., a mean difference of 100.2 Wm^{-2} in absorbed direct beam solar radiation and 34.5 Wm^{-2} in absorbed diffuse beam and reflected solar radiation. Mean radiant temperatures (T_{mrt}) at the sunny locations were 56.1–58.6 °C, and the shadow effect reduced them to half, around 27.2 °C.

Accurate meteorological and urban setting data such as Linke turbidity, ground heights and building/ground albedos should be obtained for better results from the new model.

4.1 Introduction

Body and urban morphological variables and parameters used for human radiation exchange analysis in outdoor urban areas have two main categories, human area factors and urban area factors. The human area factors include body area factors and clothing area factors. The urban area factors are sky view factor (ψ_{sky}); view factors of sunny and shaded surfaces of buildings, vegetation and ground; albedos and emissivities of buildings, vegetation and ground surfaces and transmissivities of vegetation. Body area factors for standing and walking postures which are common body postures in outdoor areas were analyzed in Chapters 1 and 2, and these factors can be easily adjusted for clothed subjects using the clothing area factor information in McCullough et al. (1985, 1989), ASHRAE (2001) and ISO9920 (2007). Also, the well documented results of surface albedos & emissivities (Arnfield 1982, Oke 1987, Brown and Gillespie 1995) and vegetation transmissivities (Oke 1987, Brown and Gillespie 1995) can be used for the variables of urban surface materials even though some value ranges are too broad, e.g., albedo of brick as 0.2-0.5 (Brown and Gillespie 1995).

One of the most important deficiencies existing in the urban area factors is how to analyze view factors between a human body and anisothermally surrounding, three-dimensional (3D) urban environments. The total angle factor between them is 360×360 spherical degrees in the vertical (altitude) and horizontal (azimuth) directions covering both the lower (ground) and upper (sky) hemispheres. The view factor is a proportion of the entire radiant environment occupied by each isothermal surface. The total view factor is 1.0 (100 %), and each isothermal surface in a hemisphere will have a value less than or equal to 0.5 (50 %).

In the daytime; if the outdoor urban area has direct beam solar radiation, each surface should be divided into at least two different isothermal surfaces, sunny and shaded, created by the sun's azimuth and altitude angles at various times and latitudes. Even though it is the same material, amounts of incident solar radiation are significantly different which affects reflected solar radiation and surface temperatures that directly influence amounts of emitted longwave radiation from the surfaces. Those divided areas are used in the calculation of longwave and reflected solar radiation. Hence, the accurate division into sunny and

shaded proportions of each uniform surface of building walls, vegetation and ground is one of the key tasks for radiation analysis in the outdoor urban area.

The sky view factor (ψ_{sky}) is a key variable in the estimation of diffuse beam solar and longwave radiation from the sky. Several methods to find ψ_{sky} have been tested: the geometric method (Oke 1981, Burt et al. 1982, Johnson and Watson 1984, Watson and Johnson 1987), the fisheye lens photographic method (Steyn 1980, Johnson and Watson 1984), computer analysis of fisheye lens photographs (Steyn et al. 1986, Clark and Follin 1988, Holmer 1992, Chapman et al. 2001, Grimmond et al. 2001, Holmer et al. 2001, Chapman and Thornes 2004, Gál et al. 2007) and 3D computer modeling (Dozier and Frew 1990, Fu and Rich 1999, Souza et al. 2003, Rodrigues et al. 2004, Rzepa and Gromek 2006). For continuously changing urban morphology, the fisheye lens photographic method is not applicable because the method can only simulate already built environments, meaning an unbuilt environment cannot be analyzed using the method because the environment does not exist in reality. 3D computer simulation is the best method for ψ_{sky} analysis when analyzing future urban environments. Gál et al. (2009) recently compared raster- and vector-based ψ_{sky} methods. They noted that there was no significant difference between the two methods, that the vector-based ψ_{sky} method could create more accurate results and that the raster-based method required significantly shorter time. Therefore, for dealing with a large area such as an entire city, a raster-based 3D computer simulation method that can analyze view factors of sunny and shaded surfaces of building walls, vegetation and the ground and ψ_{sky} at each location of outdoor urban areas will work well for the radiation analysis of complex outdoor urban settings.

Several computer software programs have been developed which can deal with ψ_{sky} as well as the shade effect: TownScope (Teller and Azar 2001, Azar 2004), RayMan (Matzarakis et al. 2000 & 2007), ENVI-met (Bruse and Fleer 1998, Bruse 1999 & 2008), Solar Analyst (Fu and Rich 1999), Urban Infoscapes (Richens 1997, Ratti and Baker 2003, Ratti and Richens 1999 & 2004, Ratti et al. 2006) and SOLWEIG (Lindberg et al. 2008).

The above 6 computer programs have their own advantages and disadvantages. In the radiation analyses of outdoor urban areas, many researchers have ignored vegetation, but vegetation has a much different surface temperature than buildings affecting longwave radiation analysis and a different

reflectivity and transmissivity for solar radiation. Therefore, the vegetation view factor has to be separated from the view factors of buildings and other structures in the sky hemisphere. For this reason, only two computer modeling programs, RayMan and ENVI-met, can be used in the comparison analysis with measured radiation data. Solar Analyst, Urban Infoscapes and SOLWEIG do not include the effect of vegetation[1]. TownScope considers the effect only in the calculation of direct and diffuse beam solar radiation receipt (Azar 2004).

ENVI-met has potential because it is raster-based and can include vegetation variables. A new version of ENVI-met 3.1 released in 2008 is raster (grid)-based freeware and can analyze ψ_{sky}, shading pattern, mean radiant temperature (T_{mrt}) and human thermal comfort index based on predicted mean vote (PMV, Fanger 1972). However, it can deal with only a small area up to a 250×250×30 grid. Also, the program is known to overestimate T_{mrt} during the morning up to 19 K and underestimate in the afternoon and night-time up to 9 K (Ali-Toudert 2005, p. 154, Fig. 5.16).

RayMan, although it is vector-based freeware, can analyze ψ_{sky}, T_{mrt} and thermal indices such as physiological equivalent temperature (PET, Höppe 1993 and 1999), PMV and Standard Effective Temperature (SET*, Gagge et al. 1986) and include vegetation. The program is very user friendly and has a detailed vegetation input interface. However, the program underestimated T_{mrt} at low sun altitudes, in the morning and afternoon in summertime and also at noon in October in Sweden (Thorsson et al. 2007).

Therefore, it is unclear how to adopt whole radiation exchange processes for human thermal exchange modeling in outdoor urban areas because of several constraints in urban area factors as well as the limitations of existing methods and programs.

The purpose of this chapter is to develop a new human-urban radiation exchange simulation model for outdoor urban area, combining the new human radiation exchange model (Park and Tuller model) from Chapter 3 and new urban area factors. The model will be tested with collected ψ_{sky} and radiation data at 5 locations in downtown Nanaimo, B.C., Canada and in a small park in downtown Changwon, Republic of Korea. Also, the existing 3D computer simulation programs (RayMan Pro and ENVI-met 3.1) will be tested with the same collected data, and their results will be compared with the results of the new model.

[1] The SOLWEIG model included the vegetation effect after this study (Lindberg and Grimmond 2011).

4.2 Methods

4.2.1 Study sites

To test accuracy and convenience of the urban radiation exchange model, the most urbanized area, the Central Business District (CBD), was chosen for its complex, high radiation exchanges and great possibility to create heat stress in summer. If an adequate method can be found in this area, the method will be easily adaptable to radiation exchange analysis of other urban land use types.

To conduct radiation exchange simulation, 5 locations (Nanaimo_1 to _5) and a square (Nanaimo_square) in downtown Nanaimo were chosen. 3D CAD (Computer Aided Design) computer files of the downtown area previously created by the Nanaimo Department of Engineering could be used conveniently in the simulation after changing vector-based CAD data to raster-based data. Nanaimo_1-4 are on a pedestrian passage along NE-SW tending streets and Nanaimo_5 is on a small square next to streets. Nanaimo_square is surrounded by buildings from 9 to 21 m high and located 50 m inside the streets (Fig. 4.1). Another study site is Changwon_smallpark in the centre of a small park in downtown Changwon, Republic of Korea (Fig. 4.2). The site is surrounded by buildings from 13 to 50 m high.

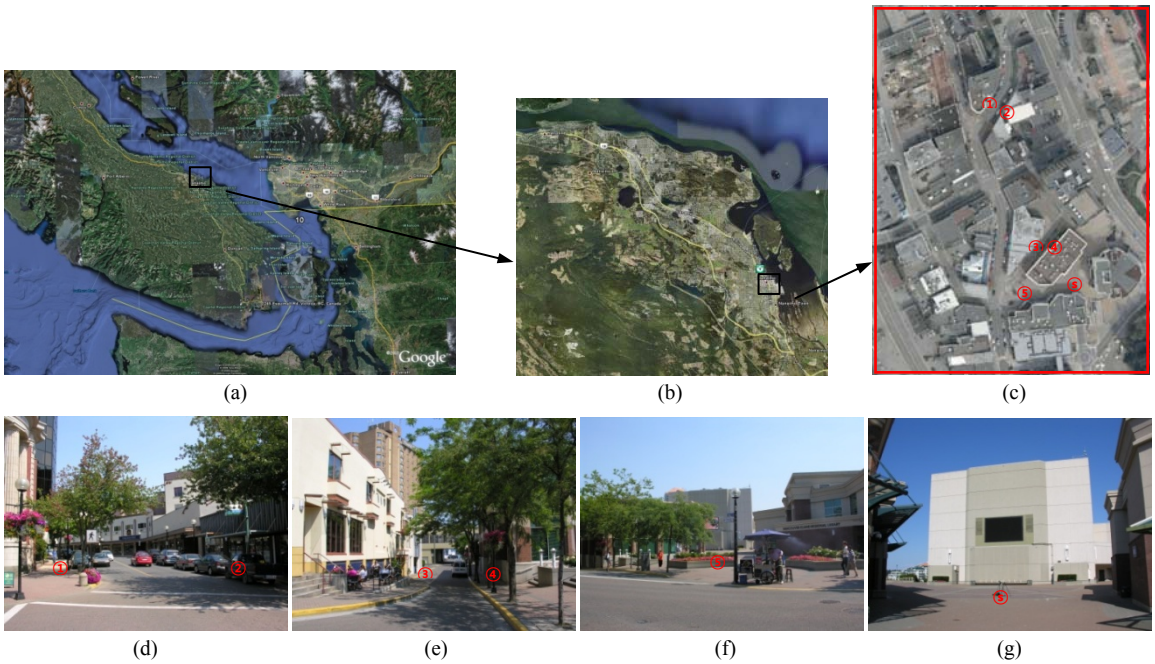

Fig. 4.1 Nanaimo study sites: downtown Nanaimo, B.C., Canada: (a) Nanaimo in small scale, (b) the city of Nanaimo, (c) Nanaimo Study site, (d) Nanaimo_1 & _2, (e) Nanaimo_3 & _4, (f) Nanaimo_5, (g) Nanaimo_square. (a)-(c) from Google maps and (d)-(g) from street photographs

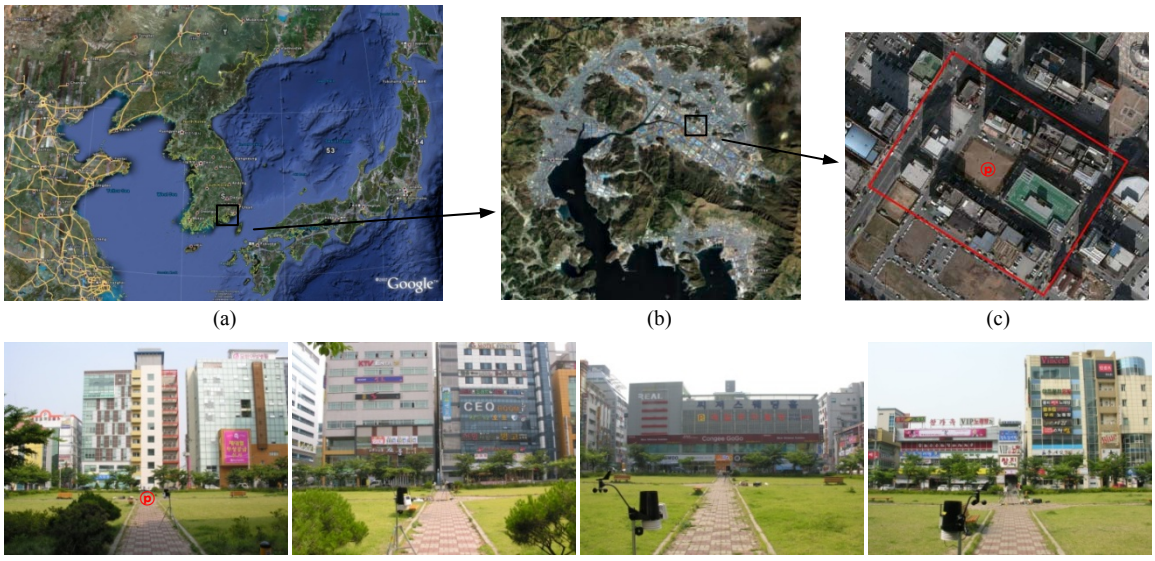

(a) (b) (c)

(d) (e) (f) (g)

Fig. 4.2 Changwon study site: small park in downtown Changwon, Republic of Korea: (a) Changwon in small scale, (b) the city of Changwon, (c) Changwon Study site, (d) northwest view, (e) northeast view, (f) southeast view, (g) southwest view. (a)-(b) from Google maps, (c) from air photographs and (d)-(g) from street photographs by direction

4.2.2 Materials

4.2.2.1 Meteorological data

Data collection dates in downtown Nanaimo were set to the time of greatest heat stress throughout the year, July and August (Table 4.1). Air temperature can be an indicator of the radiant environment. For data collection in downtown Changwon, June was selected instead of July or August because the latter two months are a rainy season in the Republic of Korea and the normal mean daily maximum air temperature at Masan meteorological centre, the nearest to Changwon, in June was close to that at Nanaimo Airport in July and August (Table 4.2).

Table 4.1 1971-2000 air temperature (T_a) normals at Nanaimo Airport, B.C., Canada[a]

T_a (°C)	Jan	Feb	Mar	Apr	May	Jun	**Jul**	**Aug**	Sep	Oct	Nov	Dec	Year
Daily Mean	2.7	4.2	6.1	8.8	12.3	15.2	17.9	18	14.8	9.7	5.4	2.9	9.8
Standard Deviation	1.6	1.5	1.1	1	1.2	1.1	1.1	1.1	1.2	0.8	1.6	1.7	0.6
Daily Maximum	6.2	8.2	10.9	14.1	17.8	20.5	**24**	**24.2**	20.9	14.6	9.1	6.1	14.7
Daily Minimum	-0.8	0	1.3	3.4	6.7	9.7	11.8	11.7	8.6	4.8	1.5	-0.4	4.9

[a] data source: Environment Canada, Canadian Climate Normals 1971-2000 (http://www.climate.weatheroffice.ec.gc.ca/climate_normals/index_e.html)

Table 4.2 1971-2000 normal air temperature (T_a) at Masan meteorological centre, the nearest station to Changwon, Republic of Korea[a]

T_a (°C)	Jan	Feb	Mar	Apr	May	**Jun**	Jul	Aug	Sep	Oct	Nov	Dec	Year
Daily Mean	2.8	4.5	8.6	14.0	18.3	21.6	25.3	26.6	22.8	17.4	11.0	5.3	14.9
Daily Maximum	7.4	9.3	13.5	19.2	23.3	**25.7**	28.8	30.3	27.0	22.4	15.9	10.4	19.4
Daily Minimum	-1.1	0.3	4.4	9.5	14.1	18.4	22.6	23.7	19.3	13.1	6.7	1.1	11.0

[a] data source: Korea Meteorological Administration, Average Climatic Data 1971-2000 (http://www.kma.go.kr/sfc/sfc_03_05.jsp)

To find albedos and surface temperatures of buildings, vegetation and ground surfaces, albedo tests were conducted in Nanaimo on August 6, 2008 (noon) and July 28, 2009 (morning, noon and afternoon). Surface temperatures were measured at the Nanaimo site on August 5, 2008 (noon) and July 26, 2009 (morning, noon and afternoon).

Radiation data collections were conducted on August 5, 2008 (noon) and on July 26, 2009 (morning, noon and afternoon) at the Nanaimo_1-5 locations and on July 27, 2009 (9:00–16:00) at Nanaimo_square. Changwon data were collected on June 11, 2009 (11:30–17:00). Two observation methods were used: a transect method for Nanaimo_1-5 and single, point source measurements for Nanaimo_square and Changwon_smallpark (see Table 4.3). The sky condition was clear and cloudless on all the data collection days.

Solar radiation was collected using 2 pyranometers (CMP 11 made by Kipp & Zonen, Delft, the Netherlands and Middleton EP08 made by Carter-Scott Design, Melbourne, Australia). The spectral ranges of the CMP 11 and Middleton EP08 are 285~2800 and 305~2850 nm, respectively. The sensitivity of the CMP 11 is 8.31 μV/Wm^{-2}. The accuracy of Middleton EP08 is 5 % and its sensitivity is 7.29 μV/Wm^{-2}. Total net all-wave radiation (incoming solar and longwave radiation minus outgoing solar and longwave radiation) was collected using a net radiometer (NR Lite made by Kipp & Zonen, Delft, the Netherlands) (Fig. 4.3a). Its spectral range is 200~100,000 nm, and its sensitivity is 13.8 μV/Wm^{-2}. The 2 pyranometers were installed oppositely, each pyranometer covered half a sphere (ground or sky hemisphere). The instruments were set 1.2 meters above the ground, and all radiation data were stored every 5 seconds in a CR23X micrologger (Campbell Scientific, Inc.). Radiation data at Nanaimo_1-5 were measured for about 10 minutes at each location, and the mean of the 5 second values over the period of observation was used in further analysis. Those at Nanaimo_square and Changwon_smallpark were done continually during the entire observation period at these stations, and the 1 minute mean taken at the even hour and half hour was

used in further analysis, i.e., 12:00 mean datum was calculated from 12:00:00 to 12:00:55. During the radiation measurements, surface temperature, wind speed, air temperature and humidity at each location were also measured. Surface temperatures of various building walls, the ground and vegetation surfaces were measured using an infrared thermometer (Raytek PM Plus made by Raytek, Santa Cruz, CA, USA; accuracy ± 0.5 °C). The emissivity of the infrared thermometer was set to 1.0, and the surface temperatures were read to one tenth of a degree Celsius. Several spots on an isothermal surface were measured mostly at a height of 3 meters above the ground and their mean values were used in this study. Wind speed was measured with a Kestrel 2000 Pocket Weather Meter (Nielsen-Kellerman, USA; accuracy ± 3 %) for 5 minutes at each Nanaimo_1-5 location and for 5 minutes every half an hour at Nanaimo_square and Changwon_smallpark. The instrument was held at 1.2 meters above the ground facing into the wind. The average wind speed value at each location is stated for information only and has no role in this study. Air temperatures and humidities were measured with a sling psychrometer (dry and wet bulb temperatures) (Sato Keiryoki MFO. Co., Ltd., Japan). These were also measured at the height of 1.2 meters and read to one tenth of a degree Celsius. To avoid radiation effects, the psychrometer was kept in a wooden box at a shaded location near a measurement location until use. The rapid spinning of the psychrometer ensures that turbulent exchanges between the thermometer bulbs and air greatly outweigh any radiation effects allowing the bulbs to reach equilibrium with air temperature and humidity. Fisheye lens photographs were taken to find ψ_{sky} using a Nikon Coolpix 8700 camera with Nikon FC-E9 Fisheye converter lens and Nikon UR-E18 converter adapter (Fig. 4.3b). The ψ_{sky} values were determined using the BMSky-view computer program (Gál et al. 2007).

(a) (b)

Fig. 4.3 Measuring instruments:
(a) pyranometers and net radiometer
(b) fisheye lens photograph equipment

4.2.2.2 Urban morphological data

Urban morphological data of study sites were obtained from the Nanaimo Department of Engineering and from the ECOGIS lab at Changwon National University (http://home.changwon.ac.kr/ecogis). These included 3D building shapes, road and pedestrian passages and digital elevation model files. Vegetation sizes and locations were measured *in situ* and input manually.

The provided urban morphological data were vector-based. To convert the height data to raster-based, the feature→raster conversion function of the ArcGIS 9.2 toolbox was used. The raster-based height data were exported to ASCII text files. Four input text files (ground height, obstruction height, ground type and building azimuth angle data) were made for each site. For further information, see 'How to prepare the four urban setting files' in Appendix B.

4.2.3 Theory of the new simulation model

The new computer program is Microsoft Windows-based, written using Microsoft Visual Basic 2008. Visual Basic is easy to learn, and it is simple to create a new program. Also, the language is used in ArcGIS which is widely used software for geographic information analysis.

The program consisted of time, geographical information, meteorological information, human area factor, urban setting and analysis, albedo and emissivity and simulation parts (Fig. 4.4). Basic input data are listed in Table 4.3. All results are exported as image files (sky view factors and radiation results) and text files [sky view factors from surfaces (c:\Skyviewfactor.txt), view factors at the height of 1.2 m without trees (c:\Obstructviewfactor.txt), view factors at the height of 1.2 m with trees and surface temperatures (c:\ViewfactorandTs.txt) and radiation and mean radiant temperature (T_{mrt}) results (c:\Radiationresult.txt)]. The manual for the model is attached in Appendix B. Important computer codes are shown in Appendix C.

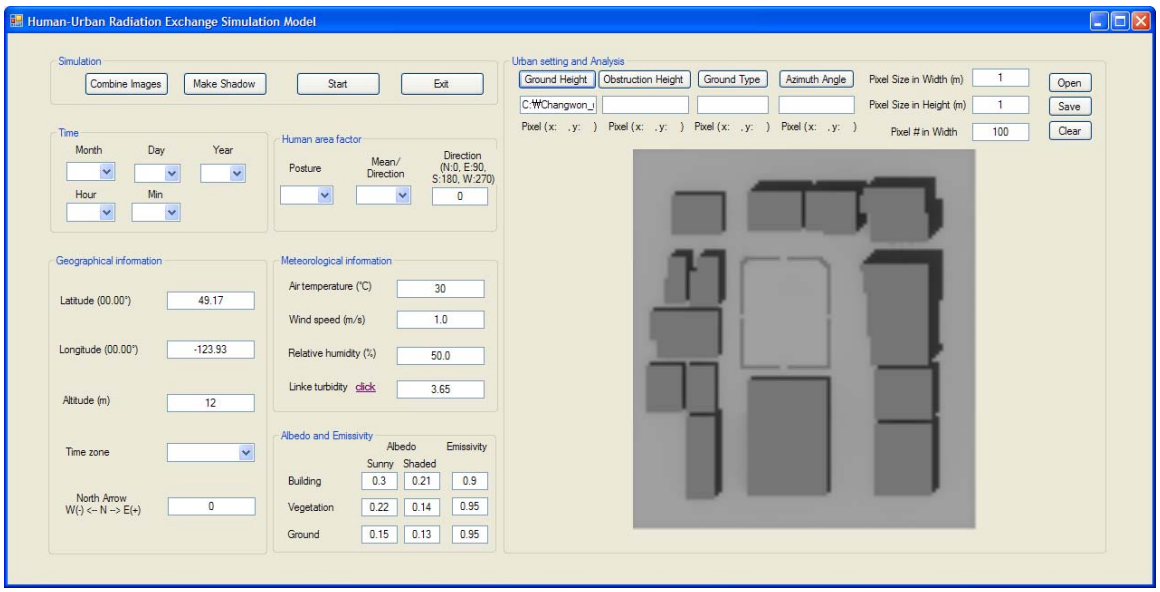

Fig. 4.4 Main window of the new human-urban radiation exchange simulation program

Table 4.3 Basic input data for the radiation simulation

	Nanaimo, B.C., Canada	**Changwon**, Republic of Korea
Latitude (°)	49°10’ N (49.17° N)	35°13’ N (35.22° N)
Longitude (°)	123°56’ W (123.93° W)	128°41’ E (128.68° E)
Altitude (m)	12	17
Time Zone	UTC-8/GMT-8	UTC+9/GMT+9
North Arrow Rotation Angle (°)	0	45
Dimensions (grid: x×y×z)	124×166×unlimited	95×105×unlimited
Grid size (m)	2×2×1	2×2×1

Aug.5, 2008					July 26, 2009					July 27, 2009					June 11, 2009				
Location	Time	Sunny/ Shady	T_a	*RH*	Location *Morning*	Time	Sunny/ Shady	T_a	*RH*	Location	Time	Sunny/ Shady	T_a	*RH*	Location	Time	Sunny/ Shady	T_a	*RH*
1	12:05	sunny	28.6	54.4	1	9:07	sunny	25.0	68.5	Square	9:00	Sunny	24.2	72.3	Small Park	11:30	sunny	28.1	36
2	12:27	shady	28.6	54.4	2	9:23	shady	24.2	71.4		10:00	Sunny	25.7	68.2		12:00	sunny	28.3	34
3	12:51	sunny	30.1	47.7	3	9:37	sunny	25.1	68.9		11:00	Sunny	27.0	64.4		12:30	sunny	28.7	33
4	13:12	shady	27.2	52.7	4	9:45	shady	25.0	68.5		12:00	Sunny	28.3	61.1		13:00	sunny	27.8	41
5	13:30	sunny	28.2	50.6	5	10:00	sunny	25.2	71.1		13:00	Sunny	30.4	56.9		13:30	sunny	27.9	41
4	13:48	shady	27.0	55.0	4	10:12	shady	25.5	67.7		14:00	Sunny	29.7	59.6		14:00	sunny	28.6	38
3	14:00	sunny	27.0	55.0	3	10:20	sunny	24.7	69.3		15:00	Sunny	31.2	55.7		14:30	sunny	29.3	40
2	14:20	shady	27.8	51.5	2	10:35	shady	24.9	69.3		16:00	Sunny	32.2	53.3		15:00	sunny	29.2	40
1	14:37	sunny	30.0	46.5	1	10:44	sunny	25.0	68.9							15:30	sunny	28.8	41
					Noon	Time	Sunny/ Shady	T_a	*RH*							16:00	sunny	28.8	44
					1	12:08	sunny	22.9	77.7							16:30	sunny	28.9	42
					2	12:14	shady	22.9	77.7							17:00	sunny	29.1	42
					3	12:34	sunny	26.0	70.0										
					4	12:46	shady	26.0	70.0										
					5	13:00	sunny	24.5	71.0										
					4	13:17	shady	26.0	67.4										
					3	13:23	sunny	28.1	63.0										
					2	13:36	shady	26.2	67.9										
					1	13:43	sunny	26.2	67.9										
					Afternoon	Time	Sunny/ Shady	T_a	*RH*										
					1	14:54	shady	25.0	72.4										
					2	15:09	sunny	25.0	72.4										
					3	15:18	shady	27.2	65.6										
					4	15:28	sunny	27.2	65.6										
					5	15:38	sunny	26.7	65.5										
					4	15:46	sunny	28.7	62.4										
					3	15:53	shady	28.7	62.4										
					2	16:05	sunny	25.3	68.1										
					1	16:11	shady	25.3	68.1										

4.2.3.1 *Creating a basic image file*

Two-digit-integer-numbers from four urban setting data text files were input into the four channels of a bitmap image: azimuth angle to alpha channel, ground height to red channel, obstruction height and ground type to green channel and 0 to blue channel. The value of green channel is obstruction height+(ground type×100). If a pixel represents a building, the green value has only building height. If it is a tree, the value has tree height+2×100. This simple way can divide three different ground types (open ground, building and tree): ground when green value is 0, building when it is between 1 and 99, and tree when it is over 200. The value of blue channel will be used later for shading results.

4.2.3.2 *Shading simulation*

Shading depends on the sun's azimuth (α) and altitude (β) angles which can be calculated through Eqs. 4.1-4.7 (VDI 2001):

$$\beta = \sin^{-1}[\sin\zeta\sin\delta + \cos\zeta\cos\delta\cos\omega] \quad (4.1)$$

$$\alpha = \cos^{-1}[(\sin\zeta\sin\beta - \sin\delta)/(\cos\zeta\cos\beta)] \quad (4.2)$$

$$\delta = \sin^{-1}[0.3978\sin(c - 77.51 + 1.92\sin c)] \quad (4.3)$$

$$c = 0.9856 \cdot J - 2.72 \quad (4.4)$$

$$\omega = (TLT - 720min) \cdot 0.25°/min \quad (4.5)$$

$$TLT = LT - (TimeZoneL - RealL) \cdot 4min/° + Z \quad (4.6)$$

$$Z = -7.66\sin c - 9.87\sin(2c + 24.99 + 3.83\sin c) \quad (4.7)$$

ζ is latitude of the observation point (°). δ is declination of the sun (solar zenith angle above the equator at noon on the day of observation) which varies between -23.44° at the winter solstice via 0° at the equinox to 23.44° at the summer solstice. α is set positive westwards of south=0° and negative eastwards. J is the Julian day (1 to 365 or 366 in the year). ω is solar hour angle (angle between the hour circle through the sun at the time of observation and the meridian). It is 0 at true solar noon, positive in the afternoon and negative in the morning. TLT is true local time in minutes. LT is mean local time in minutes of the observation site's time zone. *TimeZoneL* and *RealL* are central longitude of the time zone of the

observation point and real longitude of the observation point, respectively. *Z* is the equation of time, the difference between apparent and mean solar time. It ranges from -14 to +16 minutes.

Whether a ground surface is shaded or how much of a building/tree is shaded can be defined by comparison of the observation point with other points which are located between the observation point and the sun. When the location of the observation point is (x, y), the locations of other points ($x1$, $y1$) are:

$$x1 = x + i \tag{4.8}$$

$$y1 = y + (x1 - x) \times \tan(90 + \alpha) \tag{4.9}$$

when i is from 1 to n (image width). x, y and i are all integers. The angle of height difference between (x, y) and ($x1$, $y1$) is calculated:

$$eleangle = \tan^{-1}\left[\frac{(allheight1 - allheight)}{\sqrt{(x1 - x)^2 + (y1 - y)^2}}\right] \tag{4.10}$$

allheight and *allheight1* are the sum of ground height and obstruction height at (x, y) and ($x1$, $y1$).

When the observation point (x, y) is on the ground, if *eleangle* ≥ sun's altitude (β) angle the ground is shaded, and if *eleangle* < β the point is sunny. When the point is on a building or tree, if *eleangle* ≥ β angle the whole building/tree is shaded. If *eleangle* < β angle, *eleangle* is calculated repeatedly after *allheight* is reduced every 1 meter until *eleangle* ≥ β angle to find the proportion of shaded building/tree surface. These values are input to the blue channel of a bitmap image: 0 for sunny ground, 1 for shaded ground, 0 when the whole building/tree surface is sunny, and 1 or more for shaded building/tree height.

4.2.3.3 *View Factor (ψ)*

For view factor analysis, Johnson and Watson's (1984) fisheye lens photographic method modified from Steyn (1980) and Oke's (1987) basin equation and canyon and valley equation were tested with reference data from Raber and Hutchinson's (1947) chart and Johnson and Watson's (1984) equation/Watson and Johnson's (1987) chart in a simple urban model (Fig. 4.5).

Johnson and Watson's (1984) fisheye lens photographic method is for non-symmetrical canyons of finite length:

$$\psi_o = \frac{1}{2\pi} sin \frac{\pi}{2n} \sum_{i=0}^{n} sin\left[\frac{\pi(2i-1)}{2n}\right] \alpha_i \tag{4.11}$$

$$\psi_{sky} = 1 - \psi_o \tag{4.12}$$

The weighting factor for each annulus is:

$$\psi_o/\alpha_i = \frac{1}{2\pi} sin \frac{\pi}{2n} sin \left[\frac{\pi(2i-1)}{2n}\right] \tag{4.13}$$

ψ_o and ψ_{sky} are obstruction and sky view factors. ψ_o/α_i is the weighting factor of *i*-th annulus. π radians is 180° here. *n* is the number of annuli. α_i is the angular width (°) of the obstruction in the *i*-th annulus.

To use the method; firstly, the three-dimensional urban settings, buildings and trees, should be converted to a two dimensional, circular, fisheye lens photographic image. If there is a building or tree, its bottom will be located at the edge of the photograph and its top can be calculated using Steyn's (1980) equation (Fig. 4.6):

$$r = \frac{2R(90-\beta)}{\pi} \tag{4.14}$$

r is the radius from a center to its top. R is the radius of a fisheye lens photograph. β is building elevation angle.

ψ_o can be calculated in the computer simulation using Eq. 4.15:

$$\psi_o = \sum_{j=0}^{2\pi} \sum_{i=r}^{n} \frac{1}{2\pi} sin \frac{\pi}{2n} sin \left[\frac{\pi(2i-1)}{2n}\right] \alpha_i \tag{4.15}$$

In this study, the annuli were set to cover 300 meters which seemed enough distance for ψ_{sky} analysis in urban areas. For example; if a pixel width is 2 meters, the number of annuli will be 150. Two values of α_i were used: 5° and 10°. *j* is azimuth angle from 0° to 2π (360°), for example 72 azimuthal directions (2.5, 7.5·····352.5, 357.5°) for α_i = 5° and 36 azimuthal directions (5, 15·····345, 355°) for α_i = 10°. ψ_{sky} can be found by subtracting ψ_o from 1.0.

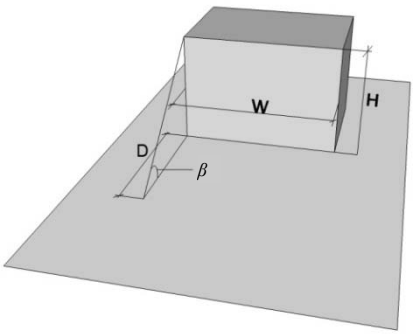

Fig. 4.5 A simple model for view factor analysis

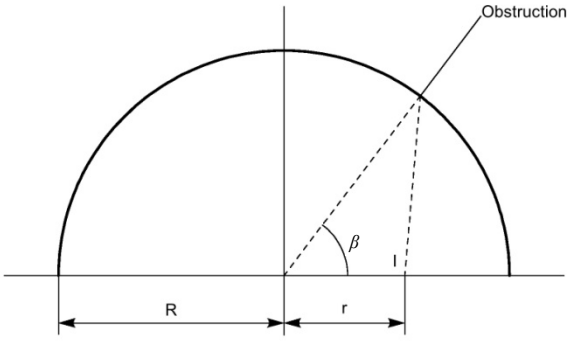

Fig. 4.6 Fisheye lens projection (equiangular). I = the top line of obstruction

Oke's (1987) equations are:

$$\psi_{sky} = \cos^2\beta \quad \text{for basin} \tag{4.16}$$

$$\psi_{sky} = \cos\beta \quad \text{for a symmetrical canyon or valley of infinite length} \tag{4.17}$$

$$\psi_o = 1 - \psi_{sky} \tag{4.18}$$

The reference values from Raber and Hutchinson's (1947) chart and Johnson and Watson's (1984) equation/Watson and Johnson's (1987) chart were well matched, only up to a 0.003 difference, and did not change when the building height increased (Table 4.4). However, computer programmed Johnson and Watson's (1984) fisheye lens photographic method and Oke's (1987) equations produced more errors, up to 0.095, when W/D (=H/D) values increased which means the observation point was closer to the building and the building was wider. Less errors occurred when the building height increased except Oke's (1987) canyon and valley equation which made more errors. Interestingly, computer programmed Johnson and Watson's (1984) every 10° method and Oke's (1987) basin equation created exactly the same results. Among the three ways, Johnson and Watson's (1984) 5° increment method was selected in the new model to analyze view factors. When the mean building height in urban CBD areas is 15 meters or over, the method has decreasing errors with increasing building heights and W/D (=H/D) ratios.

It should be noted here that H/D=W/D of 1/3 and 1/2 in the simulation are not very realistic in real urban settings because H/D≠W/D is usual at these ratios. However, the simulation was conducted to test how accurately the computer programmed codes could estimate view factors.

View factor analyses were conducted twice in this study. The first analysis was to find ψ_{sky} for estimating diffuse beam solar radiation incident on the building, tree and ground surfaces. This is needed to compute reflected solar radiation from each surface. The detailed process is explained later in section 4.2.3.4.1.3 on reflected solar radiation.

The second analysis was to find ψ_{sky} and view factors of building, tree and ground surfaces which were separated into sunny and shaded proportions. Also, the observation point was assumed at the height of 1.2 meters (mean height of the centre of the human body torso area) from the ground surface so that the surface view factors must be divided into two: upper surface view factors (upper-sunny-building surface view factor, upper-shaded-building surface view factor, upper-sunny-tree surface view factor, upper-shaded-tree surface view factor, upper-sunny-ground surface view factor and upper-shaded-ground surface

view factor) and lower surface view factors (lower-sunny-building surface view factor, lower-shaded-building surface view factor, lower-sunny-tree surface view factor, lower-shaded-tree surface view factor, lower-sunny-ground surface view factor and lower-shaded-ground surface view factor). The upper ground surface view factor is a visible proportion of ground located higher than the observation point. Those view factors were used to compute amounts of reflected solar radiation and longwave radiation from the surfaces.

Table 4.4 View factor test. Differences are the absolute differences with Johnson and Watson (1984) and Watson and Johnson (1987)

H[a] (m)	W/D[b] = H/D	Manual		Computer program							
		Raber and Hutchinson's (1947) chart	Johnson and Watson's (1984) equation/ Watson and Johnson's (1987) chart	Johnson and Watson's (1984) fisheye lens photographic method				Oke's (1987) equation			
								Basin		Valley and Canyon	
				5°	10°	Diff. with 5°	Diff. with 10°	5° & 10°	Diff.	5° & 10°	Diff.
6	6		0.797	0.702	0.710	0.095	0.087	0.710	0.087	0.843	0.046
	3	0.839	0.839	0.794	0.813	0.045	0.026	0.813	0.026	0.902	0.063
	2	0.873	0.876	0.850	0.843	0.026	0.033	0.843	0.033	0.918	0.042
	1	0.946	0.944	0.936	0.949	0.008	0.005	0.949	0.005	0.974	0.030
	1/2	0.987	0.986	0.987	0.984	0.001	0.002	0.984	0.002	0.992	0.006
	1/3	0.995	0.995	0.996	0.995	0.001	0.000	0.995	0.000	0.997	0.002
12	6		0.797	0.754	0.767	0.043	0.030	0.767	0.030	0.876	0.079
	3	0.839	0.839	0.820	0.816	0.019	0.023	0.816	0.023	0.903	0.064
	2	0.873	0.876	0.862	0.880	0.014	0.004	0.880	0.004	0.938	0.062
	1	0.946	0.944	0.944	0.949	0.000	0.005	0.949	0.005	0.974	0.030
	1/2	0.987	0.986	0.987	0.985	0.001	0.001	0.985	0.001	0.992	0.006
	1/3	0.995	0.995	0.995	0.995	0.000	0.000	0.995	0.000	0.997	0.002
24	6		0.797	0.782	0.769	0.015	0.028	0.769	0.028	0.877	0.080
	3	0.839	0.839	0.828	0.840	0.011	0.001	0.840	0.001	0.917	0.078
	2	0.873	0.876	0.874	0.880	0.002	0.004	0.880	0.004	0.938	0.062
	1	0.946	0.944	0.944	0.949	0.000	0.005	0.949	0.005	0.974	0.030
	1/2	0.987	0.986	0.987	0.985	0.001	0.001	0.985	0.001	0.992	0.006
	1/3	0.995	0.995	0.995	0.995	0.000	0.000	0.995	0.000	0.997	0.002

[a] H=building height (m)
[b] W=building segment width (m); D=distance between the observation point and the building surface, perpendicular to building surface (m)

4.2.3.4 *Analytical basic concept of radiation*

$$R^+ = K\downarrow + K\uparrow = {K_b}^+ + {K_d}^+ + {K_r}^+ = {K_b}^+ + {K_d}^+ + {K_{ro}}^+ + {K_{rveg}}^+ + {K_{rg}}^+$$

$$= \begin{Bmatrix} \frac{K_b}{sin\beta} t + K_d(\psi_{sky} + 0.3\psi_{veg\ in\ sky}) + (K_{bo\_slope} + K_{do\_slope})\psi_o a_o \\ +(K_{bveg\_slope} + K_{dveg\_slope})\psi_{veg} a_{veg} \\ +\left[(K_{bg\_slope} + K_{dg\_slope})\psi_g + \left({K_{ro}}^+ + {K_{rveg}}^+\right)(1 - \psi_{sky})\right] a_g \end{Bmatrix} \quad (4.19)$$

$$L^+ = L\downarrow + L\uparrow = {L_a}^+ + {L_o}^+ + {L_{veg}}^+ + {L_g}^+$$

$$= \begin{Bmatrix} \varepsilon_{sky}\sigma {T_a}^4 \psi_{sky} + \left[\varepsilon_o \sigma {T_o}^4 \psi_o + (1 - \varepsilon_o)\psi_{w-sky} {L_a}^+\right] \\ + \left[\varepsilon_{veg}\sigma {T_{veg}}^4 \psi_{veg} + (1 - \varepsilon_{veg})\psi_{w-sky} {L_a}^+\right] + \left[\varepsilon_g \sigma {T_g}^4 \psi_g + (1 - \varepsilon_g)\left({L_a}^+ + {L_o}^+ + {L_{veg}}^+\right)\right] \end{Bmatrix} \quad (4.20)$$

$$Q^* = R^* + L^* = \begin{Bmatrix} \left[f_p \cdot f_{eff} \cdot {K_b}^+ + \frac{1}{2} f_{eff}\left({K_d}^+ + {K_{ro}}^+ + {K_{rveg}}^+ + {K_{rg}}^+\right)\right](1 - \alpha_b) \\ + \frac{1}{2} f_{eff}\left({L_a}^+ + {L_o}^+ + {L_{veg}}^+ + {L_g}^+\right)\varepsilon_b \end{Bmatrix} \quad (4.21)$$

where R^+ and L^+ are solar and longwave radiation incident on the human body surface. Q^*, R^* and L^* are absorbed total, solar and longwave radiation on the human body surface. ${K_b}^+$, ${K_d}^+$ and ${K_r}^+$ are direct beam, diffuse beam and reflected solar radiation incident on the human body surface. ${K_r}^+$ is divided into ${K_{ro}}^+$, ${K_{rveg}}^+$ and ${K_{rg}}^+$ which are solar radiation reflected by buildings, trees and ground surfaces, respectively. t is transmissivity [obstructed by building=0, open sky=1 and obstructed by trees=0.15(spruce) to 0.75(willow) dependent on canopy density (Brown and Gillespie 1995)]. K_{bo_slope}, K_{bveg_slope} and K_{bg_slope} are direct beam solar radiation incident on building, tree and ground surfaces, respectively. K_{do_slope}, K_{dveg_slope} and K_{dg_slope} are diffuse beam solar radiation incident on building, tree and ground surfaces, respectively. ψ_{sky}, $\psi_{veg\ in\ sky}$, ψ_o, ψ_{veg} and ψ_g are view factors of sky, trees in the sky, buildings, trees and ground. ψ_{w-sky} is the view factor of sky seen from the building/tree surfaces. a_o, a_{veg}, a_g and a_b are albedos of buildings, trees, ground and human body surfaces. ${L_a}^+$, ${L_o}^+$, ${L_{veg}}^+$ and ${L_g}^+$ are longwave radiation coming from the sky, building and tree surfaces in the sky hemisphere and ground surface reaching the human body surface. ε_{sky}, ε_o, ε_{veg}, ε_g and ε_b are emissivities of the sky, building, tree, ground and human body surfaces. T_a, T_o, T_{veg} and T_g are air temperature and surface temperatures of buildings, trees and ground (K). In both solar and longwave radiation, re-reflected radiation (radiation received by the buildings and trees after being reflected from the surfaces that is then again reflected by the buildings and trees) was not included because its quantity is small. For example, when the biggest ${K_{rg}}^+$ and ψ_o in this study were 125 Wm^{-2} and 0.598 (sunny surface: 0.541, shaded surface: 0.057) at Nanaimo_3 at 12:34 P.M., July 26, 2009, re-reflected solar

radiation by building surfaces was only 10.0 Wm^{-2} (=0.3×125×0.267) when the view factor of ground seen from the building surface (ψ_{w-sky}) was calculated with Eq. 4.22 (Fig. 4.7):

$$\psi_{w-sky} = 0.7718{\psi_{sky}}^3 - 1.2046{\psi_{sky}}^2 + 0.8718\psi_{sky} + 0.0609 \quad (4.22)$$

The formula is a combination of Noilhan's (1981) ψ_{w-sky} formula for an infinite canyon and Oke's (1987) ψ_{sky} formula for a basin. In the formula, Oke's (1987) basin formula was used because his basin formula estimated more accurate view factors than his valley and canyon formula in the view factor test (Table 4.4).

Noilhan's (1981) ψ_{w-sky} formula is:

$$\psi_{w-sky} = \frac{1}{2}\left\{\frac{H}{D} + 1 - \left[\left(\frac{H}{D}\right)^2 + 1\right]^{1/2} / \left(\frac{H}{D}\right)\right\} \quad \text{for } H > 0 \quad (4.23)$$

where H is wall height and D is the perpendicular distance between a wall surface and the observation point (Fig. 4.5).

Oke's (1987) ψ_{sky} formula for a basin is:

$$\psi_{sky} = \cos^2\left[tan^{-1}\left(\frac{H}{D}\right)\right] \quad (4.24)$$

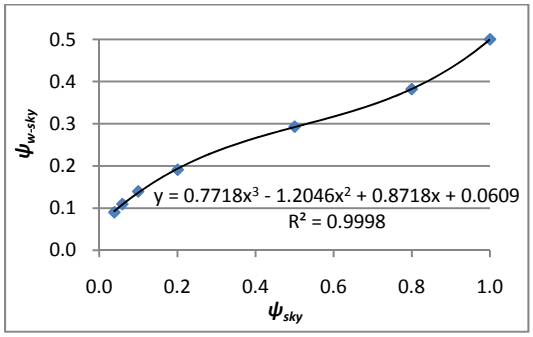

H/D	$\psi_{w\text{-}sky}$	ψ_{sky}
0	0.500	1.000
0.5	0.382	0.800
1	0.293	0.500
2	0.191	0.200
3	0.140	0.100
4	0.110	0.059
5	0.090	0.038

Fig. 4.7 Comparison between sky (ψ_{sky}) and wall-sky view factors (ψ_{w-sky})

4.2.3.4.1 *Solar radiation* (*R*)

4.2.3.4.1.1 Clear sky direct beam solar radiation (K_b)

$$K_b = K_{bo} \cdot k \cdot sin\beta \cdot \exp(-0.8662 \cdot \gamma \cdot T_L \cdot m) \quad \text{(Rigollier et al. 2000)} \quad (4.25)$$

K_{bo} is the solar constant (1367 Wm^{-2}). k is the adjustment to the solar constant for the variation of sun-earth distance (d) from its mean value ($\bar{d}$) during the year:

$$k = \left(\frac{\bar{d}}{d}\right)^2 = 1 + 0.03344 \cdot \cos(0.9856 \cdot J - 2.72) \quad \text{(VDI 2001)} \tag{4.26}$$

d is shortest near the beginning of January (k =1.034) and longest near the beginning of July (k =0.967). $\exp(-0.8662 \cdot \gamma \cdot T_L \cdot m)$ represents the direct beam transmittance under cloudless skies (Rigollier et al. 2000). m is the relative optical air mass that expresses the ratio of the optical path length of the solar beam through the atmosphere to the optical path length through a standard atmosphere at sea level with the sun at the zenith (Rigollier et al. 2000):

$$m = \left(\frac{p}{p_0}\right) / [\sin\beta + 0.50572(\beta + 6.07995)^{-1.6364}] \text{ (Kasten and Young 1989)} \tag{4.27}$$

$$\frac{p}{p_0} = \exp\left(-\frac{h}{8434.5}\right) \tag{4.28}$$

$$\beta = \beta_0 + \Delta\beta \tag{4.29}$$

$$\Delta\beta = 0.061359 \frac{0.1594 + 1.123\beta_0 + 0.065656{\beta_0}^2}{1 + 28.9344\beta_0 + 277.397{\beta_0}^2} \tag{4.30}$$

As the solar attitude decreases, the relative optical path length increases. The relative optical path length also decreases with increasing station height above sea level, h. β is the solar altitude (°) corrected from the original solar altitude (β_0) by the atmospheric refraction component ($\Delta\beta$) (Rigollier et al. 2000). γ is defined as the integrated optical thickness of the terrestrial atmosphere free of clouds, water vapour and aerosols (Rigollier et al. 2000):

$$\gamma = 1/(6.6296 + 1.7513m - 0.1202m^2 + 0.0065m^3 - 0.00013m^4) \text{ if } m \leq 20 \ (\beta_0 \geq 1.9°)$$

$$\gamma = 1/(10.4 + 0.718m) \text{ if } m > 20 \ (\beta_0 < 1.9°) \quad \text{(Kasten 1996)} \tag{4.31}$$

T_L is the Linke turbidity factor that is used to characterize the degree of transparency of the atmosphere and represents the number of clean, dry atmospheres necessary to produce the observed attenuation, resulting from the additional and highly variable effects of water vapour and aerosols (Ineichen and Perez 2002). This can be found in the Soda-is website (http://www.soda-is.com/eng/ services/climat_free_eng.php) (Polo et al. 2009). Monthly mean T_L values of the Nanaimo (49º10'N, 123º56'W) and Changwon (35º13'N, 128º41'E) sites are listed in Table 4.5. In this study, the data collection dates in Nanaimo were July 26 and 27, 2009. The mean of July and August, 3.65, was used in the simulation. For Changwon, the June T_L value, 4.2, was used.

Table 4.5 Monthly mean Linke turbidity factors (T_L) of study sites, Nanaimo and Changwon, in 2009

Month	1	2	3	4	5	6	7	8	9	10	11	12	Mean
Nanaimo	2.6	3.1	3.1	3.4	3.7	3.3	3.4	3.9	3.3	3.0	3.0	2.7	3.2
Changwon	2.1	2.3	3.1	3.5	3.8	4.2	4.8	4.7	4.1	3.4	2.7	2.4	3.4

4.2.3.4.1.2 Diffuse beam solar radiation (K_d)

K_d can be estimated with the formula modified from Rigollier et al. (2000):

$$K_d = K_{d\_iso} + K_{d\_aniso} = t_r(K_{bo} \cdot k \cdot T_{rd} \cdot F_d) + (1 - t_r)(K_{bo} \cdot k \cdot T_{rd} \cdot F_d) \quad (4.32)$$

$$t_r = \exp(-0.8662 \cdot \gamma \cdot T_L \cdot m) \quad (4.33)$$

$$T_{rd} = -1.5843\times10^{-2}+3.0543\times10^{-2}\ T_L+3.797\times10^{-4}\ T_L^2 \quad (4.34)$$

$$F_d = A_0+A_1\sin\beta+A_2(\sin\beta)^2 \quad (4.35)$$

$$A_0 = 2.6463\times10^{-1}-6.1581\times10^{-2}\ T_L+3.1408\times10^{-3}\ T_L^2 \quad (4.36)$$

$$A_1 = 2.0402+1.8945\times10^{-2}\ T_L-1.1161\times10^{-2}\ T_L^2 \quad (4.37)$$

$$A_2 = -1.3025+3.9231\times10^{-2}\ T_L+8.5079\times10^{-3}\ T_L^2 \quad (4.38)$$

K_d is composed of isotropic (K_{d_iso}) and anisotropic (K_{d_aniso}) sky parts divided by the sun's location because the intensity of skylight is not distributed uniformly in a clear sky. K_d around the sun is much greater than elsewhere. T_{rd} is the diffuse transmission function at the zenith. It depends on turbidity. If the turbidity decreases which means it is a very clean atmosphere, T_{rd} will decrease. F_d is the diffuse angular function depending on the solar altitude angle. Both the T_{rd} and F_d equations are defined for an optical air mass (m) of 2. A_0, A_1 and A_2 are coefficients dependent on the Linke turbidity factor (T_L).

4.2.3.4.1.3 Reflected solar radiation (K_r) from buildings (K_{ro}), trees (K_{rveg}) and ground (K_{rg}) surfaces

To compute quantities of reflected solar radiation (K_r), direct beam (K_{b_slope}) and diffuse beam (K_{d_slope}) incident on each slope must first be calculated. The result is then multiplied by each surface's albedo (a):

$$K_r = (K_{b\_slope} + K_{d\_slope})a \quad (4.39)$$

Equations of K_{b_slope} and K_{d_slope} can be estimated with Oke's (1987) equation:

$$K_{bo\_slope} = K_b{}^+ cosZ_{sl} = K_b{}^+[cosz \cdot cosA + sinz \cdot sinA \cdot cos(\alpha - \quad_{sl})]$$

$$= K_b{}^{+}[sinz \cdot cos(\alpha - \alpha_{sl})]$$

$$= K_b{}^{+}[cos\beta \cdot cos(\alpha - \alpha_{sl})] \quad \text{for building surfaces,} \quad (4.40)$$

$$K_{bveg\_slope} = K_b{}^{+}(sin\beta + cosZ_{sl})/2$$

$$= \frac{K_b{}^{+}[sin\beta + cos\beta \cdot cos(\alpha - \alpha_{sl})]}{2} \quad \text{for tree surfaces,} \quad (4.41)$$

$$K_{bg\_slope} = K_b{}^{+}sin\beta \quad \text{for ground surfaces} \quad (4.42)$$

$$K_{d\_slope} = K_d\psi_{sky} \quad \text{for all surfaces} \quad (4.43)$$

Z_{sl} is the angle between the perpendicular to the slope and the sun. z is the zenith angle of the sun. A is the slope angle. If it is a building surface (A = 90°), $cosA = 0\ and\ sinA = 1$. If it is a horizontal ground surface (A = 0°), $cosA = 1\ and\ sinA = 0$. α is the azimuth angle of the sun (from North) and α_{sl} is the azimuth angle of the slope (from North). Tree surfaces were assumed half horizontal and half vertical. For the ψ_{sky} simulation here, the simulation points for building and tree surfaces were set at half their height to get a mean ψ_{sky} between their bottom and top. The mean ψ_{sky} values were used as representative values of each building or tree surface for further radiation analysis. K_{d_slope} can be expressed as K_{do_slope} for building surfaces, K_{dveg_slope} for tree surfaces and K_{dg_slope} for ground surfaces with different ψ_{sky} values obtained for each surface. Therefore, reflected solar radiation by building (K_{ro}), tree (K_{rveg}) and ground (K_{rg}) surfaces can be stated as:

$$K_{ro} = \left(K_{bo\_slope} + K_{do\_slope}\right)a_o \quad (4.44)$$

$$K_{rveg} = \left(K_{bveg\_slope} + K_{dveg\_slope}\right)a_{veg} \quad (4.45)$$

$$K_{rg} = \left(K_{bg\_slope} + K_{dg\_slope}\right)a_g \quad (4.46)$$

where a_o, a_{veg} and a_g are albedos of building, tree and ground surfaces.

Previous results of albedos of typical urban materials are listed in Table 4.6. However, the ranges are too broad, and it is difficult for people to choose adequate albedo values for their simulations. For this study, albedo tests were conducted on August 6, 2008 (noon) and July 28, 2009 (morning, noon and afternoon). Albedos of 6 wall materials, 3 ground materials and vegetation (trees) were measured 124 times, 66 on sunny materials and 58 on shaded (Table 4.7).

Table 4.6 Radiative properties of typical urban materials and areas [modified from Oke (1987, p. 281) and Arnfield (1982, p. 104)]

Surface		Albedo		Emissivity
		Oke (1987)	Arnfield (1982)	Oke (1987)
Road	Asphalt	0.05–0.20	0.10	0.95
Wall	Concrete	0.10–0.35	0.27	0.71–0.90
	Brick	0.20–0.40	Red: 0.32 Yellow(buff): 0.40 White(cream): 0.60	0.90–0.92
	Stone	0.20–0.35	0.32	0.85–0.95
	Wood			0.90
Roof	Tar and gravel	0.08–0.18	0.14	0.92
	Tile	0.10–0.35		0.90
	Slate	0.10		0.90
	Thatch	0.15–0.20	Shingle: 0.25	
	Corrugated iron	0.10–0.16		0.13–0.28
Window	Clear glass zenith angle less than 40°	0.08	0.09	0.87–0.94
	Zenith angle 40 to 80°	0.09–0.52		0.87–0.94
Paint	White, whitewash	0.50–0.90	0.69	0.85–0.95
	Red, brown, green	0.20–0.35		0.85–0.95
	Black	0.02–0.15	Dark: 0.28	0.90–0.98
Urban area	Range	0.10–0.27		0.85–0.96
	Mean	0.15		~0.95

The mean albedo of wall materials was 0.25 (25 %) from the mean albedo of sunny materials, 0.3 (30 %), and of shaded materials, 0.21 (21 %) (Table 4.8). Vegetation had a slightly lower mean albedo of 0.2 (20 %) than that of wall materials from 0.22 (22 %) sunny and 0.14 (14 %) shaded. Ground had much lower mean albedo of 0.11 (11 %) and similar results for sunny, 0.11 (11 %), and shaded, 0.12 (12 %). However, the variation among materials was large. For example, stucco, 0.4 (40 %), as wall material and concrete, 0.15 (15 %), as ground material had almost twice the mean albedos as brick, 0.21 (21 %), and asphalt, 0.07 (7 %), respectively. Also, some weird albedo values were obtained. The window and tree albedos at Nanaimo_1 on July 28 noon time were 0.71 (71 %) and 0.61 (61 %), respectively, which were much higher than mean values, 0.2 (20 %) for the sunny window surface and 0.21 (21 %) for the sunny tree surface. These unusually high values were excluded in the calculation.

For better simulations, adapting adequate albedo values for each surface instead of using mean values is definitely the best choice but, in reality, figuring out correct values and inputting them for each surface is laborious and time-consuming. In this study, mean albedos of sunny and shaded walls and vegetation were used. Mean albedos of concrete ground surfaces [sunny: 0.15 (15 %) and shaded: 0.13 (13 %)] were used because concrete is the most common urban sidewalk material.

Table 4.7 Number of urban surface albedo measurements

Materials \ Time		Aug. 6, 2008			July 28, 2009									All		
		Noon			Morning			Noon			Afternoon					
		Sunny	Shaded	All	Sunny	Shaded	All	Sunny	Shaded	All	Sunny	Shaded	All	Sunny	Shaded	All
Wall	Brick	1	2	3	2	3	5	1	3	4	2	3	5	6	11	17
	Stucco	1	1	2	3	3	6	4	2	6	2	5	7	10	11	21
	Concrete		2	2	2	1	3	3	1	4	1	3	4	6	7	13
	Tile				1	1	2	1	1	2	1	1	2	3	3	6
	Window	3	4	7	2	2	4	3	3	6		6	6	8	15	23
	Wood		1	1		1	1		1	1		1	1	0	4	4
Vegetation					3		3	2		2	1	1	2	6	1	7
Ground	Brick	8	3	11	1		1	4		4	4		4	17	3	20
	Asphalt	1		1	1		1	1		1	1		1	4	0	4
	Concrete	1	1	2	1		1	1		1	3	2	5	6	3	9
Total		15	14	29	16	11	27	20	11	31	15	22	37	**66**	**58**	**124**

Table 4.8 Albedos of urban surfaces

Materials			Aug. 6, 2008 Noon Max.	Min.	Mean Sunny	Mean Shaded	Mean All	July 28, 2009 Morning Max.	Min.	Mean Sunny	Mean Shaded	Mean All	Noon[a] Max.	Min.	Mean Sunny	Mean Shaded	Mean All	Afternoon Max.	Min.	Mean Sunny	Mean Shaded	Mean All	Mean of Materials Sunny	Shaded	All	Mean of Wall, Vegetation and Ground Sunny	Shaded	All
Wall	Brick	Red	0.30	0.16	0.30	0.16	0.23	0.27	0.19	0.27	0.19	0.23				0.27	0.27	0.28	0.15	0.21	0.22	0.21	0.26	0.21	0.24			
		Brown				0.19	0.19	0.18	0.13	0.18	0.15	0.16	0.25	0.20	0.25	0.21	0.22	0.27	0.10	0.27	0.10	0.18	0.23	0.16	0.19			
		Mean			0.30	0.18	0.22			0.23	0.16	0.19			0.25	0.23	0.23			0.24	0.18	0.20	**0.26**	**0.19**	**0.21**			
	Stucco	Ivory			0.69		0.69	0.47	0.34	0.47	0.34	0.40	0.58	0.55	0.58	0.55	0.56	0.52	0.49		0.51	0.51	0.58	0.47	0.54			
		Grey				0.26	0.26	0.41	0.30	0.41	0.30	0.35	0.46	0.25	0.36		0.36	0.34	0.16	0.21	0.34	0.25	0.33	0.30	0.31			
		Yellow								0.50		0.50			0.47		0.47				0.30	0.30	0.49	0.30	0.42	**0.30**	**0.21**	**0.25**
		Brown									0.12	0.12				0.24	0.24				0.31	0.31		0.22	0.22			
		Mean			0.69	0.26	0.47			0.46	0.25	0.36			0.44	0.39	0.42			0.21	0.39	0.34	**0.45**	**0.32**	**0.40**			
	Concrete		0.28	0.22		0.25	0.25	0.22	0.16	0.19	0.19	0.19	0.46	0.11	0.28	0.24	0.27	0.25	0.14	0.25	0.15	0.18	**0.24**	**0.21**	**0.22**			
	Tile (orange brown)							0.26	0.24	0.26	0.24	0.25	0.41	0.25	0.41	0.26	0.33	0.41	0.11	0.41	0.11	0.26	**0.36**	**0.20**	**0.28**			
	Window		0.22	0.08	0.15	0.15	0.15	0.41	0.09	0.26	0.12	0.19	0.20	0.12	0.20	0.15	0.17	0.31	0.08		0.22	0.22	**0.20**	**0.16**	**0.18**			
	Wood (beige brown)					0.10	0.10				0.16	0.16				0.21	0.21				0.25	0.25		**0.18**	**0.18**			
Vegetation			0.17	0.13	0.16		0.16	0.25	0.16	0.21		0.21			0.21		0.21	0.28	0.14	0.28	0.14	0.21	**0.22**	**0.14**	**0.20**	**0.22**	**0.14**	**0.20**
Ground	Brick	Red	0.18	0.09	0.12	0.14	0.13								0.08		0.08	0.11	0.09	0.10	0.10	0.10	0.10	0.12	0.10			
		Dark Red			0.09		0.09																0.09		0.09			
		Brown			0.17		0.17																0.17		0.17			
		Dark Brown			0.08		0.08																0.08		0.08			
		Grey	0.13	0.10	0.10	0.13	0.11				0.10	0.10	0.11	0.08	0.10		0.10	0.14	0.10	0.14	0.10	0.12	0.11	0.11	0.11	**0.11**	**0.12**	**0.11**
		Orange													0.08		0.08			0.15		0.15	0.12		0.12			
		Mean			0.11	0.13	0.12				0.10	0.10			0.09		0.09			0.12		0.12	**0.11**	**0.12**	**0.11**			
	Asphalt				0.07		0.07			0.08		0.08			0.07		0.07			0.07		0.07	**0.07**		**0.07**			
	Concrete		0.16	0.15	0.16	0.15	0.15			0.16		0.16			0.15		0.15	0.16	0.09	0.12	0.10	0.11	**0.15**	**0.13**	**0.14**			

[a] The albedos of window and trees at location 1 at noon were 0.71 and 0.61, respectively. These values were excluded because they were unusually high and likely erroneous.

4.2.3.4.2 *Longwave radiation* (*L*)

In longwave radiation analysis, sky emissivity (ε_{sky}) and surface temperatures of buildings, vegetation and the ground are key variables.

4.2.3.4.2.1 Sky emissivity (ε_{sky})

Prata (1996)'s sky emissivity formula for clear sky conditions is used:

$$\varepsilon_{sky} = 1 - \left(1 + 46.5\frac{e_a}{T_a}\right) \times \exp\left[-\left(1.2 + 3.0 \times 46.5\frac{e_a}{T_a}\right)^{0.5}\right] \quad (4.47)$$

but, Jonsson et al. (2006) found the formula overestimated by 0.04 during daytime. In this study, 0.04 was subtracted from the ε_{sky} values of the formula. Vapour pressure (e_a) is calculated with Antoine's equation (Parsons 1993):

$$e_a = RH \times \exp\left(18.956 - \frac{4030.18}{T_a + 235}\right) \text{ (hPa)} \quad (4.48)$$

4.2.3.4.2.2 Surface temperature

Another limitation of existing methods is to find the surface temperature which is a required variable to estimate the quantity of longwave radiation emitted from building, tree or ground surfaces. Surface temperature is always changing dependent on radiation, latent and sensible heat flux densities and the thermal properties of the materials.

Longwave radiation from the ground surface (L_g) without any obstruction in the sky hemisphere is the sum of emitted longwave radiation from the ground surface created by the ground surface emissivity (ε_g) and temperature (T_g) and longwave radiation from the sky hemisphere reflected by the ground surface (Oke 1987):

$$L\uparrow = L_g + (1-\varepsilon_g)L\downarrow = \varepsilon_g \sigma {T_g}^4 + (1-\varepsilon_g)L\downarrow \quad (4.49)$$

Frequently, the T_g effect is approximated by using T_a which is widely available in climate data. Sellers (1965) approximated the first term of the L_g equation:

$$\varepsilon_g \sigma {T_g}^4 \approx \varepsilon_g \sigma {T_a}^4 + 4\varepsilon_g \sigma {T_a}^3 (T_g - T_a) \quad (4.50)$$

Later, Holtslag and van Ulden (1983) compared measured net radiation (Q) data on a grass surface when mean cloud cover was 50 % with the second term of Sellers's (1965) equation:

$$4\varepsilon_g \sigma {T_a}^3 (T_g - T_a) = 0.12Q \quad (4.51)$$

Offerle et al. (2003) modified Eq. 4.51 by including surface albedo and changing Q to total incoming solar radiation from the sky hemisphere ($K\downarrow$):

$$L\uparrow = L_g + (1-\varepsilon_g)L\downarrow = \varepsilon_g \sigma {T_g}^4 + (1-\varepsilon_g)L\downarrow = \varepsilon_g \sigma {T_a}^4 + 0.08K\downarrow (1-a_g) + (1-\varepsilon_g)L\downarrow \quad (4.52)$$

$$\varepsilon_g \sigma {T_g}^4 + (1-\varepsilon_g)L\downarrow = \varepsilon_g \sigma {T_a}^4 + 0.08\left(K_{bg\_slope} + K_{dg\_slope}\right)(1-a_g) + (1-\varepsilon_g)L\downarrow \quad (4.53)$$

$$T_g = \sqrt[4]{{T_a}^4 + \frac{0.08(K_{bg\_slope} + K_{dg\_slope})(1-a_g)}{\varepsilon_g \sigma}} \quad (4.54)$$

With a_g = 0.15, $K\downarrow$ = 1000 Wm^{-2} and T_a = 300 K, the correction is equivalent to $T_g - T_a$ = 11 K on a dry surface (Offerle et al. 2003).

The other surface temperatures, T_o and T_{veg}, can be obtained from the same formula for T_g with different values of solar radiation incident on the surface and also different albedos:

$$T_o = \sqrt[4]{{T_a}^4 + \frac{0.08(K_{bo\_slope} + K_{do\_slope})(1-a_o)}{\varepsilon_o \sigma}} \quad (4.55)$$

$$T_{veg} = \sqrt[4]{{T_a}^4 + \frac{0.08(K_{bveg\_slope} + K_{dveg\_slope})(1-a_{veg})}{\varepsilon_{veg} \sigma}} \quad (4.56)$$

To test how well the equations work, measured surface temperatures on August 5 (noon) and July 26 (morning, noon and afternoon) were compared with the results of Eqs. 4.54-4.56. In this study, ε_g and ε_{veg} are assumed to be 0.95 and ε_o 0.9, which were used in urban energy studies (Masson 2000, Lemonsu et al. 2004). Mean albedos (a_o = 0.3, a_g = 0.11 and a_{veg} = 0.22) of sunny building, ground and vegetation surfaces were used instead of 0.08. Mean sunny ground surface albedo (0.11) was used instead of sunny concrete ground surface albedo (0.15) used for the reflected solar radiation analysis because the two study sites had more brick ground surfaces.

During the two days at the Nanaimo site, 147 urban surface temperatures were measured, 71 on sunny surfaces and 76 on shaded (Table 4.9). Measured surface temperatures on the sunny surfaces were

compared with the results of Eqs. 4.54-4.56 (Table 4.10). The formula mean estimates were 8.3 K and 2.6 K less on the ground and wall surfaces, respectively, and 1.2 K more on the vegetation surfaces. The absolute mean difference of all surfaces was 7.3 K: ground surface, 8.7 K; vegetation surface, 5.3 K; and wall surfaces, 2.6 K. The formulas made large differences, up to 15.9 K on the asphalt surface around noon. Ground and vegetation surfaces had greater differences around noon than morning and afternoon. Conversely, wall surfaces had less differences around noon. This shows the effect of the sun angle more perpendicular on the vertical wall surfaces for direct beam solar radiation. Some surfaces had lower surface temperatures than the formulas'.

The shaded surface temperatures were close to air temperatures (Table 4.11), so they were compared with air temperatures, not the results of Eqs. 4.54-4.56. Only the vegetation surface had a difference greater than 1 K, 1.3 K more, and wall and ground surfaces had only 0.4 K differences. However, the absolute mean difference of all surfaces was 2.4 K: ground surface, 3.6 K; wall surface, 1.7 K; and vegetation surface, 1.3 K. The largest difference between them was from the ground surfaces during the afternoon of July 26, up to 7.9 K, on brick and small gravel concrete. All surfaces had greater differences in the afternoon, and vegetation surfaces had a large mean difference in the morning, too.

To modify surface temperature estimation, those differences dependent on time on sunny and shaded surfaces should be included. Mean morning, noon and afternoon differences on July 26, 2009, at the Nanaimo_5 station were plotted (Fig. 4.8). Best-fit polynomial equations of each sunny and shaded surface were found. The differences estimated by the equations were added to surface temperatures predicted by Eqs. 4.54-4.56.

Table 4.9 Number of urban surface temperature measurements

Materials \ Time		Aug. 5, 2008			July 26, 2009									All		
		Noon			Morning			Noon			Afternoon					
		Sunny	Shaded	All	Sunny	Shaded	All	Sunny	Shaded	All	Sunny	Shaded	All	Sunny	Shaded	All
Wall	Brick	2	3	5	1	3	4		3	3	3	1	4	6	10	16
	Concrete	1	1	2	1	2	3	1	2	3	1	1	2	4	6	10
	Cement	1	3	4		1	1				1		1	2	4	6
	Stucco	1	2	3	2	2	4	2	2	4	2	2	4	7	8	15
	Window	2	4	6	2		2	1	1	2				5	5	10
	Tile	1		1										1		1
	Wood		1	1		2	2		2	2	1	1	2	1	6	7
Vegetation		3		3	3	1	4	1	1	2	1	2	3	8	4	12
Ground	Brick	4	2	6	4	6	10	5	4	9	5	4	9	18	16	34
	Small gravel concrete	2	1	3	2		2	2		2	3	3	6	9	4	13
	Concrete	1		1		2	2		3	3	2	1	3	3	6	9
	Cement		2	2											2	2
	Asphalt	1		1	2	2	4	2	1	3	2	2	4	7	5	12
Total		19	19	38	17	21	38	14	19	33	21	17	38	**71**	**76**	**147**

Table 4.10 Differences between measured sunny ground, wall and vegetation surface temperatures and those estimated using Offerle et al.'s (2003) formulas (Eqs. 4.54-4.56): measured minus estimated (K)

Time \ Materials			Wall								Veg.	Ground						Mean
			Brick	Concrete	Cement	Stucco	Window	Tile	Wood	Mean		Brick	Small gravel concrete	Concrete	Cement	Asphalt	Mean	
Aug. 5, 2008	Mean	Noon	11.6	2.6	-6.8	-5.9	4.9	13.6		3.3	-7.9	7.0	8.1	9.9		-2.9	5.5	3.1
July 26, 2009	Mean	Morning	11.1	-1.5		-1.4	5.1			3.3	-1.7	0.9	3.9			6.5	3.8	2.9
		Noon		-0.9		-0.4	3.1			0.6	8.1	12.8	13.3			15.9	14.0	7.4
		Afternoon	3.2	0.3	-2.2	-0.1			13.8	3.0	-3.6	10.0	9.4	8.2		12.9	10.1	5.2
		All day	7.2	-0.7	-2.2	-0.6	4.1		13.8	2.3	1.0	7.9	8.9	8.2		11.7	9.3	5.2
Mean			8.6	0.1	-4.5	-1.9	4.4	13.6	13.8	**2.6**	**-1.2**	7.7	8.7	9.0		8.1	**8.3**	**4.6**
Absolute mean			8.6	1.3	4.5	1.9	3.3	13.6	13.8	**2.6**	**5.3**	7.7	8.7	9.0		9.5	**8.7**	**7.3**

Table 4.11 Differences between measured shaded ground, wall and vegetation surface temperatures and air temperature: T_a minus T_g, T_o or T_{veg} (K)

Time \ Materials			Wall								Veg.	Ground						Mean
			Brick	Concrete	Cement	Stucco	Window	Tile	Wood	Mean		Brick	Small gravel concrete	Concrete	Cement	Asphalt	Mean	
Aug. 5, 2008	Mean	Noon	-1	-0.4	2.1	-1.1	1.4		-3.2	-0.4		5.1	-2		4.2		2.4	0.6
July 26, 2009	Mean	Morning	0.3	-0.3	1.2	-1			-1.2	-0.2	1.9	1		1.2		1.2	1.1	0.5
		Noon	0	1.1		0.4	-0.7		-0.8	0	0.1	1.6		1.8		1	1.5	0.5
		Afternoon	-1.5	-2.9		0.6			-5.5	-2.3	1.9	-7.9	-7.9	-3.1		-5.9	-6.2	-3.6
		All day	-0.4	-0.7	1.2	0	-0.7		-2.5	-0.5	1.3	-1.8	-7.9	0		-1.2	-2.7	-1.2
Mean			-0.6	-0.6	1.7	-0.3	0.3		-2.7	**-0.4**	**1.3**	-0.1	-5	0	4.2	-1.2	**-0.4**	**-0.2**
Absolute mean			2.4	1.2	1.7	0.8	1.6		2.7	**1.7**	**1.3**	4.0	5.0	2.0	4.2	3.0	**3.6**	**2.4**

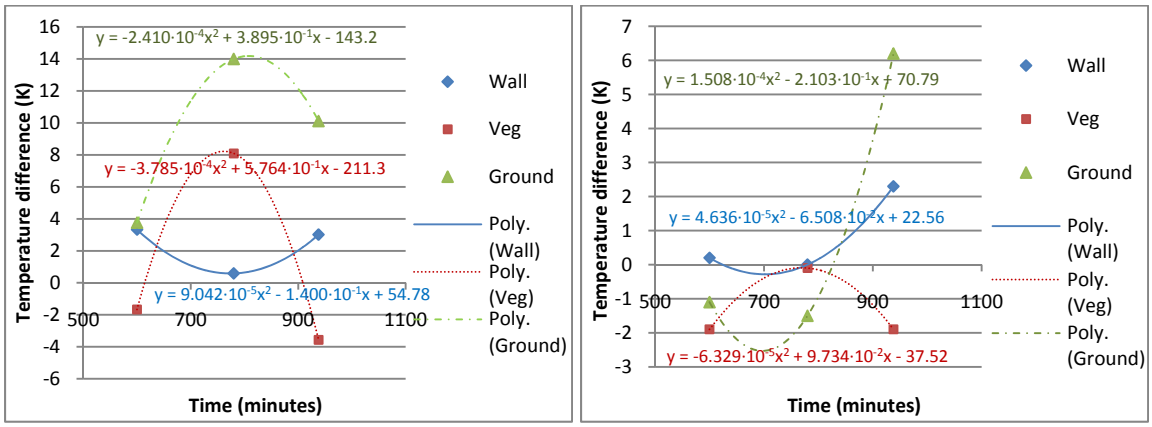

(a) (b)

Fig. 4.8 Surface temperature differences: (a) sunny surfaces and (b) shaded surfaces. Time (minutes) is minutes from midnight standard time, i.e., 600=10:00, 780=13:00 and 938=15:38 that are actual observation times

4.2.3.5 *Sensitivity test*

Default date and time for the tests were solar noon on July 31th, 2010. The location was 49N, a medium latitude among major cities in Canada (lowest: Toronto 43° 39', highest: Edmonton 53° 34'), and 120W, the standard meridian for the Pacific time zone. Altitude was 0 (zero) meters above sea level. Air temperature (T_a) and relative humidity (RH) were fixed at 23 °C and 50 %, which are similar to average daily maximum air temperature and average relative humidity at 1500 local standard time at Vancouver and Victoria in

summer (Canadian Climate Normals 1971–2000 http://climate.weatheroffice.gc.ca/climate_normals/index_e.html). The solar altitude for the selected time and location was 59.3°. The solar radiation at the top of the atmosphere (solar constant) was assumed to be 1367 Wm^{-2}.

Firstly, tests for meteorological variables were conducted (Fig. 4.9). The range of Linke turbidity (T_L) for the test was 3.0–4.0 because the mean July-August, 2009 was 3.65 T_L at Nanaimo, B.C. A T_L change of 0.5 made a 52.0±1.5 Wm^{-2} difference in direct beam solar radiation incident on the human body surface (K_b^+), and a site latitude variation of 5° created a 14.9±1.6 Wm^{-2} difference (Fig. 4.9a). Also, diffuse beam solar radiation (K_d) changed 20.8±0.3 Wm^{-2} per 0.5 T_L and 0.9±0.4 Wm^{-2} per 5° latitude. The range of T_a was 23–31 °C, and that of *RH* was 10–90 %. A 1 °C change in air temperature (T_a) created a mean 7.5 Wm^{-2} change in longwave radiation from the sky (L_a). The effects of a relative humidity change of 10 % on L_a ranged from a maximum of 12.9 Wm^{-2} at low relative humidities to a minimum of 5.8 Wm^{-2} at high relative humidities at 23 °C T_a (Fig. 4.9b).

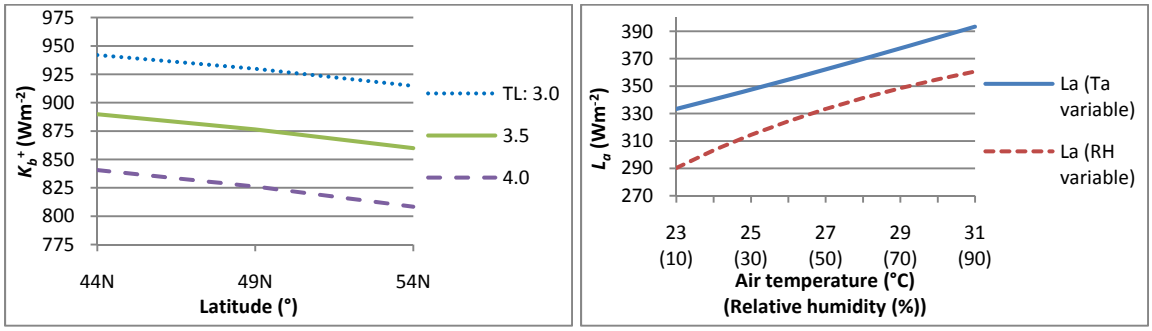

(a) (b)

Fig. 4.9 Sensitivity tests of the Linke turbidity factor, latitude, air temperature and relative humidity: (a) incident direct beam solar radiation on the human body surface (K_b^+) dependent on Linke turbidity factors (T_L) at various latitudes and (b) longwave radiation from the sky dependent on air temperature (T_a) and relative humidity (*RH*). *RH* effects were tested with a fixed T_a value of 23°C

Secondly, the effects of sky view factors (ψ_{sky}) on solar and longwave radiation were tested over the range of 0.54–0.923 (Fig. 4.10a). A simple ψ_{sky} simulation (2–36 m distance from a 12 m wide and 24 m high building) was used. Longwave radiation from the sky (L_a) and from obstructions (L_o) had more rapid changes than the other radiation components. L_a and L_o had a mean change of 33.5 and 47.0 Wm^{-2}, respectively, per 0.1 ψ_{sky} change. The next most sensitive variables were solar radiation reflected by obstructions in the sky hemisphere (K_{ro}, mean 16.0 Wm^{-2}) and K_d (mean 12.7 Wm^{-2}). Rapid increases of K_{ro} and L_o and decreases of K_{rg} and L_g around 0.54 ψ_{sky} seemed to be caused by a lower ψ_{sky} estimation of the

computer program (Fig. 4.10a). In human body surface related variable tests, ± 0.1 albedo (a_b) and ± 0.01 emissivity (ε_b) of the body surface from the frequently used values in modelling, 0.3 a_b and 0.97 ε_b, were conducted. A 0.1 change in a_b yielded a 24.7 Wm^{-2} difference (K_b^*: 13.5, $K_d^*+K_r^*$: 11.2 Wm^{-2}) in total absorbed all-wave radiation (Q^*), and a ε_b change of 0.01 gave a 3.9 Wm^{-2} difference in absorbed longwave radiation (L^*) (Fig. 4.10b). Those a_b and ε_b changes consequently made 3.7 and 0.5 °C differences in T_{mrt}, respectively (Fig. 4.10c).

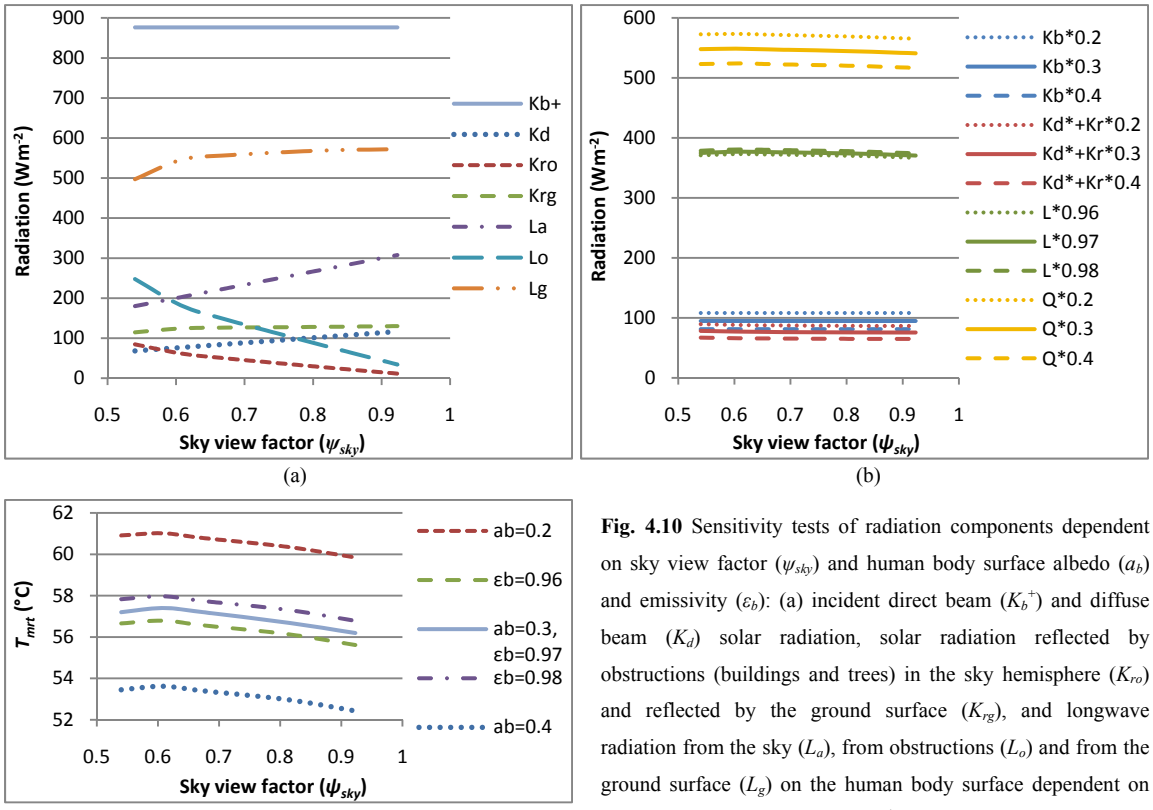

Fig. 4.10 Sensitivity tests of radiation components dependent on sky view factor (ψ_{sky}) and human body surface albedo (a_b) and emissivity (ε_b): (a) incident direct beam (K_b^+) and diffuse beam (K_d) solar radiation, solar radiation reflected by obstructions (buildings and trees) in the sky hemisphere (K_{ro}) and reflected by the ground surface (K_{rg}), and longwave radiation from the sky (L_a), from obstructions (L_o) and from the ground surface (L_g) on the human body surface dependent on ψ_{sky}, (b) absorbed direct beam (K_b^*), diffuse and reflected solar radiation ($K_d^*+K_r^*$), longwave radiation (L^*) and total all-wave radiation (Q^*) on the human body surface dependent on a_b (0.2, 0.3 and 0.4) and ε_b (0.96, 0.97 and 0.98) at various ψ_{sky} values, and (c) mean radiant temperature (T_{mrt}) dependent on a_b (0.2, 0.3 and 0.4) and ε_b (0.96, 0.97 and 0.98) at various ψ_{sky} values. Default a_b and ε_b are 0.3 and 0.97

Thirdly, urban surface albedos were tested (Fig. 4.11). Albedos were tested in increments of 0.1 within the following ranges: 0.3–0.7 for building walls (a_o), 0.12–0.52 for trees (a_{veg}) and 0.15–0.55 for the ground (a_g). With an open ψ_{sky} of around 0.6, 0.1 albedo changes of a_o, a_{veg} and a_g created differences of about 20, 17 and 84 Wm^{-2} in K_{ro}, K_{rveg} and K_{rg}, respectively (Fig. 4.11a, b and c). Thus, those changes made 0.9, 0.8 and 3.4 °C differences in T_{mrt}, respectively (Fig. 4.11d, e and f). The differences of reflected solar

radiation and T_{mrt} vary with open sky view factor and decrease at higher ψ_{sky} values. In the test of albedo change effects, a_o effects were most sensitive to ψ_{sky} changes. With a 0.1 increase in ψ_{sky}, K_{ro} decreased from around 15 Wm^{-2} at a_o = 0.3 to around 36 Wm^{-2} at a_o = 0.7. The effects of a_{veg} on the amount of K_{rveg} were 30 % less than those of a_o because of tree transmissivity, 30 % (0.3). The a_g did not make large differences in K_{rg}, from around 1.5 Wm^{-2} at a_g = 0.15 to around 6 Wm^{-2} at a_g = 0.55.

In summary, modelled human radiation is sensitive to the albedo changes. Especially, variations in a_b and a_g had the most effect on human radiation exchange.

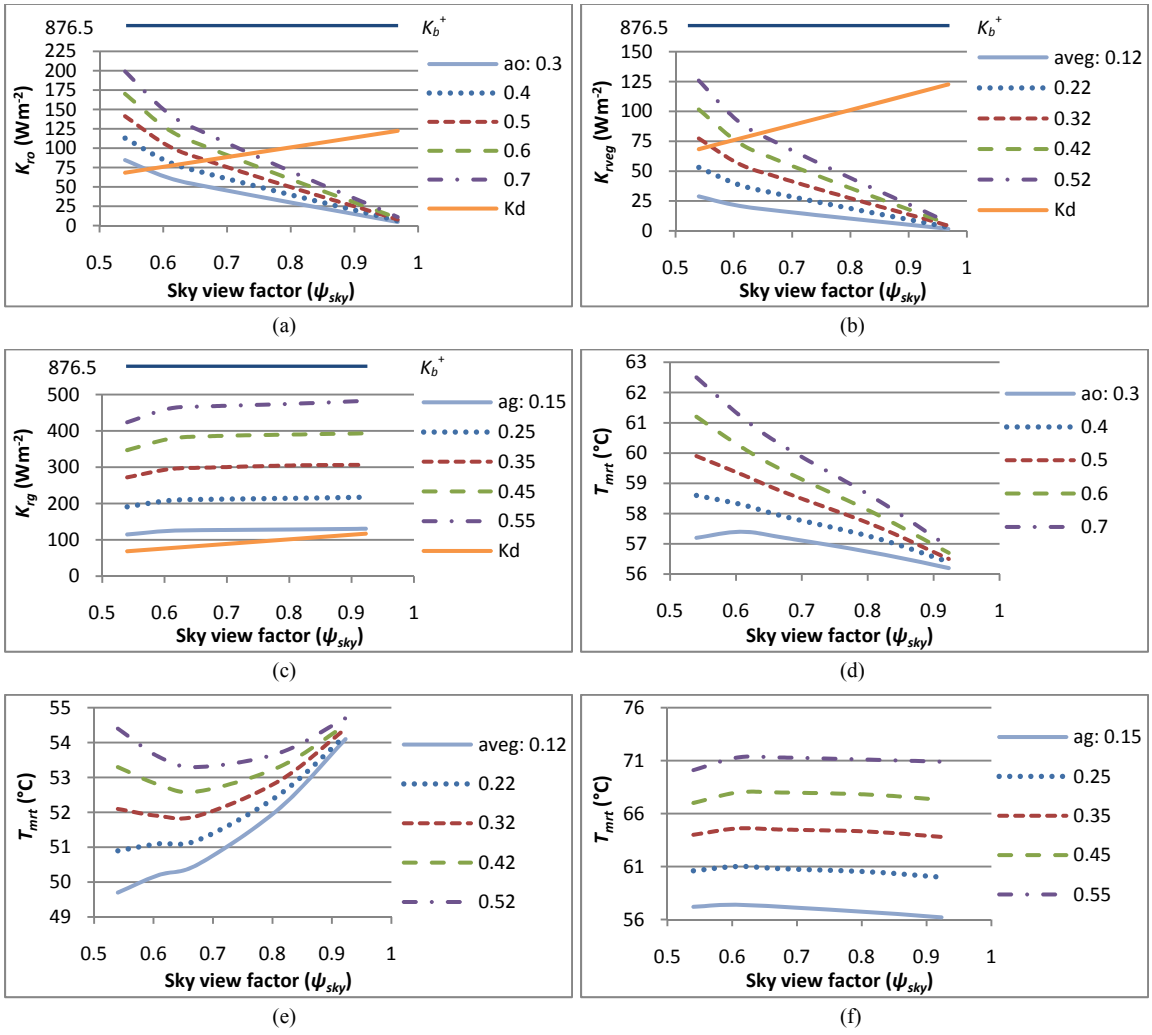

Fig. 4.11 Sensitivity tests of surface albedos: solar radiation reflected (a) by buildings dependent on building surface albedos (a_o: 0.3-0.7), (b) by trees dependent on tree surface albedos (a_{veg}: 0.22-0.62) and (c) by the ground surface dependent on ground surface albedos (a_g: 0.15-0.55) with various sky view factors, and mean radiant temperature (T_{mrt}) dependent on (d) building surface albedos (a_o: 0.3-0.7), (e) tree surface albedos (a_{veg}: 0.12-0.52) and (f) ground surface albedos (a_g: 0.15-0.55). Direct beam (K_b^+) = 876.5 Wm^{-2} and diffuse beam (K_d) solar radiation incident on the human body surface were estimated at solar noon on July 31th, 2010 at 49N, 120W

4.2.4 Basic settings and theories of RayMan Pro and ENVI-met 3.1

Two 3D computer simulation modeling programs, RayMan Pro (http://www.urbanclimate.net/rayman/index.htm) and ENVI-met 3.1 (http://www.envi-met.com), were used in the comparison because they are the most advanced, are free and have been updated regularly. Detailed, required input data for the computer simulations are listed in Table 4.12. Data input windows of the programs were shown in Fig. 4.12 for RayMan Pro and in Fig. 4.13 for ENVI-met 3.1. Topography input data for RayMan with a grid size less than 10 meters did not work properly, so a 10×10 meter grid was used. In the ENVI-met data input windows, topography is assumed to be a horizontal ground surface so it is not necessary to prepare topographic input data. Obstructions (buildings and trees) and ground surface type (loam, concrete, brick, asphalt and so on) were input as a minimum 2 (x axis)×2 (y)×1 (z) meter grid which is much larger than the minimum 0.5 meter grid suggested in its manual. Data input with 1 meter grid size for each dimension did not work and continuously made errors in ENVI-met. Potential temperature and specific humidity values at the height of 2500 meters in the upper air were obtained from the National Climatic Data Center, NOAA Satellite and Information Service, USA (http://www1.ncdc.noaa.gov/pub/data/igra/data-y2d/). The upper air data of Cheju (WMO station number: 47185, 33.28ºN 126.17ºE) were used for the Changwon site. Those of Quillayute (WMO station number: 72797, 47.57ºN 124.30ºW), WA, USA were used for Nanaimo. The results of ψ_{sky}, air and ground temperatures and individual quantities of solar and longwave radiation from the computer simulation programs were compared with measured microclimatic data from the Nanaimo and Changwon study sites.

Table 4.12 Input geographical and climatic data for RayMan and ENVI-met simulations

Computer simulation programs		Initial input data	Study sites			
			Nanaimo, B.C., Canada			Changwon, Korea
RayMan		Date	Aug. 5, 2008	July 26, 2009	July 27, 2009	June 11, 2009
		Time	12:00–14:40	9:00–10:45 12:00–13:45 14:50–16:15	9:00–16:00	11:30–17:00
		Latitude	49° 10'N			35° 13'N
		Longitude	123° 56'W			128° 41'E
		Time zone	UTC-8/GMT-8			UTC+9/GMT+9
		Elevation (m)	12			17
		Air temperature (°C)	27.0–30.1	22.9–28.7	24.2–32.2	27.8–29.3
		Relative humidity (%)	46.5–55.0	62.4–77.7	53.3–72.3	33.0–45.0
		Cloud cover (octas)	0			0
		Wind speed (m/s)	0.4–1.3	0.3–1.3	0.4–1.5	0.9–2.2
		Albedo of the surroundings	0.3			
ENVI-met		Start simulation at time	6:00	6:00	8:00	8:00
		Total simulation time (hr)	12	24	12	12
		Dimensions (grid: x×y×z)	124×166×25			95×105×25
		Horizontal grid size (m)	2			2
		Vertical grid size (m)	1			1
		Rotation out of grid North (°)	0			-45
		Number of nesting grids	3			5
		Wind speed 10 m above ground (m/s)	3.6	1.9	1.1	2.1
		Wind direction (°, N=0, clockwise)	260	180	30	281
		Relative humidity 2 m above ground (%)	62	82	83	53.9
		Initial air temperature at a height of 2500 m (°C)	10.7	11.7	15.1	10.7
		Specific humidity at a height of 2500 m (g/kg)	2.7	7.6	5.9	0.5
		Albedo of Walls	0.2			
		Albedo of Roofs	0.3			

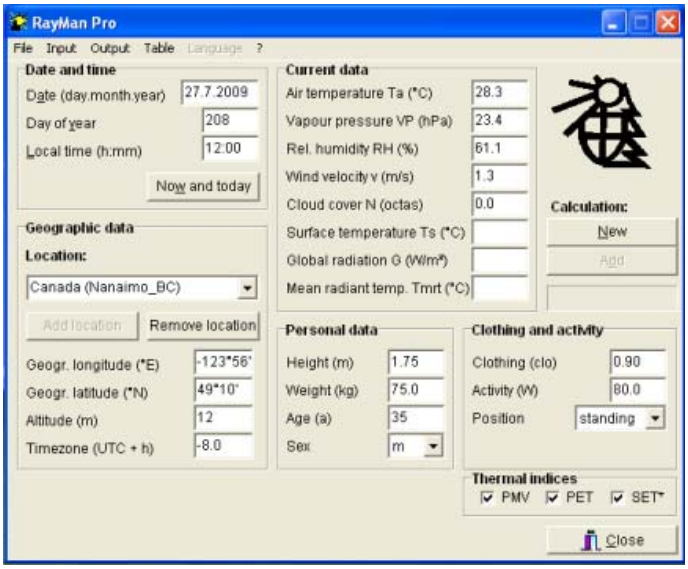

(a)

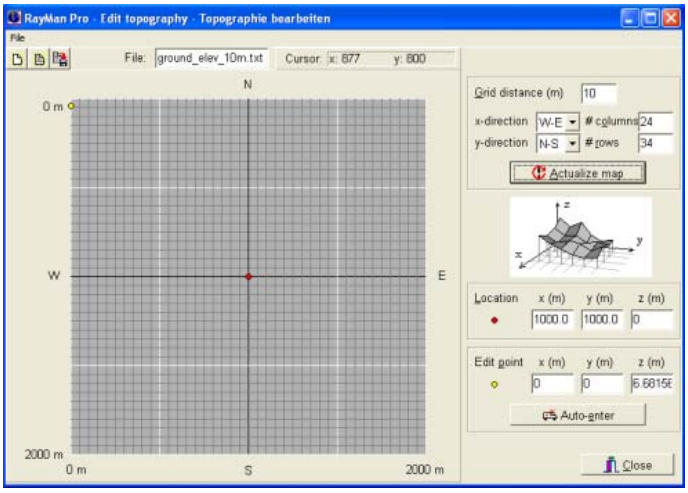

(b)

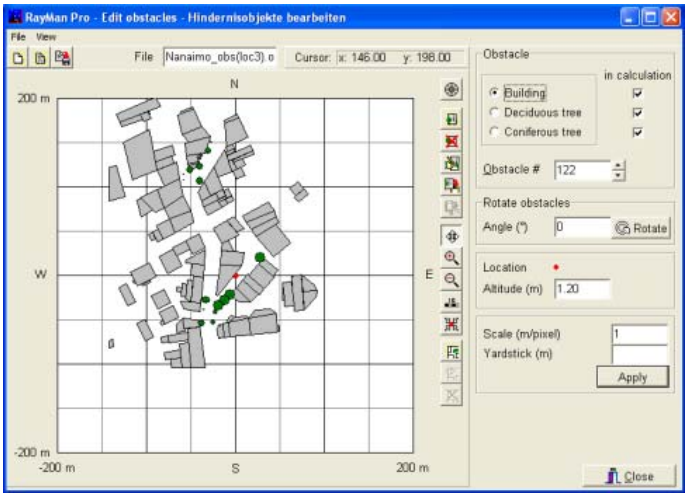

(c)

Fig. 4.12 RayMan Pro program windows: (a) main window, (b) topography input window and (c) obstacles (buildings and trees) input window

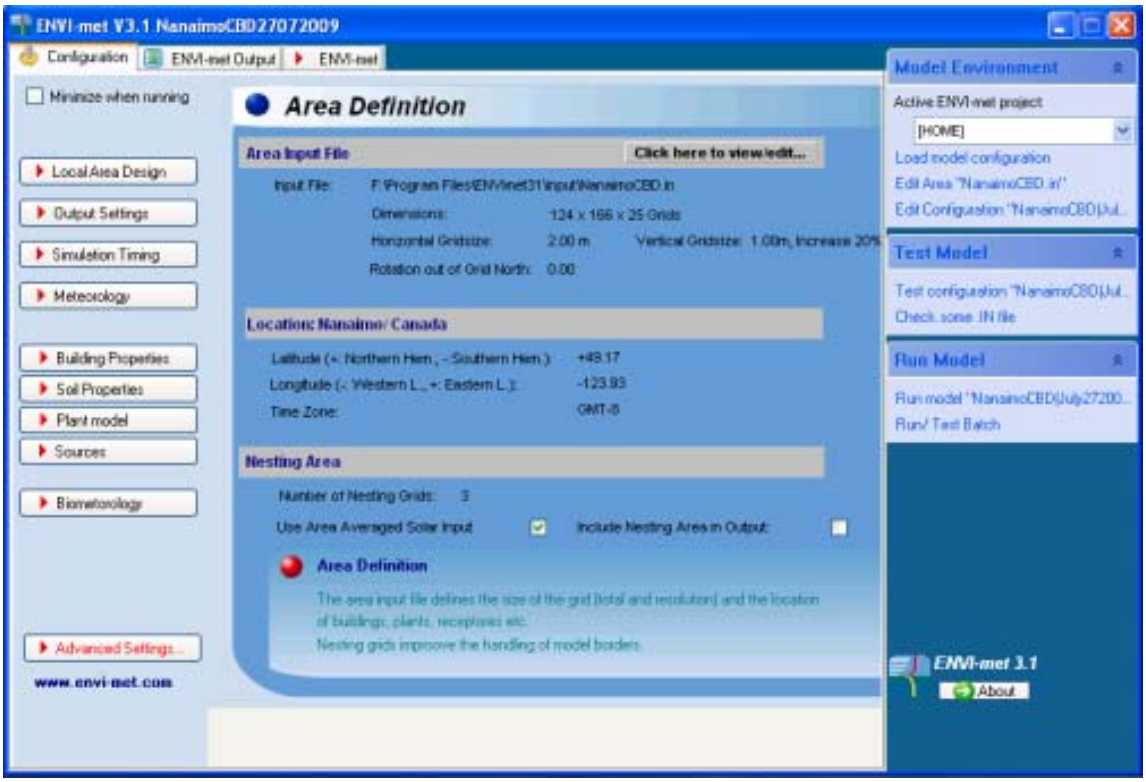

(a)

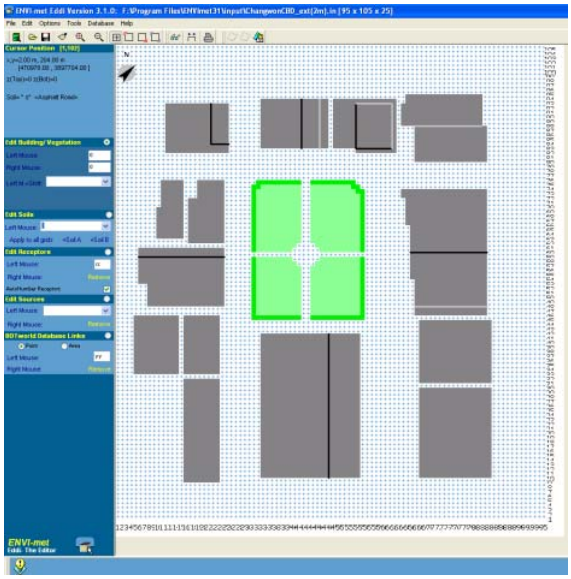

(b)

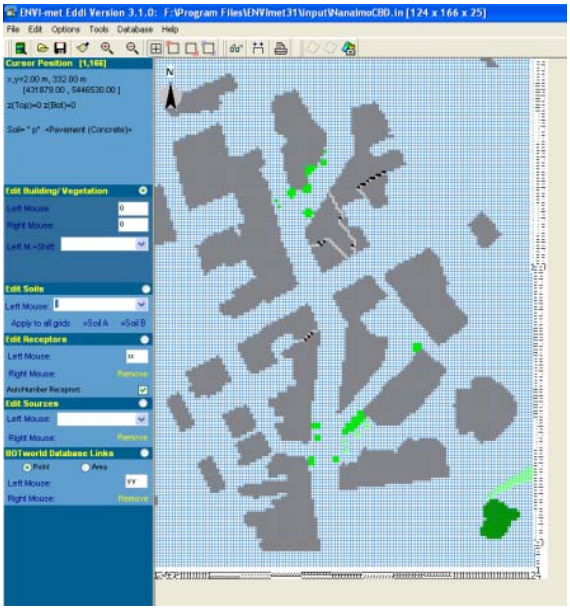

(c)

Fig. 4.13 ENVI-met 3.1 program windows: (a) main window, (b) data input window for Changwon and (c) data input window for Nanaimo

The known, basic radiation formulas of the two simulation programs for cloudless sky conditions are shown next.

4.2.4.1 *RayMan Pro* (from Matzarakis et al. 2010)

Global solar radiation (G_0) for no obstructions in the sky hemisphere is estimated by:

$$G_0 = 0.84 \cdot K_{bo} \cdot \cos z \cdot \exp(-0.027 \cdot P/P_0 \cdot T_L/\cos z) \quad \text{(VDI 1994)} \tag{4.57}$$

where K_{bo} is the solar constant (1367 Wm^{-2}), z is zenith angle (°), P is the local atmospheric pressure (hPa) and P_0 is the normal pressure at sea level (1013 hPa).

Solar radiation (R) is the sum of direct beam solar radiation (K_b) and diffuse beam solar radiation (K_d):

$$R = K_b + K_d = G_0 \text{ for unobstructed skies} \tag{4.58}$$

K_b is estimated by:

$$K_b = K_{bo} \cdot \cos z \cdot \exp(-T_L \cdot \gamma \cdot m \cdot P/P_0)(1 - N/8) \quad \text{(Jendritzky et al. 1990)} \tag{4.59}$$

$$m = 1/[\sin\beta + 0.50572(\beta + 6.07995)^{-1.6364}] \quad \text{(Kasten and Young 1989)} \tag{4.60}$$

$$\gamma = 1/(0.9m + 9.4) \quad \text{for } z < 85° \quad \text{(Kasten 1980)} \tag{4.61}$$

where γ is the vertical optical thickness of the standard (Rayleigh) atmosphere, m is the relative optical air mass and N is the degree of cloudiness in octas. In this study, N is 0 with cloudless sky condition. β is solar altitude (°) which can be found very easily from the Solar Position Calculator, NOAA Earth System Research Lab (http://www.srrb.noaa.gov/highlights/sunrise/azel.html).

K_d is estimated by:

$$K_d = K_{d0}(1 - N/8) + K_{d8} \cdot N/8 \quad \text{(Valko 1966)} \tag{4.62}$$

where K_d can be computed linearly between the two extreme cloudiness values, cloudless (N=0) and overcast (N=8). In this study, N is 0 for a cloudless sky condition so that K_d is:

$$K_d = K_{d0} \tag{4.63}$$

$$K_{d0} = K_{d0\_iso} + K_{d0\_aniso} \tag{4.64}$$

$$K_{d0\_iso} = (G_0 - K_b)(1 - t_r)\psi_{sky} \tag{4.65}$$

$$K_{d0\_aniso} = (G_0 - K_b)\, t_r \tag{4.66}$$

$$t_r = K_b/(K_{bo} \cdot \cos z) \tag{4.67}$$

where K_{d0} consists of an isotropic (K_{d0_iso}) and anisotropic (K_{d0_aniso}) components. t_r is the transmittance of the atmosphere for K_b. K_{d0_aniso} comes from near the sun, so it is included in the calculation of K_{d0} only when the sun is visible at the incident location.

For longwave radiation (L) from the surrounding environment, longwave radiation from the sky (L_a) and from the ground (L_g) are calculated via (Falkenberg and Bolz 1949, Monteith and Unsworth 1990, Oke 1987, VDI 1994):

$$L = L_a + L_g \tag{4.68}$$

$$L_a = \sigma \cdot T_a^4 (0.82 - 0.25 \cdot 10^{-0.0945 \cdot e_a})[1 + 0.21(N/8)^{2.5}] \tag{4.69}$$

$$L_g = \varepsilon \cdot \sigma \cdot T_g^4 + (1-\varepsilon)\, L_a \quad \text{(Oke 1987)} \tag{4.70}$$

$$T_g = T_a + (Q + Q_s)/[(6.2 + 4.26 \cdot v)(1 + 1/B)] \quad \text{(Oke 1987)} \tag{4.71}$$

where e_a is vapour pressure (hPa) and T_g is the ground surface temperature (K). Q is the net radiation of the ground surface [$= (1-a_g) \cdot R + L_a - L_g$, a_g is the albedo of ground surface, assumed as 0.3], Q_s is the soil heat flux density ($=-0.19 \cdot Q$ if $Q > 0$ and $-0.32 \cdot Q$ if $Q < 0$), v is the wind speed and B is the Bowen ratio. Both L_g and T_g values can be calculated iteratively (Matzarakis et al. 2010).

In RayMan Pro's radiation formulas, two limitations are revealed. There are no reflected solar radiation and longwave radiation components for obstructions (buildings and trees) in the sky hemisphere. Moreover, we can see its formulas do not include ψ_{sky} in the longwave radiation from the sky hemisphere and sunny/shaded view factors in both the solar and longwave radiation calculations. Therefore, it can be expected that its estimated longwave radiation will be less than the collected radiation data because of the missing emitted longwave radiation component from higher surface temperatures and emissivities of obstructions than the sky. The effect of the missing reflected solar radiation component by obstructions depends on the diffuse beam from the obstructed sky, the albedos of the obstructions and the total solar radiation incident on the obstructions.

4.2.4.2 *ENVI-met 3.1* [its radiation formulas based on Taesler and Andersson (1984)]

K_b is estimated by:

$$K_b = \{k \cdot K_{bo} \cdot \exp[-(\zeta_r + \zeta_d)m] - w\} \tag{4.72}$$

$$\zeta_r = \lambda^{-4}\, 0.00816 \tag{4.73}$$

$$\zeta_d = \lambda^{-1.3}\tau \quad \text{(given by Ångström)} \tag{4.74}$$

$$m = 1/\sin\beta \quad \text{for } \beta > 10°$$

$$m=1.22[1.0144/\sin(\beta+1.44) - 0.49] \quad \text{for } \beta \leq 10° \quad \text{(Liljequist 1979)} \quad (4.75)$$

$$w=70+2.8 \cdot e_a \cdot m \quad \text{(Liljequist 1979)} \quad (4.76)$$

where ζ_r and ζ_d are attenuation coefficients due to molecular scattering and turbidity respectively. λ is solar wavelength (=0.48μm which is the maximum wavelength of solar radiation), and τ is the turbidity coefficient from early Swedish data by Volz (1968) (Table 4.13). w is reduction of solar radiation by water vapour absorption.

Table 4.13 The turbidity coefficient (τ) from early Swedish data (Taesler and Andersson 1984, originally from Volz 1968)

Month	1	2	3	4	5	6	7	8	9	10	11	12
τ (clear sky condition)	0.04	0.04	0.05	0.06	0.07	0.07	0.065	0.06	0.055	0.05	0.04	0.04

K_d is estimated by:

$$K_d = \eta \cdot G_0 = \eta \cdot [K_b \sin \beta/(1-\eta)] = K_b \sin \beta \, [\eta/(1-\eta)] \quad (4.77)$$

$$\eta = 1/[1+8(\sin \beta)^{0.7}] \quad \text{(Brown and Isfält 1974)} \quad (4.78)$$

where η is the dependence of K_d on solar altitude.

For longwave radiation, there are no specific equations published yet. In its website manual, the formula concept is:

$$L = \psi_{sky}[t_{veg} \times L_a + (1-t_{veg}) \times L_{veg}] + (1-\psi_{sky}) \times \max(L_{env}, L_g) \quad (4.79)$$

where t_{veg} is a transmission factor of vegetation (no plants, t_{veg}=1; very dense vegetation, t_{veg}=0). L_{env} is longwave radiation from an averaged surface temperature of the surrounding environment in the program, and L_g is longwave radiation from the ground surface. The 'max' function means the higher value between the two is used.

This program also has certain known limitations. The values of the direct, diffuse and reflected solar radiation do not include the variables of inclination and exposure of the surface because the ground surface is assumed horizontal (http://www.envi-met.com/htmlhelp/hs520.htm). Vegetation effect in the fraction of sky obstructed by buildings ($1-\psi_{sky}$) is ignored because the program developers, Bruse and Fleer (1998), thought it is only effective for the longwave radiation budget when only vegetation obscures the sky (http://www.envi-met.com/htmlhelp/hs540.htm). However, on a hot summer day it is expected that the wall surface temperature of a typical building made of concrete or bricks will be much higher than the leaf

surface temperature when direct beam solar radiation is incident on both surfaces. This means vegetation can reduce total incoming longwave radiation when it obscures warmer building surfaces. Therefore, neglect of the vegetation obscuring building surfaces effect seems to be an incorrect assumption.

4.3 Results

This section will show the results of comparisons of sky view factor, air temperature, ground surface temperature and radiation between the collected data and the results of the new human-urban radiation exchange simulation model (New model), RayMan and ENVI-met.

4.3.1 Sky view factor (ψ_{sky}) comparison

Sky view factors estimated by the three models were compared with those determined from fish-eye lens photographs. In the sky view factor analysis, location 2 at Nanaimo (Nanaimo_2) was excluded because pedestrian arcades and awnings at this location could not be expressed in the computer simulation modeling (Fig. 4.14b).

Overall, all models (New model, RayMan and ENVI-met) underestimated greatly except the New model and ENVI-met at one location, Nanaimo_4 (Table 4.14 and Fig. 4.15a). The new model made better estimates, 9.8 % absolute mean difference, than the other two models, 16.9 % by ENVI-met and 42.6 % by RayMan. The differences between the collected data and New model were less than 8 % except at Nanaimo_5 and _square which were 21 and 18 %, respectively. Those large differences at the two locations came from ground height input data errors. The ground height data were obtained from the contour data, but in urban areas ground heights are easily changed by building construction. Building sites should be on the same ground height, so ground heights near buildings are changing along with the bottom heights of the buildings. For example, the ground heights from the contour data were 11 meters at Nanaimo_4, 10 meters at Nanaimo_5 and 9 meters at Nanaimo_square, but the grounds of Nanaimo_5 and _square were the same height and around 3 meters higher than Nanaimo_4.

RayMan's sky view factor estimates averaged 38 % less than the collected data at Nanaimo_3, 4, square and Changwon_smallpark and underestimated by about 53 % when the locations had trees nearby (Nanaimo_1 & 5). ENVI-met had less differences with the collected values than RayMan and had results close to those of the New model. The difference between the New model and ENVI-met seems to come from ENVI-met 3.1 not including ground elevation data in the simulation, although a new version, 4.0, will include a digital elevation model in the future (see V3.1 online manual in www.envi-met.com).

The highest coefficient of determination (r^2) between the measured and three models' sky view factors was for the New model, 0.938 (Fig. 4.15b). ENVI-met (0.906) was higher than RayMan (0.843). As expected, the combination of New model-ENVI-met (0.943) had a little higher r^2 than the combinations of New model-RayMan (0.926) and RayMan-ENVI-met (0.933) (Fig. 4.15c).

How those underestimates in the models affect radiation analysis will be discussed in the section 4.3.4 on radiation comparison.

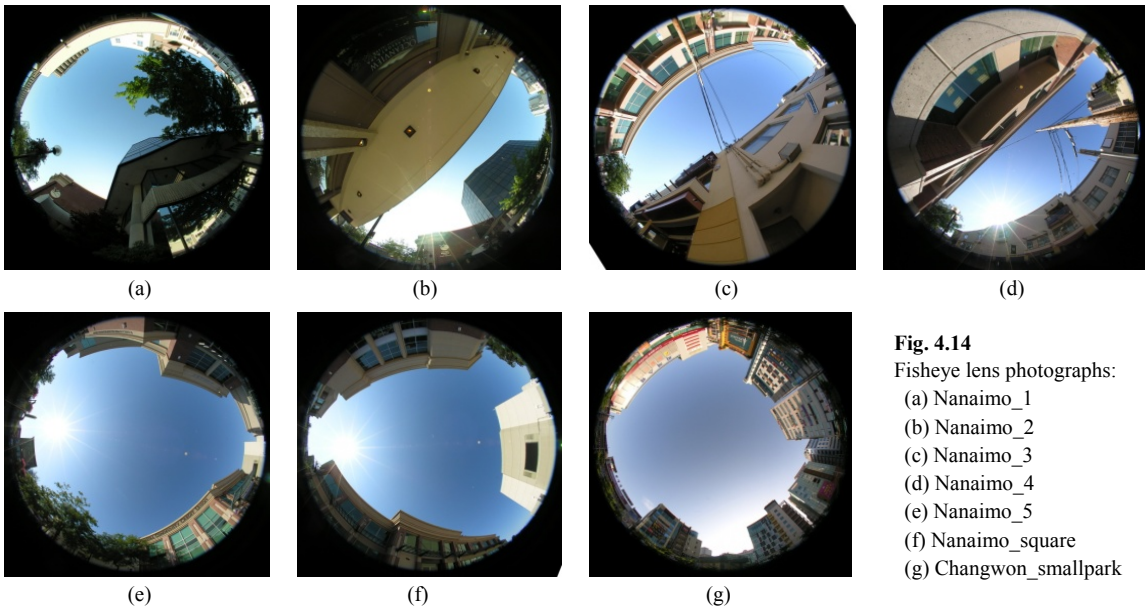

Fig. 4.14
Fisheye lens photographs:
(a) Nanaimo_1
(b) Nanaimo_2
(c) Nanaimo_3
(d) Nanaimo_4
(e) Nanaimo_5
(f) Nanaimo_square
(g) Changwon_smallpark

Table 4.14 Sky view factor (ψ_{sky}) comparison between collected and computer simulated results from New model, RayMan and ENVI-met. Collected ψ_{sky} values were determined using BMSky-view computer program (Gál et al. 2007)

Location	Collected ψ_{sky}	New model	RayMan	ENVI-met	New model-Collected		RayMan-Collected		ENVI-met-Collected	
					difference	%	difference	%	difference	%
Nanaimo_1	0.427	0.416	0.203	0.368	-0.011	-2.6	-0.224	-52.5	-0.059	-13.8
Nanaimo_3	0.408	0.391	0.255	0.377	-0.017	-4.2	-0.153	-37.5	-0.031	-7.6
Nanaimo_4	0.349	0.374	0.212	0.420	0.025	7.2	-0.137	-39.3	0.071	20.3
Nanaimo_5	0.843	0.666	0.399	0.619	-0.177	-21.0	-0.444	-52.7	-0.224	-26.6
Nanaimo_square	0.778	0.638	0.468	0.636	-0.140	-18.0	-0.310	-39.8	-0.142	-18.3
Changwon_smallpark	0.785	0.741	0.521	0.670	-0.044	-5.6	-0.264	-33.6	-0.115	-14.7
Mean						-7.4		-42.6		-10.1
Absolute mean						9.8		42.6		16.9

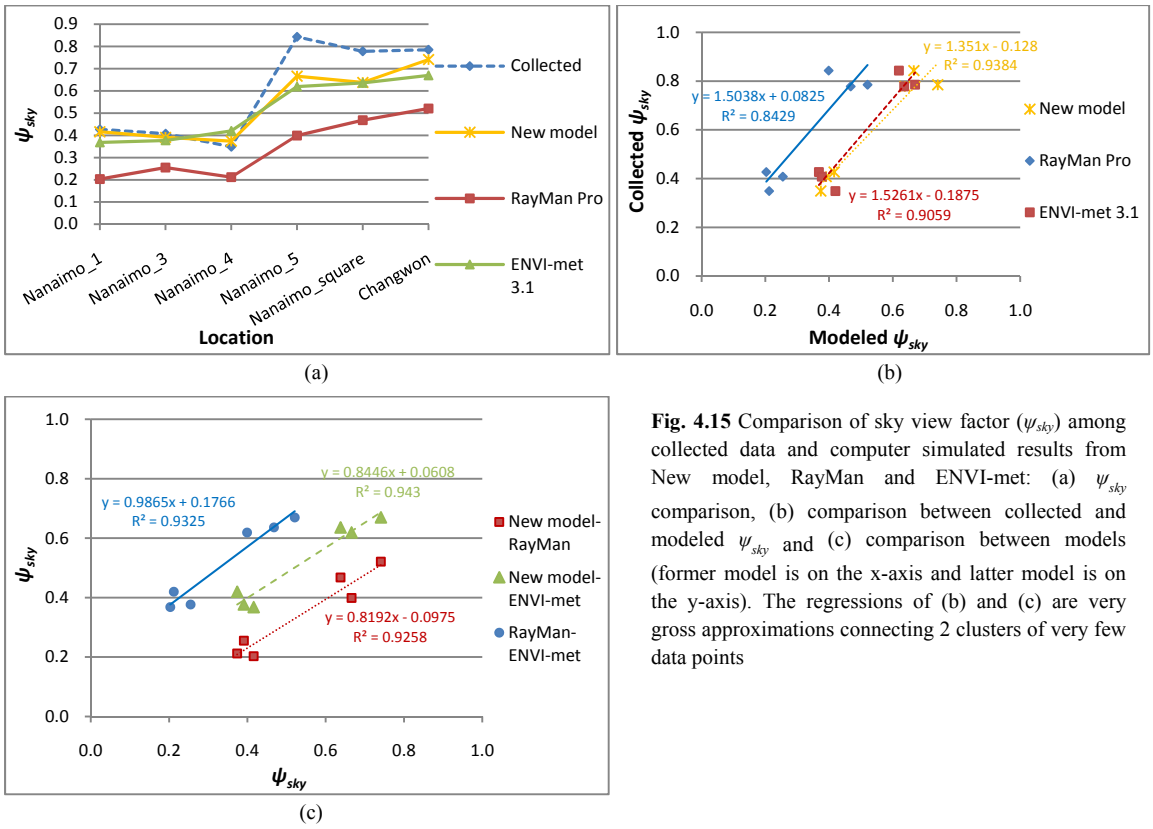

Fig. 4.15 Comparison of sky view factor (ψ_{sky}) among collected data and computer simulated results from New model, RayMan and ENVI-met: (a) ψ_{sky} comparison, (b) comparison between collected and modeled ψ_{sky} and (c) comparison between models (former model is on the x-axis and latter model is on the y-axis). The regressions of (b) and (c) are very gross approximations connecting 2 clusters of very few data points

4.3.2 Air temperature (T_a) comparison

The New model and RayMan require air temperatures as initial input data, so only results from ENVI-met were compared with the measured T_a data. Overall, ENVI-met underestimated at all locations during the daytime: mean differences of 10.8 °C on August 5 in 2008, 7.4 °C on July 26, 8.4 °C on July 27 and 11.3 °C on June 11 in 2009 (Fig. 4.16 & Table 4.15). Moreover, the daytime T_a ranges between the maximum T_a values and the minimum T_a values were also underestimated at all Nanaimo sites. ENVI-met estimates were closer to observed values at Changwon. These results are similar to those of Emmanuel et al. (2007) who mentioned ENVI-met underestimated daytime T_a and estimated a narrower diurnal range compared with measured T_a in Sri Lanka. The effect of underestimated T_a by ENVI-met for radiation analysis will be shown in the section 4.3.4.3 on radiation comparison.

The r^2 values between ENVI-met and measured air temperature were very low, up to 0.182, except in the July 27 data, 0.934 (Fig. 4.16). The r^2 was low at both sunny and shaded locations (Fig. 4.17). The

July 27 data have a high r^2, but air temperature differences increase gradually during the daytime from 6.0 °C at 9:00 to 11.0 °C at 16:00 (Fig. 4.16c).

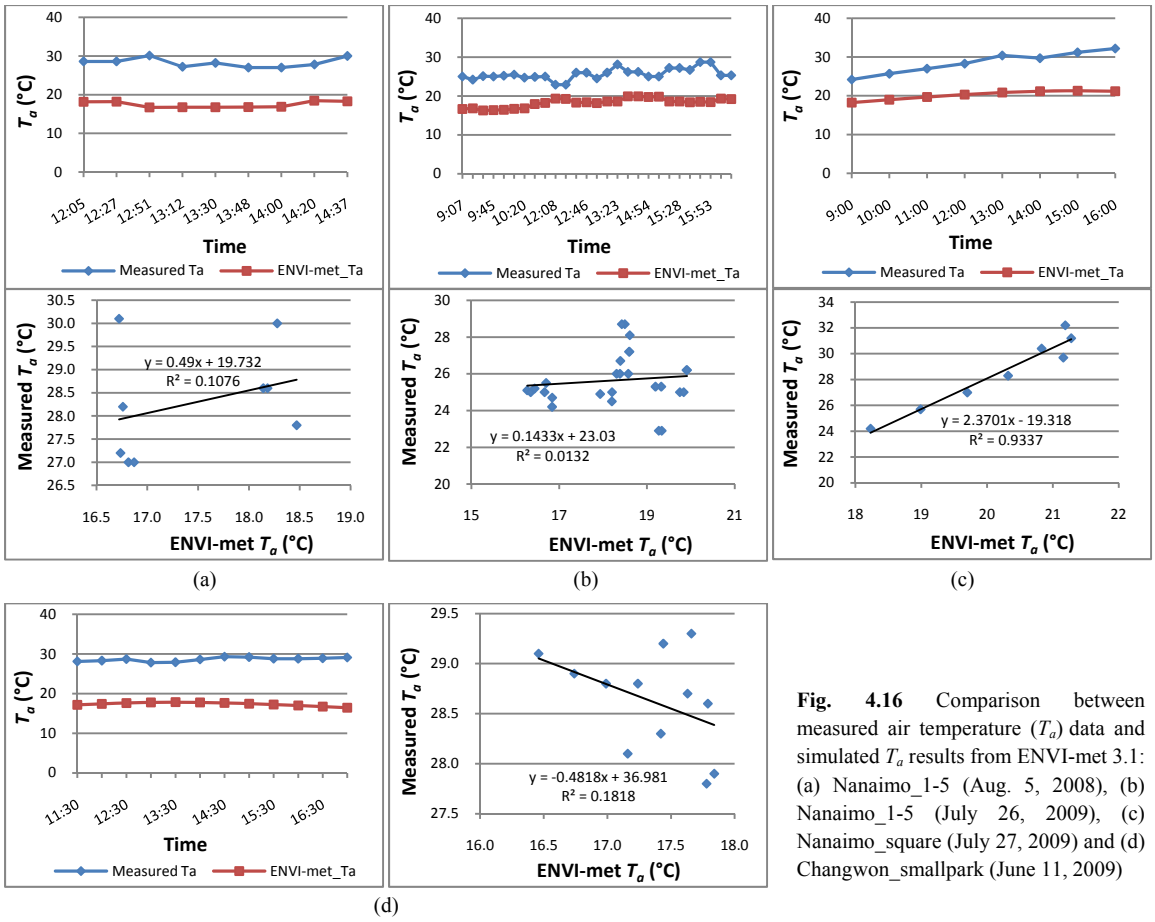

Fig. 4.16 Comparison between measured air temperature (T_a) data and simulated T_a results from ENVI-met 3.1: (a) Nanaimo_1-5 (Aug. 5, 2008), (b) Nanaimo_1-5 (July 26, 2009), (c) Nanaimo_square (July 27, 2009) and (d) Changwon_smallpark (June 11, 2009)

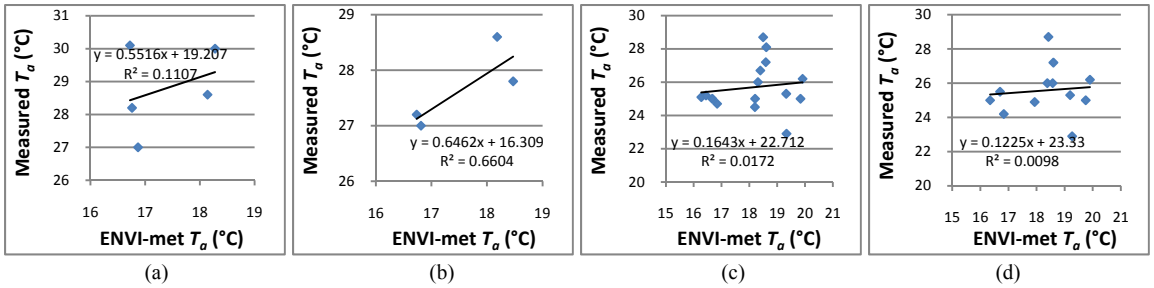

Fig. 4.17 Comparison of measured and simulated air temperature (T_a) from ENVI-met 3.1 at sunny and shaded Nanaimo locations: (a) sunny locations (Aug. 5, 2008), (b) shaded locations (Aug. 5, 2008), (c) sunny locations (July 26, 2009) and (d) shaded locations (July 26, 2009)

Table 4.15 Comparison of air temperature (T_a) between measured data and computer simulated results from ENVI-met 3.1

Date/ Site	Time	Location	Solar Time	Sun/ Shade	Measured T_a (°C)	ENVI-met T_a (°C)	Difference (°C) (ENVI-met - Measured)	T_a range (°C)		
Aug. 5, 2008 (Nanaimo, B.C., Canada)	Noon	1	12:05	sunny	28.6	18.1	-10.5			
		2	12:27	shady	28.6	18.2	-10.4			
		3	12:51	sunny	30.1	16.7	-13.4			
		4	13:12	shady	27.2	16.7	-10.5			
		5	13:30	sunny	28.2	16.8	-11.4		Measured T_a	ENVI-met_ T_a
		4	13:48	shady	27.0	16.8	-10.2	Maximum	30.1	18.5
		3	14:00	sunny	27.0	16.9	-10.1	Minimum	27.0	16.7
		2	14:20	shady	27.8	18.5	-9.3	Mean	28.3	17.4
		1	14:37	sunny	30.0	18.3	-11.7	Range	3.1	1.7
Aug. 26, 2009 (Nanaimo, B.C., Canada)	Morning	1	9:07	sunny	25.0	16.7	-8.3			
		2	9:23	shady	24.2	16.8	-7.4			
		3	9:37	sunny	25.1	16.3	-8.8			
		4	9:45	shady	25.0	16.4	-8.6			
		5	10:00	sunny	25.2	16.4	-8.8			
		4	10:12	shady	25.5	16.7	-8.8			
		3	10:20	sunny	24.7	16.8	-7.9			
		2	10:35	shady	24.9	17.9	-7.0			
		1	10:44	sunny	25.0	18.2	-6.8			
	Noon	1	12:08	sunny	22.9	19.3	-3.6			
		2	12:14	shady	22.9	19.3	-3.6			
		3	12:34	sunny	26.0	18.3	-7.7			
		4	12:46	shady	26.0	18.4	-7.6			
		5	13:00	sunny	24.5	18.2	-6.3			
		4	13:17	shady	26.0	18.6	-7.4			
		3	13:23	sunny	28.1	18.6	-9.5			
		2	13:36	shady	26.2	19.9	-6.3			
		1	13:43	sunny	26.2	19.9	-6.3			
	Afternoon	1	14:54	shady	25.0	19.8	-5.3			
		2	15:09	sunny	25.0	19.8	-5.2			
		3	15:18	shady	27.2	18.6	-8.6			
		4	15:28	sunny	27.2	18.6	-8.6			
		5	15:38	sunny	26.7	18.4	-8.3			
		4	15:46	sunny	28.7	18.5	-10.2	Maximum	28.7	19.9
		3	15:53	shady	28.7	18.4	-10.3	Minimum	22.9	16.3
		2	16:05	sunny	25.3	19.3	-6.0	Mean	25.6	18.3
		1	16:11	shady	25.3	19.2	-6.1	Range	5.8	3.6
Aug. 27, 2009 (Nanaimo, B.C., Canada)	Daytime	Square	9:00	sunny	24.2	18.2	-6.0			
			10:00	sunny	25.7	19.0	-6.7			
			11:00	sunny	27.0	19.7	-7.3			
			12:00	sunny	28.3	20.3	-8.0			
			13:00	sunny	30.4	20.8	-9.6	Maximum	32.2	21.3
			14:00	sunny	29.7	21.2	-8.5	Minimum	24.2	18.2
			15:00	sunny	31.2	21.3	-9.9	Mean	28.6	20.2
			16:00	sunny	32.2	21.2	-11.0	Range	8.0	3.1
June 11, 2009 (Changwon, Korea)	Daytime	Smallpark	11:30	sunny	28.1	17.2	-10.9			
			12:00	sunny	28.3	17.4	-10.9			
			12:30	sunny	28.7	17.6	-11.1			
			13:00	sunny	27.8	17.8	-10.0			
			13:30	sunny	27.9	17.8	-10.1			
			14:00	sunny	28.6	17.8	-10.8			
			14:30	sunny	29.3	17.7	-11.6			
			15:00	sunny	29.2	17.4	-11.8			
			15:30	sunny	28.8	17.2	-11.6	Maximum	29.3	17.8
			16:00	sunny	28.8	17.0	-11.8	Minimum	27.8	16.5
			16:30	sunny	28.9	16.7	-12.2	Mean	28.6	17.3
			17:00	sunny	29.1	16.5	-12.6	Range	1.5	1.4

4.3.3 Ground surface temperature (T_g) comparison

Surface temperature formulas of the New model were developed using empirical data at Nanaimo_1-5 on August 5, 2008, and July 26, 2009. Therefore, only the model estimates from Nanaimo_square on July 27 and from Changwon_smallpark on June 11, 2009 were compared with the measured T_g data and the RayMan and ENVI-met results (Fig. 4.18 and Table 4.16). For RayMan and ENVI-met, all datasets were compared with the measured data.

The New model seems to overestimate a little around noon and underestimate during early morning and late afternoon. The model had a much lower absolute mean difference with the measured T_g data, only 1.8 °C, at Nanaimo_square than did RayMan, 5.8 °C, and ENVI-met, 13.2 °C. This could be expected because the formula for estimating T_g values used measured T_g data at Nanaimo sites on the other days. At Changwon_smallpark, the model had a greater absolute mean difference, 4.7 °C, than at Nanaimo_square. Both locations have the same ground surface material, bricks, but their albedos were different: 11 % at Nanaimo_square and 19 % at Changwon_smallpark. Higher albedo at the latter location reduced both absorbed solar radiation and surface temperature. This created a larger T_g difference at Changwon.

The New model had the highest r^2 with the measured T_g data. It was 0.931 at Nanaimo_square and lower, 0.583, at Changwon_smallpark (Figs. 4.18c & d). The model also had very strong r^2 values with ENVI-met T_g estimates: 0.960 at Nanaimo_square and 0.995 at Changwon_ smallpark.

RayMan generally overestimated T_g values at both sunny and shaded locations before the highest radiation exchange period during the daytime around 13:00–14:00 and predicted oppositely later in the day (Figs. 4.18a-d). This phenomenon happened earlier, around 11:00, at Nanaimo_square (Fig. 4.18c).

ENVI-met underestimated T_g values the same as T_a at the sunny locations and overestimated them slightly at some shaded Nanaimo_1-5 locations before 14:00 but underestimated again at both sunny and shaded locations later in the day (Figs. 4.18a & b). Underestimates of T_g values by ENVI-met at the sunny locations such as Nanaimo_square and Changwon_smallpark are clearly shown in Figs. 4.15c & d. Also, the ENVI-met-measured ground temperature difference was greater at the sunny locations (10.7 °C mean) than at the shaded locations (4.3 °C) at Nanaimo_1-5 on both Aug. 5, 2008, and July 26, 2009.

RayMan, however, had almost the same difference at the sunny locations (4.4 °C) as at the shaded locations (4.5 °C). At Changwon_smallpark, both programs had less differences with the measured data than at Nanaimo_1-5, absolute mean 3.3 °C by RayMan and 7.8 °C by ENVI-met. The reason seems to come from the more polluted sky condition at Changwon creating lower amounts of incoming solar radiation with its higher T_L value, i.e., 3.65 T_L at Nanaimo sites and 4.2 at the Changwon site, and a little bit higher ground surface albedo than that at Nanaimo creating less absorbed solar radiation.

The r^2 values between the measured data and ENVI-met results were higher, mean 0.870 in Nanaimo and 0.543 in Changwon, than those between the measured data and RayMan results, 0.711 and 0.317, respectively (Fig. 4.18). Mean r^2 values between RayMan and ENVI-met were 0.836 and 0.647, respectively. The r^2 on Aug. 5, 2008 was the highest, 0.946, between RayMan and the measured data, but the results came from a very limited number of observations so the averaged r^2 for the three days at the Nanaimo sites looks more logical.

Both programs create significant T_g differences, i.e., absolute mean 4.5 °C by RayMan and 10.6 °C by ENVI-met through the sunny locations of all datasets. T_g differences will directly affect the quantities of emitted longwave radiation from the ground surface. The results will be shown in section 4.3.4 on radiation comparison.

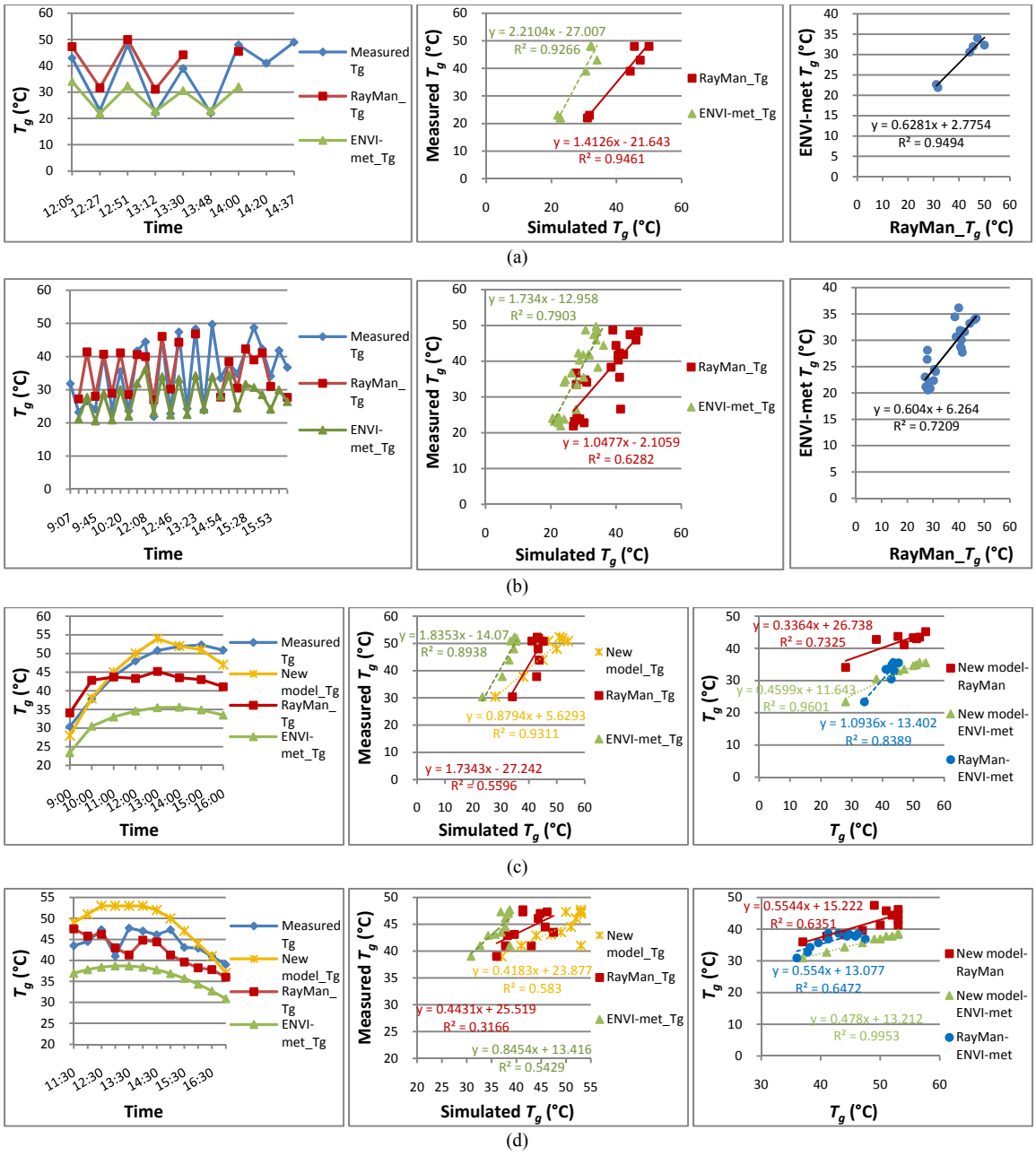

Fig. 4.18 Comparison between measured ground surface temperature (T_g) and computer simulated T_g from RayMan, ENVI-met and the New model: (a) comparison at Nanaimo_1-5 on Aug. 5, 2008, (b) comparison at Nanaimo_1-5 on July 26, 2009, (c) comparison at Nanaimo_square on July 27, 2009 and (d) comparison at Changwon_smallpark on June 11, 2009 (former model is on the x-axis and latter model is on the y-axis)

Table 4.16 Comparison of ground surface temperature (T_g) between measured data and computer simulated results from RayMan, ENVI-met and the New model

Date/ Site	Time	Location	Solar Time	Sun/ Shade	Measured T_g	New model _T_g	RayMan _T_g	ENVI-met_T_g	T_g Difference		
									New model-Measured	RayMan-Measured	ENVI-met-Measured
Aug. 5, 2008 (Nanaimo, B.C., Canada)	Noon	1	12:05	sunny	43		47.3	34		4.3	-9
		3	12:51	sunny	48		50	32.3		2	-15.7
		4	13:12	shady	22		31.1	22.7		9.1	0.7
		5	13:30	sunny	39		44.2	30.6		5.2	-8.4
		4	13:48	shady	22			22.8			0.8
		3	14:00	sunny	48		45.5	32		-2.5	-16
		1	14:37	sunny	49						
		Absolute Mean								**4.6**	**8.4**
Aug. 26, 2009 (Nanaimo, B.C., Canada)	Morning	1	9:07	sunny	31.8						
		3	9:37	sunny	26.6		41.4	27.7		14.8	1.1
		4	9:45	shady	24.1		28	20.5		3.9	-3.6
		5	10:00	sunny	40.3		40.7	28.8		0.4	-11.5
		4	10:12	shady	23.9		28.9	20.9		5	-3
		3	10:20	sunny	35.5		41.1	30.1		5.6	-5.4
		1	10:44	sunny	41.7		40.6	31.9		-1.1	-9.8
		Absolute Mean								**5.1**	**5.7**
	Noon	1	12:08	sunny	44.4		40	36.2		-4.4	-8.2
		3	12:34	sunny	45.9		46.1	33.9		0.2	-12
		4	12:46	shady	22.8		30.2	22.4		7.4	-0.4
		5	13:00	sunny	47.4		44.3	33.2		-3.1	-14.2
		4	13:17	shady	24.3			22.5			-1.8
		3	13:23	sunny	48.3		46.8	34.2		-1.5	-14.1
		1	13:43	sunny	49.7			33.9			-15.8
		Absolute Mean								**3.3**	**9.5**
	Afternoon	1	14:54	shady	33.5		27.8	28.1		-5.7	-5.4
		3	15:18	shady	34.8		30.5	24.5		-4.3	-10.3
		4	15:28	sunny	41.9		42.3	31.6		0.4	-10.3
		5	15:38	sunny	48.7		39	30.7		-9.7	-18
		4	15:46	sunny	42.3		41.1	28.5		-1.2	-13.8
		3	15:53	shady	34.1		31	24.1		-3.1	-10
		1	16:11	shady	36.7		27.7	26.4		-9	-10.3
		Absolute Mean								**4.8**	**11.2**
Aug. 27, 2009 (Nanaimo, B.C., Canada)	Daytime	Square	9:00	sunny	30.4	28	34.1	23.4	-2.4	3.7	-7
			10:00	sunny	37.8	38	42.8	30.5	0.2	5	-7.3
			11:00	sunny	43.9	45	43.7	33	1.1	-0.2	-10.9
			12:00	sunny	48	50	43.3	34.6	2.0	-4.7	-13.4
			13:00	sunny	50.8	54	45.2	35.5	3.2	-5.6	-15.3
			14:00	sunny	51.9	52	43.5	35.6	0.1	-8.4	-16.4
			15:00	sunny	52.3	51	43	34.9	-1.3	-9.3	-17.4
			16:00	sunny	50.9	47	41.1	33.5	-3.9	-9.8	-17.5
			Absolute Mean						**1.8**	**5.8**	**13.2**
June 11, 2009 (Changwon, Korea)	Daytime	Smallpark	11:30	sunny	43.5	49	47.5	36.9	5.5	4	-6.6
			12:00	sunny	44.5	51	45.8	37.8	6.5	1.3	-6.7
			12:30	sunny	47.3	53	46.2	38.4	5.7	-1.1	-8.9
			13:00	sunny	41	53	43	38.7	12	2	-2.3
			13:30	sunny	47.7	53	41.3	38.7	5.3	-6.4	-9
			14:00	sunny	47	53	44.8	38.4	6	-2.2	-8.6
			14:30	sunny	46.1	52	44.4	37.8	5.9	-1.7	-8.4
			15:00	sunny	47.3	50	41.3	36.9	2.7	-6	-10.5
			15:30	sunny	43.1	47	39.6	35.7	3.9	-3.5	-7.4
			16:00	sunny	42.9	44	38.2	34.3	1.1	-4.7	-8.6
			16:30	sunny	41	41	37.8	32.7	0	-3.2	-8.3
			17:00	sunny	39	37	36	30.9	-2	-3	-8.1
			Absolute Mean						**4.7**	**3.3**	**7.8**

4.3.4 Radiation comparison

In the RayMan and ENVI-met programs, there were no individual output data of reflected solar radiation by the ground surface ($K\uparrow$). The $K\uparrow$ values were assumed to be 15 % of total incoming solar radiation from the sky hemisphere ($K\downarrow$) and added to the total solar radiation results (R^+) for the comparison. 15% is the same ground albedo used in the New model.

Some results at the Nanaimo_1-5 locations during Aug. 5, 2008, and July 26, 2009 were not used in the comparison because wrong shadow patterns were created by inaccurate and incorrect input data, i.e., too simple building wall and roof-top shapes and incorrect ground heights.

The comparison results are shown below for each model.

4.3.4.1 New Model

The New model results were compared with the collected radiation data of each day (Fig. 4.19 & Table 4.17). The results were close to the collected data: mean 11 Wm^{-2} underestimate (17 Wm^{-2} at sunny locations) in solar radiation, 4 Wm^{-2} underestimate (3 Wm^{-2} overestimate at sunny locations) in longwave radiation and 15 Wm^{-2} underestimate (19 Wm^{-2} at sunny locations) in total radiation (Tables 4.18 & 4.19). The absolute means were higher than the normal means: 37 Wm^{-2} (42 Wm^{-2} at sunny locations) in solar radiation, 29 Wm^{-2} (30 Wm^{-2} at sunny locations) in longwave radiation and 66 Wm^{-2} (71 Wm^{-2} at sunny locations) in total radiation.

High r^2 in solar radiation, over 0.987, affected high r^2 in total radiation, over 0.982 (Fig. 4.19). The r^2 in longwave radiation varied widely from low, 0.226 at Changwon_smallpark, to high, 0.953 at Nanaimo_square.

In the comparison of radiation components, incoming solar radiation from the sky hemisphere ($K\downarrow$) was estimated very well: mean 13.9 Wm^{-2} underestimate at the sunny locations and 7.1 Wm^{-2} overestimate at the shaded locations at Nanaimo_1-5 and 5 Wm^{-2} overestimate at Changwon_smallpark. The exception was at Nanaimo_square which had a 22 Wm^{-2} overestimate (Table 4.19). The r^2 was extremely high, 0.995 (Fig. 4.20b).

Several reasons can be considered for the $K\downarrow$ overestimate at Nanaimo_square. ψ_{sky} at Nanaimo_square was underestimated by 0.14, 0.638, by the New model compared with 0.778 in the fisheye lens photograph. This means more $K\downarrow$ will come with higher ψ_{sky}, and the $K\downarrow$ overestimate will increase if the fisheye lens photograph ψ_{sky} was used. For example, K_d (85 Wm^{-2}) and $K_{ro}+K_{rveg}$ (17 Wm^{-2}) at noon on July 27, 2009 (Table 4.17) would change to 104 Wm^{-2} and 10 Wm^{-2} when ψ_{sky} increases by 0.14. The net difference will be 12 Wm^{-2} more overestimate from 34 Wm^{-2} to 46 Wm^{-2} (Table 4.18). Therefore, lower estimated ψ_{sky} is not the reason. Overestimated $K\downarrow$ differences at Nanaimo_square were reduced in the afternoon (Table 4.18). One possible factor could be: Linke turbidity (T_L). The monthly mean T_L values were used in the simulation, so the true T_L value at Nanaimo_square was lower on that day. Moreover, T_L values change during the daytime from high around noon to low in the morning and afternoon (Ineichen and Perez 2002). Therefore, the constant T_L value does not take into account the variation throughout the day.

In reflected solar radiation by the ground surface ($K\uparrow$), July 26 and 27, 2009 results at Nanaimo_1-5 and Nanaimo_square had lower mean differences, only 3.9 Wm^{-2} at the sunny locations and 2.0 Wm^{-2} at the shaded location, than Aug. 5, 2008, 43 Wm^{-2} and 30 Wm^{-2}, and June 11, 2009 at Changwon_smallpark, 34 Wm^{-2}. It is hard to explain the differences of Aug. 5, 2009 due to a small sample size. However, the Changwon_smallpark results clearly show the differences created by the gap in ground albedos between the value used in the simulation (0.15) and the real one (0.19). Higher actual ground albedo at Changwon_smallpark made those underestimates in the simulation. The r^2 was high, 0.876.

Incoming longwave radiation from the sky hemisphere ($L\downarrow$) differences were very small, only up to a mean 16 Wm^{-2}, but r^2 was very low, only 0.118 (Table 4.19 & Fig. 4.20b). Those of incoming longwave radiation from the ground hemisphere ($L\uparrow$) had similar results to those of $L\downarrow$. The mean difference was up to 16 Wm^{-2} except one shaded location datum at Nanaimo_4 on Aug. 5, 2008, mean 34 Wm^{-2} overestimate. The r^2 was much higher, 0.6, than that for $L\downarrow$. As explained in section 4.3.3 on T_g comparison, the $L\uparrow$ overestimates at Changwon_smallpark were created by the higher ground albedo than the one used in the simulation because the high surface albedo could reduce absorbed solar radiation and reduce surface temperature.

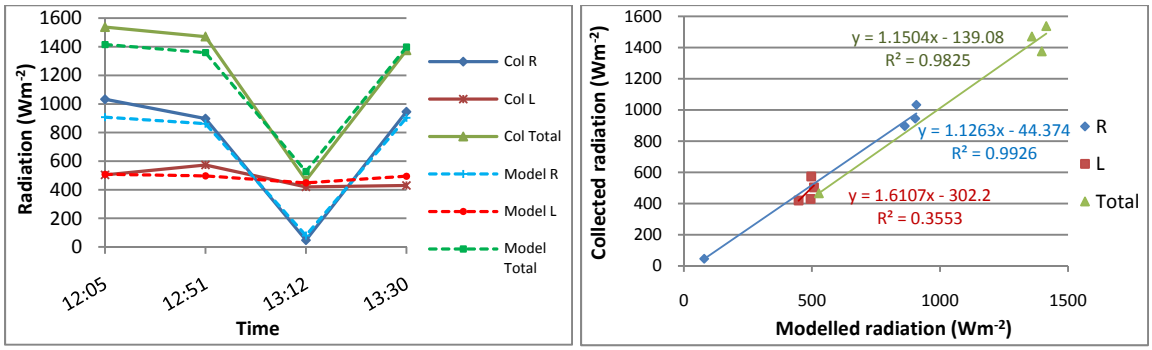

(a)

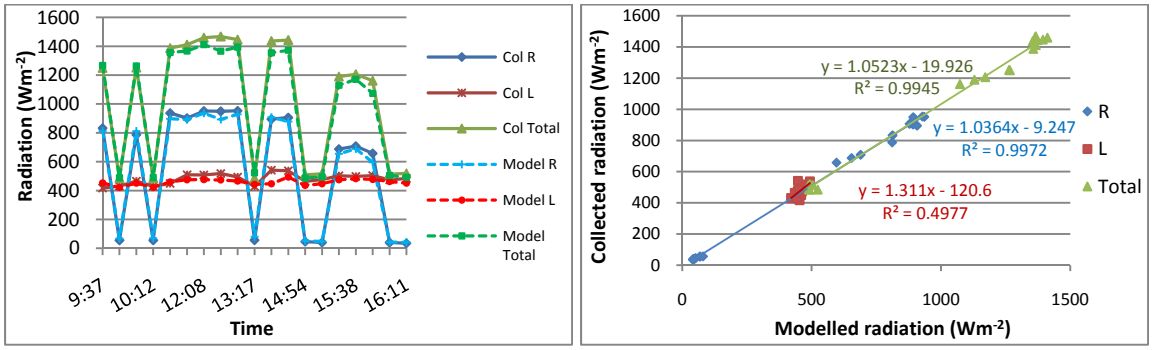

(b)

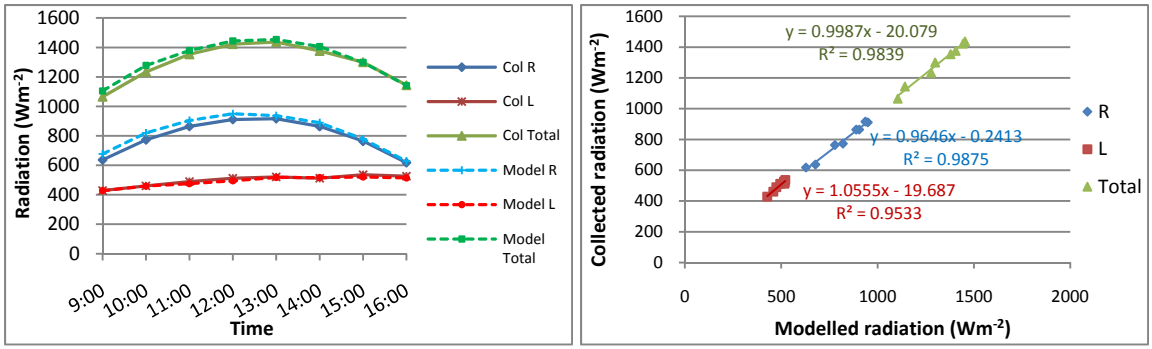

(c)

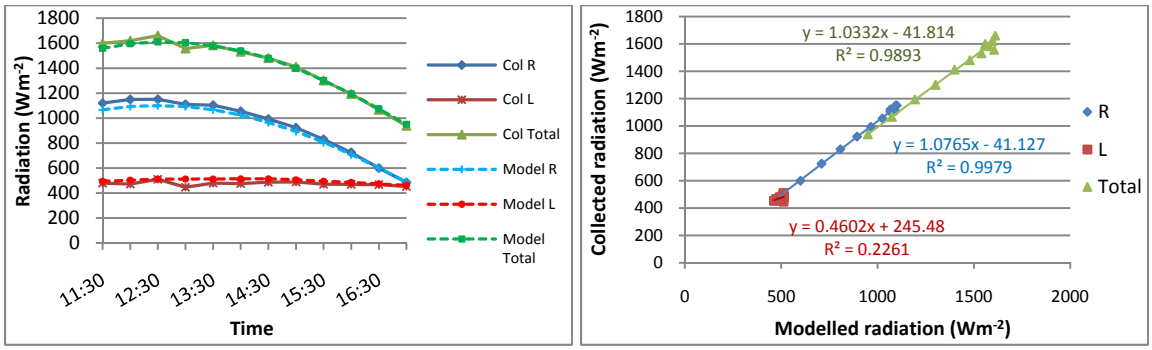

(d)

Fig. 4.19 Radiation comparison between collected data and New model results: (a) Nanaimo_1-5 (Aug. 5, 2008), (b) Nanaimo_1-5 (July 26, 2009), (c) Nanaimo_square (July 27, 2009) and (d) Changwon_smallpark (June 11, 2009)

Table 4.17 Comparison between collected radiation data and New model results (Wm^{-2})

Date/ Site	Time	Location	Solar Time	Sun/ Shade	Collected data							New model results														R-*R*	L-*L*	Total -*Total*
					R			*L*			*Total*[a]	R						L							Total			
												K↓				*K*↑	Total	*L*↓				*L*↑	Total				
					K↓	*K*↑	Total	*L*↓	*L*↑	Total		K_b	K_d	$K_{ro}+K_{rveg}$	Total	K_{rg}		L_a	L_o	L_{veg}	Total	L_g						
Aug. 5, 2008 (Nanaimo, B.C., Canada)	Noon	1	12:05	sunny	863	170	1033	224	280	504	1537	725	57	13	795	113	908	79	80	48	207	301	508	1415	-126	4	-122
		3	12:51	sunny	770	128	897	274	300	574	1471	721	52	6	779	83	862	75	130	2	208	289	497	1359	-35	-77	-112
		4	13:12	shady	39	8	47	205	215	420	466	0	32	10	41	38	79	68	129	2	200	248	448	527	33	28	61
		5	13:30	sunny	821	124	945	166	264	430	1375	695	90	22	806	97	903	124	48	30	202	293	495	1398	-42	64	22
		4	13:48	shady	35	29	64	204	215	419	483																
		3	14:00	sunny	768	61	829	227	298	524	1354																
		1	14:37	sunny	717	122	839	255	303	557	1397																
July 26, 2009 (Nanaimo, B.C., Canada)	Morning	1	9:07	sunny	589	87	677	220	244	464	1140																
		3	9:37	sunny	747	86	833	190	227	417	1250	576	50	80	706	107	813	71	136	2	209	244	454	1267	-20	37	17
		4	9:45	shady	49	7	55	210	221	431	486	0	29	31	60	8	68	68	131	2	201	220	421	489	13	-10	3
		5	10:00	sunny	691	96	787	195	270	465	1252	619	88	13	720	92	812	122	50	26	198	254	452	1263	24	-13	12
		4	10:12	shady	49	7	56	209	220	429	485	0	30	30	61	9	69	68	131	2	201	220	421	491	14	-8	6
		3	10:20	sunny	816	122	937	196	254	450	1387	652	51	76	779	118	897	71	133	2	205	255	460	1357	-40	10	-30
		1	10:44	sunny	778	124	902	233	276	509	1411	686	56	46	788	104	892	76	82	48	206	269	474	1367	-10	-34	-44
	Noon	1	12:08	sunny	829	122	952	223	285	508	1460	749	57	13	819	117	936	73	74	45	193	283	476	1411	-16	-33	-48
		3	12:34	sunny	837	113	949	228	290	518	1467	749	52	6	807	86	893	73	123	2	198	275	473	1366	-57	-45	-102
		4	12:46	shady	35	3	38	207	217	424	461																
		5	13:00	sunny	830	123	953	199	294	493	1447	740	91	10	841	87	929	122	53	20	194	272	466	1394	-25	-28	-53
		4	13:17	shady	44	12	57	207	221	428	485	0	32	10	42	39	81	69	127	2	198	245	443	524	24	15	39
		3	13:23	sunny	797	98	895	242	300	541	1436	725	52	33	810	98	908	75	125	2	202	286	489	1396	13	-94	-81
		1	13:43	sunny	788	118	906	233	304	537	1443	706	57	10	773	105	879	77	76	47	200	294	494	1372	-27	-44	-71
	Afternoon	1	14:54	shady	26	20	46	215	249	463	509	0	34	8	42	10	52	76	80	44	200	235	435	487	6	-28	-22
		3	15:18	shady	33	8	41	223	253	476	516	0	30	10	39	8	48	74	130	2	206	241	447	495	7	-29	-22
		4	15:28	sunny	623	65	688	226	277	502	1190	533	46	15	595	60	655	71	135	2	207	268	475	1129	-33	-27	-61
		5	15:38	sunny	612	96	708	199	299	498	1206	512	84	11	607	83	689	124	53	25	202	280	482	1171	-19	-16	-34
		4	15:46	sunny	586	72	658	226	278	504	1161	494	45	16	554	42	596	72	138	2	212	265	477	1073	-62	-27	-88
		3	15:53	shady	32	8	40	222	251	474	514	0	27	10	37	5	42	76	134	2	212	251	463	505	2	-11	-9
		1	16:11	shady	30	5	35	224	259	484	519	0	28	9	37	4	41	76	82	43	201	250	451	492	6	-33	-27
July 27, 2009 (Nanaimo, B.C., Canada)	Daytime	Square	9:00	sunny	569	68	637	190	238	428	1065	495	77	23	595	82	677	115	80	2	196	231	428	1105	40	-1	40
			10:00	sunny	690	83	773	199	262	460	1234	617	82	24	723	97	820	117	80	2	200	259	459	1278	46	-2	45
			11:00	sunny	772	92	864	207	282	490	1354	703	84	23	809	95	905	120	80	2	202	272	475	1379	41	-15	26
			12:00	sunny	811	100	911	215	297	512	1423	745	85	17	846	104	949	122	81	2	205	290	495	1444	38	-17	21
			13:00	sunny	815	101	916	214	307	521	1437	738	85	9	832	105	937	126	83	2	212	306	518	1454	20	-3	17
			14:00	sunny	766	98	864	202	311	512	1376	684	84	13	781	108	889	125	83	2	211	306	517	1406	25	5	30
			15:00	sunny	675	89	764	223	313	536	1300	588	81	14	684	95	778	128	86	2	216	305	521	1299	14	-15	-1
			16:00	sunny	545	73	618	218	308	526	1144	459	76	15	550	78	628	130	89	2	221	293	514	1142	10	-12	-2
June 11, 2009 (Changwon, Korea)	Daytime	Smallpark	11:30	sunny	947	173	1120	199	281	480	1600	801	117	11	928	138	1066	132	49	13	193	300	493	1559	-54	14	-41
			12:00	sunny	967	182	1149	188	284	471	1620	822	117	13	952	141	1093	131	52	13	196	307	503	1596	-56	32	-24
			12:30	sunny	970	181	1151	215	295	510	1661	828	117	13	957	142	1100	132	52	13	196	315	511	1611	-51	1	-50
			13:00	sunny	933	177	1110	175	271	446	1556	820	117	16	952	141	1093	133	51	13	197	315	512	1605	-17	66	48
			13:30	sunny	929	174	1103	185	295	480	1583	796	117	16	928	138	1066	133	52	13	198	315	512	1578	-37	33	-5
			14:00	sunny	888	167	1055	184	292	476	1531	759	116	18	893	132	1025	134	52	13	199	315	514	1539	-30	37	8
			14:30	sunny	836	158	993	198	290	487	1481	709	116	17	841	124	965	137	53	13	202	311	514	1479	-28	26	-2
			15:00	sunny	773	150	923	195	294	488	1411	647	114	18	779	115	893	136	54	12	202	304	506	1399	-30	18	-12
			15:30	sunny	693	138	831	191	279	470	1301	574	111	18	703	104	807	136	54	12	201	293	494	1301	-24	24	0
			16:00	sunny	601	124	725	191	278	469	1193	494	107	17	618	91	709	137	54	11	203	283	485	1194	-16	16	1
			16:30	sunny	498	102	600	195	272	467	1067	409	100	16	524	76	600	136	55	10	201	272	474	1074	0	7	7
			17:00	sunny	403	82	486	188	265	453	939	320	92	14	426	62	488	137	56	10	203	259	462	950	2	9	11

[a] total here indicates added total amounts of radiation, not net-radiation, coming from upper (↓) and lower (↑) hemispheres divided by the height of 1.2 m, mean height of torso (chest and abdomen). This is an important value to compute radiation quantities for the vertical standing human body.

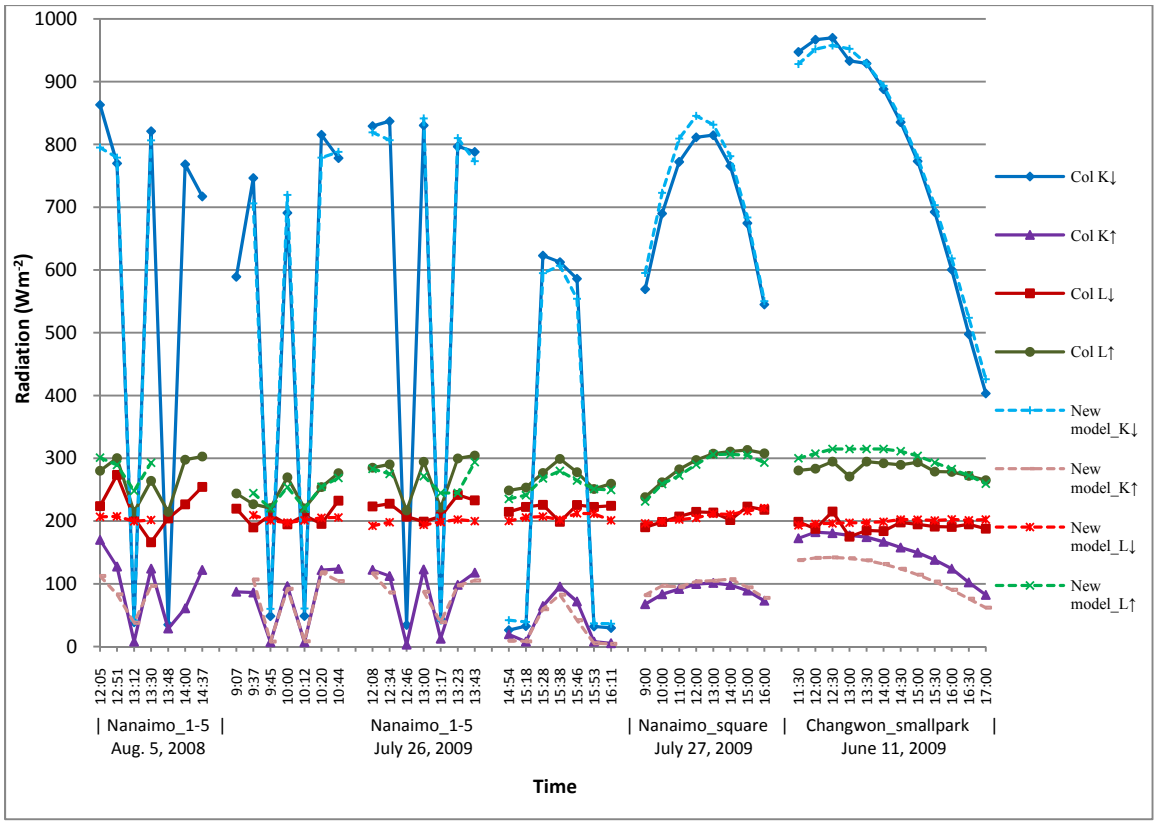

(a)

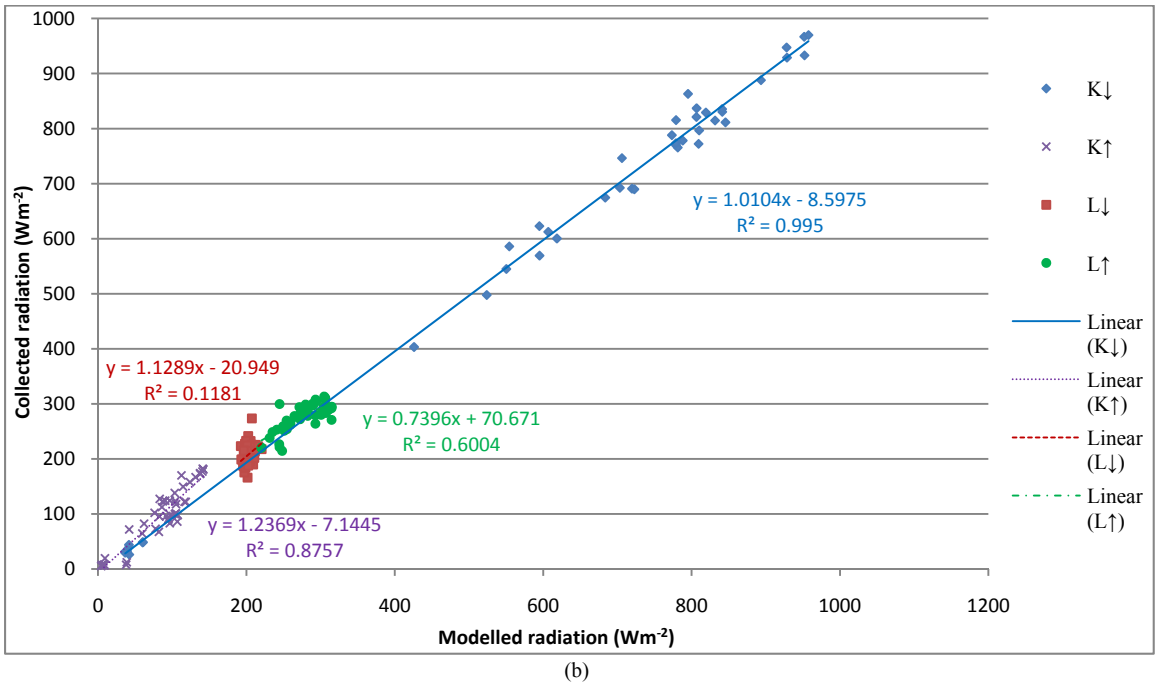

(b)

Fig. 4.20 Comparison and scatter plot of radiation components between collected data and New model results: (a) comparison of radiation components and (b) scatter plot

Table 4.18 Differences in solar and longwave radiation components between collected data and New model results (Wm^{-2})

Date/ Site	Time	Location	Solar Time	Sun/ Shade	Differences (New model results-Collected data)							Absolute differences						
					R			*L*			Total	*R*			*L*			Total
					K↓	*K*↑	Total	*L*↓	*L*↑	Total		*K*↓	*K*↑	Total	*L*↓	*L*↑	Total	
Aug. 5, 2008 (Nanaimo, B.C., Canada)	Noon	1	12:05	sunny	-68	-58	-126	-17	21	4	-122	68	58	126	17	21	38	164
		3	12:51	sunny	9	-44	-35	-66	-11	-77	-112	9	44	53	66	11	77	130
		4	13:12	shady	2	30	33	-5	34	28	61	2	30	33	5	34	39	71
		5	13:30	sunny	-15	-27	-42	36	29	64	22	15	27	42	36	29	64	107
		4	13:48	shady														
		3	14:00	sunny														
		1	14:37	sunny														
July 26, 2009 (Nanaimo, B.C., Canada)	Morning	1	9:07	sunny														
		3	9:37	sunny	-40	21	-20	19	17	37	17	40	21	61	19	17	37	98
		4	9:45	shady	11	1	13	-9	0	-10	3	11	1	13	9	0	10	23
		5	10:00	sunny	29	-4	24	3	-16	-13	12	29	4	33	3	16	18	51
		4	10:12	shady	12	2	14	-8	0	-8	6	12	2	14	8	0	8	21
		3	10:20	sunny	-37	-4	-40	10	0	10	-30	37	4	40	10	0	10	50
		1	10:44	sunny	10	-19	-10	-27	-8	-34	-44	10	19	29	27	8	34	64
	Noon	1	12:08	sunny	-10	-6	-16	-31	-2	-33	-48	10	6	16	31	2	33	48
		3	12:34	sunny	-30	-26	-57	-30	-15	-45	-102	30	26	57	30	15	45	102
		4	12:46	shady														
		5	13:00	sunny	11	-36	-25	-5	-23	-28	-53	11	36	47	5	23	28	74
		4	13:17	shady	-2	26	24	-9	24	15	39	2	26	29	9	24	33	61
		3	13:23	sunny	13	-1	13	-39	-55	-94	-81	13	1	14	39	55	94	108
		1	13:43	sunny	-15	-13	-27	-33	-10	-44	-71	15	13	27	33	10	44	71
	Afternoon	1	14:54	shady	16	-10	6	-15	-14	-28	-22	16	10	26	15	14	28	54
		3	15:18	shady	6	1	7	-17	-12	-29	-22	6	1	7	17	12	29	36
		4	15:28	sunny	-28	-5	-33	-19	-9	-27	-61	28	5	33	19	9	27	61
		5	15:38	sunny	-6	-13	-19	3	-19	-16	-34	6	13	19	3	19	22	41
		4	15:46	sunny	-32	-30	-62	-13	-13	-27	-88	32	30	62	13	13	27	88
		3	15:53	shady	5	-3	2	-11	0	-11	-9	5	3	7	11	0	11	18
		1	16:11	shady	7	-1	6	-23	-10	-33	-27	7	1	8	23	10	33	41
July 27, 2009 (Nanaimo, B.C., Canada)	Daytime	Square	9:00	sunny	26	15	40	6	-7	-1	40	26	15	40	6	7	13	53
			10:00	sunny	33	14	46	1	-3	-2	45	33	14	46	1	3	4	50
			11:00	sunny	37	3	41	-5	-10	-15	26	37	3	41	5	10	15	55
			12:00	sunny	34	4	38	-10	-7	-17	21	34	4	38	10	7	17	55
			13:00	sunny	17	4	20	-2	-1	-3	17	17	4	20	2	1	3	24
			14:00	sunny	16	9	25	9	-4	5	30	16	9	25	9	4	13	38
			15:00	sunny	9	5	14	-7	-8	-15	-1	9	5	14	7	8	15	30
			16:00	sunny	5	5	10	3	-15	-12	-2	5	5	10	3	15	17	27
June 11, 2009 (Changwon, Korea)	Daytime	Smallpark	11:30	sunny	-19	-35	-54	-6	19	14	-41	19	35	54	6	19	25	79
			12:00	sunny	-15	-41	-56	8	24	32	-24	15	41	56	8	24	32	88
			12:30	sunny	-12	-39	-51	-19	20	1	-50	12	39	51	19	20	39	90
			13:00	sunny	19	-36	-17	22	44	66	48	19	36	56	22	44	66	121
			13:30	sunny	-1	-37	-37	12	20	33	-5	1	37	37	12	20	33	70
			14:00	sunny	5	-35	-30	15	23	37	8	5	35	41	15	23	37	78
			14:30	sunny	6	-34	-28	5	22	26	-2	6	34	39	5	22	26	66
			15:00	sunny	5	-35	-30	8	10	18	-12	5	35	40	8	10	18	58
			15:30	sunny	11	-35	-24	10	14	24	0	11	35	45	10	14	24	69
			16:00	sunny	18	-34	-16	12	4	16	1	18	34	52	12	4	16	68
			16:30	sunny	26	-26	0	6	0	7	7	26	26	52	6	0	7	59
			17:00	sunny	22	-20	2	15	-6	9	11	22	20	43	15	6	20	63

Table 4.19 Maximum, minimum and mean values of radiation differences between collected data and New model results (Wm^{-2})

Date	Location	Radiation differences	Normal values							Absolute values						
			R			*L*			Total	*R*			*L*			Total
			K↓	*K*↑	Total	*L*↓	*L*↑	Total		*K*↓	*K*↑	Total	*L*↓	*L*↑	Total	
Aug. 5, 2008	sunny	Max.	9	-27	-35	36	29	64	22	68	58	126	66	29	77	164
		Min.	-68	-58	-126	-66	-11	-77	-122	9	27	42	17	11	38	107
		Mean	-25	-43	-68	-16	13	-3	-71	31	43	74	40	20	60	134
	shady	Max.	2	30	33	-5	34	28	61	2	30	33	5	34	39	71
		Min.	2	30	33	-5	34	28	61	2	30	33	5	34	39	71
		Mean	2	30	33	-5	34	28	61	2	30	33	5	34	39	71
July 26, 2009	sunny	Max.	29	21	24	19	17	37	17	40	36	62	39	55	94	108
		Min.	-40	-36	-62	-39	-55	-94	-102	6	1	14	3	0	10	41
		Mean	-11	-11	-23	-14	-13	-26	-49	22	15	37	19	16	35	71
	shady	Max.	16	26	24	-8	24	15	39	16	26	29	23	24	33	61
		Min.	-2	-10	2	-23	-14	-33	-27	2	1	7	8	0	8	18
		Mean	8	2	10	-13	-2	-15	-5	8	6	15	13	9	22	36
July 27, 2009	sunny	Max.	37	15	46	9	-1	5	45	37	15	46	10	15	17	55
		Min.	5	3	10	-10	-15	-17	-2	5	3	10	1	1	3	24
		Mean	22	7	29	-1	-7	-8	22	22	7	29	5	7	12	42
June 11, 2009	sunny	Max.	26	-20	2	22	44	66	48	26	41	56	22	44	66	121
		Min.	-19	-41	-56	-19	-6	1	-50	1	20	37	5	0	7	58
		Mean	5	-34	-28	7	16	24	-5	13	34	47	12	17	29	76
Sunny location mean			1	-18	-17	-4	1	-3	-19	20	22	42	15	15	30	71
Overall mean			2	-13	-11	-5	1	-4	-15	17	20	37	15	14	29	66

4.3.4.2 *RayMan Pro*

RayMan Pro clearly underestimates solar radiation at the sunny locations and overestimates at the shaded locations (Fig. 4.21 & Table 4.20). Direct beam solar radiation cannot reach shaded locations. Only diffuse beam and reflected solar radiation will affect the amounts of incoming solar radiation. However, this program does not have the reflected solar radiation component, so only diffuse beam solar radiation is effective at the shaded locations. The shaded locations had overestimates in diffuse beam solar radiation even though the estimated ψ_{sky} values were underestimated (Table 4.14 & Fig. 4.15).

Due to the omitted reflected solar radiation component, the RayMan results are incoming solar radiation only from the upper (sky) hemisphere. In Fig. 4.19a, only incoming solar radiation from the sky hemisphere ($K\downarrow$) is compared. $K\downarrow$ of locations with lower ψ_{sky} values, Nanaimo_1-4 on Aug. 5, 2008 and July 26, 2009 were underestimated by a mean of 46 Wm^{-2} (absolute mean: 49 Wm^{-2}) at the sunny locations and overestimated by a mean of 123 Wm^{-2} (absolute mean is the same) at the shaded locations. Those with more open skies, Nanaimo_square on July 27, 2009 and Changwon_smallpark on June 11, 2009 were estimated closely. The mean was 9.25 Wm^{-2} absolute difference (Tables 4.21 & 4.22). Therefore, it can be

noted that RayMan had good solar radiation estimates from the sky hemisphere only at higher ψ_{sky} locations. To estimate total solar radiation from both the sky and ground hemispheres, RayMan needs components of reflected solar radiation from obstructions in the sky hemisphere and from the ground hemisphere and more precise formulas for the diffuse beam solar radiation component as well as ψ_{sky} estimation.

The r^2 between estimated and observed solar radiation was very high, over 0.983 (Figs. 4.21 & 4.22b) although the real differences were large, mean 21 Wm^{-2} (sunny locations only: 50 Wm^{-2}) and absolute mean 62 Wm^{-2} (sunny locations only: 52 Wm^{-2}) (Table 4.22).

In longwave radiation analysis, there are two incoming directions: from the sky hemisphere ($L\downarrow$) and from the ground hemisphere ($L\uparrow$). As RayMan does not include ψ_{sky} effects in the formula of longwave radiation from the sky (L_a) and does not have a longwave radiation from obstructions component (L_o), the estimated $L\downarrow$ values by RayMan should be a lot lower than the observed $L\downarrow$ values. The reason is obvious because the surrounding obstructions will have much higher surface temperatures and emissivities than the sky. RayMan's $L\downarrow$ results were comprised of the effects of two variables, air temperature (T_a) and vapour pressure (e_a), so the range was very narrow and did not change with ψ_{sky} (Fig. 4.22a). More open sky locations such as Nanaimo_5, Nanaimo_square and Changwon_smallpark have close results with the collected $L\downarrow$ data, e.g., mean 16 Wm^{-2} difference at Nanaimo_square and 1 Wm^{-2} at Changwon_smallpark (Table 4.22). As expected, there was a very weak r^2 with RayMan's $L\downarrow$ results, only 0.021 (Fig. 4.22b).

The ground surface is representative of the ground hemisphere because the height of radiation measurement is 1.2 m and measuring instruments are located horizontally so that the ground surface temperature must be most effective in its $L\uparrow$ analysis if obstructions shown in the ground hemisphere do not have extremely higher or lower surface temperatures than the ground surface temperature. RayMan's $L\uparrow$ results follow the same pattern as T_g: RayMan overestimates before noon and underestimates after. The r^2 with RayMan's $L\uparrow$ results was 0.555 and the real differences only averaged 3 Wm^{-2} (absolute mean: 15 Wm^{-2}) for all datasets which were much better results than the differences of $L\downarrow$, mean 19 Wm^{-2} (absolute mean: 21 Wm^{-2}) (Fig. 4.22b & Table 4.22). The r^2 of total longwave radiation (L) varied from 0.321 at Changwon_smallpark to 0.840 at Nanaimo_square.

The r^2 between the collected data and RayMan results was very high for solar radiation from the sky hemisphere, and low for longwave radiation, especially longwave radiation from the sky hemisphere (Fig. 4.22b). Similar to the high solar radiation r^2 values, those for total radiation were very strong, over 0.940. The real radiation differences were also moderate: mean 21 Wm^{-2} (absolute mean: 62 Wm^{-2}) in solar radiation, 22 Wm^{-2} (36 Wm^{-2}) in longwave radiation and 44 Wm^{-2} (97 Wm^{-2}) in total radiation (Table 4.22).

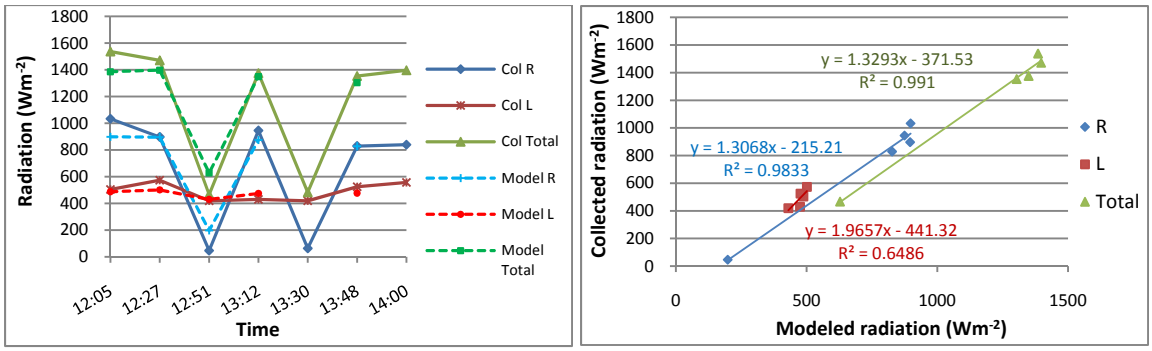

(a)

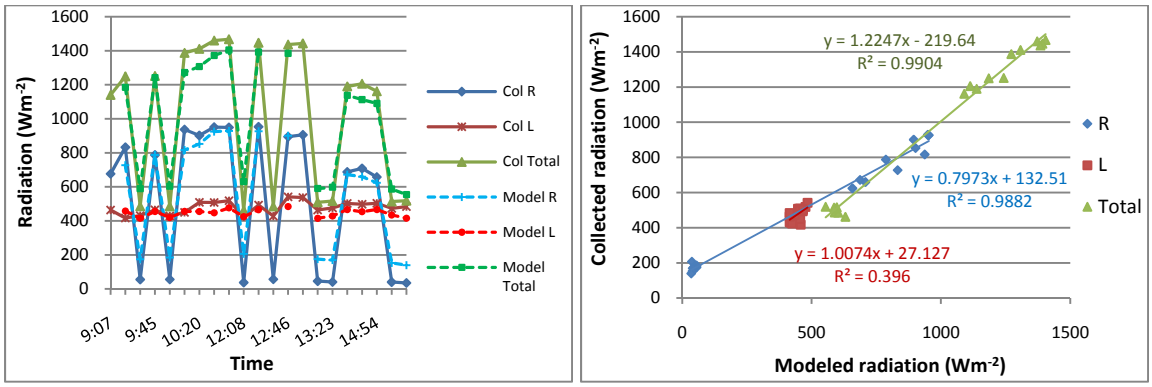

(b)

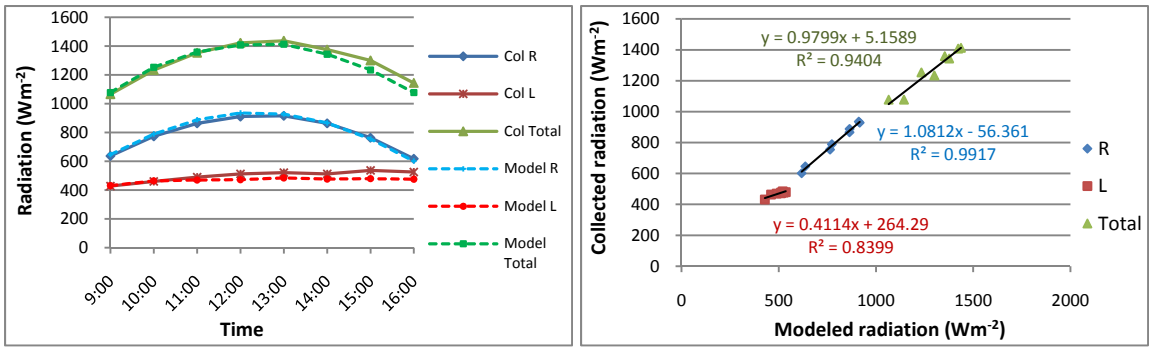

(c)

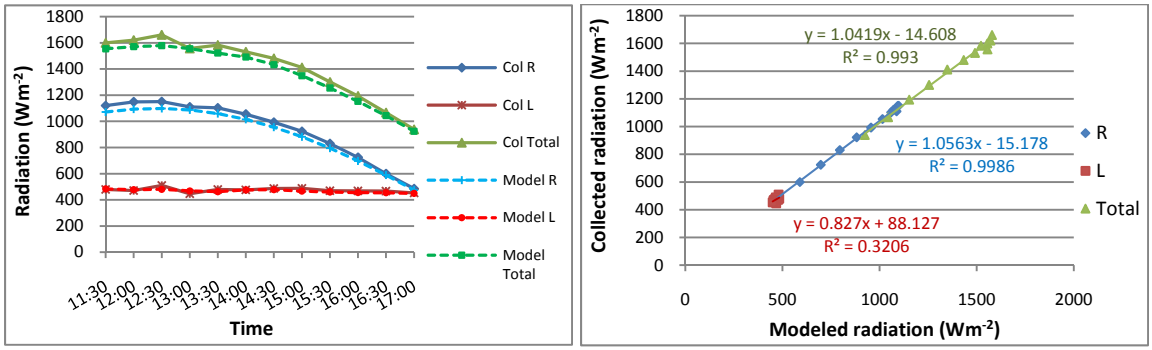

(d)

Fig. 4.21 Radiation comparison between collected data and RayMan Pro results: (a) Nanaimo_1-5 (Aug. 5, 2008), (b) Nanaimo_1-5 (July 26, 2009), (c) Nanaimo_square (July 27, 2009) and (d) Changwon_smallpark (June 11, 2009)

Table 4.20 Comparison between collected radiation data and RayMan Pro results (Wm^{-2})

Date/ Site	Time	Location	Solar Time	Sun/ Shade	Collected data							RayMan Pro results								R-*R*	L-*L*	Total-*Total*
					R			*L*			*Total*	R				L			Total			
					K↓	*K*↑	Total	*L*↓	*L*↑	Total		G_0	K_b	K_d	Total	L_a	L_g	Total				
Aug. 5, 2008 (Nanaimo, B.C., Canada)	Noon	1	12:05	sunny	863	170	1033	224	280	504	1537	821	694	87	898	192	295	488	1386	-135	-17	-152
		3	12:51	sunny	770	128	897	274	300	574	1471	817	690	90	896	196	305	501	1397	-1	-73	-74
		4	13:12	shady	39	8	47	205	215	420	466	806	0	172	198	188	242	430	628	151	11	162
		5	13:30	sunny	821	124	945	166	264	430	1375	792	663	98	875	191	284	475	1349	-70	44	-26
		4	13:48	shady	35	29	64	204	215	419	483											
		3	14:00	sunny	768	61	829	227	298	524	1354	760	629	90	827	188	289	477	1304	-2	-48	-50
		1	14:37	sunny	717	122	839	255	303	557	1397											
July 26, 2009 (Nanaimo, B.C., Canada)	Morning	1	9:07	sunny	589	87	677	220	244	464	1140											
		3	9:37	sunny	747	86	833	190	227	417	1250	678	541	91	727	183	274	458	1185	-106	41	-65
		4	9:45	shady	49	7	55	210	221	431	486	693	0	151	174	183	232	416	589	119	-15	103
		5	10:00	sunny	691	96	787	195	270	465	1252	720	585	100	787	184	272	455	1243	0	-9	-9
		4	10:12	shady	49	7	56	209	220	429	485	740	0	160	184	184	235	419	603	128	-10	119
		3	10:20	sunny	816	122	937	196	254	450	1387	752	618	92	816	182	273	456	1272	-121	6	-115
		1	10:44	sunny	778	124	902	233	276	509	1411	785	653	89	852	183	272	455	1307	-50	-54	-103
	Noon	1	12:08	sunny	829	122	952	223	285	508	1460	845	716	88	925	178	269	447	1372	-27	-61	-88
		3	12:34	sunny	837	113	949	228	290	518	1467	845	716	91	928	186	291	476	1405	-21	-42	-63
		4	12:46	shady	35	3	38	207	217	424	461	842	0	179	206	186	239	425	631	169	1	169
		5	13:00	sunny	830	123	953	199	294	493	1447	837	707	98	927	182	284	466	1392	-27	-28	-54
		4	13:17	shady	44	12	57	207	221	428	485											
		3	13:23	sunny	797	98	895	242	300	541	1436	822	692	91	900	191	293	484	1385	5	-57	-52
		1	13:43	sunny	788	118	906	233	304	537	1443											
	Afternoon	1	14:54	shady	26	20	46	215	249	463	509	702	0	153	175	183	232	415	590	129	-49	81
		3	15:18	shady	33	8	41	223	253	476	516	655	0	147	169	189	240	429	598	128	-47	81
		4	15:28	sunny	623	65	688	226	277	502	1190	634	497	87	672	189	278	466	1138	-16	-36	-52
		5	15:38	sunny	612	96	708	199	299	498	1206	612	475	99	659	188	266	454	1113	-49	-44	-93
		4	15:46	sunny	586	72	658	226	278	504	1161	594	456	86	624	193	274	467	1090	-34	-37	-71
		3	15:53	shady	32	8	40	222	251	474	514	578	0	133	153	193	242	434	587	112	-39	73
		1	16:11	shady	30	5	35	224	259	484	519	535	0	121	139	184	231	415	554	104	-69	35
July 27, 2009 (Nanaimo, B.C., Canada)	Daytime	Square	9:00	sunny	569	68	637	190	238	428	1065	597	459	103	646	181	250	431	1078	9	3	12
			10:00	sunny	690	83	773	199	262	460	1234	718	583	104	789	185	279	464	1253	16	3	20
			11:00	sunny	772	92	864	207	282	490	1354	801	670	103	888	188	282	470	1359	24	-19	5
			12:00	sunny	811	100	911	215	297	512	1423	841	712	102	936	192	281	472	1408	25	-40	-15
			13:00	sunny	815	101	916	214	307	521	1437	835	706	102	928	197	288	485	1413	12	-36	-24
			14:00	sunny	766	98	864	202	311	512	1376	783	651	103	867	195	282	477	1343	3	-36	-33
			15:00	sunny	675	89	764	223	313	536	1300	689	552	104	755	199	280	479	1234	-9	-57	-66
			16:00	sunny	545	73	618	218	308	526	1144	559	422	102	602	202	274	476	1077	-16	-50	-67
June 11, 2009 (Changwon, Korea)	Daytime	Small park	11:30	sunny	947	173	1120	199	281	480	1600	950	842	89	1071	189	295	484	1555	-49	4	-45
			12:00	sunny	967	182	1149	188	284	471	1620	968	863	88	1093	189	289	478	1571	-56	6	-50
			12:30	sunny	970	181	1151	215	295	510	1661	973	868	88	1099	190	291	480	1579	-52	-30	-82
			13:00	sunny	933	177	1110	175	271	446	1556	963	857	88	1087	189	279	468	1555	-23	22	-1
			13:30	sunny	929	174	1103	185	295	480	1583	940	831	90	1059	189	274	463	1522	-44	-17	-61
			14:00	sunny	888	167	1055	184	292	476	1531	902	791	92	1015	190	286	476	1491	-40	0	-40
			14:30	sunny	836	158	993	198	290	487	1481	852	737	95	956	193	285	477	1433	-38	-10	-48
			15:00	sunny	773	150	923	195	294	488	1411	790	670	97	882	193	274	467	1348	-41	-22	-63
			15:30	sunny	693	138	831	191	279	470	1301	716	592	99	795	192	268	460	1255	-36	-10	-46
			16:00	sunny	601	124	725	191	278	469	1193	633	506	100	697	192	264	455	1152	-28	-14	-41
			16:30	sunny	498	102	600	195	272	467	1067	542	414	98	589	192	262	454	1044	-10	-13	-23
			17:00	sunny	403	82	486	188	265	453	939	445	320	93	475	193	257	449	924	-11	-4	-15

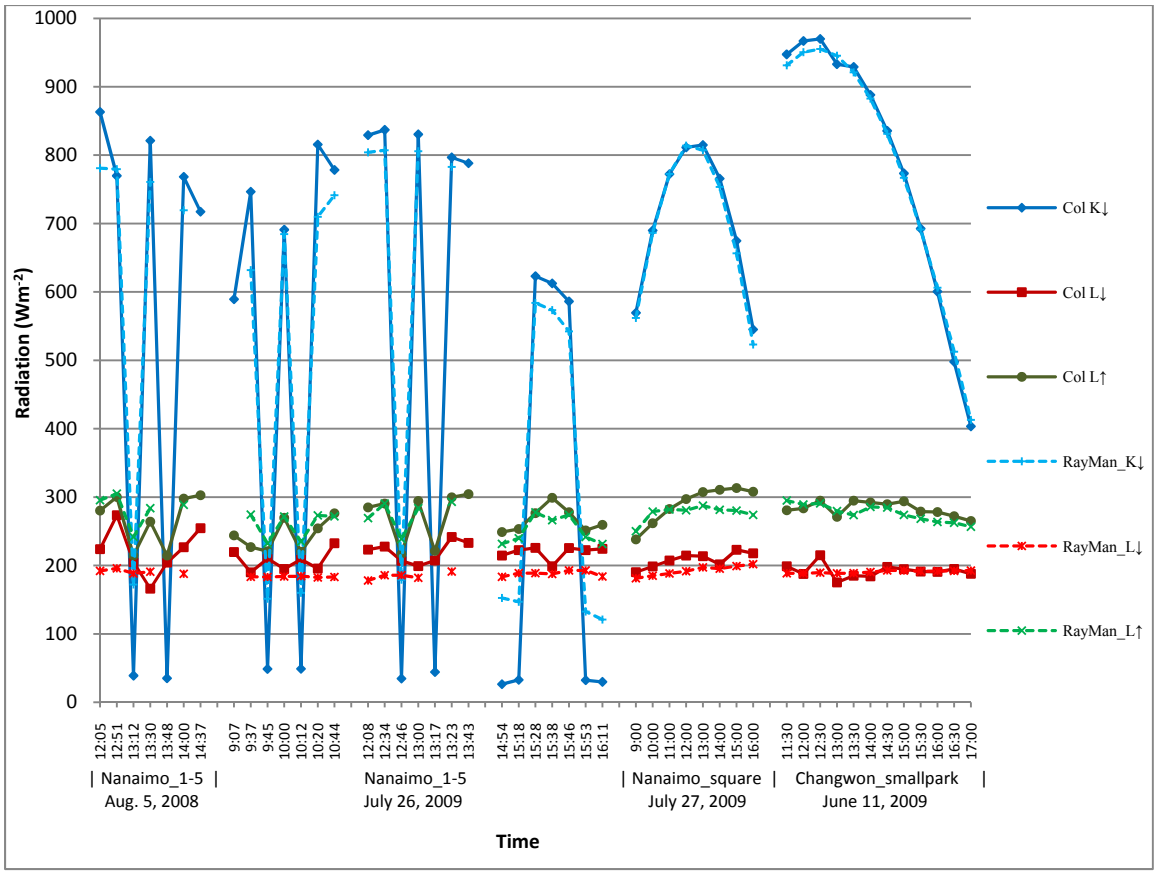

(a)

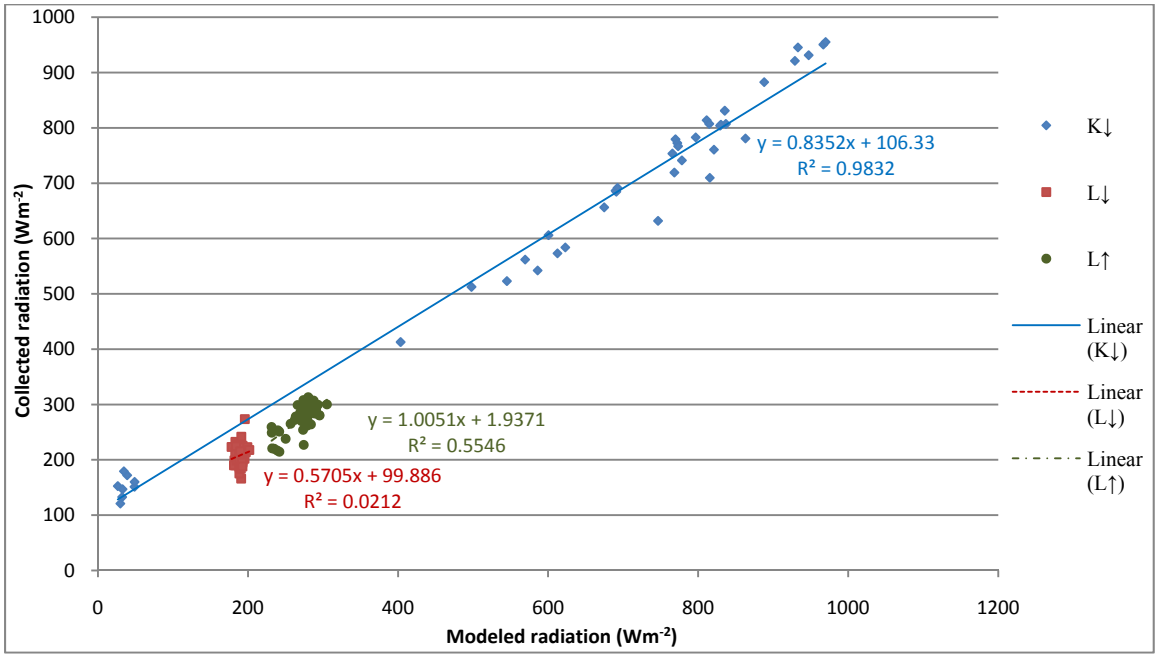

(b)

Fig. 4.22 Comparison and scatter plot of radiation components between collected data and RayMan Pro results: (a) comparison of radiation components and (b) scatter plot

Table 4.21 Differences in solar and longwave radiation components between collected data and RayMan Pro results (Wm^{-2})

Date/ Site	Time	Location	Solar Time	Sun/ Shade	Differences (RayMan results-Collected data)						Absolute differences					
					R		*L*			Total	*R*		*L*			Total
					$K\downarrow$	Total	$L\downarrow$	$L\uparrow$	Total		$K\downarrow$	Total	$L\downarrow$	$L\uparrow$	Total	
Aug. 5, 2008 (Nanaimo, B.C., Canada)	Noon	1	12:05	sunny	-82	-152	-32	15	-17	-168	82	152	32	15	47	198
		3	12:51	sunny	10	-74	-78	5	-73	-146	10	74	78	5	83	156
		4	13:12	shady	133	162	-17	27	11	172	133	162	17	27	44	206
		5	13:30	sunny	-60	-26	25	20	44	18	60	26	25	20	44	70
		4	13:48	shady												
		3	14:00	sunny	-49	-50	-39	-9	-48	-98	49	50	39	9	48	98
		1	14:37	sunny												
July 26, 2009 (Nanaimo, B.C., Canada)	Morning	1	9:07	sunny												
		3	9:37	sunny	-115	-65	-6	47	41	-24	115	65	6	47	54	119
		4	9:45	shady	103	103	-27	12	-15	88	103	103	27	12	38	142
		5	10:00	sunny	-6	-9	-11	2	-9	-19	6	9	11	2	13	22
		4	10:12	shady	111	119	-25	15	-10	109	111	119	25	15	39	158
		3	10:20	sunny	-106	-115	-13	19	6	-109	106	115	13	19	32	147
		1	10:44	sunny	-37	-103	-49	-4	-54	-157	37	103	49	4	54	157
	Noon	1	12:08	sunny	-25	-88	-45	-16	-61	-149	25	88	45	16	61	149
		3	12:34	sunny	-30	-63	-42	0	-42	-104	30	63	42	0	42	105
		4	12:46	shady	145	169	-21	22	1	170	145	169	21	22	43	212
		5	13:00	sunny	-25	-54	-17	-11	-28	-82	25	54	17	11	28	82
		4	13:17	shady												
		3	13:23	sunny	-14	-52	-51	-6	-57	-109	14	52	51	6	57	109
		1	13:43	sunny												
	Afternoon	1	14:54	shady	126	81	-31	-17	-49	32	126	81	31	17	49	129
		3	15:18	shady	114	81	-34	-14	-47	34	114	81	34	14	47	128
		4	15:28	sunny	-39	-52	-37	1	-36	-88	39	52	37	1	38	90
		5	15:38	sunny	-39	-93	-11	-33	-44	-137	39	93	11	33	44	137
		4	15:46	sunny	-44	-71	-33	-4	-37	-108	44	71	33	4	37	108
		3	15:53	shady	100	73	-30	-9	-39	34	100	73				73
		1	16:11	shady	91	35	-40	-28	-69	-33	91	35	40	28	69	104
July 27, 2009 (Nanaimo, B.C., Canada)	Daytime	Square	9:00	sunny	-7	12	-9	12	3	15	7	12	9	12	21	33
			10:00	sunny	-3	20	-14	17	3	23	3	20	14	17	31	50
			11:00	sunny	0	5	-19	-1	-19	-15	0	5	19	1	19	24
			12:00	sunny	2	-15	-23	-17	-40	-54	2	15	23	17	40	54
			13:00	sunny	-7	-24	-17	-20	-36	-60	7	24	17	20	36	60
			14:00	sunny	-12	-33	-6	-29	-36	-69	12	33	6	29	36	69
			15:00	sunny	-18	-66	-24	-33	-57	-123	18	66	24	33	57	123
			16:00	sunny	-22	-67	-16	-34	-50	-117	22	67	16	34	50	117
June 11, 2009 (Changwon, Korea)	Daytime	Small park	11:30	sunny	-16	-45	-10	14	4	-41	16	45	10	14	25	70
			12:00	sunny	-16	-50	1	5	6	-43	16	50	1	5	6	56
			12:30	sunny	-15	-82	-26	-4	-30	-111	15	82	26	4	30	111
			13:00	sunny	13	-1	13	8	22	21	13	1	13	8	22	23
			13:30	sunny	-8	-61	4	-21	-17	-78	8	61	4	21	25	86
			14:00	sunny	-5	-40	6	-7	0	-40	5	40	6	7	13	53
			14:30	sunny	-4	-48	-5	-5	-10	-58	4	48	5	5	10	58
			15:00	sunny	-6	-63	-2	-20	-22	-85	6	63	2	20	22	85
			15:30	sunny	-1	-46	0	-11	-10	-56	1	46	0	11	11	57
			16:00	sunny	6	-41	1	-15	-14	-55	6	41	1	15	16	57
			16:30	sunny	15	-23	-3	-10	-13	-36	15	23	3	10	13	36
			17:00	sunny	9	-15	5	-8	-4	-18	9	15	5	8	13	28

Table 4.22 Maximum, minimum and mean values of radiation differences between collected data and RayMan Pro results (Wm^{-2})

Date	Location	Radiation difference	Normal values						Absolute values					
			R		*L*			Total	*R*		*L*			Total
			K↓	Total	*L*↓	*L*↑	Total		*K*↓	Total	*L*↓	*L*↑	Total	
Aug. 5, 2008	sunny	Max.	10	-26	25	20	44	18	82	152	78	20	83	198
		Min.	-82	-152	-78	-9	-73	-168	10	26	25	5	44	70
		Mean	-45	-75	-31	8	-23	-98	50	75	43	12	55	131
	shady	Max.	133	162	-17	27	11	172	133	162	17	27	44	206
		Min.	133	162	-17	27	11	172	133	162	17	27	44	206
		Mean	133	162	-17	27	11	172	133	162	17	27	44	206
July 26, 2009	sunny	Max.	-6	-9	-6	47	41	-19	115	115	51	47	61	157
		Min.	-115	-115	-51	-33	-61	-157	6	9	6	0	13	22
		Mean	-44	-70	-29	0	-29	-99	44	70	29	13	42	111
	shady	Max.	145	169	-21	22	1	170	145	169	40	28	69	212
		Min.	91	35	-40	-28	-69	-33	91	35	21	9	38	104
		Mean	113	95	-30	-3	-33	62	113	95	30	17	46	141
July 27, 2009	sunny	Max.	2	20	-6	17	3	23	22	67	24	34	57	123
		Min.	-22	-67	-24	-34	-57	-123	0	5	6	1	19	24
		Mean	-8	-21	-16	-13	-29	-50	9	30	16	20	36	66
June 11, 2009	sunny	Max.	15	-1	13	14	22	21	16	82	26	21	30	111
		Min.	-16	-82	-26	-21	-30	-111	1	1	0	4	6	23
		Mean	-2	-43	-1	-6	-7	-50	10	43	6	11	17	60
Sunny location mean			-22	-50	-17	-4	-21	-71	25	52	20	14	34	86
Overall mean			4	-21	-19	-3	-22	-44	42	62	21	15	36	97

4.3.4.3 *ENVI-met 3.1*

All radiation data from ENVI-met were from the height of 1 m above the ground surface instead of 1.2 m because of the program's limitation of no decimal height data input function. This program, overall, greatly overestimated solar radiation and underestimated longwave radiation (Fig. 4.23 & Table 4.23). The differences in solar radiation became greater at lower solar altitudes, in the morning and afternoon. Those for longwave radiation became bigger in the afternoon. Because of larger overestimates in solar radiation compared with underestimates in longwave radiation, total radiation was overestimated at both the sunny and shaded locations (Tables 4.24 & 4.25).

The online website manual notes "The value of the direct shortwave radiation is given as the maximum possible value, including shading effects but not including the inclination and exposition of the surface. For the diffuse and reflected shortwave radiation, the values for a horizontal surface are given" (http://www.envi-met.com/htmlhelp/hs520.htm). This means the program does not seem to target precise solar radiation simulation. Also, reflected solar radiation by the ground surface (*K*↑) seems internally

calculated using a set albedo of the ground surface, so there is no individual output of $K\uparrow$ dependent on actual surface albedo.

This program overestimated incoming solar radiation from the sky hemisphere ($K\downarrow$) by around 125 Wm^{-2} at Nanaimo_1-5 on Aug. 5, 2008 and July 26, 2009 at the shaded locations and a mean of 372 Wm^{-2} at the sunny locations (Fig. 4.24a & Table 4.25).

Longwave radiation from the sky hemisphere ($L\downarrow$) was much closer to the collected data than the $K\downarrow$ results at both sunny and shaded locations. The mean differences were from 13 Wm^{-2} to 40 Wm^{-2} and no typical pattern was found. Differences between observed and modeled longwave radiation from the ground hemisphere ($L\uparrow$) were larger in the afternoon, following the pattern of T_g (Tables 4.16 & 4.24). The observed and modeled $L\uparrow$ values at shaded locations were very close, a mean 3 Wm^{-2} overestimate on Aug. 5, 2008 and 16 Wm^{-2} underestimate on July 26, 2009 (Table 4.25). Also, the results were closer at sunny Changwon_smallpark, a mean 22 Wm^{-2} underestimate, than at sunny Nanaimo locations, a mean 36 Wm^{-2} underestimate, as expected from the T_g results (Table 4.16). ENVI-met 3.1 largely underestimates longwave radiation from the sky (L_a) due to low T_a estimates (Table 4.15) and underestimates longwave radiation from the ground (L_g) due to low T_g estimates (Table 4.16). ENVI-met worked better for the longwave radiation estimate in the more turbid sky condition of Changwon_smallpark.

The r^2 values for the individual site/date cases were very high, over 0.964 and 0.942, for solar radiation and total radiation, respectively (Fig. 4.23). Also, $K\downarrow$ of the entire data set had a good r^2, 0.935 (Fig. 4.24). However, the r^2 values of $L\downarrow$ and $L\uparrow$ were only 0.180 and 0.699, respectively. The real radiation differences were very significant: mean 377 Wm^{-2} (absolute mean: 377 Wm^{-2}) for total solar radiation, -57 Wm^{-2} (absolute mean: 58 Wm^{-2}) for total longwave radiation and 320 Wm^{-2} (absolute mean: 435 Wm^{-2}) for total radiation (Table 4.25).

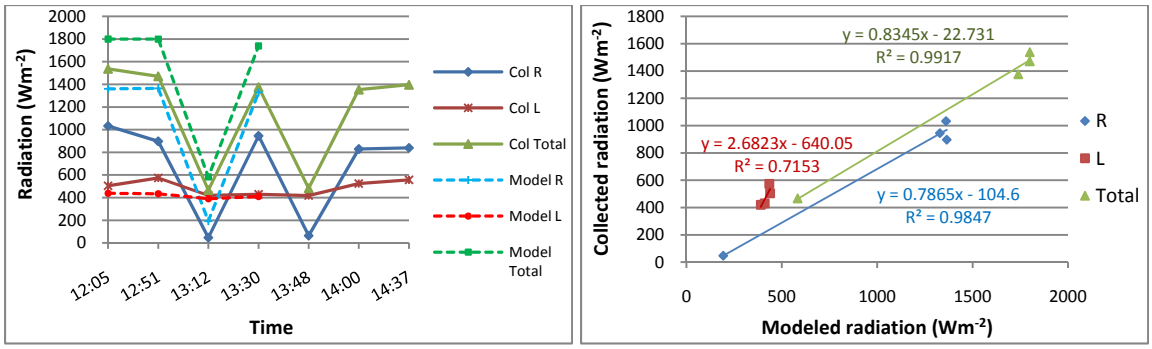

(a)

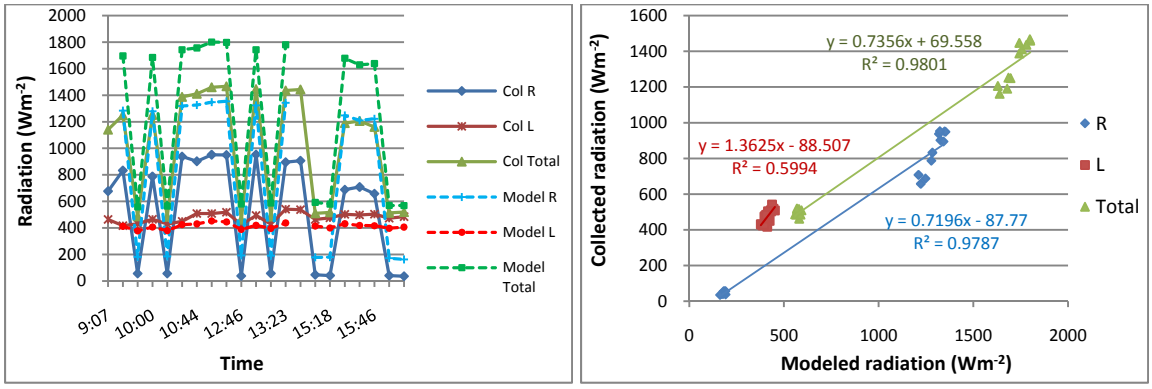

(b)

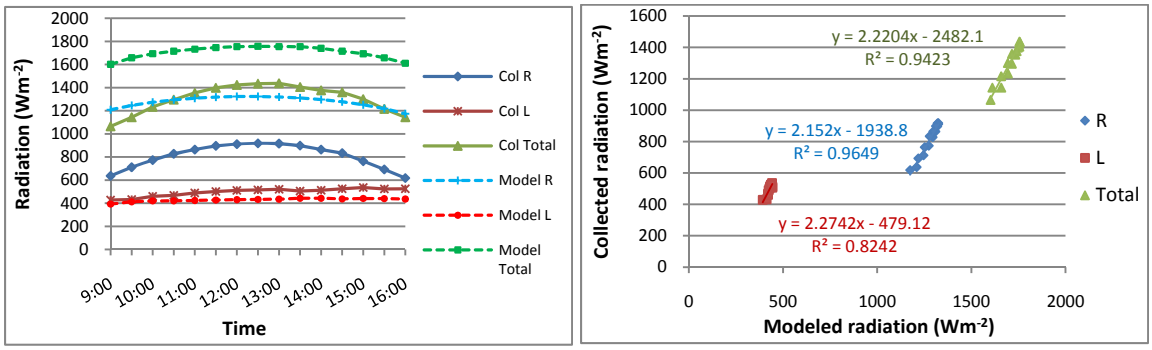

(c)

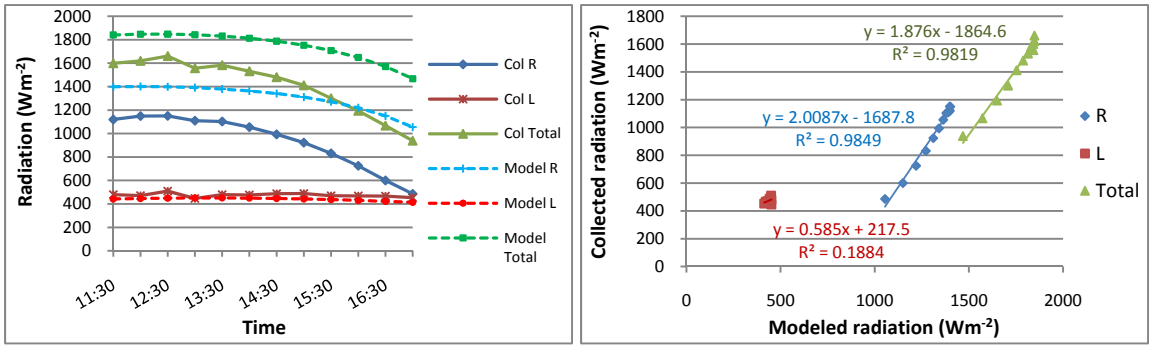

(d)

Fig. 4.23 Radiation comparison between collected data and ENVI-met 3.1 results: (a) Nanaimo_1-5 (Aug. 5, 2008), (b) Nanaimo_1-5 (July 26, 2009), (c) Nanaimo_square (July 27, 2009) and (d) Changwon_smallpark (June 11, 2009)

Table 4.23 Comparison between collected radiation data and ENVI-met 3.1 results (Wm^{-2})

Date/ Site	Time	Location	Solar Time	Sun/ Shade	Collected data							ENVI-met 3.1 results										R-*R*	L-*L*	Total-*Total*
					R			*L*			*Total*	R				L					Total			
												K↓			Total	*L*↓			*L*↑	Total				
					K↓	*K*↑	Total	*L*↓	*L*↑	Total		K_b	K_d	K_r		L_a	L_o	Total	L_g					
Aug. 5, 2008 (Nanaimo, B.C., Canada)	Noon	1	12:05	sunny	863	170	1033	224	280	504	1537	1017	53	114	1361	62	124	186	252	438	1800	328	-66	262
		3	12:51	sunny	770	128	897	274	300	574	1471	1015	46	125	1365	49	138	188	247	435	1799	468	-139	329
		4	13:12	shady	39	8	47	205	215	420	466	0	50	118	193	61	112	173	217	390	583	146	-30	117
		5	13:30	sunny	821	124	945	166	264	430	1375	1009	79	68	1329	100	69	169	241	410	1739	384	-20	364
		4	13:48	shady	35	29	64	204	215	419	483													
		3	14:00	sunny	768	61	829	227	298	524	1354													
		1	14:37	sunny	717	122	839	255	303	557	1397													
July 26, 2009 (Nanaimo, B.C., Canada)	Morning	1	9:07	sunny	589	87	677	220	244	464	1140													
		3	9:37	sunny	747	86	833	190	227	417	1250	958	41	118	1284	49	130	180	232	412	1696	452	-5	447
		4	9:45	shady	49	7	55	210	221	431	486	0	46	112	181	61	105	167	211	378	559	126	-53	72
		5	10:00	sunny	691	96	787	195	270	465	1252	972	74	65	1279	100	70	171	236	406	1685	491	-58	433
		4	10:12	shady	49	7	56	209	220	429	485		47	113	185	62	106	168	212	379	564	129	-50	80
		3	10:20	sunny	816	122	937	196	254	450	1387	982	44	121	1319	50	134	184	240	424	1743	381	-26	356
		1	10:44	sunny	778	124	902	233	276	509	1411	992	51	111	1326	64	120	185	246	430	1756	424	-79	346
	Noon	1	12:08	sunny	829	122	952	223	285	508	1460	1007	53	112	1348	66	127	193	260	452	1801	397	-56	341
		3	12:34	sunny	837	113	949	228	290	518	1467	1007	46	124	1353	52	141	193	252	445	1798	404	-73	331
		4	12:46	shady	35	3	38	207	217	424	461		50	117	192	64	108	172	216	388	580	154	-36	119
		5	13:00	sunny	830	123	953	199	294	493	1447	1004	80	68	1324	105	64	169	250	419	1743	370	-74	296
		4	13:17	shady	44	12	57	207	221	428	485		50	116	191	64	115	180	217	396	587	134	-32	102
		3	13:23	sunny	797	98	895	242	300	541	1436	999	45	123	1343	52	132	184	253	437	1780	448	-104	344
		1	13:43	sunny	788	118	906	233	304	537	1443													
	Afternoon	1	14:54	shady	26	20	46	215	249	463	509		48	107	178	67	114	181	234	414	592	132	-49	83
		3	15:18	shady	33	8	41	223	253	476	516		40	116	180	52	125	177	223	399	579	139	-77	63
		4	15:28	sunny	623	65	688	226	277	502	1190	934	43	108	1248	64	122	187	245	431	1679	560	-71	489
		5	15:38	sunny	612	96	708	199	299	498	1206	924	67	62	1211	105	72	177	242	418	1629	503	-79	424
		4	15:46	sunny	586	72	658	226	278	504	1161	915	42	106	1223	64	117	181	235	416	1639	565	-87	477
		3	15:53	shady	32	8	40	222	251	474	514		38	112	172	52	124	176	221	397	569	132	-76	55
		1	16:11	shady	30	5	35	224	259	484	519		42	99	163	66	112	178	228	406	568	127	-78	49
July 27, 2009 (Nanaimo, B.C., Canada)	Daytime	Square	9:00	sunny	569	68	637	190	238	428	1065	921	64	67	1209	96	78	173	219	392	1602	572	-36	537
			9:30	sunny	633	79	712	185	247	432	1144	947	68	68	1246	97	80	177	236	413	1659	534	-19	515
			10:00	sunny	690	83	773	199	262	460	1234	967	71	70	1274	98	82	179	241	420	1694	500	-40	460
			10:30	sunny	736	92	828	198	269	468	1295	981	73	71	1294	99	77	175	245	421	1715	466	-47	420
			11:00	sunny	772	92	864	207	282	490	1354	992	75	72	1309	100	75	175	249	424	1733	445	-66	379
			11:30	sunny	798	99	897	211	291	501	1398	999	76	72	1319	100	75	176	252	428	1746	422	-74	348
			12:00	sunny	811	100	911	215	297	512	1423	1002	77	72	1324	101	75	177	254	431	1754	413	-81	332
			12:30	sunny	819	99	918	214	302	516	1434	1002	77	72	1324	102	75	177	256	433	1757	406	-82	324
			13:00	sunny	815	101	916	214	307	521	1437	999	76	72	1320	103	75	178	257	435	1755	404	-86	318
			13:30	sunny	796	102	899	200	306	506	1405	993	75	72	1311	103	83	186	258	443	1754	412	-63	350
			14:00	sunny	766	98	864	202	311	512	1376	983	74	71	1297	103	82	186	257	443	1740	433	-69	364
			14:30	sunny	739	95	834	214	311	525	1359	970	72	70	1278	104	77	181	257	437	1715	444	-88	356
			15:00	sunny	675	89	764	223	313	536	1300	951	69	69	1252	104	83	186	255	441	1693	488	-95	393
			15:30	sunny	612	81	693	214	309	523	1216	927	66	67	1218	103	84	187	253	440	1658	525	-83	442
			16:00	sunny	545	73	618	218	308	526	1144	895	62	65	1174	103	83	186	251	437	1611	556	-89	467
June 11, 2009 (Changwon, Korea)	Daytime	Smallpark	11:30	sunny	947	173	1120	199	281	480	1600	1059	88	70	1399	108	71	180	262	442	1841	279	-38	241
			12:00	sunny	967	182	1149	188	284	471	1620	1060	88	70	1401	109	72	181	265	446	1847	252	-25	227
			12:30	sunny	970	181	1151	215	295	510	1661	1058	88	70	1398	109	73	182	267	449	1848	248	-61	187
			13:00	sunny	933	177	1110	175	271	446	1556	1053	87	70	1391	110	73	183	268	451	1842	281	5	286
			13:30	sunny	929	174	1103	185	295	480	1583	1046	85	69	1380	110	73	183	268	451	1831	277	-29	248
			14:00	sunny	888	167	1055	184	292	476	1531	1034	83	68	1364	110	73	183	267	450	1813	309	-27	282
			14:30	sunny	836	158	993	198	290	487	1481	1019	80	67	1341	109	72	182	265	447	1788	348	-41	307
			15:00	sunny	773	150	923	195	294	488	1411	998	77	66	1311	109	71	180	262	442	1753	388	-46	342
			15:30	sunny	693	138	831	191	279	470	1301	969	72	64	1271	108	70	178	258	436	1708	441	-34	407
			16:00	sunny	601	124	725	191	278	469	1193	932	67	62	1219	107	69	176	253	430	1649	495	-39	455
			16:30	sunny	498	102	600	195	272	467	1067	882	60	58	1150	106	68	174	248	422	1572	550	-45	505
			17:00	sunny	403	82	486	188	265	453	939	812	52	54	1055	105	66	171	242	413	1468	569	-40	529

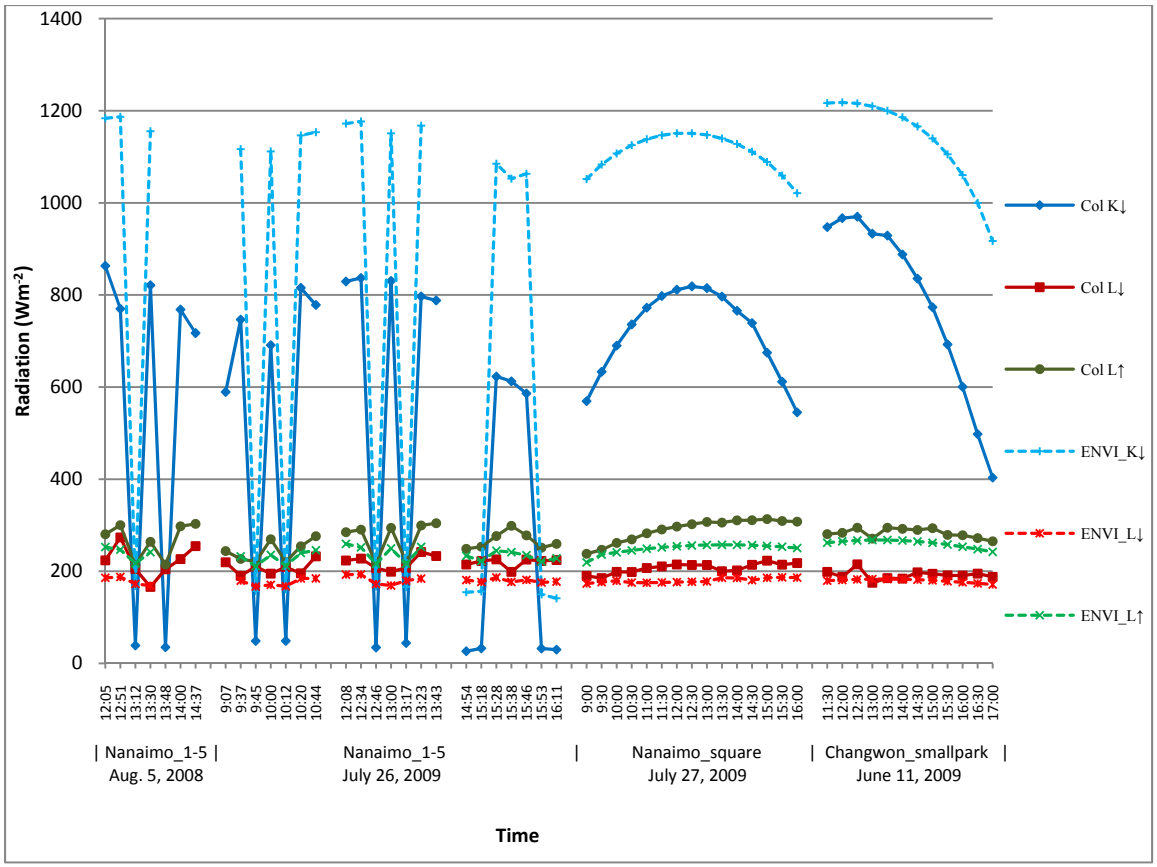

(a)

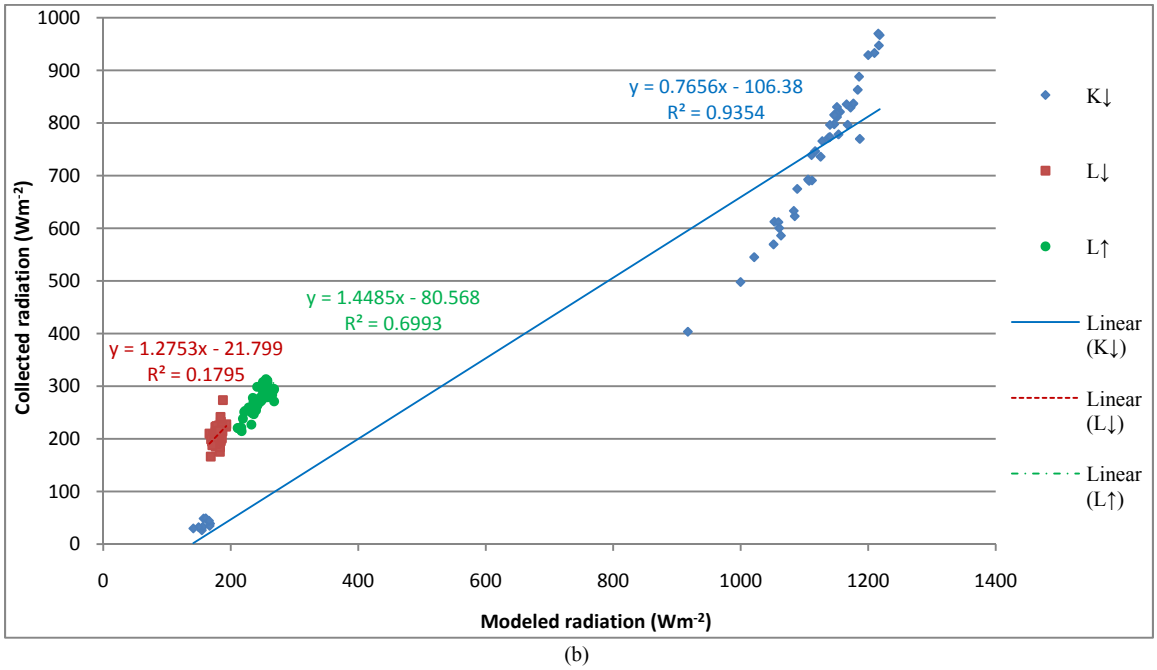

(b)

Fig. 4.24 Comparison and scatter plot of radiation components between collected data and ENVI-met 3.1 results: (a) comparison of radiation components and (b) scatter plot

Table 4.24 Differences in solar and longwave radiation components between collected data and ENVI-met 3.1 results (Wm^{-2})

Date/ Site	Time	Location	Solar Time	Sun/ Shade	Differences (ENVI-met results-Collected data)						Absolute differences					
					R		*L*			Total	*R*		*L*			Total
					K↓	Total	*L*↓	*L*↑	Total		*K*↓	Total	*L*↓	*L*↑	Total	
Aug. 5, 2008 (Nanaimo, B.C., Canada)	Noon	1	12:05	sunny	321	328	-38	-28	-66	262	321	328	38	28	66	394
		3	12:51	sunny	417	468	-86	-53	-139	329	417	468	86	53	139	607
		4	13:12	shady	129	146	-32	3	-30	117	129	146	32	3	35	181
		5	13:30	sunny	335	384	3	-23	-20	364	335	384	3	23	25	409
		4	13:48	shady												
		3	14:00	sunny												
		1	14:37	sunny												
July 26, 2009 (Nanaimo, B.C., Canada)	Morning	1	9:07	sunny												
		3	9:37	sunny	370	452	-10	5	-5	447	370	452	10	5	16	467
		4	9:45	shady	109	126	-43	-10	-53	72	109	126	43	10	53	179
		5	10:00	sunny	421	491	-24	-34	-58	433	421	491	24	34	58	550
		4	10:12	shady	112	129	-41	-8	-50	80	112	129	41	8	50	179
		3	10:20	sunny	331	381	-11	-14	-26	356	331	381	11	14	26	407
		1	10:44	sunny	375	424	-48	-31	-79	346	375	424	48	31	79	503
	Noon	1	12:08	sunny	343	397	-30	-26	-56	341	343	397	30	26	56	453
		3	12:34	sunny	340	404	-35	-38	-73	331	340	404	35	38	73	477
		4	12:46	shady	132	154	-35	-1	-36	119	132	154	35	1	36	190
		5	13:00	sunny	321	370	-30	-45	-74	296	321	370	30	45	74	445
		4	13:17	shady	122	134	-28	-5	-32	102	122	134	28	5	32	166
		3	13:23	sunny	371	448	-58	-47	-104	344	371	448	58	47	104	552
		1	13:43	sunny												
	Afternoon	1	14:54	shady	128	132	-34	-15	-49	83	128	132	34	15	49	181
		3	15:18	shady	123	139	-46	-31	-77	63	123	139	46	31	77	216
		4	15:28	sunny	462	560	-39	-32	-71	489	462	560	39	32	71	631
		5	15:38	sunny	440	503	-22	-57	-79	424	440	503	22	57	79	582
		4	15:46	sunny	477	565	-44	-43	-87	477	477	565	44	43	87	652
		3	15:53	shady	117	132	-47	-30	-76	55	117	132	47	30	76	208
		1	16:11	shady	112	127	-47	-31	-78	49	112	127	47	31	78	205
July 27, 2009 (Nanaimo, B.C., Canada)	Daytime	Square	9:00	sunny	482	572	-17	-19	-36	537	482	572	17	19	36	608
			9:30	sunny	450	534	-9	-11	-19	515	450	534	9	11	19	553
			10:00	sunny	417	500	-19	-21	-40	460	417	500	19	21	40	540
			10:30	sunny	389	466	-23	-24	-47	420	389	466	23	24	47	513
			11:00	sunny	366	445	-32	-34	-66	379	366	445	32	34	66	511
			11:30	sunny	349	422	-35	-39	-74	348	349	422	35	39	74	496
			12:00	sunny	340	413	-38	-43	-81	332	340	413	38	43	81	494
			12:30	sunny	333	406	-36	-46	-82	324	333	406	36	46	82	488
			13:00	sunny	333	404	-36	-50	-86	318	333	404	36	50	86	489
			13:30	sunny	344	412	-14	-48	-63	350	344	412	14	48	63	475
			14:00	sunny	362	433	-16	-53	-69	364	362	433	16	53	69	503
			14:30	sunny	372	444	-33	-54	-88	356	372	444	33	54	88	532
			15:00	sunny	414	488	-37	-58	-95	393	414	488	37	58	95	583
			15:30	sunny	448	525	-27	-56	-83	442	448	525	27	56	83	609
			16:00	sunny	476	556	-32	-57	-89	467	476	556	32	57	89	645
June 11, 2009 (Changwon, Korea)	Daytime	Smallpark	11:30	sunny	269	279	-19	-19	-38	241	269	279	19	19	38	317
			12:00	sunny	251	252	-6	-19	-25	227	251	252	6	19	25	277
			12:30	sunny	246	248	-33	-28	-61	187	246	248	33	28	61	308
			13:00	sunny	277	281	8	-3	5	286	277	281	8	3	11	292
			13:30	sunny	271	277	-2	-27	-29	248	271	277	2	27	29	305
			14:00	sunny	298	309	-1	-25	-27	282	298	309	1	25	27	335
			14:30	sunny	331	348	-16	-25	-41	307	331	348	16	25	41	389
			15:00	sunny	367	388	-14	-32	-46	342	367	388	14	32	46	434
			15:30	sunny	413	441	-13	-21	-34	407	413	441	13	21	34	475
			16:00	sunny	460	495	-15	-25	-39	455	460	495	15	25	39	534
			16:30	sunny	502	550	-21	-24	-45	505	502	550	21	24	45	595
			17:00	sunny	514	569	-17	-23	-40	529	514	569	17	23	40	609

Table 4.25 Maximum, minimum and mean values of radiation differences between collected data and ENVI-met 3.1 results (Wm^{-2})

Date	Location	Radiation difference	Normal values						Absolute values					
			R		*L*			Total	*R*		*L*			Total
			K↓	Total	*L*↓	*L*↑	Total		*K*↓	Total	*L*↓	*L*↑	Total	
Aug. 5, 2008	sunny	Max.	417	468	3	-23	-20	364	417	468	86	53	139	607
		Min.	321	328	-86	-53	-139	262	321	328	3	23	25	394
		Mean	357	393	-40	-35	-75	318	357	393	42	35	77	470
	shady	Max.	129	146	-32	3	-30	117	129	146	32	3	35	181
		Min.	129	146	-32	3	-30	117	129	146	32	3	35	181
		Mean	129	146	-32	3	-30	117	129	146	32	3	35	181
July 26, 2009	sunny	Max.	477	565	-10	5	-5	489	477	565	58	57	104	652
		Min.	321	370	-58	-57	-104	296	321	370	10	5	16	407
		Mean	387	454	-32	-33	-65	389	387	454	32	34	66	520
	shady	Max.	132	154	-28	-1	-32	119	132	154	47	31	78	216
		Min.	109	126	-47	-31	-78	49	109	126	28	1	32	166
		Mean	119	134	-40	-16	-56	78	119	134	40	16	56	191
July 27, 2009	sunny	Max.	482	572	-9	-11	-19	537	482	572	38	58	95	645
		Min.	333	404	-38	-58	-95	318	333	404	9	11	19	475
		Mean	392	468	-27	-41	-68	400	392	468	27	41	68	536
June 11, 2009	sunny	Max.	514	569	8	-3	5	529	514	569	33	32	61	609
		Min.	246	248	-33	-32	-61	187	246	248	1	3	11	277
		Mean	350	370	-13	-22	-35	335	350	370	14	22	36	406
Sunny location mean			376	430	-25	-33	-58	372	376	430	26	33	59	489
Overall mean			330	377	-28	-30	-57	320	330	377	28	30	58	435

4.3.5 Absorbed radiation on the human body surface

The radiation comparison in section 4.3.4 showed amounts of radiation at the height of 1.2 m above the ground surface from the New model, RayMan Pro and ENVI-met 3.1. This section will show amounts of radiation absorbed on the human body surface from the New model.

Absorbed direct beam solar radiation on the human body surface (K_b^*) had narrow ranges between times at Nanaimo sunny locations, around 20 Wm^{-2}, because of the combined effects of normal incidence incoming direct beam solar radiation (K_b^+) and projected area factor (f_p) (Tables 4.26 & 4.27). For example, when time goes from noon to afternoon, K_b^+ will decrease but f_p will increase. Therefore, K_b^* will have a different pattern than K_b^+. Nanaimo_1-5 and Nanaimo_square data clearly show the different pattern of K_b^*. The highest K_b^* was at medium solar altitudes around $\beta \approx 37°$, 9:00 ($\beta \approx 40°$) and 16:00 ($\beta \approx 37°$), rather than at high solar altitudes, 12:00 ($\beta \approx 60°$). Changwon_smallpark K_b^* data were also similar, highest around 16:30 ($\beta \approx 36°$), and, it had more than double the range between maximum and minimum K_b^*, 43.2 Wm^{-2}, than the range at Nanaimo sunny locations, 19.7 Wm^{-2}. The ranges in K_b^+ (215.0 Wm^{-2}) and f_p (0.151) between

times of maximum and minimum K_b^* at Changwon_smallpark were twice those of K_b^+ (mean: 100.0 Wm^{-2}) and f_p (mean: 0.068) at Nanaimo sunny locations.

The mean K_b^* difference between the sunny and shaded locations at Nanaimo_1-5 was 100.2 Wm^{-2}. Absorbed diffuse beam (K_d^*) and reflected beam (K_r^*) solar radiation had a 34.5 Wm^{-2} mean difference between the sunny and shaded locations at Nanaimo_1-5 (sunny: 51.8 Wm^{-2}, shaded: 17.3 Wm^{-2}). Nanaimo_square had a very similar mean of sunny $K_d^* + K_r^*$, 56.9 Wm^{-2}, as did the sunny locations at Nanaimo_1-5. Changwon_smallpark had a little higher mean sunny location $K_d^* + K_r^*$, 71.3 Wm^{-2}, than those at Nanaimo sunny locations. The Changwon site's higher ψ_{sky} increased its amounts of K_d (Tables 4.14 & 4.17). The range between maximum and minimum $K_d^* + K_r^*$ at Changwon_smallpark, 30.8 Wm^{-2}, was more than double the range at Nanaimo_square, 10.7 Wm^{-2}, which was very similar to the ratio between their ranges of K_b^*.

Total absorbed longwave radiation by the human body (L^*) was much higher than total absorbed solar radiation ($R^* = K_b^* + K_d^* + K_r^*$). Mean L^* was around 400 Wm^{-2} at the sunny locations: 388.6 Wm^{-2} at Nanaimo_1-5, 397.9 Wm^{-2} at Nanaimo_square and 404.1 Wm^{-2} at Changwon_smallpark. The shaded locations at Nanaimo_1-5 had a 31.4 Wm^{-2} lower mean, 357.2 Wm^{-2}, than the sunny locations at Nanaimo_1-5. Therefore, it can be said that a shadow at a small location can make a moderate difference in absorbed longwave radiation in urban areas if the shaded area with its lower surface temperature covers large proportions of the urban surface view factors at the location.

The shadow effect for human body total absorbed radiation in the daytime is dominantly controlled by absorbed solar radiation, i.e., mean difference 100.2 Wm^{-2} in K_b^* and 34.5 Wm^{-2} in $K_d^* + K_r^*$ compared to 31.4 Wm^{-2} in L^* between the sunny and shaded locations at Nanaimo_1-5.

The mean total absorbed radiation (Q^*) was around 556 Wm^{-2} at the sunny locations: 540.5 Wm^{-2} at Nanaimo_1-5, 559.1 Wm^{-2} at Nanaimo_square and 557.0 Wm^{-2} at Changwon_smallpark. The shaded locations at Nanaimo_1-5 had a 166.1 Wm^{-2} lower mean, 374.4 Wm^{-2}.

Absorbed radiation can be converted to mean radiant temperatures (T_{mrt}) (Fanger 1972):

$$T_{mrt} = \left[\frac{f_p K_b{}^+(1-a_b) + 0.5(K_d{}^+ + K_r{}^+)(1-a_b) + 0.5\varepsilon_b L^+}{\varepsilon_b \sigma}\right]^{0.25} - 273.15 \qquad (4.80)$$

The definition of T_{mrt} is "uniform temperature of black surroundings (emissivity ε=1.0) which will give the same radiant heat loss from the person" (Fanger 1972).

Both Changwon_smallpark and Nanaimo_square, 58.6 °C, had 2.5 °C greater mean T_{mrt} values than that of the sunny locations of Nanaimo_1-5, 56.1 °C. The mean T_{mrt} of the shaded locations at Nanaimo_1-5 was reduced to almost half, 27.2 °C, which is the benefit of the shadow effect. Shadows eliminate direct beam solar radiation and reduce solar radiation reflected from the adjacent ground and vertical surfaces of buildings and trees. It lowers surface temperatures of the ground and vertical objects.

Table 4.26 Absorbed radiation on the human body surface

Date/Site	Time	Location	Solar time	K_b^+ (Wm^{-2})	f_p	K_b^{*a} (Wm^{-2})	$K_d^*+K_r^*$ (Wm^{-2})	L^* (Wm^{-2})	Q^* (Wm^{-2})	T_{mrt} (°C)
Aug. 5, 2008 (Nanaimo, B.C., Canada)	Noon	1	12:05	857.6	0.19	95.4	53.5	411.8	560.7	59.2
		3	12:51	856.4	0.191	95.9	41.4	403.0	540.3	56.1
		4	13:12	0	0.195	0	23.2	363.2	386.4	29.6
		5	13:30	848.4	0.199	98.9	61.0	401.1	561.0	59.2
		4	13:48							
		3	14:00							
		1	14:37							
July 26, 2009 (Nanaimo, B.C., Canada)	Morning	1	9:07							
		3	9:37	805.0	0.23	108.2	69.3	367.8	545.3	56.9
		4	9:45	0	0.226	0	19.9	341.5	361.4	24.6
		5	10:00	821.0	0.219	105.4	56.5	366.3	528.2	54.2
		4	10:12	0	0.214	0	20.3	341.7	361.9	24.7
		3	10:20	832.6	0.211	102.7	71.9	372.9	547.5	57.2
		1	10:44	843.8	0.201	99.4	60.3	384.7	544.4	56.7
	Noon	1	12:08	863.1	0.182	91.7	54.7	385.7	532.0	54.8
		3	12:34	863.2	0.181	91.6	42.1	383.7	517.4	52.5
		4	12:46							
		5	13:00	860.7	0.184	92.8	55.2	377.6	525.6	53.8
		4	13:17	0	0.188	0	23.6	359.2	382.8	28.9
		3	13:23	856.1	0.189	94.9	53.4	396.2	544.5	56.7
		1	13:43	850.3	0.195	97.2	50.4	400.4	547.9	57.2
	Afternoon	1	14:54	0	0.224	0	15.1	352.9	368.0	26.0
		3	15:18	0	0.234	0	13.9	362.5	376.4	27.6
		4	15:28	787.9	0.239	110.2	35.5	385.1	530.8	54.6
		5	15:38	778.6	0.243	110.9	52.0	390.9	553.7	58.1
		4	15:46	770.7	0.247	111.4	30.1	386.8	528.3	54.3
		3	15:53	0	0.25	0	12.4	375.1	387.5	29.8
		1	16:11	0	0.258	0	12.0	365.5	377.5	27.9
July 27, 2009 (Nanaimo, B.C., Canada)	Daytime	Square	9:00	771.3	0.247	111.4	53.4	346.8	511.5	51.6
			10:00	820.3	0.22	105.6	59.5	371.9	537.0	55.6
			11:00	849.3	0.196	97.6	59.1	385.0	541.8	56.3
			12:00	862.1	0.183	92.3	60.0	401.3	553.6	58.1
			13:00	860.2	0.185	93.2	58.1	419.7	570.9	60.7
			14:00	843.5	0.202	99.6	59.9	419.3	578.8	61.8
			15:00	809.8	0.227	107.5	55.5	422.3	585.3	62.7
			16:00	754.6	0.253	111.9	49.3	416.7	578.0	61.7
June 11, 2009 (Changwon, Korea)	Daytime	Smallpark	11:30	839.5	0.138	67.9	77.6	399.9	545.4	56.9
			12:00	845.3	0.125	61.8	79.4	407.8	549.0	57.4
			12:30	847.0	0.12	59.6	79.5	414.5	553.5	58.1
			13:00	844.7	0.126	62.5	79.9	415.2	557.7	58.7
			13:30	838.2	0.141	69.1	78.9	415.5	563.4	59.6
			14:00	827.4	0.159	77.0	77.8	416.5	571.3	60.7
			14:30	811.8	0.179	85.1	75.0	416.6	576.7	61.5
			15:00	790.8	0.2	92.4	72.1	410.4	574.9	61.2
			15:30	763.8	0.22	98.2	67.9	400.7	566.8	60.1
			16:00	729.4	0.239	101.9	62.7	393.5	558.1	58.8
			16:30	686.2	0.256	102.8	56.2	384.1	543.1	56.5
			17:00	632.0	0.271	100.2	49.1	374.7	523.9	53.6

[a] $K_b^* = (f_p \times f_{eff} \times K_b^+) \times (1-a_b) = (f_p \times 0.836 \times K_b^+) \times 0.7$

Table 4.27 Maximum, minimum, mean and range of absorbed radiation on the human body surface

Site/Date	Sun/Shade		K_b^+ (Wm^{-2})	f_p	K_b^* (Wm^{-2})	$K_d^*+K_r^*$ (Wm^{-2})	L^* (Wm^{-2})	Q^* (Wm^{-2})	T_{mrt} (°C)
Nanaimo_1-5 (Aug. 5, 2008 & July 26, 2009)	Sunny	Max.	863.2	0.247	111.4	71.9	411.8	561.0	59.2
		Min.	770.7	0.181	91.6	30.1	366.3	517.4	52.5
		Range	92.5	0.066	19.8	41.8	45.5	43.6	6.7
		Mean	834.5	0.206	100.2	51.8	388.6	540.5	56.1
	Shade	Max.	0	0.258	0	23.6	375.1	387.5	29.8
		Min.	0	0.188	0	12.0	341.5	361.4	24.6
		Range	0	0.070	0	11.6	33.6	26.1	5.2
		Mean	0	0.224	0	17.3	357.2	374.4	27.2
	Sunny+Shade	Max.	863.2	0.258	111.4	71.9	411.8	561.0	59.2
		Min.	0	0.181	0	12.0	341.5	361.4	24.6
		Range	863.2	0.077	111.4	59.9	70.3	199.6	34.6
		Mean	543.3	0.213	65.5	40.3	377.2	483.0	46.1
Nanaimo_square (July 27, 2009)	Sunny	Max.	862.1	0.253	111.9	60.0	422.3	585.3	62.7
		Min.	754.6	0.183	92.3	49.3	346.8	511.5	51.6
		Range	107.5	0.070	19.6	10.7	75.5	73.8	11.1
		Mean	821.4	0.214	102.4	56.9	397.9	557.1	58.6
Changwon_smallpark (June 11, 2009)	Sunny	Max.	847.0	0.271	102.8	79.9	416.6	576.7	61.5
		Min.	632.0	0.120	59.6	49.1	374.7	523.9	53.6
		Range	215.0	0.151	43.2	30.8	41.9	52.8	7.9
		Mean	788.0	0.181	81.5	71.3	404.1	557.0	58.6

4.4 Discussion

Large differences in $K\downarrow$ between the collected radiation data and the New model results occurred at Nanaimo_square and Nanaimo_3 in the morning and in $K\uparrow$ at Changwon_smallpark (see Fig. 4.20a & Table 4.18). The main reasons appear to be T_L for Nanaimo_square, building surface albedo (a_o) for Nanaimo_3 and ground surface albedo (a_g) for Changwon_smallpark. A test of the effect of changing the model inputs was conducted.

The mean monthly T_L values were 3.4 in July and 3.9 in August, so the test increased T_L from 3.65 ($= \frac{3.4+3.9}{2}$) used in the analyses of Nanaimo_1-5 and Nanaimo_square to 3.85. For a_g of Changwon_smallpark, the input value was increased from 0.15 to 0.19 which was found from the collected data. Also, stucco was the main building surface material at Nanaimo_3, so the collected a_o values were used in the test, 0.45 for sunny and 0.32 for shaded building surfaces.

The 0.2 increase of T_L value for Nanaimo_square reduced by more than half the mean $K\downarrow$ difference between the collected radiation data and the New model results from 22.0 to 10.7 Wm^{-2} (Table 4.28). The $K\uparrow$ differences of Changwon_smallpark showed how the correct a_g value should be used. The differences were reduced greatly from a mean of -33.8 to -2.9 Wm^{-2}. The a_o test for Nanaimo_3 showed the effectiveness of using adequate a_o values for $K\downarrow$ estimates. Differences between observations and model output changed from -40.5 to 1.5 Wm^{-2} at 9:37 and -36.6 to 1.5 Wm^{-2} at 10:20 (Table 4.28). Also, the increase of $K\uparrow$ values at Nanaimo_3 could clearly represent the unequal scattering direction of high albedo building surface materials. In the reflected solar radiation analysis, the scattering was assumed equal for all visible directions, but the results show high albedo building surface materials might act like a very smooth surface and scatter most solar radiation forward at an angle. Therefore, these building surface materials affect amounts of solar radiation received by the upper pyranometer but have little effect on solar radiation received by the bottom pyranometer because most solar radiation reflected by these building surface materials below the observation height, 1.2 m, will go forward to the ground surface. That is why the differences of $K\uparrow$ values increased only 64 %, (26.8 Wm^{-2} at 9:37 and 24.2 Wm^{-2} at 10:20), of the changed differences of $K\downarrow$ values (42.0 Wm^{-2} at 9:37 and 38.1 Wm^{-2} at 10:20, Table 4.28).

Therefore, most differences can be reduced greatly if proper variables and parameters of urban settings for each site can be used.

In previous studies, Thorsson et al. (2007) mentioned RayMan underestimates T_{mrt} at low solar altitudes in summer and also at noon in October in Sweden. This study reveals the program underestimates total radiation during all daylight hours in summer in Nanaimo, B.C., Canada and Changwon, Republic of Korea. Ali-Toudert (2005) stated ENVI-met overestimates T_{mrt} in the morning and underestimates it in the afternoon and at night-time. This study shows it continually overestimates throughout the day in summer at both study sites. Its overestimation of total radiation increases more at low solar altitudes in the morning and afternoon.

RayMan Pro underestimated and ENVI-met 3.1 overestimated total radiation throughout the day. Limitations of RayMan Pro include the lack of a reflected solar radiation component and inaccurate estimates of sky view factor, ground surface temperature and diffuse beam solar radiation. ENVI-met 3.1 allowed no topographic input data and had inaccurate estimates of air and ground surface temperatures and both direct beam and diffuse beam solar radiation.

Operating time is another important issue. RayMan Pro can only analyze one location each time, so the results were obtained instantaneously. ENVI-met 3.1 can simulate many locations at one time, but the results took 2–3 days for a 12 hour simulation for small urban sites with less than a 180×180×25 grid. The main reason for the different simulation time between the two programs is RayMan Pro analyzes only radiation data but ENVI-met 3.1 analyzes wind velocity as well as radiation. ENVI-met 3.1 cannot deal with a large urban site such as an entire city, but seems to work OK for a small urban site.

Table 4.28 Effects of Linke turbidity and albedo changes on differences between observed and modeled solar radiation incoming from the sky hemisphere ($K\downarrow$) and reflected by the ground surface ($K\uparrow$)

Location	Time	T_L: 3.65	T_L: 3.85
		$K\downarrow$ [a] (Wm^{-2})	$K\downarrow$ (Wm^{-2})
Nanaimo_square	9:00	25.6	15.1
	10:00	32.8	21.3
	11:00	37.1	25.1
	12:00	34.2	22.0
	13:00	16.8	4.8
	14:00	15.7	4.0
	15:00	8.9	-2.1
	16:00	5.2	-4.8
	Mean	22.0	10.7

Location	Time	a_g: 0.15	a_g: 0.19
		$K\uparrow$ [b] (Wm^{-2})	$K\uparrow$ (Wm^{-2})
Changwon_smallpark	11:30	-34.8	1.8
	12:00	-40.9	-3.7
	12:30	-38.7	-1.1
	13:00	-36.4	1.4
	13:30	-36.8	-0.6
	14:00	-35.3	-0.2
	14:30	-33.8	-0.8
	15:00	-35.0	-4.7
	15:30	-34.6	-7.4
	16:00	-33.5	-9.5
	16:30	-25.5	-5.3
	17:00	-20.2	-4.1
	Mean	-33.8	-2.9

Location	Time	a_o: 0.3 for sunny 0.21 for shaded		a_o: 0.45 for sunny 0.32 for shaded	
		$K\downarrow$ (Wm^{-2})	$K\uparrow$ (Wm^{-2})	$K\downarrow$ (Wm^{-2})	$K\uparrow$ (Wm^{-2})
Nanaimo_3	9:37	-40.5	20.8	1.5	47.6
	10:20	-36.6	-3.6	1.5	20.6

[a] $K\downarrow$: $K\downarrow$ differences (modeled minus observed data)
[b] $K\uparrow$: $K\uparrow$ differences (modeled minus observed data)

4.5 Conclusions

A new human-urban radiation simulation model was developed which had body area factors of the contemporary Canadian adult population. Important urban area factors (albedos and temperatures of building, tree and ground surfaces) were estimated from the urban settings of the Nanaimo site. The New model was tested with the collected radiation data of the two study sites: Nanaimo, B.C., Canada and Changwon, Republic of Korea. The model made very small differences with the collected data, mean 15 Wm^{-2} (19 Wm^{-2} at only sunny locations), and the r^2 between them were very strong, over 0.987, in solar and total radiation and a little weaker in longwave radiation. It showed much better results than two other computer simulation programs, RayMan Pro and ENVI-met 3.1.

Several concerns of urban area modeling arose for better results. Firstly, accurate urban setting data should be acquired, i.e., ground elevation, building height and tree height. Ground elevations at urban sites are changing from contour lines in existing maps because of construction. Secondly, the computer program codes of the view factor analysis method in the New model should be modified for pedestrian streets although the analytical equation from Johnson and Watson (1984) works accurately in mathematical simulations. The view factor method was accurate when the observation location was away from the buildings, but the method created some errors when the location was close to buildings, like a sidewalk for pedestrians. Thirdly, separate input functions of albedos and emissivities for each surface material will make more accurate simulations. As shown in the discussion and Table 4.8, the ground albedos were different although the surface materials were the same. Small differences in albedos created large errors. RayMan Pro has a separate input function for the building and tree surfaces, and ENVI-met 3.1 has the same function for the ground surface. Fourthly, automatic detection of building azimuth angles and ground surface slope angles can reduce time and labour and provide more accurate estimation. The computer coding for this automation will be done in the next version. Lastly, a simulation function for each individual location can shorten computer running time. The current version of the New model simulates all outdoor locations at one time, so it took 1-2 hours for each study site. This part will be included in the next version.

More precise methods for exploring urban area factors should be developed for microclimatic human-urban radiant environments. The modified new human-urban radiation exchange simulation model will allow more accurate estimation for landscape and urban planning/design at various scales from a small site to an entire city. Also, this model can be expanded for human thermal sensation/comfort modeling to include sensible and latent heat flux density components.

References

Ali-Toudert F (2005) Dependence of Outdoor Thermal Comfort on Street Design in Hot and Dry Climate. Berichte des Meteorologischen Institutes der Universität Freiburg Nr. 15, http://www.freidok.uni-freiburg.de/volltexte/2078

Arnfield AJ (1982) An approach to the estimation of the surface radiative properties and radiation budgets of cities. Physical Geography 3(2): 97–122

ASHRAE (2001) Thermal Comfort. In: ASHRAE handbook - Fundamentals, Chapter 8. American Society of Heating, Refrigerating and Air-conditioning Engineers, Inc., Atlanta

Azar S (2004) Urban software: TownScope III. IAUC Newsletter 4: 2-3. http://www.urban-climate.org/Iauc0004.pdf

Brown G, Isfält E (1974) Solinstrålning och Solavskärmning, (Solar Irradiation and Sun Shading Devices), Report R19. National Swedish Council for Building Research, Stockholm, Sweden

Brown RD, Gillespie TJ (1995) Microclimatic Landscape Design: Creating Thermal Comfort and Energy Efficiency. John Wiley & Sons Inc., New York

Bruse M, Fleer H (1998) Simulating surface-plant-air interactions inside urban environments with a three dimensional numerical model. Environmental Modelling and Software 13: 373-384

Bruse M (1999) Simulating microscale climate interactions in complex terrain with a high-resolution numerical model: A case study for the Sydney CBD Area. Proceedings International Conference on Urban Climatology & International Congress of Biometeorology, Sydney, 8-12 Nov.

Bruse M (2008) ENVI-met website. http://www.envi-met.com

Burt JE, O'Rourke PA, Terjung WH (1982) View-factors leading to the simulation of human heat stress and radiant exchange: an algorithm. Archives for Meteorology, Geophysics, and Bioclimatology, Series B, 30: 321-331

Chapman L, Thornes JE, Bradley AV (2001) Rapid determination of canyon geometry parameters for use in surface radiation budgets. Theoretical and Applied Climatology 69: 81-89

Chapman L, Thornes JE (2004) Real-time sky-view factor calculation and approximation. Journal of Atmospheric and Oceanic Technology 5: 730-741

Clark JA, Follin GM (1988) A simple "equal area" calibration for fisheye photography. Agricultural and Forest Meteorology 44: 19-25

Dozier J, Frew J (1990) Rapid calculation of terrain parameters for radiation modeling from digital elevation data. IEEE Transactions on Geoscience and Remote Sensing 28(5): 963-969

Emmanuel R, Rosenlund H, Johansson E (2007) Urban shading-a design option for the tropics? A study in Colombo, Sri Lanka. International Journal of Climatology 27: 1995-2004 doi: 10.1002/joc.1609

Falkenberg G, Bolz HM (1949) Neue Bestimmung der Konstanten der Angströmschen Strahlungsformel. Zeitschrift für Meteorologie 3: 97

Fanger PO (1972) Thermal Comfort: Analysis and Applications in Environmental Engineering. McGraw-Hill, New York

Fu P, Rich PM (1999) Design and implementation of the solar analyst: an ArcView extension for modeling solar radiation at landscape scales. Proceedings of the 19th Annual ESRI user conference, San Diego. http://gis.esri.com/library/userconf/proc99/proceed/papers/pap867/p867.htm

Gagge AP, Fobelets A, Berglund LG (1986) A standard predictive index of human response to the thermal environment. ASHRAE Transactions 92(2B): 709-731

Gál T, Rzepa M, Gromek B, Unger J (2007) Comparison between sky view factor values computed by two different methods in an urban environment. ACTA Climatologica et Chorologica, Universitatis Szegediensis, Tomus 40-41: 17-26

Gál T, Lindberg F, Unger J (2009) Computing continuous sky view factors using 3D urban raster and vector databases: Comparison and application to urban climate. Theoretical and Applied Climatology 95: 111-123. doi: 10.1007/s00704-007-0362-9

Grimmond CSB, Potter SK, Zutter HN, Souch C (2001) Rapid methods to estimate sky-view factors applied to urban areas. International Journal of Climatology 21(7): 903-913

Holmer B (1992) A simple operative method for determination of sky view factors in complex urban canyons from fisheye photographs. Meteorologische Zeitschrift, N. F. 1: 236-239

Holmer B, Postgård U, Eriksson M (2001) Sky view factors in forest canopies calculated with IDRISI. Theoretical and Applied Climatology 68: 33-40

Holtslag AAM, van Ulden AP (1983) A simple scheme for daytime estimates of the surface fluxes from routine weather data. Journal of Climate and Applied Meteorology 22: 517-529

Höppe PR (1993) Heat balance modeling. Experientia 49: 741-746. doi: 10.1007/BF01923542

Höppe PR (1999) The physiological equivalent temperature – a universal index for the biometeorological assessment of the thermal environment. International Journal of Biometeorology 43: 71-75. doi: 10.1007/s004840050118

Ineichen P, Perez R (2002) A new airmass independent formulation for the Linke turbidity coefficient. Solar Energy 73(3): 151-157

ISO9920 (2007) ISO 9920: Ergonomics of the Thermal Environment: Estimation of Thermal Insulation and Water Vapour Resistance of a Clothing Ensemble. ISO, Geneva

Jendritzky G, Menz H, Schirmer H, Schmidt-Kessen W (1990) Methodik zur raumbezogenen Bewertung der thermischen Komponente im Bioklima des Menschen (Fortgeschriebenes Klima-Michel-Modell). Beitr Akad Raumforsch Landesplan, No. 114

Johnson GT, Watson ID (1984) The determination of view-factors in urban canyons. Journal of Climate and Applied Meteorology 23: 329-335

Jonsson P, Eliasson I, Holmer B, Grimmond CSB (2006) Longwave incoming radiation in the Tropics: results from field work in three African cities. Theoretical and Applied Climatology 85:185-201

Kasten F (1980) A simple parametrization of the pyrheliometric formula for determining the Linke turbidity factor. Meteorologische Rundsch 33: 124–127

Kasten F, Young AT (1989) Revised optical air mass tables and approximation formula. Applied Optics 28: 4735-4738

Kasten F (1996) The Linke turbidity factor based on improved values of the integral Rayleigh optical thickness. Solar Energy 56: 239-244

Lindberg F, Holmer B, Thorsson S (2008) SOLWEIG 1.0 – Modelling spatial variations of 3D radiant fluxes and mean radiant temperature in complex urban settings. International Journal of Biometeorology 52(7): 697-713

Lindberg F, Grimmond CSB (2011) The influence of vegetation and building morphology on shadow patterns and mean radiant temperatures in urban areas: model development and evaluation. Theoretical and Applied Climatology, doi: 10.1007/s00704-010-0382-8

Lemonsu A, Grimmond CSB, Masson V (2004) Modeling the surface energy balance of the core of an old Mediterranean city: Marseille. Journal of Applied Meteorology 43: 312-327

Liljequist GH (1979) Meteorologi: Strålning, Dept. of Meteorology, University of Uppsala, Uppsala

Masson V (2000) A physically-based scheme for the urban energy budget in atmospheric models. Boundary-Layer Meteorology 94: 357-397

Matzarakis A, Rutz F, Mayer H (2000) Estimation and calculation of the mean radiant temperature within urban structures. In: de Dear RJ, Kalma JD, Oke TR, Auliciems A (eds.) Biometeorology and Urban Climatology at the Turn of the Millennium. ICB-ICUC'99, Sydney, WCASP-50, WMO/TD No 1026, 273-278

Matzarakis A, Rutz F, Mayer H (2007) Modelling radiation fluxes in simple and complex environments-application of the RayMan model. International Journal of Biometeorology 51: 323-334

Matzarakis A, Rutz F, Mayer H (2010) Modelling radiation fluxes in simple and complex environments: basics of the RayMan model. International Journal of Biometeorology 54: 131-139

McCullough EA, Jones BW, Huck J (1985) A comprehensive data base for estimating clothing insulation. ASHRAE Transactions 91: 29-47

McCullough EA, Jones BW, Tamura T (1989) A data base for determining the evaporative resistance of clothing. ASHRAE Transactions 94: 316-328

Monteith JL, Unsworth M (1990) Principles of Environmental Physics, 2nd edition. Elsevier, Oxford

Noilhan J (1981) A model for the net total radiation flux at the surfaces of a building. Building and Environment 16: 259-266

Offerle B, Grimmond CSB, Oke TR (2003) Parameterization of net all-wave radiation for urban areas. Journal of Applied Meteorology 42(8): 1157-1174

Oke TR (1981) Canyon geometry and the nocturnal urban heat island: comparison of scale model and field observations. International Journal of Climatology 1: 237–254

Oke TR (1987) Boundary Layer Climates. Methuen, London

Parsons K (1993) Human Thermal Environments: The Effects of Hot, Moderate and Cold Environments on Human Health, Comfort and Performance-the Principles and the Practice. Taylor & Francis Inc., London

Polo J, Zarzalejo LF, Martín L, Navarro AA, Marchante R (2009) Estimation of daily Linke turbidity factor by using global irradiance measurements at solar noon. Solar Energy 83: 1177-1185. doi: 10.1016/j.solener.2009.01.018

Prata AJ (1996) A new long-wave formula for estimating downward clearsky radiation at the surface. Quarterly Journal of the Royal Meteorological Society 122:1127–1151

Raber BF, Hutchinson FW (1947) Panel Heating and Cooling Analysis. John Wiley, New York

Ratti C, Baker N (2003) Urban infoscapes: new tools to inform city design and planning. Architectural Research Quarterly 7(1): 63-74

Ratti C, Richens P (1999) Urban texture analysis with image processing techniques. CAAD futures Digital Proceedings, 49-64

Ratti C, Richens P (2004) Raster analysis of urban form. Environment and Planning B: Planning and Design 31: 297-309

Ratti C, Di Sabatino S, Britter R (2006) Urban texture analysis with image processing techniques: Winds and dispersion. Theoretical and Applied Climatology 84: 77-90

Richens P (1997) Image processing for urban scale environmental modelling. Proceedings of the International Conference Building Simulation '97-Prague, 163-171

Rigollier C, Bauer O, Wald L (2000) On the clear sky model of the ESRA–European Solar Radiation Atlas–with respect to the heliosat method. Solar Energy 68(1): 33-48

Rodrigues DS, Souza LCL, Mendes JFG (2004) Enhancing 3DSKYVIEW extension performance. In: Leeuwen JPV, Timmermans HJP (eds.) Recent Advances in Design and Decision Support Systems in Architecture and Urban Planning, Kluwer academic publishers, P. O. Box 17, 3300 AA Dordrecht, The Netherlands. ISBN: 978-1-4020-2408-5. 325-340

Rzepa M, Gromek B (2006) Variability of sky view factor in the main street canyon in the center of Lódź. 6th International Conference on Urban Climate, Göteborg, Sweden, 854-857

Sellers WD (1965) Physical Climatology. The University of Chicago Press, Chicago

Souza LCL, Rodrigues DS, Mendes JFG (2003) Sky view factors estimation using a 3D-GIS extension. 8th International IBPSA Conference, Eindhoven, Netherlands, August 11~14, 1227-1234

Steyn DG (1980) The calculation of view factors from fisheye-lens photographs. Atmosphere-Ocean 18(3): 254-258

Steyn DG, Hey JE, Watson ID, Johnson GT (1986) The determination of sky view-factors in urban environments using video imagery. Journal of Atmospheric and Oceanic technology 3(4): 759-764

Taesler R, Andersson C (1984) A method for solar radiation computations using routine meteorological observations. Energy and Buildings 7: 341-352

Teller J, Azar S (2001) TownScope 2 – A computer system to support solar access decision-making. Solar Energy 70(3): 187-200

Thorsson S, Lindberg F, Eliasson I, Holmer B (2007) Different methods for estimating the mean radiant temperature in an outdoor urban setting. International Journal of Climatology 27: 1983-1993 doi: 10.1002/joc.1537

Valko P (1966) Die Himmelsstrahlung in ihrer Beziehung zu vershiedenen Parametern. Archives for Meteorology, Geophysics, and Bioclimatology B 14: 337-359

VDI (1994) 3789 Part 2: Environmental Meteorology. Interactions between Atmosphere and Surfaces; Calculation of the Short- and Long Wave Radiation. Beuth, Berlin

VDI (2001) 3789 Part 3: Environmental Meteorology. Interactions between Atmosphere and Surfaces; Calculation of Spectral Irradiances in the Solar Wavelength Range. Beuth, Berlin

Volz FE (1968) Turbidity at Uppsala from 1909 to 1922 from Sjöström's Solar Radiation Measurements. Communications Series B, No. 28, Swedish Meteorological and Hydrological Institute, 100-104

Watson ID, Johnson GT (1987) Graphical estimation of sky view-factors in urban environments. International Journal of Climatology 7: 193-197

Chapter 5. Summary and Conclusions

The investigation and modeling of radiation exchange between the human body and its surrounding environments was described in Chapters 1–4. The body area factors, effective radiation area factor (f_{eff}) and projected area factor (f_p^*=projected area/total body surface area, and f_p=projected area/effective radiation area), were determined from a sample of 139 adults for standing posture (Chapter 1) and for walking posture (Chapter 2).

The radiation components of five existing human thermal exchange models (Burt, COMFA, MENEX, OUT_SET*, RayMan models) and one experimental model (six-directional method) for estimating quantities of human body absorbed radiation in outdoor areas were compared with a new model (Park and Tuller model) using radiation data collected in Guelph, Ontario, Canada (Chapter 3).

Urban area factors, surface albedos and temperatures, were obtained from downtown Nanaimo, B.C., Canada and shown in Chapter 4. These factors are important for human radiation exchange simulation in outdoor urban areas. These urban area factors were included in a new human-urban radiation exchange simulation model for outdoor urban areas. The new model was compared with two other existing three-dimensional computer simulation programs, RayMan Pro and ENVI-met 3.1, as well as the measured microclimatic data including both solar and longwave radiation in Chapter 4.

The major findings are:

1. Differences in human body factors (f_p and f_{eff}) between genders (male or female) and body types [normal- or over-weight BMI (Body Mass Index) categories] for standing posture were relatively small. For most general modeling studies, a single value can be used regardless of gender or BMI category without seriously affecting the projected results.

2. There were only minor differences in directionless f_p values between genders and stride positions for walking posture. The directional f_p differences between normal-weight male and normal-weight female models were also small. However, directional f_p values had greater differences between azimuth angles. Large differences occurred at low altitude angles which are closest to perpendicular to the vertical body surface. Differences decrease with increasing altitude angles.

3. f_{eff} values between standing (0.826) and walking (0.846) postures were not too different. The mean f_{eff} (0.836) can be applied in most general modeling studies where applications to a variety of people both standing and walking are of interest. However, f_p values should be selected carefully because directional and directionless f_p differences were significant at some azimuth angles.

4. In the differences between human radiation exchange models, the key variable was the projected area factor (f_p^*). The RayMan model had the closest f_p^* values to those of the new human radiation exchange model of Park and Tuller, 0.025-0.035 lower. This made the RayMan model underestimate net all-wave radiation up to 29 Wm^{-2} compared with the Park and Tuller model, an amount that can be important in human thermal exchange. Therefore, proper f_p and f_{eff} values should be used for accurate estimation of absorbed solar and net longwave radiation. The Park and Tuller model's body area factors (f_p and f_{eff}) show promise for improved analysis of radiation exchange of the contemporary adult body.

5. The new human-urban radiation exchange simulation model has a detailed view factor analysis system. It can estimate 12 different view factors (sunny/shaded × building/vegetation/ground surfaces × upper/lower hemispheres at the height of 1.2 meters). It can separate vegetation view factors from building view factors in the upper hemisphere. Also, the model used the most recent, detailed urban area factors: sunny/shaded surface albedos and temperatures of buildings, vegetation and the ground. The model had very small differences with the collected radiation data. It estimated much better results than two other computer simulation programs, RayMan Pro and ENVI-met 3.1. The model produces two different types of results: amounts of radiation or mean radiant temperature which can be used as input data for most human thermal exchange (comfort) models, including predicted mean vote (PMV), physiological equivalent temperature (PET) and universal thermal climate index (UTCI). The detailed radiation data are useful at the stage of design and the mean radiant temperature data are useful at the stage of planning. A planner with detailed radiation data can analyze the type and amount of radiation that affects most of the designated area and which radiant surface should be modified to improve the thermal environment. However, mean radiant temperature data allow planners to analyze general thermal condition of the area but they cannot modify it because mean radiant temperature is one sum value which does not show detailed effects of surrounding radiant environments. Therefore, the model provides a tool that will enable urban planners, landscape

architects and developers to include effects on outdoor human thermal exchange (comfort) in both the planning and design stages of their projects.

However, this study has several limitations:

1. Among body factors, clothing area factors were not tested. For more realistic simulations, the factors should be analyzed seasonally and by clothing insulation. Further studies will analyze clothing area factors and combine these with the created body models of this study. The results will be included in the next version of the model.

2. Body area factors (f_p and f_{eff}) were not tested using real human bodies or mannequins. Those factors are important parameters for the model. The method of developing the parameters was based on methods and theories widely used in the field of biometeorology. However, detailed real tests including the entire body area have never been done. Recently, a flexible solar panel was developed. These panels can make tests of solar radiation incident on the human body possible. On the other hand, it is still difficult to directly measure longwave radiation.

3. The new human-urban radiation exchange simulation model has several limitations:

a. no cloud effect is included;

b. each pixel of the ground surface is assumed to be horizontal;

c. only one albedo and emissivity value is allowed for each sunny/shaded building, tree or ground surface;

d. the model would benefit from surface temperature formulas that take into account the more complete energy budget of the surface;

e. the urban albedos and surface temperatures were taken at only a limited number of sites and in the warm season. The model needs to be tested for cold conditions, other latitudes and so on; and

f. a somewhat long simulation time. 124×166 grid area (248 m × 332 m when the grid size is 2 m) simulation of the Nanaimo site took around 2 hours. The operating system was Microsoft Windows XP. The CPU was Intel Core Duo E8400 at 3.0 Ghz and memory ram was 3.5 GBytes.

These limitations will be modified in further studies. Input functions allowing different ground slope angles, albedo and emissivity for each individual ground surface and vertical obstruction type will be coded in the next version. Programming simulation for individual locations of interest, not whole areas, can

effectively reduce simulation time. More tests for estimating surface temperatures should be conducted for a variety of materials and situations. If better formulas are available, they will be included in the next version of the model.

A later model will also include the sitting posture and the cloudiness effect as well as specific Linke turbidity values which are useful in planning studies and in simulating air pollution effects on human radiation exchange. Therefore, the modified new human-urban radiation exchange simulation model will give landscape and urban planners a better, easy-to-use but accurate tool. This will allow consideration of human radiation exchange in their practices and facilitate creation of more sustainable urban environments for human beings.

The model can be used in two ways: (1) It can simulate existing outdoor environments to assess some of the effects of assumed future climates. If these are found to be unfavourable, the model can be used to quickly and easily investigate the viability of different ground surface and vertical obstruction modifications to maintain a comfortable radiation environment. (2) It can simulate the effects of future development options. The model can test the effects of different obstruction heights and spacing, building and ground materials, vegetation types and so on. Planners and others interested in urban and landscape design can use the model in both ways to create thermally comfortable areas. More detailed explanations are given in Appendix D.

This study explored all processes for analyzing human-urban radiation exchange from basic theories to three-dimensional computer simulation. I hope this study can contribute to creating better living environments for human beings.

Appendix A: Survey form and poster of human body area factor

This appendix has the participant consent form and survey poster which were used in the human body data collection at the Commonwealth Recreation Centre in Victoria, B.C., Canada.

Department of Geography, University of Victoria
P. O. Box 3050, Victoria, B.C., V8W 3P5
Phone : +1 250 721~7327, Fax : +1 250 721~6216

Participant Consent Form

Radiation exchange between an ergonomic human body and surrounding urban environments for human thermal comfort

You are being invited to participate in a study entitled **Radiation exchange between an ergonomic human body and surrounding urban environments for human thermal comfort** that is being conducted by Sookuk Park.

Sookuk Park is a PhD student in the department of Geography at the University of Victoria and you may contact him if you have further questions by e-mail: sooland@uvic.ca or telephone: 721-7345.

As a graduate student, I am required to conduct research as part of the requirements for a degree in PhD. It is being conducted under the supervision of Dr. Stanton E. Tuller. You may contact my supervisor at 721-7332.

The purpose of this research project is to increase our understanding of human thermal exchange in urban environments and provide some knowledge and tools to allow planners to more easily and accurately assess the effects of different urban morphologies. The focus of this study is radiation exchange, both solar and longwave, between the ergonomic human body, especially standing and walking postures, and the surrounding thermal environments.

Research of this type is important because this study updates methods in human bioclimatology, making them more applicable to the present-day, adult population. The results will supply important information for models of human thermal exchange and can be applied to develop easy-to-use procedures that can be applied by urban planners, designers and landscape architects to assess human radiation exchange and create more comfortable, healthy outdoor and indoor spaces. Creating more comfortable outdoor spaces will also encourage human health and local businesses.

You are being asked to participate in this study as it requires participants who have an average adult body shape which can be easily identified by visual interpretation.

If you agree to voluntarily participate in this research, your participation will include your height, weight, age, natural standing pose and walking poses. It will take less than 1 minute. Before the procedure, you have to fill in the consent form which has your name, signature and date, and check your age categories. The procedure is that you have to stand on a scale on the ground for 5 seconds with your natural standing pose (at that time, I will record your weight), step down the scale and walk 5 meters (4-6 steps). During that time, your body shape will be collected by my assistants using digital cameras and camcorders 10 meters away from you at this location. Your height will be collected from your taken standing pose image.

Participation in this study may cause some inconvenience to you, including your showing your weight, age and body shape. However, there are no known or anticipated risks to you by participating in this research.

The potential benefits of your participation in this research include that the results have direct application for models of human thermal exchange and can be applied to develop easy-to-use procedures that can be applied by urban planners, designers and landscape architects to assess human radiation exchange and create more comfortable, healthy outdoor and indoor spaces. Comfortable environments will reduce human thermal stress and encourage people to utilize the downtown activity.

Your participation in this research must be completely voluntary. If you do decide to participate, you may withdraw at any time without any consequences or any explanation. If you do withdraw from the study your data will not be used.

In terms of protecting your anonymity and confidentiality and the confidentiality of the data, your body shape will be collected 10 meters away from your body and stored only in my personal computer with password. And, your original images will be erased after digitizing the outer edge of your body shape. Therefore, your anonymity and confidentiality including the confidentiality of the data will be perfectly protected.

Data from this study will be disposed of the following ways: 1. The image files will be protected with password in my personal computer, and the original files in camcorders and digital cameras will be destroyed after being exported to my personal computer; 2. All data is digital images, so the images in digital cameras and computers will be deleted with a delete key, and images in camcorders will be also destroyed by taking other scenes.

It is anticipated that the results of this study will be shared with others in the following ways: presentations at scholarly meetings, published articles and my thesis.

In addition to being able to contact the researcher and the supervisor at the above phone numbers, you may verify the ethical approval of this study, or raise any concerns you might have, by contacting the Associate Vice-President, Research at the University of Victoria (250-472-4545).

Your signature below indicates that you understand the above conditions of participation in this study and that you have had the opportunity to have your questions answered by the researchers.

_____	_____	_____
Name of Participant	*Signature*	*Date*

A copy of this consent will be left with you, and a copy will be taken by the researcher.

Item # 1. Age Categories

20~24	25~29	30~34	35~39	40~44	45~49	50~54	55~59	60~64	65~69	70+
____	____	____	____	____	____	____	____	____	____	____

Item # 2. Weight

_____ kg

Item # 3. Height

_____cm

Survey Poster

University of Victoria | British Columbia Canada

S. Park, a PhD candidate, Dept. of Geography
P.O.Box 3050, Victoria, B.C., V8W 3P5
Phone : (250) 721~ 7345, Fax : (250) 721~ 6216
E-mail : sooland@uvic.ca

Radiation Exchange between The Ergonomic Human Body and The Surrounding Urban Environments for Human Thermal Comfort

Purpose : The purpose of this research project is to increase our understanding of human thermal exchange in urban environments and provide some knowledge and tools to allow planners to more easily and accurately assess the effects of different urban morphologies.

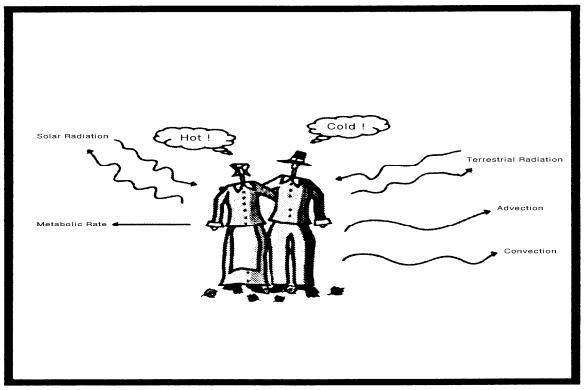

Procedure : **It will take less than 1 minute.**

1. Stand on a scale for 5 seconds with your natural standing pose
2. Step down to the ground
3. Walk naturally 5 meters (4~6 steps)
4. Fill in the consent form

Methods :

Importing to the computer Wiping out the original images

☺ **Your anonymity and confidentiality including the data will be perfectly protected.**

Appendix B: Manual for the new human-urban radiation exchange simulation model

This appendix has the manual for the human-urban radiation exchange simulation computer model.

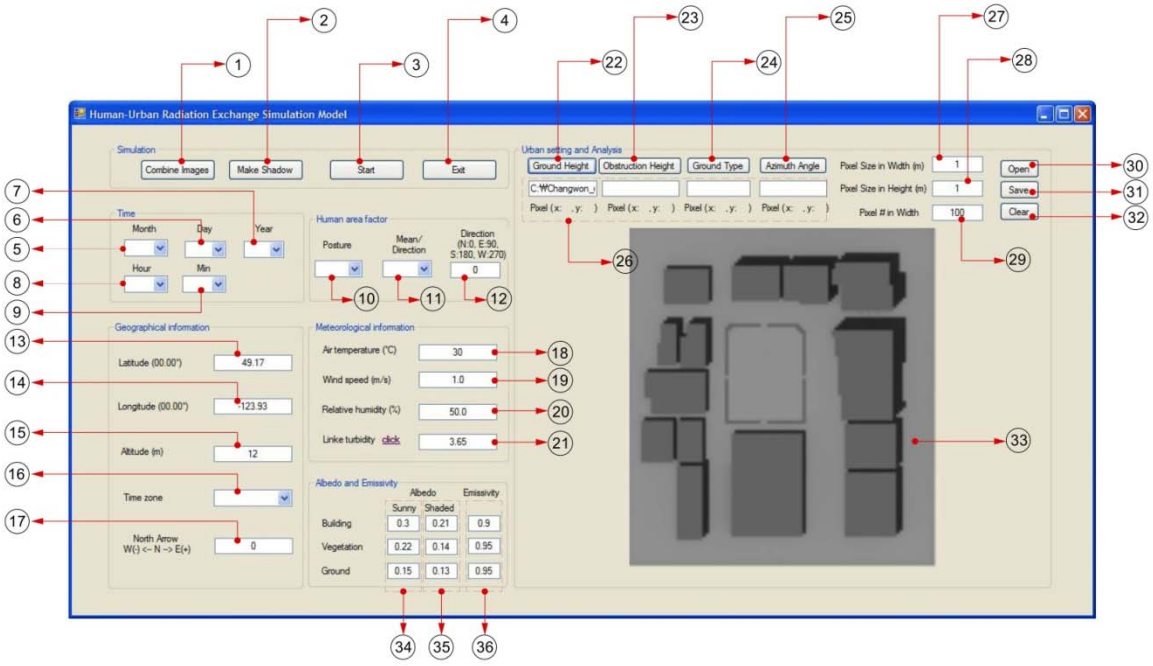

Fig. B.1 Manual window of the human-urban radiation exchange simulation model

Simulation section:

① (Button 10) Combine Images: making an image for simulation combining ㉒ Ground Height, ㉓ Obstruction Height, ㉔ Ground Type and ㉕ Azimuth Angle

② (Button 2) Make Shadow: creating shadow patterns using the combined image of four urban setting data, ㉒-㉕

③ (Button 7) Start: running the whole simulation processes

④ (Button 6) Exit: exit from the program. The model will be closed.

Time section:

⑤ (ComboBox 1) Month: 1 (January)-12 (December)

⑥ (ComboBox 2) Day: 1-31

⑦ (ComboBox 3) Year: 1950-2050

⑧ (ComboBox 4) Hour: 1-24

⑨ (ComboBox 5) Minute: 0-59

Human area factor section:

⑩ (ComboBox 7) Posture: standing, walking or mean of standing and walking

⑪ (ComboBox 8) Mean/Direction: mean or direction of posture

⑫ (TextBox 14) Direction: direction of posture. This is required only when Direction in ⑪ is chosen.

Geographical information section:

⑬ (TextBox 1) Latitude (00.00°): decimal degree of latitude without unit (°), e.g., latitude of Nanaimo site is 49º10′N which is 49.17

⑭ (TextBox 2) Longitude (00.00°): decimal degree of longitude without unit (°), and longitude is expressed as positive when it is in the east and negative when in the west, e.g., longitude of Nanaimo site is 123º56'W which is -123.93

⑮ (TextBox 3) Altitude (m): ground height above the sea level

⑯ (ComboBox 6) Time zone: GMT-12:00 International date line west ~ GMT+12:00 Fiji, Auckland, Wellington, Petroparlovsk-Kamchatsky

⑰ (TextBox 15) North arrow [W(-)←N(0)→E(+)]: the rotation of north arrow, a western way from the north is minus values and an eastern way from the north is plus values.

Meteorological information section:

⑱ (TextBox 4) Air temperature (°C): dry bulb temperature

⑲ (TextBox 5) Wind speed (ms^{-1}): wind speed at the height of 1.2 meters. The wind speed data column is not required in the radiation simulation but made for further development.

⑳ (TextBox 6) Relative humidity (%): relative humidity in percent

㉑ (TextBox 7) Linke turbidity: this value can be found at the Soda-is website (http://www.soda-is.com/eng/services/ climat_free_eng.php) that will be automatically connected when click is clicked. The values are monthly.

Urban setting and Analysis section:

㉒ (Button 3) Ground Height: ground height data as a text file (.txt) or an image file (.bmp)

㉓ (Button 1) Obstruction Height: obstruction (buildings and trees) height data as a text file (.txt) or an image file (.bmp)

㉔ (Button 5) Ground Type: ground type (ground/building or tree) data as a text file (.txt) or an image file (.bmp)

㉕ (Button 11) Azimuth Angle: building azimuth angle data as a text file (.txt) or an image file (.bmp)

㉖ (TextBox 8, 9, 12, 13; Label 14, 15, 18, 19) four textboxes will show the file folders and names selected in ㉒-㉕, and four labels will show the pixel numbers of the x-axis and y-axis.

㉗ (TextBox 10) Pixel Size in Width (m): the size of one pixel in the x- and y-axis directions

㉘ (TextBox 16) Pixel Size in Height (m): the size of one pixel in the z-axis direction

㉙ (TextBox 11) Pixel # in Width: pixel number in the x-axis direction

㉚ (Button 8) Open: showing an image file in the ㉝ Picturebox

㉛ (Button 4) Save: saving an image of the ㉝ Picturebox

㉜ (Button 9) Clear: clearing an image of the ㉝ Picturebox

Picturebox:

㉝ (PictureBox 1) Picturebox: showing all images during the processes

Albedo and Emissivity:

㉞ (TextBox 17, 18, 19) Albedos of sunny surfaces of building, vegetation and ground

㉟ (TextBox 20, 21, 22) Albedos of shaded surfaces of building, vegetation and ground

㊱ (TextBox 23, 24, 25) Emissivities of building, vegetation and ground surfaces

How to prepare the four urban setting files:

Fig. B.2 explains how to create the four text files for a site. Raster image is made of pixels. In this study, a bitmap image was selected. Its pixel is composed of 4 channels: alpha (opacity), red, green and blue channels. Each channel can have a value between 0 and 255. In the data input text file, only two digit numbers are used for each pixel which means the input value for each pixel is limited to between 0 and 99 (Figs. B.2b and c). However, the new model has setting options of pixel width and height, so the real input value can be extended enough to express high-rise buildings and trees. For example, when a building height is 150 meters the height can be input as 75 in the text datum and 2 in pixel height. In the ground type file, only two numbers were used: 0 for ground and building and 2 for tree (Fig. B.2d). In the azimuth angle file, the angle is the direction which a building surface faces and is clockwise from north (0°) through east (90°), south (180°) and west (270°), and the increment is 10°, so 18 is input as 180° and 9 as 90° (Fig. B.2e).

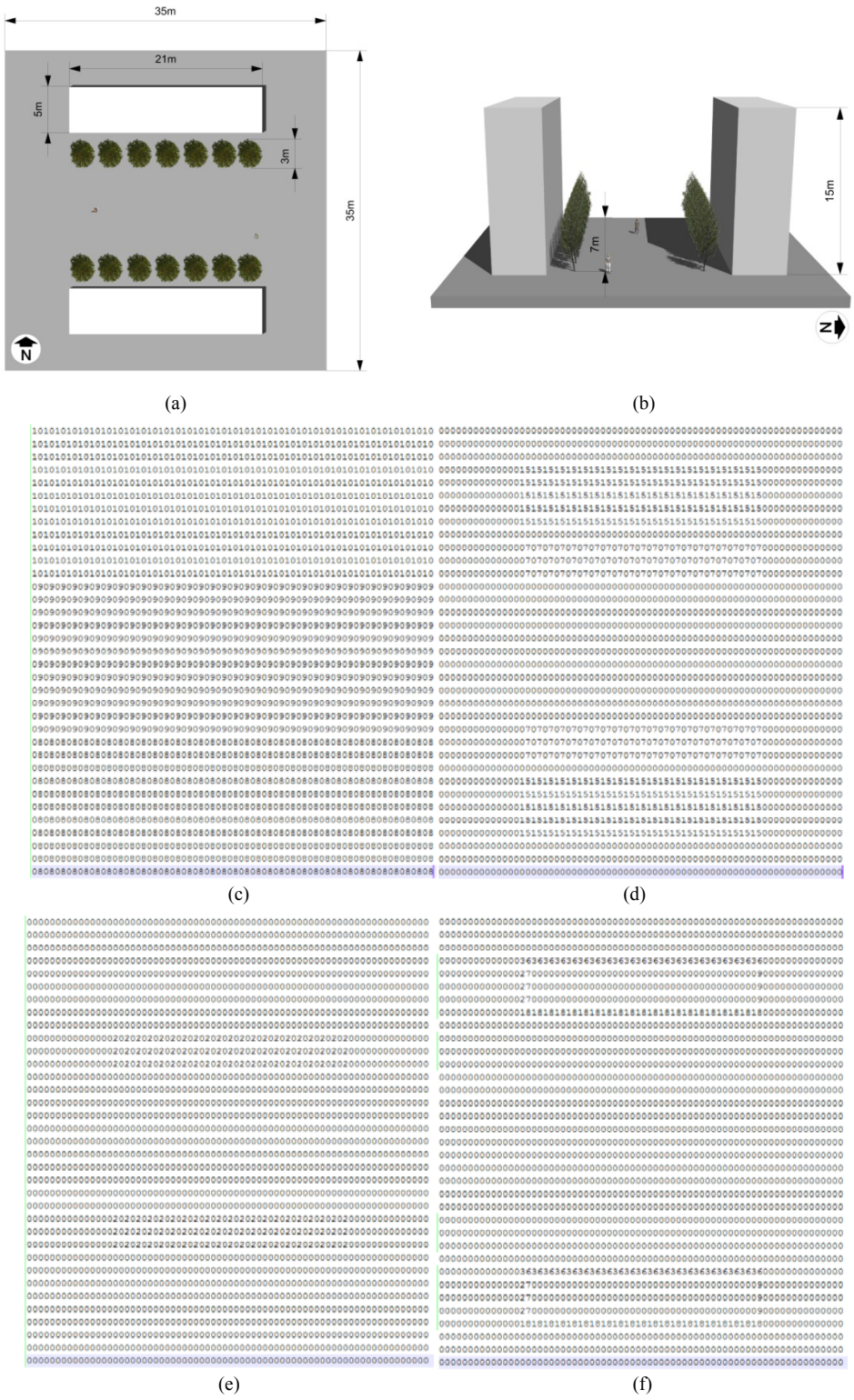

(a) (b)

(c) (d)

(e) (f)

Fig. B.2 Example of urban setting data text files: (a) horizontal view, (b) bird view, (c) ground height text file, (d) obstruction height text file, (e) ground type text file and (f) azimuth angle text file

How to run the simulation:

1. Adjust date and time data in the time section (⑤-⑨).

2. Input and adjust all required data in the geographical (⑬-⑰) and meteorological (⑱-㉑) information including albedos and emissivities of sunny and shaded building, vegetation and ground surfaces (㉞-㊱).

3. Set human body area (⑩-⑫) sections. For a simple analysis, a setting of 'standing and walking' → 'mean' will be fine. When it is set to 'mean', the direction value is not required. For a specific analysis, a posture and its direction should be defined for precise results. The direction runs clockwise from the north (0).

4. Click and choose four urban setting files (㉒-㉕), and input pixel data (㉗-㉙).

5. Click 'Start' button (③).

6. As the results, the first results (reflected solar radiation, surface temperatures and sky view factors of each pixel) will be automatically saved in C:\Skyviewfactor.txt, and a pop-up window 'Save a Sky View Factor Image File' will be opened. Input a file name and push 'Save' button or click 'Cancel' button if you don't want to save the image file. The text file can be read in proper programs, e.g., Notepad, Notepad++, Microsoft Office Excel and so on.

7. The second results (view factors of sunny and shaded ground and building surfaces without tree surfaces received to each ground pixel) will be saved in C:\Obstructviewfactor.txt, and a pop-up window 'Save a Building View Factor Image File' will be shown. Next procedure is same as 5.

8. The third results (view factors and surface temperatures of sunny and shaded ground, building and tree surfaces received to each ground pixel) and the last results (sky view factors, all radiation, human area factors and mean radiant temperatures) will be saved in C:\ViewfactorandTs.txt and in C:\Radiationresult.txt, respectively. Two pop-up windows 'Save a Urban Radiation Map Image File' showing total radiation received to each ground pixel at the height of 1.2 meters and 'Save a Human Radiation Map image File' showing total radiation absorbed to the human body surface will be consecutively shown. Next procedure is same as 5.

9. When the simulation is done, click the 'Exit' button (④).

10. For simulations at other times, adjust all required data through 1-3 and start again. For different sites, set all data through 1-4 and click start.

Appendix C: Important computer codes of the new human-urban radiation exchange simulation model

Shadow casting

```
Private Sub Button2_Click_1(ByVal sender As System.Object, ByVal e As System.EventArgs) Handles Button2.Click
    'j is Julian day
    Dim j As Integer
    Dim k As Single

    Select Case ComboBox1.SelectedIndex
      Case 0 : j = ComboBox2.SelectedIndex + 1
      Case 1 : j = 32 + ComboBox2.SelectedIndex
      Case 2 : j = 60 + ComboBox2.SelectedIndex
      Case 3 : j = 91 + ComboBox2.SelectedIndex
      Case 4 : j = 121 + ComboBox2.SelectedIndex
      Case 5 : j = 152 + ComboBox2.SelectedIndex
      Case 6 : j = 182 + ComboBox2.SelectedIndex
      Case 7 : j = 213 + ComboBox2.SelectedIndex
      Case 8 : j = 244 + ComboBox2.SelectedIndex
      Case 9 : j = 274 + ComboBox2.SelectedIndex
      Case 10 : j = 305 + ComboBox2.SelectedIndex
      Case 11 : j = 335 + ComboBox2.SelectedIndex
    End Select

    'Direct beam solar radiation calculation
    'beta: solar altitude, k: the sun-earth distance correction, Rayop: Rayleigh optical thickness, Linket: Linke turbidity, Airmass: the relative optical air mass
    'z: elevation, t: atmospheric transmissivity
    Dim Kbo, z, Linket, xx, alti, lati, longi, CMT, TLT, Timezone, betaorg, decl, solarh, solazi As Double

    Kbo = 1367
    alti = TextBox3.Text
    Linket = TextBox7.Text
    xx = 0.9856 * j - 2.72
    k = 1 + 0.03344 * Math.Cos(xx * Math.PI / 180)
    Timezone = ComboBox6.SelectedIndex
    z = -7.66 * Math.Sin(xx * Math.PI / 180) - 9.87 * Math.Sin((2 * xx + 24.99 + 3.83 * Math.Sin(xx * Math.PI / 180)) * Math.PI /_
180)
    lati = TextBox1.Text
    longi = Int(TextBox2.Text)
    CMT = (ComboBox4.SelectedIndex + 1) * 60 + ComboBox5.SelectedIndex

    Select Case ComboBox6.SelectedIndex
      Case 0 : Timezone = -180
      Case 1 : Timezone = -165
      Case 2 : Timezone = -150
      Case 3 : Timezone = -135
      Case 4 : Timezone = -120
      Case 5 : Timezone = -105
      Case 6 : Timezone = -90
      Case 7 : Timezone = -75
      Case 8 : Timezone = -60
      Case 9 : Timezone = -45
      Case 10 : Timezone = -30
      Case 11 : Timezone = -15
      Case 12 : Timezone = 0
      Case 13 : Timezone = 15
      Case 14 : Timezone = 30
      Case 15 : Timezone = 45
      Case 16 : Timezone = 60
      Case 17 : Timezone = 75
      Case 18 : Timezone = 90
      Case 19 : Timezone = 105
```

```
            Case 20 : Timezone = 120
            Case 21 : Timezone = 135
            Case 22 : Timezone = 150
            Case 23 : Timezone = 165
            Case 24 : Timezone = 180
        End Select

        TLT = CMT - (Timezone - longi) * 4 + z
        decl = Math.Asin((0.3978 * Math.Sin((xx - 77.51 + 1.92 * Math.Sin(xx * Math.PI / 180)) * Math.PI / 180))) * 180 / Math.PI
        solarh = (TLT - 720) * 0.25
        betaorg = Math.Asin(Math.Sin(lati * Math.PI / 180) * Math.Sin(decl * Math.PI / 180) + Math.Cos(lati * Math.PI / 180) *_
Math.Cos(decl * Math.PI / 180) * Math.Cos(solarh * Math.PI / 180)) * 180 / Math.PI  'Solar elevation angle

        solazi = Math.Acos((Math.Sin(lati * Math.PI / 180) * Math.Sin(betaorg * Math.PI / 180) - Math.Sin(decl * Math.PI / 180)) /_
(Math.Cos(lati * Math.PI / 180) * Math.Cos(betaorg * Math.PI / 180))) * 180 / Math.PI  'Solar azimuth angle. Positive westwards
(afternoon) of south=0 and negative eastwards (morning)
        If CMT < 720 Then
            solazi = -solazi + TextBox15.Text
        ElseIf CMT > 720 Then
            solazi = solazi + TextBox15.Text
        Else
            solazi = TextBox15.Text
        End If

'Analyzing shadow proportions
        Dim newimage As Bitmap = PictureBox1.Image
        Dim x, y, x1, y1, pGreen1 As Integer
        Dim allheight, allheight1, allheight2, elevation, eleangle, pGreen, pGreenh, pGreenhh As Double
        Try
            ' Loop through the images pixels to reset blue color which number represents the shading analysis result.

            If betaorg > 0 Then
                If solazi < -26.565 And solazi >= -90 Then
                    For x = 0 To newimage.Width - 1 Step 1
                        For y = 0 To newimage.Height - 1 Step 1
                            pGreenhh = 0
                            Dim pixelColor As Color = newimage.GetPixel(x, y)
                            If pixelColor.G > 200 Then
                                pGreen = (pixelColor.G - 200)      'tree height=pixelColor.G-200
                            Else
                                pGreen = pixelColor.G
                            End If

                            allheight = pixelColor.R + pGreen * TextBox16.Text

                            For x1 = x + 1 To (newimage.Width – 1) Step 1
                                If x1 >= 0 and x1 <= (newimage.Width - 1) Then
                                    y1 = y + CInt((x1 - x) * Math.Tan((90 + solazi) * Math.PI / 180))   'solazi is solar azimuth angle.
                                    If y1 = y Then
                                        y1 = y + 1
                                    End If
                                    If y1 >= 0 and y1 <= (newimage.Height - 1) Then     'input angle value (90-solar azimuth angle)

                                        Dim pixelcolor1 As Color = newimage.GetPixel(x1, y1)

                                        If pixelcolor1.G > 200 Then
                                            pGreen1 = (pixelcolor1.G - 200)
                                        Else
                                            pGreen1 = pixelcolor1.G
                                        End If

                                        allheight1 = pixelcolor1.R + pGreen1 * TextBox16.Text
                                        elevation = (allheight1 - allheight) / Math.Sqrt(((x - x1) * TextBox10.Text) ^ 2 + ((y - y1) *_
TextBox10.Text) ^ 2)
                                        eleangle = Math.Atan(elevation) * 180 / Math.PI

                                        If pGreen > 0 And pGreen1 > 0 And pGreen = pGreen1 And (y1 - y) = 1 Then
                                            eleangle = 90
                                        End If
```

```
                        If eleangle >= betaorg Then
                            pixelColor = newimage.GetPixel(x, y)
                            If pGreen = 0 Then
                                Dim newColor As Color = Color.FromArgb(pixelColor.A, pixelColor.R, pixelColor.G, pGreen + 1)
'Shaded ground, building or tree pixel. Shaded ground has 1 value.
                                newimage.SetPixel(x, y, newColor)
                            Else
                                Dim newColor As Color = Color.FromArgb(pixelColor.A, pixelColor.R, pixelColor.G, pGreen)
'Shaded whole height of building or tree
                                newimage.SetPixel(x, y, newColor)
                            End If

                            Exit For
                        Else
                            pGreenh = pGreen
                            Do While eleangle < betaorg   'Comparing with solar elevation angle

                                pGreenh -= 1

                                If pGreenh = -1 Then
                                    pixelColor = newimage.GetPixel(x, y)
                                    Dim newColor1 As Color = Color.FromArgb(pixelColor.A, pixelColor.R, pixelColor.G, pGreenhh)
'Sunny ground, building or tree pixel.
                                    newimage.SetPixel(x, y, newColor1)
                                    eleangle = betaorg
                                Else
                                    allheight2 = pixelColor.R + pGreenh * TextBox16.Text
                                    elevation = (allheight1 - allheight2) / Math.Sqrt(((x - x1) * TextBox10.Text) ^ 2 + ((y - y1) *_
TextBox10.Text) ^ 2)
                                    eleangle = Math.Atan(elevation) * 180 / Math.PI
                                    pixelColor = newimage.GetPixel(x, y)
                                    If pGreenhh < pGreenh And eleangle > betaorg Then
                                        pGreenhh = pGreenh
                                    End If
                                    Dim newColor1 As Color = Color.FromArgb(pixelColor.A, pixelColor.R, pixelColor.G, pGreenhh)
'pGreen is the shaded height of building or tree.
                                    newimage.SetPixel(x, y, newColor1)
                                End If
                            Loop
                        End If
                    End If
                End If
            Next
            Dim pixel1 As Color = newimage.GetPixel(x, y)
            Dim Shadedata As String = x & ", " & y & " Azimuth: " & pixel1.A & " Ground height: " & pixel1.R & " Obstruct
height: " & pixel1.G & " Shade obstruct height: " & pixel1.B & vbCrLf
            My.Computer.FileSystem.WriteAllText("C:\Shadedata.txt", Shadedata, True)
        Next
    Next
ElseIf solazi < -90 Then
    For x = 0 To newimage.Width - 1 Step 1
        For y = newimage.Height - 1 To 0 Step -1
            pGreenhh = 0
            Dim pixelColor As Color = newimage.GetPixel(x, y)
            If pixelColor.G > 200 Then
                pGreen = (pixelColor.G - 200)    'tree height=pixelColor.G-200
            Else
                pGreen = pixelColor.G
            End If

            allheight = pixelColor.R + pGreen * TextBox16.Text

            For x1 = x + 1 To newimage.Width - 1 Step 1
                If x1 >= 0 and x1 <= (newimage.Width – 1) Then
                    y1 = y - CInt((x1 - x) * Math.Tan((90 - solazi) * Math.PI / 180))
                    If y1 = y Then
                        y1 = y - 1
                    End If
                    If y1 >= 0 and y1 <= (newimage.Height –1) Then    'input angle value (90-solar azimuth angle)
```

```
                        Dim pixelcolor1 As Color = newimage.GetPixel(x1, y1)

                        If pixelcolor1.G > 200 Then
                            pGreen1 = (pixelcolor1.G - 200)
                        Else
                            pGreen1 = pixelcolor1.G
                        End If

                        allheight1 = pixelcolor1.R + pGreen1 * TextBox16.Text
                        elevation = (allheight1 - allheight) / Math.Sqrt(((x - x1) * TextBox10.Text) ^ 2 + ((y - y1) *_
TextBox10.Text) ^ 2)
                        eleangle = Math.Atan(elevation) * 180 / Math.PI
                        If pGreen > 0 And pGreen1 > 0 And pGreen = pGreen1 And (y - y1) = 1 Then
                            eleangle = 90
                        End If
                        If eleangle >= betaorg Then
                            pixelColor = newimage.GetPixel(x, y)
                            If pGreen = 0 Then
                                Dim newColor As Color = Color.FromArgb(pixelColor.A, pixelColor.R, pixelColor.G, pGreen + 1)
'Shaded ground, building or tree pixel. Shaded ground has 1 value.
                                newimage.SetPixel(x, y, newColor)
                            Else
                                Dim newColor As Color = Color.FromArgb(pixelColor.A, pixelColor.R, pixelColor.G, pGreen)
'Shaded whole height of building or tree
                                newimage.SetPixel(x, y, newColor)
                            End If

                            Exit For
                        Else
                            pGreenh = pGreen
                            Do While eleangle < betaorg   'Comparing with solar elevation angle

                                pGreenh -= 1

                                If pGreenh = -1 Then
                                    pixelColor = newimage.GetPixel(x, y)
                                    Dim newColor1 As Color = Color.FromArgb(pixelColor.A, pixelColor.R, pixelColor.G, pGreenhh)
'Sunny ground, building or tree pixel.
                                    newimage.SetPixel(x, y, newColor1)
                                    eleangle = betaorg
                                Else
                                    allheight2 = pixelColor.R + pGreenh * TextBox16.Text
                                    elevation = (allheight1 - allheight2) / Math.Sqrt(((x - x1) * TextBox10.Text) ^ 2 + ((y - y1) *_
TextBox10.Text) ^ 2)
                                    eleangle = Math.Atan(elevation) * 180 / Math.PI
                                    pixelColor = newimage.GetPixel(x, y)
                                    If pGreenhh < pGreenh And eleangle > betaorg Then
                                        pGreenhh = pGreenh
                                    End If
                                    Dim newColor1 As Color = Color.FromArgb(pixelColor.A, pixelColor.R, pixelColor.G, pGreenhh)
'pGreen is the shaded height of building or tree.
                                    newimage.SetPixel(x, y, newColor1)
                                End If
                            Loop
                        End If
                    End If
                End If
            Next
            Dim pixel1 As Color = newimage.GetPixel(x, y)
            Dim Shadedata As String = x & ", " & y & " Azimuth: " & pixel1.A & " Ground height: " & pixel1.R & " Obstruct
height: " & pixel1.G & " Shade obstruct height: " & pixel1.B & vbCrLf
            My.Computer.FileSystem.WriteAllText("C:\Shadedata.txt", Shadedata, True)
        Next
    Next

ElseIf solazi > 26.565 And solazi <= 90 Then

    For x = newimage.Width - 1 To 0 Step -1
        For y = 0 To newimage.Height - 1 Step 1
            pGreenhh = 0
```

```
                Dim pixelColor As Color = newimage.GetPixel(x, y)
                If pixelColor.G > 200 Then
                   pGreen = (pixelColor.G - 200)    'tree height=pixelColor.G-200
                Else
                   pGreen = pixelColor.G
                End If

                allheight = pixelColor.R + pGreen * TextBox16.Text

                For x1 = x - 1 To 0 Step -1

                   If x1 >= 0 and x1 <= (newimage.Width – 1) Then
                      y1 = y + CInt((x - x1) * Math.Tan((90 - solazi) * Math.PI / 180))
                      If y1 = y Then
                         y1 = y + 1
                      End If
                      If y1 >= 0 and y1 <= (newimage.Height - 1) Then    'input angle value (90-solar azimuth angle)

                         Dim pixelcolor1 As Color = newimage.GetPixel(x1, y1)

                         If pixelcolor1.G > 200 Then
                            pGreen1 = (pixelcolor1.G - 200)
                         Else
                            pGreen1 = pixelcolor1.G
                         End If

                         allheight1 = pixelcolor1.R + pGreen1 * TextBox16.Text
                         elevation = (allheight1 - allheight) / Math.Sqrt(((x - x1) * TextBox10.Text) ^ 2 + ((y - y1) *_
TextBox10.Text) ^ 2)
                         eleangle = Math.Atan(elevation) * 180 / Math.PI
                         If pGreen > 0 And pGreen1 > 0 And pGreen = pGreen1 And (y1 - y) = 1 Then
                            eleangle = 90
                         End If
                         If eleangle >= betaorg Then
                            pixelColor = newimage.GetPixel(x, y)
                            If pGreen = 0 Then
                               Dim newColor As Color = Color.FromArgb(pixelColor.A, pixelColor.R, pixelColor.G, pGreen + 1)
'Shaded ground, building or tree pixel. Shaded ground has 1 value.
                               newimage.SetPixel(x, y, newColor)
                            Else
                               Dim newColor As Color = Color.FromArgb(pixelColor.A, pixelColor.R, pixelColor.G, pGreen)
'Shaded whole height of building or tree
                               newimage.SetPixel(x, y, newColor)
                            End If

                            Exit For
                         Else
                            pGreenh = pGreen
                            Do While eleangle < betaorg   'Comparing with solar elevation angle

                               pGreenh -= 1

                               If pGreenh = -1 Then
                                  pixelColor = newimage.GetPixel(x, y)
                                  Dim newColor1 As Color = Color.FromArgb(pixelColor.A, pixelColor.R, pixelColor.G, pGreenhh)
'Sunny ground, building or tree pixel.
                                  newimage.SetPixel(x, y, newColor1)
                                  eleangle = betaorg
                               Else
                                  allheight2 = pixelColor.R + pGreenh * TextBox16.Text
                                  elevation = (allheight1 - allheight2) / Math.Sqrt(((x - x1) * TextBox10.Text) ^ 2 + ((y - y1) *_
TextBox10.Text) ^ 2)
                                  eleangle = Math.Atan(elevation) * 180 / Math.PI
                                  pixelColor = newimage.GetPixel(x, y)
                                  If pGreenhh < pGreenh And eleangle > betaorg Then
                                     pGreenhh = pGreenh
                                  End If
                                  Dim newColor1 As Color = Color.FromArgb(pixelColor.A, pixelColor.R, pixelColor.G, pGreenhh)
'pGreen is the shaded height of building or tree.
                                  newimage.SetPixel(x, y, newColor1)
```

```
                        End If
                    Loop
                End If
            End If
        End If
    Next
    Dim pixel1 As Color = newimage.GetPixel(x, y)
    Dim Shadedata As String = x & ", " & y & " Azimuth: " & pixel1.A & " Ground height: " & pixel1.R & " Obstruct
height: " & pixel1.G & " Shade obstruct height: " & pixel1.B & vbCrLf
    My.Computer.FileSystem.WriteAllText("C:\Shadedata.txt", Shadedata, True)
  Next
Next
ElseIf solazi > 90 Then
  For x = newimage.Width - 1 To 0 Step -1
    For y = newimage.Height - 1 To 0 Step -1
      pGreenhh = 0
      Dim pixelColor As Color = newimage.GetPixel(x, y)
      If pixelColor.G > 200 Then
        pGreen = (pixelColor.G - 200)    'tree height=pixelColor.G-200
      Else
        pGreen = pixelColor.G
      End If

      allheight = pixelColor.R + pGreen * TextBox16.Text

      For x1 = x - 1 To 0 Step -1

        If x1 >= 0 and x1 <= (newimage.Width – 1) Then
          y1 = y - CInt((x - x1) * Math.Tan((90 + solazi) * Math.PI / 180))
          If y1 = y Then
            y1 = y - 1
          End If
          If y1 >= 0 and y1 <= (newimage.Height – 1) Then    'input angle value (90-solar azimuth angle)

            Dim pixelcolor1 As Color = newimage.GetPixel(x1, y1)

            If pixelcolor1.G > 200 Then
              pGreen1 = (pixelcolor1.G - 200)
            Else
              pGreen1 = pixelcolor1.G
            End If

            allheight1 = pixelcolor1.R + pGreen1 * TextBox16.Text
            elevation = (allheight1 - allheight) / Math.Sqrt(((x - x1) * TextBox10.Text) ^ 2 + ((y - y1) *_
TextBox10.Text) ^ 2)
            eleangle = Math.Atan(elevation) * 180 / Math.PI
            If pGreen > 0 And pGreen1 > 0 And pGreen = pGreen1 And (y - y1) = 1 Then
              eleangle = 90
            End If
            If eleangle >= betaorg Then
              pixelColor = newimage.GetPixel(x, y)
              If pGreen = 0 Then
                Dim newColor As Color = Color.FromArgb(pixelColor.A, pixelColor.R, pixelColor.G, pGreen + 1)
'Shaded ground, building or tree pixel. Shaded ground has 1 value.
                newimage.SetPixel(x, y, newColor)
              Else
                Dim newColor As Color = Color.FromArgb(pixelColor.A, pixelColor.R, pixelColor.G, pGreen)
'Shaded whole height of building or tree
                newimage.SetPixel(x, y, newColor)
              End If

              Exit For
            Else
              pGreenh = pGreen
              Do While eleangle < betaorg   'Comparing with solar elevation angle

                pGreenh -= 1

                If pGreenh = -1 Then
                  pixelColor = newimage.GetPixel(x, y)
```

```
                                    Dim newColor1 As Color = Color.FromArgb(pixelColor.A, pixelColor.R, pixelColor.G, pGreenhh)
'Sunny ground, building or tree pixel.
                                    newimage.SetPixel(x, y, newColor1)
                                    eleangle = betaorg
                                Else
                                    allheight2 = pixelColor.R + pGreenh * TextBox16.Text
                                    elevation = (allheight1 - allheight2) / Math.Sqrt(((x - x1) * TextBox10.Text) ^ 2 + ((y - y1) *_
TextBox10.Text) ^ 2)
                                    eleangle = Math.Atan(elevation) * 180 / Math.PI
                                    pixelColor = newimage.GetPixel(x, y)
                                    If pGreenhh < pGreenh And eleangle > betaorg Then
                                        pGreenhh = pGreenh
                                    End If
                                    Dim newColor1 As Color = Color.FromArgb(pixelColor.A, pixelColor.R, pixelColor.G, pGreenhh)
'pGreen is the shaded height of building or tree.
                                    newimage.SetPixel(x, y, newColor1)
                                End If
                            Loop
                        End If
                    End If
                End If
            Next
            Dim pixel1 As Color = newimage.GetPixel(x, y)
            Dim Shadedata As String = x & ", " & y & " Azimuth: " & pixel1.A & " Ground height: " & pixel1.R & " Obstruct
height: " & pixel1.G & " Shade obstruct height: " & pixel1.B & vbCrLf
            My.Computer.FileSystem.WriteAllText("C:\Shadedata.txt", Shadedata, True)
        Next
    Next
ElseIf solazi = 0 Then
    For x = 0 To newimage.Width - 1 Step 1
        For y = 0 To newimage.Height - 1 Step 1
            pGreenhh = 0
            Dim pixelColor As Color = newimage.GetPixel(x, y)
            If pixelColor.G > 200 Then
                pGreen = (pixelColor.G - 200)      'tree height=pixelColor.G-200
            Else
                pGreen = pixelColor.G
            End If

            allheight = pixelColor.R + pGreen * TextBox16.Text

            For y1 = y + 1 To newimage.Height - 1 Step 1     'at noon: azimuth angle=0

                If y1 >= 0 and y1 < (newimage.Height – 1) Then
                    x1 = x
                    Dim pixelcolor1 As Color = newimage.GetPixel(x1, y1)
                    If pixelcolor1.G > 200 Then
                        pGreen1 = (pixelcolor1.G - 200)
                    Else
                        pGreen1 = pixelcolor1.G
                    End If

                    allheight1 = pixelcolor1.R + pGreen1 * TextBox16.Text
                    elevation = (allheight1 - allheight) / ((y1 - y) * TextBox10.Text)
                    eleangle = Math.Atan(elevation) * 180 / Math.PI
                    If pGreen > 0 And pGreen1 > 0 And pGreen = pGreen1 And (y1 - y) = 1 Then
                        eleangle = 90
                    End If
                    If eleangle >= betaorg Then
                        pixelColor = newimage.GetPixel(x, y)
                        If pGreen = 0 Then
                            Dim newColor As Color = Color.FromArgb(pixelColor.A, pixelColor.R, pixelColor.G, pGreen + 1)
'Shaded ground, building or tree pixel. Shaded ground has 1 value.
                            newimage.SetPixel(x, y, newColor)
                        Else
                            Dim newColor As Color = Color.FromArgb(pixelColor.A, pixelColor.R, pixelColor.G, pGreen)
'Shaded whole height of building or tree
                            newimage.SetPixel(x, y, newColor)
                        End If
```

```
                        Exit For
                    Else
                        pGreenh = pGreen
                        Do While eleangle < betaorg   'Comparing with solar elevation angle

                            pGreenh -= 1

                            If pGreenh = -1 Then
                                pixelColor = newimage.GetPixel(x, y)
                                Dim newColor1 As Color = Color.FromArgb(pixelColor.A, pixelColor.R, pixelColor.G, pGreenhh)
'Sunny ground, building or tree pixel.
                                newimage.SetPixel(x, y, newColor1)
                                eleangle = betaorg
                            Else
                                allheight2 = pixelColor.R + pGreenh * TextBox16.Text
                                elevation = (allheight2 - allheight1) / ((y - y1) * TextBox10.Text)
                                eleangle = Math.Atan(elevation) * 180 / Math.PI
                                pixelColor = newimage.GetPixel(x, y)
                                If pGreenhh < pGreenh And eleangle > betaorg Then
                                    pGreenhh = pGreenh
                                End If
                                Dim newColor1 As Color = Color.FromArgb(pixelColor.A, pixelColor.R, pixelColor.G, pGreenhh)
'pGreen is the shaded height of building or tree.
                                newimage.SetPixel(x, y, newColor1)
                            End If
                        Loop
                    End If
                End If
            Next
            Dim pixel1 As Color = newimage.GetPixel(x, y)
            Dim Shadedata As String = x & ", " & y & " Azimuth: " & pixel1.A & " Ground height: " & pixel1.R & " Obstruct
height: " & pixel1.G & " Shade obstruct height: " & pixel1.B & vbCrLf
            My.Computer.FileSystem.WriteAllText("C:\Shadedata.txt", Shadedata, True)
        Next
    Next
ElseIf solazi >= -26.565 And solazi < 0 Then
    For x = 0 To newimage.Width - 1 Step 1
        For y = 0 To newimage.Height - 1 Step 1
            pGreenhh = 0
            Dim pixelColor As Color = newimage.GetPixel(x, y)
            If pixelColor.G <> 255 Then
                If pixelColor.G > 200 Then
                    pGreen = (pixelColor.G - 200)    'tree height=pixelColor.G-200
                Else
                    pGreen = pixelColor.G
                End If

                allheight = pixelColor.R + pGreen * TextBox16.Text

                For y1 = y + 1 To newimage.Height - 1 Step 1

                    If y1 >= 0 and y1 <= (newimage.Height – 1) Then
                        x1 = x - CInt((y1 - y) * Math.Tan((solazi) * Math.PI / 180))
                        If x1 = x Then
                            x1 = x + 1
                        End If
                        If x1 >= 0 and x1 <= (newimage.Width - 1) Then     'input angle value (90-solar azimuth angle)

                            Dim pixelcolor1 As Color = newimage.GetPixel(x1, y1)

                            If pixelcolor1.G > 200 Then
                                pGreen1 = (pixelcolor1.G - 200)
                            Else
                                pGreen1 = pixelcolor1.G
                            End If

                            allheight1 = pixelcolor1.R + pGreen1 * TextBox16.Text
                            elevation = (allheight1 - allheight) / Math.Sqrt(((x - x1) * TextBox10.Text) ^ 2 + ((y - y1) *_
TextBox10.Text) ^ 2)
                            eleangle = Math.Atan(elevation) * 180 / Math.PI
```

```
                        If pGreen > 0 And pGreen1 > 0 And pGreen = pGreen1 And (y1 - y) = 1 Then
                            eleangle = 90
                        End If
                        If eleangle >= betaorg Then
                            pixelColor = newimage.GetPixel(x, y)
                            If pGreen = 0 Then
                                Dim newColor As Color = Color.FromArgb(pixelColor.A, pixelColor.R, pixelColor.G, pGreen + 1)
'Shaded ground, building or tree pixel. Shaded ground has 1 value.
                                newimage.SetPixel(x, y, newColor)
                            Else
                                Dim newColor As Color = Color.FromArgb(pixelColor.A, pixelColor.R, pixelColor.G, pGreen)
'Shaded whole height of building or tree
                                newimage.SetPixel(x, y, newColor)
                            End If

                            Exit For
                        Else
                            pGreenh = pGreen
                            Do While eleangle < betaorg   'Comparing with solar elevation angle

                                pGreenh -= 1

                                If pGreenh = -1 Then
                                    pixelColor = newimage.GetPixel(x, y)
                                    Dim newColor1 As Color = Color.FromArgb(pixelColor.A, pixelColor.R, pixelColor.G, pGreenhh)
'Sunny ground, building or tree pixel.
                                    newimage.SetPixel(x, y, newColor1)
                                    eleangle = betaorg
                                Else
                                    allheight2 = pixelColor.R + pGreenh * TextBox16.Text
                                    elevation = (allheight1 - allheight2) / Math.Sqrt(((x - x1) * TextBox10.Text) ^ 2 + ((y - y1) *_
TextBox10.Text) ^ 2)
                                    eleangle = Math.Atan(elevation) * 180 / Math.PI
                                    pixelColor = newimage.GetPixel(x, y)
                                    If pGreenhh < pGreenh And eleangle > betaorg Then
                                        pGreenhh = pGreenh
                                    End If
                                    Dim newColor1 As Color = Color.FromArgb(pixelColor.A, pixelColor.R, pixelColor.G, pGreenhh)
'pGreen is the shaded height of building or tree.
                                    newimage.SetPixel(x, y, newColor1)
                                End If
                            Loop
                        End If
                    End If
                End If
            Next
            Dim pixel1 As Color = newimage.GetPixel(x, y)
            Dim Shadedata As String = x & ", " & y & " Azimuth: " & pixel1.A & " Ground height: " & pixel1.R & "
Obstruct height: " & pixel1.G & " Shade obstruct height: " & pixel1.B & vbCrLf
            My.Computer.FileSystem.WriteAllText("C:\Shadedata.txt", Shadedata, True)
        End If
    Next
Next
ElseIf solazi > 0 And solazi <= 26.565 Then
    For x = newimage.Width - 1 To 0 Step -1
        For y = 0 To newimage.Height - 1 Step 1
            pGreenhh = 0
            Dim pixelColor As Color = newimage.GetPixel(x, y)
            If pixelColor.G <> 255 Then
                If pixelColor.G > 200 Then
                    pGreen = (pixelColor.G - 200)    'tree height=pixelColor.G-200
                Else
                    pGreen = pixelColor.G
                End If

                allheight = pixelColor.R + pGreen * TextBox16.Text

                For y1 = y + 1 To newimage.Height - 1 Step 1

                    If y1 >= 0 and y1 <= (newimage.Height – 1) Then
```

```
                        x1 = x - CInt((y1 - y) * Math.Tan((solazi) * Math.PI / 180))
                        If x1 = x Then
                            x1 = x - 1
                        End If
                        If x1 >= 0 and x1 <= (newimage.Width - 1) Then     'input angle value (90-solar azimuth angle)

                            Dim pixelcolor1 As Color = newimage.GetPixel(x1, y1)

                            If pixelcolor1.G > 200 Then
                                pGreen1 = (pixelcolor1.G - 200)
                            Else
                                pGreen1 = pixelcolor1.G
                            End If

                            allheight1 = pixelcolor1.R + pGreen1 * TextBox16.Text
                            elevation = (allheight1 - allheight) / Math.Sqrt(((x - x1) * TextBox10.Text) ^ 2 + ((y - y1) *_
TextBox10.Text) ^ 2)
                            eleangle = Math.Atan(elevation) * 180 / Math.PI
                            If pGreen > 0 And pGreen1 > 0 And pGreen = pGreen1 And (y1 - y) = 1 Then
                                eleangle = 90
                            End If
                            If eleangle >= betaorg Then
                                pixelColor = newimage.GetPixel(x, y)
                                If pGreen = 0 Then
                                    Dim newColor As Color = Color.FromArgb(pixelColor.A, pixelColor.R, pixelColor.G, pGreen + 1)
'Shaded ground, building or tree pixel. Shaded ground has 1 value.
                                    newimage.SetPixel(x, y, newColor)
                                Else
                                    Dim newColor As Color = Color.FromArgb(pixelColor.A, pixelColor.R, pixelColor.G, pGreen)
'Shaded whole height of building or tree
                                    newimage.SetPixel(x, y, newColor)
                                End If

                                Exit For
                            Else
                                pGreenh = pGreen
                                Do While eleangle < betaorg   'Comparing with solar elevation angle

                                    pGreenh -= 1

                                    If pGreenh = -1 Then
                                        pixelColor = newimage.GetPixel(x, y)
                                        Dim newColor1 As Color = Color.FromArgb(pixelColor.A, pixelColor.R, pixelColor.G, pGreenhh)
'Sunny ground, building or tree pixel.
                                        newimage.SetPixel(x, y, newColor1)
                                        eleangle = betaorg
                                    Else
                                        allheight2 = pixelColor.R + pGreenh * TextBox16.Text
                                        elevation = (allheight1 - allheight2) / Math.Sqrt(((x - x1) * TextBox10.Text) ^ 2 + ((y - y1) *_
TextBox10.Text) ^ 2)
                                        eleangle = Math.Atan(elevation) * 180 / Math.PI
                                        pixelColor = newimage.GetPixel(x, y)
                                        If pGreenhh < pGreenh And eleangle > betaorg Then
                                            pGreenhh = pGreenh
                                        End If
                                        Dim newColor1 As Color = Color.FromArgb(pixelColor.A, pixelColor.R, pixelColor.G, pGreenhh)
'pGreen is the shaded height of building or tree.
                                        newimage.SetPixel(x, y, newColor1)
                                    End If
                                Loop
                            End If
                        End If
                    End If
                Next
                Dim pixel1 As Color = newimage.GetPixel(x, y)
                Dim Shadedata As String = x & ", " & y & " Azimuth: " & pixel1.A & " Ground height: " & pixel1.R & "
Obstruct height: " & pixel1.G & " Shade obstruct height: " & pixel1.B & vbCrLf
                My.Computer.FileSystem.WriteAllText("C:\Shadedata.txt", Shadedata, True)
            End If
        Next
```

```
            Next

        End If
    Else
        MsgBox("It's not the daytime.")
    End If

Catch ex As ArgumentException
    MessageBox.Show("There was an error." & "Check the path to the image file or whether the image sizes are same.")
End Try
```

View factor and Radiation analyses

'Combining 4 datafiles

```
Try
    If Microsoft.VisualBasic.Right(TextBox8.Text, 3) = "bmp" And Microsoft.VisualBasic.Right(TextBox9.Text, 3) = "bmp" And
Microsoft.VisualBasic.Right(TextBox12.Text, 3) = "bmp" And Microsoft.VisualBasic.Right(TextBox13.Text, 3) = "bmp" Then

        ' Retrieve the image.
        Dim gheight, obstruct, gtype, azimuthB As Bitmap

        gheight = New Bitmap(TextBox9.Text, True)   'ground height
        obstruct = New Bitmap(TextBox8.Text, True)  'obstruct height: 0 ground, 1~200 building and 201~255 tree
        gtype = New Bitmap(TextBox12.Text, True)    'ground type: 0-ground & building, 2-tree
        azimuthB = New Bitmap(TextBox13.Text, True) 'building azimuth angle
        Label15.Text = "Pixel # ( x:" & gheight.Width & ", y:" & gheight.Height & ")"
        Label14.Text = "Pixel # ( x:" & obstruct.Width & ", y:" & obstruct.Height & ")"
        Label18.Text = "Pixel # ( x:" & gtype.Width & ", y:" & gtype.Height & ")"
        Label19.Text = "Pixel # ( x:" & azimuthB.Width & ", y:" & azimuthB.Height & ")"
        Dim o, p As Integer

        ' Loop through the images pixels to reset color.
        For o = 0 To gheight.Width - 1
            For p = 0 To gheight.Height - 1
                Dim pixelColor1 As Color = gheight.GetPixel(o, p)
                Dim pixelcolor2 As Color = obstruct.GetPixel(o, p)
                Dim pixelcolor3 As Color = gtype.GetPixel(o, p)
                Dim pixelcolor4 As Color = azimuthB.GetPixel(o, p)
                Dim nColor As Color = Color.FromArgb(pixelcolor4.A, pixelColor1.R, pixelcolor2.G + pixelcolor3.B * 100, 0)
'Pixelcolor.G: 0 ground, 1~200 building height, 201~255 tree height

                gheight.SetPixel(o, p, nColor)
            Next
        Next

        Dim newimage4 As Bitmap

        newimage4 = gheight
        ' Set the PictureBox to display the image.
        PictureBox1.Image = newimage4
        MsgBox("Combining the image file data is done.")
    End If

    If Microsoft.VisualBasic.Right(TextBox8.Text, 3) = "txt" And Microsoft.VisualBasic.Right(TextBox9.Text, 3) = "txt" And
Microsoft.VisualBasic.Right(TextBox12.Text, 3) = "txt" And Microsoft.VisualBasic.Right(TextBox13.Text, 3) = "txt" Then
        Dim o, p, width As Integer
        o = 0
        width = TextBox11.Text

        Dim Text1 As String() = IO.File.ReadAllLines(TextBox9.Text)
        Dim Text2 As String() = IO.File.ReadAllLines(TextBox8.Text)
        Dim Text3 As String() = IO.File.ReadAllLines(TextBox12.Text)
        Dim text4 As String() = IO.File.ReadAllLines(TextBox13.Text)
        Dim lines1 As String() = Text1
        Dim lines2 As String() = Text2
        Dim lines3 As String() = Text3
```

```
        Dim lines4 As String() = text4

        Dim newimage4 As Bitmap = New Bitmap(TextBox11.Text, Int(lines1.Length),
System.Drawing.Imaging.PixelFormat.Format32bppArgb)
        Dim Counter As Integer = 0
        For Each S1 As String In lines1
            Dim A As Integer
            For A = 1 To (TextBox11.Text * 2) Step 2
                ' Get one character.
                Dim ss1 As String = Microsoft.VisualBasic.Mid(S1, A, 2)
                Dim i1 As Integer = CInt(Val(ss1))
                o = Counter Mod width
                p = CInt(Int(Counter / width))
                Counter += 1
                Dim pixelcolor As Color = Color.FromArgb(0, i1, 0, 0)
                newimage4.SetPixel(o, p, pixelcolor)
            Next
        Next
        Dim pixelcolor1 As Color = newimage4.GetPixel(o, p)
        Counter = 0
        For Each S2 As String In lines2
            Dim A As Integer
            For A = 1 To (TextBox11.Text * 2) Step 2
                'Get one character.
                Dim ss2 As String = Microsoft.VisualBasic.Mid(S2, A, 2)
                Dim i2 As Integer = CInt(Val(ss2))
                o = Counter Mod width
                p = CInt(Int(Counter / width))
                Counter += 1
                pixelcolor1 = newimage4.GetPixel(o, p)
                Dim pixelcolor As Color = Color.FromArgb(0, pixelcolor1.R, i2, 0)
                newimage4.SetPixel(o, p, pixelcolor)
            Next
        Next
        Dim pixelcolor2 As Color = newimage4.GetPixel(o, p)
        Counter = 0
        For Each S3 As String In lines3
            Dim A As Integer
            For A = 1 To (TextBox11.Text * 2) Step 2
                'Get one character.
                Dim ss3 As String = Microsoft.VisualBasic.Mid(S3, A, 2)
                Dim i3 As Integer = CInt(Val(ss3))
                o = Counter Mod width
                p = CInt(Int(Counter / width))
                Counter += 1
                pixelcolor2 = newimage4.GetPixel(o, p)
                Dim pixelcolor As Color = Color.FromArgb(0, pixelcolor2.R, pixelcolor2.G + i3 * 100, 0)
                newimage4.SetPixel(o, p, pixelcolor)
            Next
        Next
        Dim pixelcolor3 As Color = newimage4.GetPixel(o, p)
        Counter = 0
        For Each S4 As String In lines4
            Dim A As Integer
            For A = 1 To (TextBox11.Text * 2) Step 2
                ' Get one character.
                Dim ss4 As String = Microsoft.VisualBasic.Mid(S4, A, 2)
                Dim i4 As Integer = CInt(Val(ss4))          'building azimuth angle is between 0 (north) and 18 (south) through 9 (east).
                o = Counter Mod width
                p = CInt(Int(Counter / width))
                Counter += 1

                pixelcolor3 = newimage4.GetPixel(o, p)
                Dim pixelcolor As Color = Color.FromArgb(i4, pixelcolor3.R, pixelcolor3.G, 0)
                newimage4.SetPixel(o, p, pixelcolor)

                Dim Combinedata As String = o & ", " & p & " Azimuth: " & pixelcolor.A & " Ground height: " & pixelcolor.R & "
Obstruct height: " & pixelcolor.G & vbCrLf
                My.Computer.FileSystem.WriteAllText("C:\Combinedata.txt", Combinedata, True)
            Next
```

```
            Next
            Me.PictureBox1.Image = newimage4
            Label15.Text = "Pixel # ( x:" & newimage4.Width & ", y:" & newimage4.Height & ")"
            Label14.Text = "Pixel # ( x:" & newimage4.Width & ", y:" & newimage4.Height & ")"
            Label18.Text = "Pixel # ( x:" & newimage4.Width & ", y:" & newimage4.Height & ")"
            Label19.Text = "Pixel # ( x:" & newimage4.Width & ", y:" & newimage4.Height & ")"
        End If
    Catch ex As ArgumentException
        MessageBox.Show("There was an error." & "Check the path to the image file or whether the image sizes are same.")
    End Try
```

' Sky view factor analysis and calculating each surface temperature and solar radiation reflected by building, tree and ground surface

```
    'pixelcolor.a: building azimuth angle(0~180 deg.), pixelcolor.r: ground height, pixelcolor.g: obstruct's height, pixelcolor.b: shaded building and tree's height
    Dim newimage1 As Bitmap = newimage
    Dim newimagesvf As Bitmap = New Bitmap(TextBox11.Text, newimage.Height,
System.Drawing.Imaging.PixelFormat.Format32bppArgb)

    Dim Shadeposition1, Shadeposition2, Newposition, Newposition1, Newposition2, Newpositionsh, Viewangle, shadeangle, elevationsh, Neweleangle, eleangle1, eleanglesh, shaderatio, groundsunny, groundshade, obstructsunny, obstructshade, Treeshade, Treesunny As Double
    Dim N, M, dist, annuli As Integer

    Try
        ' Loop through the images pixels to find sky view factors, reflected solar radiation, surface temperature.
        Dim SVF As Double
        For x = 0 To newimage1.Width - 1
            For y = 0 To newimage1.Height - 1
                Dim pixelcolor As Color = newimage1.GetPixel(x, y)
                SVF = 0
                If pixelcolor.G > 200 Then
                    pGreen = pixelcolor.G - 200
                Else
                    pGreen = pixelcolor.G
                End If
                allheight = pixelcolor.R + pGreen / 2 * TextBox16.Text
                For Viewangle = 2.5 To 357.5 Step 5
                    eleangle = 0
                    shadeangle = 0
                    For dist = 1 To 300 / TextBox10.Text Step 1   'maximum distance to analyze view factors is assumed 300 meters.
                        x1 = x + CInt(dist * Math.Cos(Viewangle * Math.PI / 180))
                        y1 = y + CInt(dist * Math.Sin(Viewangle * Math.PI / 180))

                        If 0 <= x1 And x1 <= (newimage1.Width - 1) Then
                            If 0 <= y1 And y1 <= (newimage1.Height - 1) Then

                                'View factor analysis
                                Dim pixelcolor1 As Color = newimage1.GetPixel(x1, y1)

                                If pixelcolor1.G > 200 Then
                                    pGreen1 = pixelcolor1.G - 200
                                Else
                                    pGreen1 = pixelcolor1.G
                                End If
                                eleangle1 = eleangle
                                allheight1 = pixelcolor1.R + pGreen1 * TextBox16.Text
                                elevation = (allheight1 - allheight) / Math.Sqrt(((x - x1) * TextBox10.Text - TextBox10.Text / 2) ^ 2 + _
((y - y1) * TextBox10.Text - TextBox10.Text / 2) ^ 2)
                                eleangle = Math.Atan(elevation) * 180 / Math.PI
                                If eleangle > 0 Then
                                    eleangle = eleangle + 90
                                End If
                                If pGreen > 0 And pGreen1 > 0 And pGreen = pGreen1 Then
                                    eleangle = 180
                                End If
                                If eleangle = 0 Or eleangle < 0 Then
```

```
                        eleangle = 90
                    End If
                    If eleangle > eleangle1 Then
                        Neweleangle = Math.Abs(eleangle - eleangle1)
                        shadeangle = shadeangle + Neweleangle
                    End If
                    If eleangle < eleangle1 Then
                        eleangle = eleangle1
                    End If
                End If
            End If
        Next
        If eleangle = 0 Then
            shadeangle = 90
        End If
        Newposition = CInt((2 * (300 / TextBox10.Text) * (180 - shadeangle)) / 180)
        For annuli = 1 To Newposition Step 1
            SVF = SVF + (1 / 360) * Math.Sin((180 / (2 * (300 / TextBox10.Text))) * Math.PI / 180) * Math.Sin(((180 * (2 *_
annuli - 1)) / (2 * (300 / TextBox10.Text))) * Math.PI / 180) * 5
        Next
    Next

    If SVF > 1 Then
        SVF = 1
    ElseIf SVF < 0 Then
        SVF = 0
    End If
    Dim Kbsl, Kdsl, Krsl, Krslsh, Ts, solazisl As Double
    solazisl = Math.Abs(solazi - TextBox15.Text + 180 - pixelcolor.A * 10)
    If solazisl >= 90 Then
        solazisl = 90
    End If
    If SVF > 0 Then
        If pixelcolor.G > 0 And pixelcolor.G < 201 Then
            Kbsl = Kb * Math.Cos(betaorg * Math.PI / 180) * Math.Cos(solazisl * Math.PI / 180)  'Direct beam solar radiation
received on the vertical building surface
            Kdsl = Kd * SVF
            Ts = Math.Sqrt(Math.Sqrt((273.15 + Ta) ^ 4 + (0.08 * (Kbsl + Kdsl) * 0.7) / (TextBox23.Text * 5.67 * 10 ^ -8))) +_
(0.00009042 * CMT ^ 2 - 0.14 * CMT + 54.78) - 273.15
            Krsl = (Kbsl + Kdsl) * TextBox17.Text
            Krslsh = Kdsl * t * TextBox20.Text
        ElseIf pixelcolor.G > 200 Then
            Kbsl = Kb * (Math.Sin(betaorg * Math.PI / 180) + Math.Cos(betaorg * Math.PI / 180) * Math.Cos(solazisl *_
Math.PI / 180)) / 2   'Direct beam solar radiation received on 1/2(the vertical building surface + the horizontal ground surface)
            Kdsl = Kd * SVF
            Ts = Math.Sqrt(Math.Sqrt((273.15 + Ta) ^ 4 + (0.08 * (Kbsl + Kdsl) * 0.78) / (TextBox24.Text * 5.67 * 10 ^ -8))) _
+ (-0.0003785 * CMT ^ 2 + 0.5764 * CMT - 211.3) - 273.15
            Krsl = (Kbsl + Kdsl) * TextBox18.Text
            Krslsh = Kdsl * t * TextBox21.Text
        Else
            If pixelcolor.B = 0 Then
                Kbsl = Kb * Math.Sin(betaorg * Math.PI / 180)
                Kdsl = Kd * SVF
            Else
                Kbsl = 0
                Kdsl = Kd * SVF
            End If
            Ts = Math.Sqrt(Math.Sqrt((273.15 + Ta) ^ 4 + (0.08 * (Kbsl + Kdsl) * 0.89) / (TextBox25.Text * 5.67 * 10 ^ -8))) _
+ (-0.000241 * CMT ^ 2 + 0.3895 * CMT - 143.2) - 273.15
            Krsl = (Kbsl + Kdsl) * TextBox19.Text
            Krslsh = Kdsl * t * TextBox22.Text
        End If
    Else
        Kbsl = 0
        Kdsl = 0
        Krsl = 0
        Krslsh = 0
        Ts = Ta
    End If
```

```
            Dim SkyViewFactor As String = x & ", " & y & " Sun elevation: " & betaorg.tostring("f1") & " Sun azimuth: " &
solazi.tostring("f1") & " Kr: " & Krsl.ToString("F1") & " Krsh: " & Krslsh.ToString("F1") & " Kb: " & Kbsl.ToString("F1") & " Kd: "
& Kdsl.ToString("F1") & " Ts: " & Ts.ToString("F1") & " SVF: " & SVF.ToString("F3") & vbCrLf
            My.Computer.FileSystem.WriteAllText("C:\Skyviewfactor.txt", SkyViewFactor, True)
            If Krsl > 255 Then
              Krsl = Krsl / 10 + 200
              Krslsh = Krslsh + 200
            End If
            'exporting sky view factors (SVF)
            Dim newColorsvf As Color = Color.FromArgb(CInt(Krslsh), CInt(Krsl), CInt(Ts), CInt(SVF * 100))
            newimagesvf.SetPixel(x, y, newColorsvf)
          Next
        Next
        PictureBox1.Image = newimagesvf
      Catch ex As ArgumentException
        MessageBox.Show("There was an error in first view analysis.")
      End Try

      Try
        ' Call the Process.Start method to open the default browser
        ' with a URL:
        Dim SaveFileDialog1 As New SaveFileDialog()
        SaveFileDialog1.Filter = "Bitmap Image|*.bmp"
        SaveFileDialog1.Title = "Save a Sky View Factor Image File"
        SaveFileDialog1.ShowDialog()
        ' If the file name is not an empty string open it for saving.
        If SaveFileDialog1.FileName <> "" Then
          ' Saves the Image via a FileStream created by the OpenFile method.
          Dim fs As System.IO.FileStream = CType _
            (SaveFileDialog1.OpenFile(), System.IO.FileStream)
          ' Saves the Image in the appropriate ImageFormat based upon the
          ' file type selected in the dialog box.
          ' NOTE that the FilterIndex property is one-based.
          Select Case SaveFileDialog1.FilterIndex
            Case 1
              Me.PictureBox1.Image.Save(fs, _
                System.Drawing.Imaging.ImageFormat.Bmp)
          End Select
          fs.Close()
        End If
      Catch ex As Exception
        ' The error message
        MessageBox.Show("Unable to save the file.")
      End Try


' Building view factor analysis (sky view factor without trees)

      Dim newimage2 As Bitmap = newimage
      Dim buildingviewfactor As Bitmap = New Bitmap(TextBox11.Text, newimage.Height,
System.Drawing.Imaging.PixelFormat.Format32bppArgb)
      Try

        Dim annuliup, Uppergposition1, Uppergposition2, groundshadeup1, groundsunnyup1, SVF, oriangle, groundshade1,
groundsunny1, obstructshade1, obstructsunny1, pGreen2, distance, distance1, shaderatiog, obstructshadeg1, Obstructsunnyg1 As
Double
        oriangle = Math.Atan((TextBox10.Text / 2) / 1.2) * 180 / Math.PI
        ' Loop through the images pixels to find building view factors excluding tree property.
        Neweleangle = 0
        eleangle = -90 + oriangle

        For x = 0 To newimage2.Width - 1
          For y = 0 To newimage2.Height - 1
            Dim pixelcolor As Color = newimage2.GetPixel(x, y)
            groundsunny1 = 0
            groundsunnyup1 = 0
            groundshadeup1 = 0
            groundshade1 = 0
            obstructshade1 = 0
            obstructsunny1 = 0
```

```
            obstructshadeg1 = 0
            Obstructsunnyg1 = 0
            SVF = 0
            If pixelcolor.G = 0 Then
               For Viewangle = 2.5 To 357.5 Step 5
                  N = 0
                  pGreen2 = 1.2
                  allheight = pixelcolor.R + pGreen2
                  eleangle = -90 + oriangle
                  Newposition = CInt((2 * (300 / TextBox10.Text) * oriangle) / 180)
                  If pixelcolor.B = 0 Then
                     For annuli = 1 To Newposition Step 1
                        groundsunny1 = groundsunny1 + (1 / 360) * Math.Sin((180 / (2 * (300 / TextBox10.Text))) * Math.PI / 180) *_
Math.Sin(((180 * (2 * annuli - 1)) / (2 * (300 / TextBox10.Text))) * Math.PI / 180) * 5
                     Next
                  ElseIf pixelcolor.B = 1 Then
                     For annuli = 1 To Newposition Step 1
                        groundshade1 = groundshade1 + (1 / 360) * Math.Sin((180 / (2 * (300 / TextBox10.Text))) * Math.PI / 180) *_
Math.Sin(((180 * (2 * annuli - 1)) / (2 * (300 / TextBox10.Text))) * Math.PI / 180) * 5
                     Next
                  End If
                  For dist = 1 To 300 / TextBox10.Text Step 1    'maximum distance to analyze view factors is assumed 300 meters.
                     x1 = x + CInt(dist * Math.Cos(Viewangle * Math.PI / 180))
                     y1 = y + CInt(dist * Math.Sin(Viewangle * Math.PI / 180))
                     If 0 <= x1 And x1 <= (newimage2.Width - 1) And 0 <= y1 And y1 <= (newimage2.Height - 1) Then
                        distance = Math.Sqrt(((x - x1) * TextBox10.Text + TextBox10.Text / 2) ^ 2 + ((y - y1) * TextBox10.Text +_
TextBox10.Text / 2) ^ 2)
                        distance1 = Math.Sqrt(((x - x1) * TextBox10.Text - TextBox10.Text / 2) ^ 2 + ((y - y1) * TextBox10.Text -_
TextBox10.Text / 2) ^ 2)
                        'View factor analysis
                        Dim pixelcolor1 As Color = newimage2.GetPixel(x1, y1)
                        If pixelcolor1.G = 0 Or pixelcolor1.G > 200 Then          'View factor analysis for the ground surface
                           eleangle1 = eleangle
                           allheight1 = pixelcolor1.R
                           elevation = (allheight1 - allheight) / distance
                           eleangle = Math.Atan(elevation) * 180 / Math.PI
                           If eleangle > eleangle1 Then
                              If eleangle1 <= 0 Then
                                 Newposition1 = CInt((2 * (300 / TextBox10.Text) * (90 + eleangle1)) / 180)
                              ElseIf eleangle1 > 0 Then
                                 Newposition1 = CInt((2 * (300 / TextBox10.Text) * (90 - eleangle1)) / 180)
                              End If
                              If eleangle <= 0 Then
                                 Newposition2 = CInt((2 * (300 / TextBox10.Text) * (90 + eleangle)) / 180)
                              ElseIf eleangle > 0 Then
                                 Newposition2 = CInt((2 * (300 / TextBox10.Text) * (90 - eleangle)) / 180)
                              End If
                              If eleangle1 >= 0 Then
                                 Uppergposition1 = Newposition1
                                 Newposition1 = (300 / TextBox10.Text)
                              End If
                              If eleangle >= 0 Then
                                 Uppergposition2 = Newposition2
                                 Newposition2 = (300 / TextBox10.Text)
                              End If
                              If Newposition1 = (300 / TextBox10.Text) Then
                                 Newposition1 = (300 / TextBox10.Text) - 1
                              End If
                              If Uppergposition1 > (300 / TextBox10.Text) Then
                                 Uppergposition1 = (300 / TextBox10.Text)
                              End If
                              If Uppergposition2 > (300 / TextBox10.Text) Then
                                 Uppergposition2 = (300 / TextBox10.Text)
                              End If
                              If pixelcolor1.B = 0 Then
                                 For annuli = Newposition1 + 1 To Newposition2 Step 1
                                    groundsunny1 = groundsunny1 + (1 / 360) * Math.Sin((180 / (2 * (300 / TextBox10.Text))) * _
Math.PI / 180) * Math.Sin(((180 * (2 * annuli - 1)) / (2 * (300 / TextBox10.Text))) * Math.PI / 180) * 5
                                 Next
                                 If eleangle1 <= 0 And eleangle > 0 Then
```

```
                    Uppergposition1 = (300 / TextBox10.Text)
                End If
                For annuliup = Uppergposition2 To Uppergposition1 Step 1
                    groundsunnyup1 = groundsunnyup1 + (1 / 360) * Math.Sin((180 / (2 * (300 / TextBox10.Text))) *_
Math.PI / 180) * Math.Sin(((180 * (2 * annuliup - 1)) / (2 * (300 / TextBox10.Text))) * Math.PI / 180) * 5
                Next
            Else
                For annuli = Newposition1 + 1 To Newposition2 Step 1
                    groundshade1 = groundshade1 + (1 / 360) * Math.Sin((180 / (2 * (300 / TextBox10.Text))) * _
Math.PI / 180) * Math.Sin(((180 * (2 * annuli - 1)) / (2 * (300 / TextBox10.Text))) * Math.PI / 180) * 5
                Next
                If eleangle1 <= 0 And eleangle > 0 Then
                    Uppergposition1 = (300 / TextBox10.Text)
                End If
                For annuliup = Uppergposition2 To Uppergposition1 Step 1
                    groundshadeup1 = groundshadeup1 + (1 / 360) * Math.Sin((180 / (2 * (300 / TextBox10.Text))) *_
Math.PI / 180) * Math.Sin(((180 * (2 * annuliup - 1)) / (2 * (300 / TextBox10.Text))) * Math.PI / 180) * 5
                Next
            End If
        End If
    End If

    If N = 0 Then
        If 0 < pixelcolor1.G And pixelcolor1.G <= 200 Then        'View factor analysis for building
            N = N + 1
            eleangle1 = eleangle
            pGreen1 = pixelcolor1.G
            allheight1 = pixelcolor1.R + pGreen1 * TextBox16.Text
            If pixelcolor1.B = 0 Then
                shaderatio = 0
                shaderatiog = 0
            ElseIf pixelcolor1.B > 0 Then
                If pixelcolor1.B > 1.2 Then
                    shaderatio = (pixelcolor1.B - 1.2) / (pGreen1 - 1.2)
                    shaderatiog = 1
                Else
                    shaderatio = 0
                    shaderatiog = pixelcolor1.B / 1.2
                End If
            End If
            elevation = (allheight1 - allheight) / distance1
            eleangle = Math.Atan(elevation) * 180 / Math.PI
            If eleangle > eleangle1 Then
                Newposition1 = CInt((2 * (300 / TextBox10.Text) * (90 + eleangle1)) / 180)
                Newposition2 = CInt((2 * (300 / TextBox10.Text) * (90 - eleangle)) / 180)
                Shadeposition1 = CInt(((300 / TextBox10.Text) - Newposition1) * shaderatiog)
                Shadeposition2 = CInt(((300 / TextBox10.Text) - Newposition2) * shaderatio)
                If shaderatio = 0 Then
                    For annuli = Newposition2 To (300 / TextBox10.Text) - Shadeposition2 - 1 Step 1
                        obstructsunny1 = obstructsunny1 + (1 / 360) * Math.Sin((180 / (2 * (300 / TextBox10.Text))) *
Math.PI / 180) * Math.Sin(((180 * (2 * annuli - 1)) / (2 * (300 / TextBox10.Text))) * Math.PI / 180) * 5
                    Next
                ElseIf shaderatio = 1 Then
                    For annuli = (300 / TextBox10.Text) - Shadeposition2 To (300 / TextBox10.Text) Step 1
                        obstructshade1 = obstructshade1 + (1 / 360) * Math.Sin((180 / (2 * (300 / TextBox10.Text))) *
Math.PI / 180) * Math.Sin(((180 * (2 * annuli - 1)) / (2 * (300 / TextBox10.Text))) * Math.PI / 180) * 5
                    Next
                Else
                    For annuli = Newposition2 To (300 / TextBox10.Text) - Shadeposition2 - 1 Step 1
                        obstructsunny1 = obstructsunny1 + (1 / 360) * Math.Sin((180 / (2 * (300 / TextBox10.Text))) *
Math.PI / 180) * Math.Sin(((180 * (2 * annuli - 1)) / (2 * (300 / TextBox10.Text))) * Math.PI / 180) * 5
                    Next
                    For annuli = (300 / TextBox10.Text) - Shadeposition2 To (300 / TextBox10.Text) Step 1
                        obstructshade1 = obstructshade1 + (1 / 360) * Math.Sin((180 / (2 * (300 / TextBox10.Text))) *
Math.PI / 180) * Math.Sin(((180 * (2 * annuli - 1)) / (2 * (300 / TextBox10.Text))) * Math.PI / 180) * 5
                    Next
                End If
                If shaderatiog = 0 Then
                    For annuli = Newposition1 To (300 / TextBox10.Text) - Shadeposition1 - 1 Step 1
```

```
                                    Obstructsunnyg1 = Obstructsunnyg1 + (1 / 360) * Math.Sin((180 / (2 * (300 / TextBox10.Text)))_
* Math.PI / 180) * Math.Sin(((180 * (2 * annuli - 1)) / (2 * (300 / TextBox10.Text))) * Math.PI / 180) * 5
                                Next
                            ElseIf shaderatiog = 1 Then
                                For annuli = (300 / TextBox10.Text) - Shadeposition1 To (300 / TextBox10.Text) Step 1
                                    obstructshadeg1 = obstructshadeg1 + (1 / 360) * Math.Sin((180 / (2 * (300 / TextBox10.Text))) *_
Math.PI / 180) * Math.Sin(((180 * (2 * annuli - 1)) / (2 * (300 / TextBox10.Text))) * Math.PI / 180) * 5
                                Next
                            Else
                                For annuli = Newposition1 To (300 / TextBox10.Text) - Shadeposition1 - 1 Step 1
                                    Obstructsunnyg1 = Obstructsunnyg1 + (1 / 360) * Math.Sin((180 / (2 * (300 / TextBox10.Text)))_
* Math.PI / 180) * Math.Sin(((180 * (2 * annuli - 1)) / (2 * (300 / TextBox10.Text))) * Math.PI / 180) * 5
                                Next
                                For annuli = (300 / TextBox10.Text) - Shadeposition1 To (300 / TextBox10.Text) Step 1
                                    obstructshadeg1 = obstructshadeg1 + (1 / 360) * Math.Sin((180 / (2 * (300 / TextBox10.Text))) *_
Math.PI / 180) * Math.Sin(((180 * (2 * annuli - 1)) / (2 * (300 / TextBox10.Text))) * Math.PI / 180) * 5
                                Next
                            End If
                        End If
                    End If
                End If

                If N > 0 Then
                    If 0 < pixelcolor1.G And pixelcolor1.G <= 200 Then
                        N = N + 1
                        eleangle1 = eleangle
                        pGreen1 = pixelcolor1.G
                        allheight1 = pixelcolor1.R + pGreen1 * TextBox16.Text
                        shaderatio = pixelcolor1.B / pGreen1
                        elevation = (allheight1 - allheight) / distance1
                        eleangle = Math.Atan(elevation) * 180 / Math.PI
                        Newposition1 = CInt((2 * (300 / TextBox10.Text) * (90 - eleangle1)) / 180)
                        Newposition2 = CInt((2 * (300 / TextBox10.Text) * (90 - eleangle)) / 180)
                        elevationsh = ((allheight1 - allheight) * shaderatio) / distance1
                        eleanglesh = Math.Atan(elevationsh) * 180 / Math.PI
                        Newpositionsh = CInt((2 * (300 / TextBox10.Text) * (90 - eleanglesh)) / 180)
                        If eleangle > eleangle1 Then
                            If eleanglesh > eleangle1 Then
                                For annuli = Newpositionsh To Newposition1 - 1
                                    obstructshade1 = obstructshade1 + (1 / 360) * Math.Sin((180 / (2 * (300 / TextBox10.Text))) *_
Math.PI / 180) * Math.Sin(((180 * (2 * annuli - 1)) / (2 * (300 / TextBox10.Text))) * Math.PI / 180) * 5
                                Next
                                For annuli = Newposition2 To Newpositionsh - 1
                                    obstructsunny1 = obstructsunny1 + (1 / 360) * Math.Sin((180 / (2 * (300 / TextBox10.Text))) *_
Math.PI / 180) * Math.Sin(((180 * (2 * annuli - 1)) / (2 * (300 / TextBox10.Text))) * Math.PI / 180) * 5
                                Next
                            Else
                                For annuli = Newposition2 To Newposition1 - 1
                                    obstructsunny1 = obstructsunny1 + (1 / 360) * Math.Sin((180 / (2 * (300 / TextBox10.Text))) *_
Math.PI / 180) * Math.Sin(((180 * (2 * annuli - 1)) / (2 * (300 / TextBox10.Text))) * Math.PI / 180) * 5
                                Next
                            End If
                        End If
                    End If
                End If
                If eleangle < eleangle1 Then
                    eleangle = eleangle1
                End If
            Next
            If eleangle > eleangle1 Then
                eleangle1 = eleangle
            End If
            If eleangle1 = -90 + oriangle Then
                Newposition1 = CInt((2 * (300 / TextBox10.Text) * oriangle) / 180)
                For annuli = Newposition1 + 1 To (300 / TextBox10.Text) Step 1
                    groundshade1 = groundshade1 + (1 / 360) * Math.Sin((180 / (2 * (300 / TextBox10.Text))) * Math.PI / 180) *_
Math.Sin(((180 * (2 * annuli - 1)) / (2 * (300 / TextBox10.Text))) * Math.PI / 180) * 5
                Next
            End If
```

```
                    If eleangle1 > -90 + oriangle And eleangle1 < 0 Then
                        Newposition1 = CInt((2 * (300 / TextBox10.Text) * (90 + eleangle1)) / 180)
                        For annuli = Newposition1 + 1 To (300 / TextBox10.Text) Step 1
                            groundshade1 = groundshade1 + (1 / 360) * Math.Sin((180 / (2 * (300 / TextBox10.Text))) * Math.PI / 180) *_
Math.Sin(((180 * (2 * annuli - 1)) / (2 * (300 / TextBox10.Text))) * Math.PI / 180) * 5
                        Next
                    End If
                Next
            End If

            SVF = 1 - (groundsunnyup1 + groundshadeup1 + groundsunny1 + groundshade1 + obstructshade1 + obstructsunny1 +_
obstructshadeg1 + Obstructsunnyg1 - 1)
            If SVF > 1 Then
                SVF = 1
            ElseIf SVF < 0 Then
                SVF = 0
            End If
            Dim obstructviewfactor As String = x & ", " & y & " SVF: " & SVF.ToString("f3") & " Groundsunny: " &
groundsunny1.ToString("f3") & " Groundshade: " & groundshade1.ToString("f3") & " Obstructsunny: " &
obstructsunny1.ToString("f3") & " Obstructshade: " & obstructshade1.ToString("f3") & vbCrLf
            My.Computer.FileSystem.WriteAllText("C:\Obstructviewfactor.txt", obstructviewfactor, True)
            Dim newColor4 As Color = Color.FromArgb(CInt((groundsunny1 + groundshade1) * 100), CInt((obstructsunny1 +
obstructshade1) * 100), CInt(SVF * 100))    'Sky view factors of each ground pixel without tree view factors
            buildingviewfactor.SetPixel(x, y, newColor4)
        Next
    Next
    ' Set the PictureBox to display the image
    'PictureBox1.Image = buildingviewfactor
Catch ex As ArgumentException
    MessageBox.Show("There was an error in second view analysis.")
End Try

Try
    ' Call the Process.Start method to open the default browser
    ' with a URL:
    Dim SaveFileDialog1 As New SaveFileDialog()
    SaveFileDialog1.Filter = "Bitmap Image|*.bmp"
    SaveFileDialog1.Title = "Save a Building View Factor Image File"
    SaveFileDialog1.ShowDialog()
    ' If the file name is not an empty string open it for saving.
    If SaveFileDialog1.FileName <> "" Then
        ' Saves the Image via a FileStream created by the OpenFile method.
        Dim fs As System.IO.FileStream = CType _
          (SaveFileDialog1.OpenFile(), System.IO.FileStream)
        ' Saves the Image in the appropriate ImageFormat based upon the
        ' file type selected in the dialog box.
        ' NOTE that the FilterIndex property is one-based.
        Select Case SaveFileDialog1.FilterIndex
            Case 1
                Me.PictureBox1.Image.Save(fs, _
                  System.Drawing.Imaging.ImageFormat.Bmp)
        End Select
        fs.Close()
    End If
Catch ex As Exception
    ' The error message
    MessageBox.Show("Unable to save the file.")
End Try


' View factor and Radiation analyses

    ' View factor analysis
    Dim newimage3 As Bitmap = newimage
    Dim urbantemp As Bitmap = New Bitmap(TextBox11.Text, newimage.Height, System.Drawing.Imaging.PixelFormat._
Format32bppArgb)
    Dim urbanradi As Bitmap = New Bitmap(TextBox11.Text, newimage.Height, System.Drawing.Imaging.PixelFormat._
Format32bppArgb)
    Dim Urbanmap As Bitmap = New Bitmap(TextBox11.Text, newimage.Height, System.Drawing.Imaging.PixelFormat._
Format32bppArgb)
```

```
    Dim Humanradimap As Bitmap = New Bitmap(TextBox11.Text, newimage.Height, System.Drawing.Imaging.PixelFormat._
Format32bppArgb)
    Dim MRTmap As Bitmap = New Bitmap(TextBox11.Text, newimage.Height, System.Drawing.Imaging.PixelFormat._
Format32bppArgb)
    Try
      Dim Tgsunnyup, Krgshadeup, Krgsunnyup, groundshadeup, groundsunnyup, Uppergposition1, Uppergposition2, annuliup,
Newgsunnyup, Newgshadeup, Newtshade, Newtsunny, Newgsunny, Newgshade, Newbshade, Newbsunny, Neweleangle1,
Neweleangle2, Neweleangle3, Neweleangle4, Neweleangle5, Neweleangle6, Neweleangle7, Neweleangle8 As Double
      Dim Krbsunnyg, Krbshadeg, shaderatiog, Treeshadeg, Treesunnyg, Obstructshadeg, Obstructsunnyg, Tvegsunnyg, Tbsunnyg,
Krvegsunnyg, Krvegshadeg, SVF1, oriangle, distance, distance1, Tgsunny, Krgsunny, Tvegsunny, Krvegsunny, Tbsunny, Krbsunny,
Krgshade, Krbshade, Krvegshade As Double
      Dim Krsl, Krslsh As Integer
      Neweleangle = 0 : eleangle = 0
      oriangle = Math.Atan((TextBox10.Text / 2) / 1.2) * 180 / Math.PI
      eleangle = -90 + oriangle

      ' Loop through the images pixels to find view factors.
      For x = 0 To newimage3.Width - 1
        For y = 0 To newimage3.Height - 1
          Tgsunnyup = 0
          Krgshadeup = 0
          Krgsunnyup = 0
          groundshadeup = 0
          groundsunnyup = 0
          groundsunny = 0
          groundshade = 0
          Treesunny = 0
          Treeshade = 0
          Treesunnyg = 0
          Treeshadeg = 0
          obstructsunny = 0
          obstructshade = 0
          Obstructsunnyg = 0
          Obstructshadeg = 0
          Krgsunny = 0
          Krgshade = 0
          Krvegsunny = 0
          Krvegshade = 0
          Krbsunny = 0
          Krbshade = 0
          Krvegsunnyg = 0
          Krvegshadeg = 0
          Krbsunnyg = 0
          Krbshadeg = 0
          Tgsunny = 0
          Tvegsunny = 0
          Tbsunny = 0
          Tvegsunnyg = 0
          Tbsunnyg = 0
          Newposition1 = 0
          Newposition2 = 0
          Uppergposition1 = 0
          Uppergposition2 = 0

          Dim pixelcolor As Color = newimage3.GetPixel(x, y)
          Dim oripixelcolor1 As Color = newimagesvf.GetPixel(x, y)
          If pixelcolor.B = 0 And pixelcolor.G = 0 Then
            Tgsunny = oripixelcolor1.G
            Krgsunny = oripixelcolor1.R
          ElseIf pixelcolor.G = 0 And pixelcolor.B = 1 Then
            Krgshade = oripixelcolor1.A
          End If
          SVF1 = 0

          If pixelcolor.G = 0 Then
            For Viewangle = 2.5 To 357.5 Step 5
              M = 0
              N = 0
              pGreen = 1.2
              allheight = pixelcolor.R + pGreen
```

```
                eleangle = -90 + oriangle
                Newposition = CInt((2 * (300 / TextBox10.Text) * oriangle) / 180)
                If pixelcolor.B = 0 Then
                    For annuli = 1 To Newposition Step 1
                        groundsunny = groundsunny + (1 / 360) * Math.Sin((180 / (2 * (300 / TextBox10.Text))) * Math.PI / 180) *_
Math.Sin(((180 * (2 * annuli - 1)) / (2 * (300 / TextBox10.Text))) * Math.PI / 180) * 5
                    Next
                ElseIf pixelcolor.B = 1 Then
                    For annuli = 1 To Newposition Step 1
                        groundshade = groundshade + (1 / 360) * Math.Sin((180 / (2 * (300 / TextBox10.Text))) * Math.PI / 180) *_
Math.Sin(((180 * (2 * annuli - 1)) / (2 * (300 / TextBox10.Text))) * Math.PI / 180) * 5
                    Next
                End If
                For dist = 1 To (300 / TextBox10.Text) Step 1   'maximum distance to analyze view factors is assumed 300 meters.
                    x1 = x + CInt(dist * Math.Cos(Viewangle * Math.PI / 180))
                    y1 = y + CInt(dist * Math.Sin(Viewangle * Math.PI / 180))
                    Neweleangle1 = 0
                    Neweleangle2 = 0
                    Neweleangle3 = 0
                    Neweleangle4 = 0
                    Neweleangle5 = 0
                    Neweleangle6 = 0
                    Neweleangle7 = 0
                    Neweleangle8 = 0
                    Newgsunny = 0
                    Newgshade = 0
                    Newgsunnyup = 0
                    Newgshadeup = 0
                    Newtsunny = 0
                    Newtshade = 0
                    Newbsunny = 0
                    Newbshade = 0

                    If 0 <= x1 And x1 <= (newimage3.Width - 1) And 0 <= y1 And y1 <= (newimage3.Height - 1) Then
                        distance = Math.Sqrt(((x - x1) * TextBox10.Text + TextBox10.Text / 2) ^ 2 + ((y - y1) * TextBox10.Text +_
TextBox10.Text / 2) ^ 2)
                        distance1 = Math.Sqrt(((x - x1) * TextBox10.Text - TextBox10.Text / 2) ^ 2 + ((y - y1) * TextBox10.Text -_
TextBox10.Text / 2) ^ 2)
                        'View factor analysis
                        Dim pixelcolor1 As Color = newimage3.GetPixel(x1, y1)
                        Dim oripixelcolor As Color = newimagesvf.GetPixel(x1, y1)
                        If oripixelcolor.R > 200 And oripixelcolor.A > 200 Then
                            Krsl = (oripixelcolor.R - 200) * 10 + 5
                            Krslsh = oripixelcolor.A - 200
                        Else
                            Krsl = oripixelcolor.R
                            Krslsh = oripixelcolor.A
                        End If
                        If pixelcolor1.G = 0 Then          'View factor analysis for the ground surface
                            eleangle1 = eleangle
                            allheight1 = pixelcolor1.R
                            elevation = (allheight1 - allheight) / distance
                            eleangle = Math.Atan(elevation) * 180 / Math.PI
                            If eleangle > eleangle1 Then
                                If eleangle1 <= 0 Then
                                    Newposition1 = CInt((2 * (300 / TextBox10.Text) * (90 + eleangle1)) / 180)
                                ElseIf eleangle1 > 0 Then
                                    Newposition1 = CInt((2 * (300 / TextBox10.Text) * (90 - eleangle1)) / 180)
                                End If
                                If eleangle <= 0 Then
                                    Newposition2 = CInt((2 * (300 / TextBox10.Text) * (90 + eleangle)) / 180)
                                ElseIf eleangle > 0 Then
                                    Newposition2 = CInt((2 * (300 / TextBox10.Text) * (90 - eleangle)) / 180)
                                End If
                                If eleangle1 >= 0 Then
                                    Uppergposition1 = Newposition1
                                    Newposition1 = (300 / TextBox10.Text)
                                End If
                                If eleangle >= 0 Then
                                    Uppergposition2 = Newposition2
```

```
                    Newposition2 = (300 / TextBox10.Text)
                End If
                If Newposition1 = (300 / TextBox10.Text) Then
                    Newposition1 = (300 / TextBox10.Text) - 1
                End If
                If Uppergposition1 > (300 / TextBox10.Text) Then
                    Uppergposition1 = (300 / TextBox10.Text)
                End If
                If Uppergposition2 > (300 / TextBox10.Text) Then
                    Uppergposition2 = (300 / TextBox10.Text)
                End If
                If pixelcolor1.B = 0 Then
                    For annuli = Newposition1 + 1 To Newposition2 Step 1
                        Newgsunny = Newgsunny + (1 / 360) * Math.Sin((180 / (2 * (300 / TextBox10.Text))) * Math.PI /_
180) * Math.Sin(((180 * (2 * annuli - 1)) / (2 * (300 / TextBox10.Text))) * Math.PI / 180) * 5
                    Next
                    groundsunny = groundsunny + Newgsunny
                    If groundsunny > 0 And Krsl > 50 Then
                        Tgsunny = (Tgsunny * (groundsunny - Newgsunny) + oripixelcolor.G * Newgsunny) / groundsunny
                        Krgsunny = (Krgsunny * (groundsunny - Newgsunny) + Krsl * Newgsunny) / groundsunny
                    End If
                    If eleangle1 <= 0 And eleangle > 0 Then
                        Uppergposition1 = (300 / TextBox10.Text)
                    End If
                    For annuliup = Uppergposition2 To Uppergposition1 Step 1
                        Newgsunnyup = Newgsunnyup + (1 / 360) * Math.Sin((180 / (2 * (300 / TextBox10.Text))) *_
Math.PI / 180) * Math.Sin(((180 * (2 * annuliup - 1)) / (2 * (300 / TextBox10.Text))) * Math.PI / 180) * 5
                    Next
                    groundsunnyup = groundsunnyup + Newgsunnyup
                    If groundsunnyup > 0 And Krsl > 50 Then
                        Tgsunnyup = (Tgsunnyup * (groundsunnyup - Newgsunnyup) + oripixelcolor.G * Newgsunnyup) /_
groundsunnyup
                        Krgsunnyup = (Krgsunnyup * (groundsunnyup - Newgsunnyup) + Krsl * Newgsunnyup) /_
groundsunnyup
                    End If
                Else
                    For annuli = Newposition1 + 1 To Newposition2 Step 1
                        Newgshade = Newgshade + (1 / 360) * Math.Sin((180 / (2 * (300 / TextBox10.Text))) * Math.PI /_
180) * Math.Sin(((180 * (2 * annuli - 1)) / (2 * (300 / TextBox10.Text))) * Math.PI / 180) * 5
                    Next
                    groundshade = groundshade + Newgshade
                    If groundshade > 0 Then
                        Krgshade = (Krgshade * (groundshade - Newgshade) + Krslsh * Newgshade) / groundshade
                    End If
                    If eleangle1 <= 0 And eleangle > 0 Then
                        Uppergposition1 = (300 / TextBox10.Text)
                    End If
                    For annuliup = Uppergposition2 To Uppergposition1 Step 1
                        Newgshadeup = Newgshadeup + (1 / 360) * Math.Sin((180 / (2 * (300 / TextBox10.Text))) * _
Math.PI / 180) * Math.Sin(((180 * (2 * annuliup - 1)) / (2 * (300 / TextBox10.Text))) * Math.PI / 180) * 5
                    Next
                    groundshadeup = groundshadeup + Newgshadeup
                    If groundshadeup > 0 Then
                        Krgshadeup = (Krgshadeup * (groundshadeup - Newgshadeup) + Krslsh * Newgshadeup) /_
groundshadeup
                    End If
                End If
            End If
        End If

        If M = 0 Then
            If pixelcolor1.G > 200 Then          'View factor analysis for trees
                M = M + 1
                N = N + 1
                eleangle1 = eleangle
                pGreen1 = pixelcolor1.G - 200
                allheight1 = pixelcolor1.R + pGreen1 * TextBox16.Text
                If pixelcolor1.B = 0 Then
                    shaderatio = 0
                    shaderatiog = 0
```

```
                    ElseIf pixelcolor1.B > 0 Then
                        If pixelcolor1.B > 1.2 Then
                            shaderatio = (pixelcolor1.B - 1.2) / (pGreen1 - 1.2)
                            shaderatiog = 1
                        Else
                            shaderatio = 0
                            shaderatiog = pixelcolor1.B / 1.2
                        End If
                    End If
                    elevation = (allheight1 - allheight) / distance1
                    eleangle = Math.Atan(elevation) * 180 / Math.PI
                    If eleangle > eleangle1 Then
                        Newposition1 = CInt((2 * (300 / TextBox10.Text) * (90 + eleangle1)) / 180)
                        Newposition2 = CInt((2 * (300 / TextBox10.Text) * (90 - eleangle)) / 180)
                        Shadeposition1 = CInt(((300 / TextBox10.Text) - Newposition1) * shaderatiog)
                        Shadeposition2 = CInt(((300 / TextBox10.Text) - Newposition2) * shaderatio)
                        If shaderatio = 0 Then
                            For annuli = Newposition2 To (300 / TextBox10.Text) - Shadeposition2 - 1 Step 1
                                Neweleangle1 = Neweleangle1 + (1 / 360) * Math.Sin((180 / (2 * (300 / TextBox10.Text))) *_
Math.PI / 180) * Math.Sin(((180 * (2 * annuli - 1)) / (2 * (300 / TextBox10.Text))) * Math.PI / 180) * 5
                            Next
                            Treesunny = Treesunny + Neweleangle1
                        ElseIf shaderatio = 1 Then
                            For annuli = (300 / TextBox10.Text) - Shadeposition2 To (300 / TextBox10.Text) Step 1
                                Neweleangle2 = Neweleangle2 + (1 / 360) * Math.Sin((180 / (2 * (300 / TextBox10.Text))) *_
Math.PI / 180) * Math.Sin(((180 * (2 * annuli - 1)) / (2 * (300 / TextBox10.Text))) * Math.PI / 180) * 5
                            Next
                            Treeshade = Treeshade + Neweleangle2
                        Else
                            For annuli = Newposition2 To (300 / TextBox10.Text) - Shadeposition2 - 1 Step 1
                                Neweleangle1 = Neweleangle1 + (1 / 360) * Math.Sin((180 / (2 * (300 / TextBox10.Text))) *_
Math.PI / 180) * Math.Sin(((180 * (2 * annuli - 1)) / (2 * (300 / TextBox10.Text))) * Math.PI / 180) * 5
                            Next
                            Treesunny = Treesunny + Neweleangle1
                            For annuli = (300 / TextBox10.Text) - Shadeposition2 To (300 / TextBox10.Text) Step 1
                                Neweleangle2 = Neweleangle2 + (1 / 360) * Math.Sin((180 / (2 * (300 / TextBox10.Text))) *_
Math.PI / 180) * Math.Sin(((180 * (2 * annuli - 1)) / (2 * (300 / TextBox10.Text))) * Math.PI / 180) * 5
                            Next
                            Treeshade = Treeshade + Neweleangle2
                        End If
                        If shaderatiog = 0 Then
                            For annuli = Newposition1 To (300 / TextBox10.Text) - Shadeposition1 - 1 Step 1
                                Neweleangle3 = Neweleangle3 + (1 / 360) * Math.Sin((180 / (2 * (300 / TextBox10.Text))) *_
Math.PI / 180) * Math.Sin(((180 * (2 * annuli - 1)) / (2 * (300 / TextBox10.Text))) * Math.PI / 180) * 5
                            Next
                            Treesunnyg = Treesunnyg + Neweleangle3
                        ElseIf shaderatiog = 1 Then
                            For annuli = (300 / TextBox10.Text) - Shadeposition1 To (300 / TextBox10.Text) Step 1
                                Neweleangle4 = Neweleangle4 + (1 / 360) * Math.Sin((180 / (2 * (300 / TextBox10.Text))) *_
Math.PI / 180) * Math.Sin(((180 * (2 * annuli - 1)) / (2 * (300 / TextBox10.Text))) * Math.PI / 180) * 5
                            Next
                            Treeshadeg = Treeshadeg + Neweleangle4
                        Else
                            For annuli = Newposition1 To (300 / TextBox10.Text) - Shadeposition1 - 1 Step 1
                                Neweleangle3 = Neweleangle3 + (1 / 360) * Math.Sin((180 / (2 * (300 / TextBox10.Text))) *_
Math.PI / 180) * Math.Sin(((180 * (2 * annuli - 1)) / (2 * (300 / TextBox10.Text))) * Math.PI / 180) * 5
                            Next
                            Treesunnyg = Treesunnyg + Neweleangle3
                            For annuli = (300 / TextBox10.Text) - Shadeposition1 To (300 / TextBox10.Text) Step 1
                                Neweleangle4 = Neweleangle4 + (1 / 360) * Math.Sin((180 / (2 * (300 / TextBox10.Text))) *_
Math.PI / 180) * Math.Sin(((180 * (2 * annuli - 1)) / (2 * (300 / TextBox10.Text))) * Math.PI / 180) * 5
                            Next
                            Treeshadeg = Treeshadeg + Neweleangle4
                        End If
                        If Treesunny > 0 Then
                            Tvegsunny = (Tvegsunny * (Treesunny - Neweleangle1) + oripixelcolor.G * Neweleangle1) /_
Treesunny
                            Krvegsunny = (Krvegsunny * (Treesunny - Neweleangle1) + Krsl * Neweleangle1) / Treesunny
                        End If
                        If Treeshade > 0 Then
```

```
                        Krvegshade = (Krvegshade * (Treeshade - Neweleangle2) + Krslsh * Neweleangle2) / Treeshade
                    End If
                    If Treesunnyg > 0 Then
                        Tvegsunnyg = (Tvegsunnyg * (Treesunnyg - Neweleangle3) + oripixelcolor.G * Neweleangle3) /_
Treesunnyg
                        Krvegsunnyg = (Krvegsunnyg * (Treesunnyg - Neweleangle3) + Krsl * Neweleangle3) / Treesunnyg
                    End If
                    If Treeshadeg > 0 Then
                        Krvegshadeg = (Krvegshadeg * (Treeshadeg - Neweleangle4) + Krslsh * Neweleangle4) / Treeshadeg
                    End If
                End If
            End If
        End If

        If M > 0 Then
            If pixelcolor1.G > 200 Then
                M = M + 1
                eleangle1 = eleangle
                pGreen1 = pixelcolor1.G - 200
                allheight1 = pixelcolor1.R + pGreen1 * TextBox16.Text
                shaderatio = pixelcolor1.B / pGreen1
                elevation = (allheight1 - allheight) / distance1
                eleangle = Math.Atan(elevation) * 180 / Math.PI
                Newposition1 = CInt((2 * (300 / TextBox10.Text) * (90 - eleangle1)) / 180)
                Newposition2 = CInt((2 * (300 / TextBox10.Text) * (90 - eleangle)) / 180)
                elevationsh = ((allheight1 - allheight) * shaderatio) / distance1
                eleanglesh = Math.Atan(elevationsh) * 180 / Math.PI
                Newpositionsh = CInt((2 * (300 / TextBox10.Text) * (90 - eleanglesh)) / 180)
                If eleangle > eleangle1 Then
                    If eleanglesh > eleangle1 Then
                        For annuli = Newpositionsh To Newposition1 - 1
                            Newtshade = Newtshade + (1 / 360) * Math.Sin((180 / (2 * (300 / TextBox10.Text))) * Math.PI /_
180) * Math.Sin(((180 * (2 * annuli - 1)) / (2 * (300 / TextBox10.Text))) * Math.PI / 180) * 5
                        Next
                        Treeshade = Treeshade + Newtshade
                        For annuli = Newposition2 To Newpositionsh - 1
                            Newtsunny = Newtsunny + (1 / 360) * Math.Sin((180 / (2 * (300 / TextBox10.Text))) * Math.PI /_
180) * Math.Sin(((180 * (2 * annuli - 1)) / (2 * (300 / TextBox10.Text))) * Math.PI / 180) * 5
                        Next
                        Treesunny = Treesunny + Newtsunny
                        If Treesunny > 0 Then
                            Tvegsunny = (Tvegsunny * (Treesunny - Newtsunny) + oripixelcolor.G * Newtsunny) / Treesunny
                            Krvegsunny = (Krvegsunny * (Treesunny - Newtsunny) + Krsl * Newtsunny) / Treesunny
                        End If
                        If Treeshade > 0 Then
                            Krvegshade = (Krvegshade * (Treeshade - Newtshade) + Krslsh * Newtshade) / Treeshade
                        End If
                    Else
                        For annuli = Newposition2 To Newposition1 - 1
                            Newtsunny = Newtsunny + (1 / 360) * Math.Sin((180 / (2 * (300 / TextBox10.Text))) * Math.PI /_
180) * Math.Sin(((180 * (2 * annuli - 1)) / (2 * (300 / TextBox10.Text))) * Math.PI / 180) * 5
                        Next
                        Treesunny = Treesunny + Newtsunny
                        If Treesunny > 0 Then
                            Tvegsunny = (Tvegsunny * (Treesunny - Newtsunny) + oripixelcolor.G * Newtsunny) / Treesunny
                            Krvegsunny = (Krvegsunny * (Treesunny - Newtsunny) + Krsl * Newtsunny) / Treesunny
                        End If
                    End If
                End If
            End If
        End If

        If N = 0 Then
            If 0 < pixelcolor1.G And pixelcolor1.G <= 200 Then          'View factor analysis for building
                N = N + 1
                M = M + 1
                eleangle1 = eleangle
                pGreen1 = pixelcolor1.G
                allheight1 = pixelcolor1.R + pGreen1 * TextBox16.Text
                If pixelcolor1.B = 0 Then
```

```
                    shaderatio = 0
                    shaderatiog = 0
                ElseIf pixelcolor1.B > 0 Then
                    If pixelcolor1.B > 1.2 Then
                        shaderatio = (pixelcolor1.B - 1.2) / (pGreen1 - 1.2)
                        shaderatiog = 1
                    Else
                        shaderatio = 0
                        shaderatiog = pixelcolor1.B / 1.2
                    End If
                End If
                elevation = (allheight1 - allheight) / distance1
                eleangle = Math.Atan(elevation) * 180 / Math.PI
                If eleangle > eleangle1 Then
                    Newposition1 = CInt((2 * (300 / TextBox10.Text) * (90 + eleangle1)) / 180)
                    Newposition2 = CInt((2 * (300 / TextBox10.Text) * (90 - eleangle)) / 180)
                    Shadeposition1 = CInt(((300 / TextBox10.Text) - Newposition1) * shaderatiog)
                    Shadeposition2 = CInt(((300 / TextBox10.Text) - Newposition2) * shaderatio)
                    If shaderatio = 0 Then
                        For annuli = Newposition2 To (300 / TextBox10.Text) - Shadeposition2 - 1 Step 1
                            Neweleangle5 = Neweleangle5 + (1 / 360) * Math.Sin((180 / (2 * (300 / TextBox10.Text))) *_
Math.PI / 180) * Math.Sin(((180 * (2 * annuli - 1)) / (2 * (300 / TextBox10.Text))) * Math.PI / 180) * 5
                        Next
                        obstructsunny = obstructsunny + Neweleangle5
                    ElseIf shaderatio = 1 Then
                        For annuli = (300 / TextBox10.Text) - Shadeposition2 To (300 / TextBox10.Text) Step 1
                            Neweleangle6 = Neweleangle6 + (1 / 360) * Math.Sin((180 / (2 * (300 / TextBox10.Text))) *_
Math.PI / 180) * Math.Sin(((180 * (2 * annuli - 1)) / (2 * (300 / TextBox10.Text))) * Math.PI / 180) * 5
                        Next
                        obstructshade = obstructshade + Neweleangle6
                    Else
                        For annuli = Newposition2 To (300 / TextBox10.Text) - Shadeposition2 - 1 Step 1
                            Neweleangle5 = Neweleangle5 + (1 / 360) * Math.Sin((180 / (2 * (300 / TextBox10.Text))) *_
Math.PI / 180) * Math.Sin(((180 * (2 * annuli - 1)) / (2 * (300 / TextBox10.Text))) * Math.PI / 180) * 5
                        Next
                        obstructsunny = obstructsunny + Neweleangle5
                        For annuli = (300 / TextBox10.Text) - Shadeposition2 To (300 / TextBox10.Text) Step 1
                            Neweleangle6 = Neweleangle6 + (1 / 360) * Math.Sin((180 / (2 * (300 / TextBox10.Text))) *_
Math.PI / 180) * Math.Sin(((180 * (2 * annuli - 1)) / (2 * (300 / TextBox10.Text))) * Math.PI / 180) * 5
                        Next
                        obstructshade = obstructshade + Neweleangle6
                    End If
                    If shaderatiog = 0 Then
                        For annuli = Newposition1 To (300 / TextBox10.Text) - Shadeposition1 - 1 Step 1
                            Neweleangle7 = Neweleangle7 + (1 / 360) * Math.Sin((180 / (2 * (300 / TextBox10.Text))) *_
Math.PI / 180) * Math.Sin(((180 * (2 * annuli - 1)) / (2 * (300 / TextBox10.Text))) * Math.PI / 180) * 5
                        Next
                        Obstructsunnyg = Obstructsunnyg + Neweleangle7
                    ElseIf shaderatiog = 1 Then
                        For annuli = (300 / TextBox10.Text) - Shadeposition1 To (300 / TextBox10.Text) Step 1
                            Neweleangle8 = Neweleangle8 + (1 / 360) * Math.Sin((180 / (2 * (300 / TextBox10.Text))) *_
Math.PI / 180) * Math.Sin(((180 * (2 * annuli - 1)) / (2 * (300 / TextBox10.Text))) * Math.PI / 180) * 5
                        Next
                        Obstructshadeg = Obstructshadeg + Neweleangle8
                    Else
                        For annuli = Newposition1 To (300 / TextBox10.Text) - Shadeposition1 - 1 Step 1
                            Neweleangle7 = Neweleangle7 + (1 / 360) * Math.Sin((180 / (2 * (300 / TextBox10.Text))) *_
Math.PI / 180) * Math.Sin(((180 * (2 * annuli - 1)) / (2 * (300 / TextBox10.Text))) * Math.PI / 180) * 5
                        Next
                        Obstructsunnyg = Obstructsunnyg + Neweleangle7
                        For annuli = (300 / TextBox10.Text) - Shadeposition1 To (300 / TextBox10.Text) Step 1
                            Neweleangle8 = Neweleangle8 + (1 / 360) * Math.Sin((180 / (2 * (300 / TextBox10.Text))) *_
Math.PI / 180) * Math.Sin(((180 * (2 * annuli - 1)) / (2 * (300 / TextBox10.Text))) * Math.PI / 180) * 5
                        Next
                        Obstructshadeg = Obstructshadeg + Neweleangle8
                    End If
                    If obstructsunny > 0 And Krsl > 50 Then
                        Tbsunny = (Tbsunny * (obstructsunny - Neweleangle5) + oripixelcolor.G * Neweleangle5) /_
obstructsunny
                        Krbsunny = (Krbsunny * (obstructsunny - Neweleangle5) + Krsl * Neweleangle5) / obstructsunny
```

```
                                End If
                                If obstructshade > 0 Then
                                    Krbshade = (Krbshade * (obstructshade - Neweleangle6) + Krslsh * Neweleangle6) / obstructshade
                                End If
                                If Obstructsunnyg > 0 And Krsl > 50 Then
                                    Tbsunnyg = (Tbsunnyg * (Obstructsunnyg - Neweleangle7) + oripixelcolor.G * Neweleangle7) /_
Obstructsunnyg
                                    Krbsunnyg = (Krbsunnyg * (Obstructsunnyg - Neweleangle7) + Krsl * Neweleangle7) /_
Obstructsunnyg
                                End If
                                If Obstructshadeg > 0 Then
                                    Krbshadeg = (Krbshadeg * (Obstructshadeg - Neweleangle8) + Krslsh * Neweleangle8) /_
Obstructshadeg
                                End If
                            End If
                        End If
                    End If

                    If N > 0 Then
                        If 0 < pixelcolor1.G And pixelcolor1.G <= 200 Then
                            N = N + 1
                            eleangle1 = eleangle
                            pGreen1 = pixelcolor1.G
                            allheight1 = pixelcolor1.R + pGreen1 * TextBox16.Text
                            shaderatio = pixelcolor1.B / pGreen1
                            elevation = (allheight1 - allheight) / distance1
                            eleangle = Math.Atan(elevation) * 180 / Math.PI
                            Newposition1 = CInt((2 * (300 / TextBox10.Text) * (90 - eleangle1)) / 180)
                            Newposition2 = CInt((2 * (300 / TextBox10.Text) * (90 - eleangle)) / 180)
                            elevationsh = ((allheight1 - allheight) * shaderatio) / distance1
                            eleanglesh = Math.Atan(elevationsh) * 180 / Math.PI
                            Newpositionsh = CInt((2 * (300 / TextBox10.Text) * (90 - eleanglesh)) / 180)
                            If eleangle > eleangle1 Then
                                If eleanglesh > eleangle1 Then
                                    For annuli = Newpositionsh To Newposition1 - 1
                                        Newbshade = Newbshade + (1 / 360) * Math.Sin((180 / (2 * (300 / TextBox10.Text))) * Math.PI /_
180) * Math.Sin(((180 * (2 * annuli - 1)) / (2 * (300 / TextBox10.Text))) * Math.PI / 180) * 5
                                    Next
                                    obstructshade = obstructshade + Newbshade
                                    For annuli = Newposition2 To Newpositionsh - 1
                                        Newbsunny = Newbsunny + (1 / 360) * Math.Sin((180 / (2 * (300 / TextBox10.Text))) * _
Math.PI / 180) * Math.Sin(((180 * (2 * annuli - 1)) / (2 * (300 / TextBox10.Text))) * Math.PI / 180) * 5
                                    Next
                                    obstructsunny = obstructsunny + Newbsunny
                                    If obstructsunny > 0 And Krsl > 50 Then
                                        Tbsunny = (Tbsunny * (obstructsunny - Newbsunny) + oripixelcolor.G * Newbsunny) /_
obstructsunny
                                        Krbsunny = (Krbsunny * (obstructsunny - Newbsunny) + Krsl * Newbsunny) / obstructsunny
                                    End If
                                    If obstructshade > 0 Then
                                        Krbshade = (Krbshade * (obstructshade - Newbshade) + Krslsh * Newbshade) / obstructshade
                                    End If
                                Else
                                    For annuli = Newposition2 To Newposition1 - 1
                                        Newbsunny = Newbsunny + (1 / 360) * Math.Sin((180 / (2 * (300 / TextBox10.Text))) * _
Math.PI / 180) * Math.Sin(((180 * (2 * annuli - 1)) / (2 * (300 / TextBox10.Text))) * Math.PI / 180) * 5
                                    Next
                                    obstructsunny = obstructsunny + Newbsunny
                                    If obstructsunny > 0 And Krsl > 50 Then
                                        Tbsunny = (Tbsunny * (obstructsunny - Newbsunny) + oripixelcolor.G * Newbsunny) /_
obstructsunny
                                        Krbsunny = (Krbsunny * (obstructsunny - Newbsunny) + Krsl * Newbsunny) / obstructsunny
                                    End If
                                End If
                            End If
                        End If
                    End If
                End If
            End If
        End If
    End If
    If eleangle < eleangle1 Then
        eleangle = eleangle1
```

```
                    End If
                Next

                If eleangle > eleangle1 Then
                    eleangle1 = eleangle
                End If
                If eleangle1 = -90 + oriangle Then
                    Newposition1 = CInt((2 * (300 / TextBox10.Text) * oriangle) / 180)
                    For annuli = Newposition1 + 1 To (300 / TextBox10.Text) Step 1
                        groundshade = groundshade + (1 / 360) * Math.Sin((180 / (2 * (300 / TextBox10.Text))) * Math.PI / 180) *_
Math.Sin(((180 * (2 * annuli - 1)) / (2 * (300 / TextBox10.Text))) * Math.PI / 180) * 5
                    Next
                End If
                If eleangle1 > -90 + oriangle And eleangle1 < 0 Then
                    Newposition1 = CInt((2 * (300 / TextBox10.Text) * (90 + eleangle1)) / 180)
                    For annuli = Newposition1 + 1 To (300 / TextBox10.Text) Step 1
                        groundshade = groundshade + (1 / 360) * Math.Sin((180 / (2 * (300 / TextBox10.Text))) * Math.PI / 180) *_
Math.Sin(((180 * (2 * annuli - 1)) / (2 * (300 / TextBox10.Text))) * Math.PI / 180) * 5
                    Next
                End If
            Next
        End If

        SVF1 = 1 - (groundshadeup + groundsunnyup + groundshade + groundsunny + Treeshade + Treesunny + obstructshade _
+ obstructsunny + Treeshadeg + Treesunnyg + Obstructshadeg + Obstructsunnyg - 1)

        Dim ViewfactorandTs As String = x & ", " & y & " Groundsunny: " & groundsunny.ToString("f3") & " Groundshade: "
& groundshade.ToString("f3") & " Groundsunnyup: " & groundsunnyup.ToString("f3") & " Groundshadeup: " &
groundshadeup.ToString("f3") & " Obstructsunny: " & obstructsunny.ToString("f3") & " Obstructshade: " &
obstructshade.ToString("f3") & " Treesunny: " & Treesunny.ToString("f3") & " Treeshade: " & Treeshade.ToString("f3") & "
Obstructsunnyg: " & Obstructsunnyg.ToString("f3") & " Obstructshadeg: " & Obstructshadeg.ToString("f3") & " Treesunnyg: " &
Treesunnyg.ToString("f3") & " Treeshadeg: " & Treeshadeg.ToString("f3") & " Tgsunny: " & Tgsunny.ToString("f1") & " Krgsunny:
" & Krgsunny.ToString("f1") & " Tbsunny: " & Tbsunny.ToString("f1") & " Krbsunny: " & Krbsunny.ToString("f1") & " Tvegsunny:
" & Tvegsunny.ToString("f1") & " Krvegsunny: " & Krvegsunny.ToString("f1") & vbCrLf
        My.Computer.FileSystem.WriteAllText("C:\ViewfactorandTs.txt", ViewfactorandTs, True)

        'Radiation calculation on the street
        Dim pixelcolorx As Color = newimage.GetPixel(x, y) 'Color.FromArgb(Azimuth, ground height, obstruct height, shaded
obstruct height)
        Dim pixelcolory As Color = buildingviewfactor.GetPixel(x, y) 'Color.FromArgb(CInt(SVF*100), CInt(SVF*100),
CInt(SVF*100))
        Dim Kbst, Kdst, Krst, Krg, Lg, Last, Lo, Lveg, TotalK, TotalL, ground As Double
        Dim SVF As Double = pixelcolory.B / 100
        If SVF1 > 1 Then
            SVF1 = 1
        ElseIf SVF1 < 0 Then
            SVF1 = 0
        End If
        If pixelcolorx.B = 1 Then
            Kbst = 0
            If SVF > SVF1 Then
                Kdst = t * Kd * (SVF1 + (SVF - SVF1) * 0.3)
            Else
                Kdst = t * Kd * SVF1
            End If
        Else
            Kbst = Kb
            If SVF > SVF1 Then
                Kdst = Kd * (SVF1 + (SVF - SVF1) * 0.3)
            Else
                Kdst = Kd * SVF1
            End If
        End If
        ground = groundsunny + groundshade
        Krst = (Krgsunnyup * groundsunnyup + Krgshadeup * groundshadeup + Krvegsunny * Treesunny + Krbsunny *_
obstructsunny + Krbshade * obstructshade + Krvegshade * Treeshade)
        Krg = Krgsunny * groundsunny + Krgshade * groundshade + Krvegsunnyg * Treesunnyg + Krbsunnyg * _
Obstructsunnyg + Krbshadeg * Obstructshadeg + Krvegshadeg * Treeshadeg + TextBox19.Text * (((1 - SVF1) * Krst) + _
(Treesunnyg + Treeshadeg + Obstructsunnyg + Obstructshadeg) * (Krvegsunnyg * Treesunnyg + Krbsunnyg * Obstructsunnyg +
Krbshadeg *_ Obstructshadeg + Krvegshadeg * Treeshadeg))
```

```
            Last = La * SVF1
            Lo = (TextBox23.Text * 5.67 * 10 ^ -8 * (273.15 + Tbsunny) ^ 4 * obstructsunny + TextBox23.Text * 5.67 * 10 ^ -8 *_
(273.15 + Ta + (0.00004636 * CMT ^ 2 - 0.06508 * CMT + 22.56)) ^ 4 * obstructshade) + 0.1 * Last * (0.7248 * SVF1 ^ 3 - 1.1527_
 * SVF1 ^ 2 + 0.8577 * SVF1 + 0.0616) + TextBox25.Text * 5.67 * 10 ^ -8 * (273.15 + Tgsunny) ^ 4 * groundsunnyup +_
TextBox25.Text * 5.67 * 10 ^ -8 * (273.15 + Ta + (0.0001508 * CMT ^ 2 - 0.2103 * CMT + 70.79)) ^ 4 * groundshadeup
            Lveg = Math.Abs((TextBox24.Text * 5.67 * 10 ^ -8 * (273.15 + Tvegsunny) ^ 4 * Treesunny + TextBox24.Text * 5.67_
 * 10 ^ -8 * (273.15 + Ta + (-0.00006329 * CMT ^ 2 + 0.09734 * CMT - 37.52)) ^ 4 * Treeshade) + 0.05 * Last * (0.7248 * SVF1 ^ 3_
 - 1.1527 * SVF1 ^ 2 + 0.8577 * SVF1 + 0.0616))
            Lg = TextBox24.Text * 5.67 * 10 ^ -8 * (273.15 + Tvegsunnyg) ^ 4 * Treesunnyg + TextBox24.Text * 5.67 * 10 ^ -8 *_
(273.15 + Ta + (-0.00006329 * CMT ^ 2 + 0.09734 * CMT - 37.52)) ^ 4 * Treeshadeg + TextBox23.Text * 5.67 * 10 ^ -8 * (273.15_
 + Tbsunnyg) ^ 4 * Obstructsunnyg + TextBox23.Text * 5.67 * 10 ^ -8 * (273.15 + Ta + (0.00004636 * CMT ^ 2 - 0.06508 * CMT +_
 22.56)) ^ 4 * Obstructshadeg + TextBox25.Text * 5.67 * 10 ^ -8 * (273.15 + Tgsunny) ^ 4 * groundsunny + TextBox25.Text * 5.67_
 * 10 ^ -8 * (273.15 + Ta + (0.0001508 * CMT ^ 2 - 0.2103 * CMT + 70.79)) ^ 4 * groundshade + 0.05 * (Last + Lo + Lveg)
            TotalK = Kbst + Kdst + Krst + Krg
            TotalL = Last + Lg + Lo + Lveg
            Dim TotalQ As Double
            TotalQ = TotalK + TotalL

            'Combining radiation results with human body area factors
            Dim Effectivefactor, Projectedareafactor As Double
            Dim direction As Double = Math.Abs(solazi + 180 - TextBox14.Text)
            Select Case ComboBox7.SelectedIndex
              Case 0
                Effectivefactor = 0.826
              Case 1
                Effectivefactor = 0.846
              Case 2
                Effectivefactor = 0.836
            End Select
            Select Case ComboBox8.SelectedIndex
              Case 0
                If ComboBox7.SelectedIndex = 0 Then
                  Projectedareafactor = 0.000000301 * betaorg ^ 3 - 0.0000646 * betaorg ^ 2 + 0.000834 * betaorg + 0.298
                ElseIf ComboBox7.SelectedIndex = 1 Then
                  Projectedareafactor = 0.000000367 * betaorg ^ 3 - 0.0000674 * betaorg ^ 2 + 0.000849 * betaorg + 0.297
                Else
                  Projectedareafactor = 0.000000334 * betaorg ^ 3 - 0.000066 * betaorg ^ 2 + 0.000842 * betaorg + 0.297
                End If
              Case 1
                If ComboBox7.SelectedIndex = 0 And direction >= 0 And direction < 7.5 Then
                  Projectedareafactor = 0.00000032 * betaorg ^ 3 - 0.000074 * betaorg ^ 2 + 0.00105 * betaorg + 0.343
                ElseIf ComboBox7.SelectedIndex = 0 And direction >= 7.5 And direction < 12.5 Then
                  Projectedareafactor = ((0.00000032 * betaorg ^ 3 - 0.000074 * betaorg ^ 2 + 0.00105 * betaorg + 0.343) +_
(0.000000339 * betaorg ^ 3 - 0.000076 * betaorg ^ 2 + 0.0011 * betaorg + 0.341)) / 2
                ElseIf ComboBox7.SelectedIndex = 0 And direction >= 12.5 And direction < 17.5 Then
                  Projectedareafactor = 0.000000339 * betaorg ^ 3 - 0.000076 * betaorg ^ 2 + 0.0011 * betaorg + 0.341
                ElseIf ComboBox7.SelectedIndex = 0 And direction >= 17.5 And direction < 22.5 Then
                  Projectedareafactor = ((0.000000339 * betaorg ^ 3 - 0.000076 * betaorg ^ 2 + 0.0011 * betaorg + 0.341) +_
(0.000000367 * betaorg ^ 3 - 0.0000784 * betaorg ^ 2 + 0.00114 * betaorg + 0.336)) / 2
                ElseIf ComboBox7.SelectedIndex = 0 And direction >= 22.5 And direction < 27.5 Then
                  Projectedareafactor = 0.000000367 * betaorg ^ 3 - 0.0000784 * betaorg ^ 2 + 0.00114 * betaorg + 0.336
                ElseIf ComboBox7.SelectedIndex = 0 And direction >= 27.5 And direction < 32.5 Then
                  Projectedareafactor = ((0.000000367 * betaorg ^ 3 - 0.0000784 * betaorg ^ 2 + 0.00114 * betaorg + 0.336) +_
(0.000000396 * betaorg ^ 3 - 0.0000802 * betaorg ^ 2 + 0.00119 * betaorg + 0.325)) / 2
                ElseIf ComboBox7.SelectedIndex = 0 And direction >= 32.5 And direction < 37.5 Then
                  Projectedareafactor = 0.000000396 * betaorg ^ 3 - 0.0000802 * betaorg ^ 2 + 0.00119 * betaorg + 0.325
                ElseIf ComboBox7.SelectedIndex = 0 And direction >= 37.5 And direction < 42.5 Then
                  Projectedareafactor = ((0.000000396 * betaorg ^ 3 - 0.0000802 * betaorg ^ 2 + 0.00119 * betaorg + 0.325) +_
(0.000000431 * betaorg ^ 3 - 0.0000818 * betaorg ^ 2 + 0.00121 * betaorg + 0.311)) / 2
                ElseIf ComboBox7.SelectedIndex = 0 And direction >= 42.5 And direction < 47.5 Then
                  Projectedareafactor = 0.000000431 * betaorg ^ 3 - 0.0000818 * betaorg ^ 2 + 0.00121 * betaorg + 0.311
                ElseIf ComboBox7.SelectedIndex = 0 And direction >= 47.5 And direction < 52.5 Then
                  Projectedareafactor = ((0.000000431 * betaorg ^ 3 - 0.0000818 * betaorg ^ 2 + 0.00121 * betaorg + 0.311) +_
(0.000000469 * betaorg ^ 3 - 0.0000835 * betaorg ^ 2 + 0.00129 * betaorg + 0.293)) / 2
                ElseIf ComboBox7.SelectedIndex = 0 And direction >= 52.5 And direction < 57.5 Then
                  Projectedareafactor = 0.000000469 * betaorg ^ 3 - 0.0000835 * betaorg ^ 2 + 0.00129 * betaorg + 0.293
                ElseIf ComboBox7.SelectedIndex = 0 And direction >= 57.5 And direction < 62.5 Then
                  Projectedareafactor = ((0.000000469 * betaorg ^ 3 - 0.0000835 * betaorg ^ 2 + 0.00129 * betaorg + 0.293) +_
(0.000000457 * betaorg ^ 3 - 0.0000783 * betaorg ^ 2 + 0.00119 * betaorg + 0.27)) / 2
                ElseIf ComboBox7.SelectedIndex = 0 And direction >= 62.5 And direction < 67.5 Then
```

```
            Projectedareafactor = 0.000000457 * betaorg ^ 3 - 0.0000783 * betaorg ^ 2 + 0.00119 * betaorg + 0.27
        ElseIf ComboBox7.SelectedIndex = 0 And direction >= 67.5 And direction < 72.5 Then
            Projectedareafactor = ((0.000000457 * betaorg ^ 3 - 0.0000783 * betaorg ^ 2 + 0.00119 * betaorg + 0.27) +_
(0.000000327 * betaorg ^ 3 - 0.0000592 * betaorg ^ 2 + 0.000796 * betaorg + 0.244)) / 2
        ElseIf ComboBox7.SelectedIndex = 0 And direction >= 72.5 And direction < 77.5 Then
            Projectedareafactor = 0.000000327 * betaorg ^ 3 - 0.0000592 * betaorg ^ 2 + 0.000796 * betaorg + 0.244
        ElseIf ComboBox7.SelectedIndex = 0 And direction >= 77.5 And direction < 82.5 Then
            Projectedareafactor = ((0.000000327 * betaorg ^ 3 - 0.0000592 * betaorg ^ 2 + 0.000796 * betaorg + 0.244) +_
(0.000000215 * betaorg ^ 3 - 0.0000479 * betaorg ^ 2 + 0.000979 * betaorg + 0.214)) / 2
        ElseIf ComboBox7.SelectedIndex = 0 And direction >= 82.5 And direction < 87.5 Then
            Projectedareafactor = 0.000000215 * betaorg ^ 3 - 0.0000479 * betaorg ^ 2 + 0.000979 * betaorg + 0.214
        ElseIf ComboBox7.SelectedIndex = 0 And direction >= 87.5 And direction < 92.5 Then
            Projectedareafactor = ((0.000000215 * betaorg ^ 3 - 0.0000479 * betaorg ^ 2 + 0.000979 * betaorg + 0.214) +_
(0.000000211 * betaorg ^ 3 - 0.0000504 * betaorg ^ 2 + 0.00124 * betaorg + 0.213)) / 2
        ElseIf ComboBox7.SelectedIndex = 0 And direction >= 92.5 And direction < 97.5 Then
            Projectedareafactor = 0.000000211 * betaorg ^ 3 - 0.0000504 * betaorg ^ 2 + 0.00124 * betaorg + 0.213
        ElseIf ComboBox7.SelectedIndex = 0 And direction >= 97.5 And direction < 102.5 Then
            Projectedareafactor = ((0.000000211 * betaorg ^ 3 - 0.0000504 * betaorg ^ 2 + 0.00124 * betaorg + 0.213) +_
(0.000000194 * betaorg ^ 3 - 0.0000476 * betaorg ^ 2 + 0.000775 * betaorg + 0.242)) / 2
        ElseIf ComboBox7.SelectedIndex = 0 And direction >= 102.5 And direction < 107.5 Then
            Projectedareafactor = 0.000000194 * betaorg ^ 3 - 0.0000476 * betaorg ^ 2 + 0.000775 * betaorg + 0.242
        ElseIf ComboBox7.SelectedIndex = 0 And direction >= 107.5 And direction < 112.5 Then
            Projectedareafactor = ((0.000000194 * betaorg ^ 3 - 0.0000476 * betaorg ^ 2 + 0.000775 * betaorg + 0.242) +_
(0.000000209 * betaorg ^ 3 - 0.0000502 * betaorg ^ 2 + 0.000561 * betaorg + 0.271)) / 2
        ElseIf ComboBox7.SelectedIndex = 0 And direction >= 112.5 And direction < 117.5 Then
            Projectedareafactor = 0.000000209 * betaorg ^ 3 - 0.0000502 * betaorg ^ 2 + 0.000561 * betaorg + 0.271
        ElseIf ComboBox7.SelectedIndex = 0 And direction >= 117.5 And direction < 122.5 Then
            Projectedareafactor = ((0.000000209 * betaorg ^ 3 - 0.0000502 * betaorg ^ 2 + 0.000561 * betaorg + 0.271) +_
(0.000000217 * betaorg ^ 3 - 0.0000525 * betaorg ^ 2 + 0.000431 * betaorg + 0.295)) / 2
        ElseIf ComboBox7.SelectedIndex = 0 And direction >= 122.5 And direction < 127.5 Then
            Projectedareafactor = 0.000000217 * betaorg ^ 3 - 0.0000525 * betaorg ^ 2 + 0.000431 * betaorg + 0.295
        ElseIf ComboBox7.SelectedIndex = 0 And direction >= 127.5 And direction < 132.5 Then
            Projectedareafactor = ((0.000000217 * betaorg ^ 3 - 0.0000525 * betaorg ^ 2 + 0.000431 * betaorg + 0.295) +_
(0.000000208 * betaorg ^ 3 - 0.0000527 * betaorg ^ 2 + 0.000292 * betaorg + 0.315)) / 2
        ElseIf ComboBox7.SelectedIndex = 0 And direction >= 132.5 And direction < 137.5 Then
            Projectedareafactor = 0.000000208 * betaorg ^ 3 - 0.0000527 * betaorg ^ 2 + 0.000292 * betaorg + 0.315
        ElseIf ComboBox7.SelectedIndex = 0 And direction >= 137.5 And direction < 142.5 Then
            Projectedareafactor = ((0.000000208 * betaorg ^ 3 - 0.0000527 * betaorg ^ 2 + 0.000292 * betaorg + 0.315) +_
(0.000000206 * betaorg ^ 3 - 0.0000537 * betaorg ^ 2 + 0.000235 * betaorg + 0.329)) / 2
        ElseIf ComboBox7.SelectedIndex = 0 And direction >= 142.5 And direction < 147.5 Then
            Projectedareafactor = 0.000000206 * betaorg ^ 3 - 0.0000537 * betaorg ^ 2 + 0.000235 * betaorg + 0.329
        ElseIf ComboBox7.SelectedIndex = 0 And direction >= 147.5 And direction < 152.5 Then
            Projectedareafactor = ((0.000000206 * betaorg ^ 3 - 0.0000537 * betaorg ^ 2 + 0.000235 * betaorg + 0.329) +_
(0.00000022 * betaorg ^ 3 - 0.0000561 * betaorg ^ 2 + 0.000233 * betaorg + 0.338)) / 2
        ElseIf ComboBox7.SelectedIndex = 0 And direction >= 152.5 And direction < 157.5 Then
            Projectedareafactor = 0.00000022 * betaorg ^ 3 - 0.0000561 * betaorg ^ 2 + 0.000233 * betaorg + 0.338
        ElseIf ComboBox7.SelectedIndex = 0 And direction >= 157.5 And direction < 162.5 Then
            Projectedareafactor = ((0.00000022 * betaorg ^ 3 - 0.0000561 * betaorg ^ 2 + 0.000233 * betaorg + 0.338) +_
(0.000000289 * betaorg ^ 3 - 0.0000657 * betaorg ^ 2 + 0.000522 * betaorg + 0.341)) / 2
        ElseIf ComboBox7.SelectedIndex = 0 And direction >= 162.5 And direction < 167.5 Then
            Projectedareafactor = 0.000000289 * betaorg ^ 3 - 0.0000657 * betaorg ^ 2 + 0.000522 * betaorg + 0.341
        ElseIf ComboBox7.SelectedIndex = 0 And direction >= 167.5 And direction < 172.5 Then
            Projectedareafactor = ((0.000000289 * betaorg ^ 3 - 0.0000657 * betaorg ^ 2 + 0.000522 * betaorg + 0.341) +_
(0.000000335 * betaorg ^ 3 - 0.0000717 * betaorg ^ 2 + 0.000696 * betaorg + 0.342)) / 2
        ElseIf ComboBox7.SelectedIndex = 0 And direction >= 172.5 And direction < 177.5 Then
            Projectedareafactor = 0.000000335 * betaorg ^ 3 - 0.0000717 * betaorg ^ 2 + 0.000696 * betaorg + 0.342
        ElseIf ComboBox7.SelectedIndex = 0 And direction >= 177.5 Then
            Projectedareafactor = ((0.00000032 * betaorg ^ 3 - 0.000074 * betaorg ^ 2 + 0.00105 * betaorg + 0.343) +_
(0.000000335 * betaorg ^ 3 - 0.0000717 * betaorg ^ 2 + 0.000696 * betaorg + 0.342)) / 2
        ElseIf ComboBox7.SelectedIndex = 1 And direction >= 0 And direction < 7.5 Then
            Projectedareafactor = 0.000000421 * betaorg ^ 3 - 0.0000779 * betaorg ^ 2 + 0.000973 * betaorg + 0.329
        ElseIf ComboBox7.SelectedIndex = 1 And direction >= 7.5 And direction < 12.5 Then
            Projectedareafactor = ((0.000000421 * betaorg ^ 3 - 0.0000779 * betaorg ^ 2 + 0.000973 * betaorg + 0.329) +_
(0.000000368 * betaorg ^ 3 - 0.0000704 * betaorg ^ 2 + 0.00082 * betaorg + 0.321)) / 2
        ElseIf ComboBox7.SelectedIndex = 1 And direction >= 12.5 And direction < 17.5 Then
            Projectedareafactor = 0.000000368 * betaorg ^ 3 - 0.0000704 * betaorg ^ 2 + 0.00082 * betaorg + 0.321
        ElseIf ComboBox7.SelectedIndex = 1 And direction >= 17.5 And direction < 22.5 Then
            Projectedareafactor = ((0.000000368 * betaorg ^ 3 - 0.0000704 * betaorg ^ 2 + 0.00082 * betaorg + 0.321) +_
(0.000000404 * betaorg ^ 3 - 0.000074 * betaorg ^ 2 + 0.000931 * betaorg + 0.315)) / 2
        ElseIf ComboBox7.SelectedIndex = 1 And direction >= 22.5 And direction < 27.5 Then
```

```
                Projectedareafactor = 0.000000404 * betaorg ^ 3 - 0.000074 * betaorg ^ 2 + 0.000931 * betaorg + 0.315
            ElseIf ComboBox7.SelectedIndex = 1 And direction >= 27.5 And direction < 32.5 Then
                Projectedareafactor = ((0.000000404 * betaorg ^ 3 - 0.000074 * betaorg ^ 2 + 0.000931 * betaorg + 0.315) +_
(0.000000408 * betaorg ^ 3 - 0.000074 * betaorg ^ 2 + 0.000977 * betaorg + 0.308)) / 2
            ElseIf ComboBox7.SelectedIndex = 1 And direction >= 32.5 And direction < 37.5 Then
                Projectedareafactor = 0.000000408 * betaorg ^ 3 - 0.000074 * betaorg ^ 2 + 0.000977 * betaorg + 0.308
            ElseIf ComboBox7.SelectedIndex = 1 And direction >= 37.5 And direction < 42.5 Then
                Projectedareafactor = ((0.000000408 * betaorg ^ 3 - 0.000074 * betaorg ^ 2 + 0.000977 * betaorg + 0.308) +_
(0.000000401 * betaorg ^ 3 - 0.0000716 * betaorg ^ 2 + 0.000911 * betaorg + 0.301)) / 2
            ElseIf ComboBox7.SelectedIndex = 1 And direction >= 42.5 And direction < 47.5 Then
                Projectedareafactor = 0.000000401 * betaorg ^ 3 - 0.0000716 * betaorg ^ 2 + 0.000911 * betaorg + 0.301
            ElseIf ComboBox7.SelectedIndex = 1 And direction >= 47.5 And direction < 52.5 Then
                Projectedareafactor = ((0.000000401 * betaorg ^ 3 - 0.0000716 * betaorg ^ 2 + 0.000911 * betaorg + 0.301) +_
(0.000000393 * betaorg ^ 3 - 0.0000695 * betaorg ^ 2 + 0.00089 * betaorg + 0.293)) / 2
            ElseIf ComboBox7.SelectedIndex = 1 And direction >= 52.5 And direction < 57.5 Then
                Projectedareafactor = 0.000000393 * betaorg ^ 3 - 0.0000695 * betaorg ^ 2 + 0.00089 * betaorg + 0.293
            ElseIf ComboBox7.SelectedIndex = 1 And direction >= 57.5 And direction < 62.5 Then
                Projectedareafactor = ((0.000000393 * betaorg ^ 3 - 0.0000695 * betaorg ^ 2 + 0.00089 * betaorg + 0.293) +_
(0.000000368 * betaorg ^ 3 - 0.0000656 * betaorg ^ 2 + 0.000865 * betaorg + 0.282)) / 2
            ElseIf ComboBox7.SelectedIndex = 1 And direction >= 62.5 And direction < 67.5 Then
                Projectedareafactor = 0.000000368 * betaorg ^ 3 - 0.0000656 * betaorg ^ 2 + 0.000865 * betaorg + 0.282
            ElseIf ComboBox7.SelectedIndex = 1 And direction >= 67.5 And direction < 72.5 Then
                Projectedareafactor = ((0.000000368 * betaorg ^ 3 - 0.0000656 * betaorg ^ 2 + 0.000865 * betaorg + 0.282) +_
(0.000000331 * betaorg ^ 3 - 0.0000601 * betaorg ^ 2 + 0.00079 * betaorg + 0.272)) / 2
            ElseIf ComboBox7.SelectedIndex = 1 And direction >= 72.5 And direction < 77.5 Then
                Projectedareafactor = 0.000000331 * betaorg ^ 3 - 0.0000601 * betaorg ^ 2 + 0.00079 * betaorg + 0.272
            ElseIf ComboBox7.SelectedIndex = 1 And direction >= 77.5 And direction < 82.5 Then
                Projectedareafactor = ((0.000000331 * betaorg ^ 3 - 0.0000601 * betaorg ^ 2 + 0.00079 * betaorg + 0.272) +_
(0.000000299 * betaorg ^ 3 - 0.0000559 * betaorg ^ 2 + 0.000799 * betaorg + 0.26)) / 2
            ElseIf ComboBox7.SelectedIndex = 1 And direction >= 82.5 And direction < 87.5 Then
                Projectedareafactor = 0.000000299 * betaorg ^ 3 - 0.0000559 * betaorg ^ 2 + 0.000799 * betaorg + 0.26
            ElseIf ComboBox7.SelectedIndex = 1 And direction >= 87.5 And direction < 92.5 Then
                Projectedareafactor = ((0.000000299 * betaorg ^ 3 - 0.0000559 * betaorg ^ 2 + 0.000799 * betaorg + 0.26) +_
(0.000000289 * betaorg ^ 3 - 0.0000548 * betaorg ^ 2 + 0.000806 * betaorg + 0.258)) / 2
            ElseIf ComboBox7.SelectedIndex = 1 And direction >= 92.5 And direction < 97.5 Then
                Projectedareafactor = 0.000000289 * betaorg ^ 3 - 0.0000548 * betaorg ^ 2 + 0.000806 * betaorg + 0.258
            ElseIf ComboBox7.SelectedIndex = 1 And direction >= 97.5 And direction < 102.5 Then
                Projectedareafactor = ((0.000000289 * betaorg ^ 3 - 0.0000548 * betaorg ^ 2 + 0.000806 * betaorg + 0.258) +_
(0.00000029 * betaorg ^ 3 - 0.0000546 * betaorg ^ 2 + 0.000678 * betaorg + 0.266)) / 2
            ElseIf ComboBox7.SelectedIndex = 1 And direction >= 102.5 And direction < 107.5 Then
                Projectedareafactor = 0.00000029 * betaorg ^ 3 - 0.0000546 * betaorg ^ 2 + 0.000678 * betaorg + 0.266
            ElseIf ComboBox7.SelectedIndex = 1 And direction >= 107.5 And direction < 112.5 Then
                Projectedareafactor = ((0.00000029 * betaorg ^ 3 - 0.0000546 * betaorg ^ 2 + 0.000678 * betaorg + 0.266) +_
(0.000000305 * betaorg ^ 3 - 0.0000573 * betaorg ^ 2 + 0.000681 * betaorg + 0.276)) / 2
            ElseIf ComboBox7.SelectedIndex = 1 And direction >= 112.5 And direction < 117.5 Then
                Projectedareafactor = 0.000000305 * betaorg ^ 3 - 0.0000573 * betaorg ^ 2 + 0.000681 * betaorg + 0.276
            ElseIf ComboBox7.SelectedIndex = 1 And direction >= 117.5 And direction < 122.5 Then
                Projectedareafactor = ((0.000000305 * betaorg ^ 3 - 0.0000573 * betaorg ^ 2 + 0.000681 * betaorg + 0.276) +_
(0.000000317 * betaorg ^ 3 - 0.0000595 * betaorg ^ 2 + 0.000644 * betaorg + 0.288)) / 2
            ElseIf ComboBox7.SelectedIndex = 1 And direction >= 122.5 And direction < 127.5 Then
                Projectedareafactor = 0.000000317 * betaorg ^ 3 - 0.0000595 * betaorg ^ 2 + 0.000644 * betaorg + 0.288
            ElseIf ComboBox7.SelectedIndex = 1 And direction >= 127.5 And direction < 132.5 Then
                Projectedareafactor = ((0.000000317 * betaorg ^ 3 - 0.0000595 * betaorg ^ 2 + 0.000644 * betaorg + 0.288) +_
(0.000000352 * betaorg ^ 3 - 0.0000651 * betaorg ^ 2 + 0.00075 * betaorg + 0.297)) / 2
            ElseIf ComboBox7.SelectedIndex = 1 And direction >= 132.5 And direction < 137.5 Then
                Projectedareafactor = 0.000000352 * betaorg ^ 3 - 0.0000651 * betaorg ^ 2 + 0.00075 * betaorg + 0.297
            ElseIf ComboBox7.SelectedIndex = 1 And direction >= 137.5 And direction < 142.5 Then
                Projectedareafactor = ((0.000000352 * betaorg ^ 3 - 0.0000651 * betaorg ^ 2 + 0.00075 * betaorg + 0.297) +_
(0.000000372 * betaorg ^ 3 - 0.0000683 * betaorg ^ 2 + 0.000783 * betaorg + 0.306)) / 2
            ElseIf ComboBox7.SelectedIndex = 1 And direction >= 142.5 And direction < 147.5 Then
                Projectedareafactor = 0.000000372 * betaorg ^ 3 - 0.0000683 * betaorg ^ 2 + 0.000783 * betaorg + 0.306
            ElseIf ComboBox7.SelectedIndex = 1 And direction >= 147.5 And direction < 152.5 Then
                Projectedareafactor = ((0.000000372 * betaorg ^ 3 - 0.0000683 * betaorg ^ 2 + 0.000783 * betaorg + 0.306) +_
(0.000000407 * betaorg ^ 3 - 0.000074 * betaorg ^ 2 + 0.000921 * betaorg + 0.314)) / 2
            ElseIf ComboBox7.SelectedIndex = 1 And direction >= 152.5 And direction < 157.5 Then
                Projectedareafactor = 0.000000407 * betaorg ^ 3 - 0.000074 * betaorg ^ 2 + 0.000921 * betaorg + 0.314
            ElseIf ComboBox7.SelectedIndex = 1 And direction >= 157.5 And direction < 162.5 Then
                Projectedareafactor = ((0.000000407 * betaorg ^ 3 - 0.000074 * betaorg ^ 2 + 0.000921 * betaorg + 0.314) +_
(0.00000044 * betaorg ^ 3 - 0.0000795 * betaorg ^ 2 + 0.00104 * betaorg + 0.323)) / 2
            ElseIf ComboBox7.SelectedIndex = 1 And direction >= 162.5 And direction < 167.5 Then
```

```
            Projectedareafactor = 0.00000044 * betaorg ^ 3 - 0.0000795 * betaorg ^ 2 + 0.00104 * betaorg + 0.323
        ElseIf ComboBox7.SelectedIndex = 1 And direction >= 167.5 And direction < 172.5 Then
            Projectedareafactor = ((0.00000044 * betaorg ^ 3 - 0.0000795 * betaorg ^ 2 + 0.00104 * betaorg + 0.323) +_
(0.00000044 * betaorg ^ 3 - 0.00008 * betaorg ^ 2 + 0.00102 * betaorg + 0.328)) / 2
        ElseIf ComboBox7.SelectedIndex = 1 And direction >= 172.5 And direction < 177.5 Then
            Projectedareafactor = 0.00000044 * betaorg ^ 3 - 0.00008 * betaorg ^ 2 + 0.00102 * betaorg + 0.328
        ElseIf ComboBox7.SelectedIndex = 1 And direction >= 177.5 Then
            Projectedareafactor = ((0.00000044 * betaorg ^ 3 - 0.00008 * betaorg ^ 2 + 0.00102 * betaorg + 0.328) +_
(0.000000421 * betaorg ^ 3 - 0.0000779 * betaorg ^ 2 + 0.000973 * betaorg + 0.329)) / 2
        ElseIf ComboBox7.SelectedIndex = 2 And direction >= 0 And direction < 7.5 Then
            Projectedareafactor = ((0.00000032 * betaorg ^ 3 - 0.000074 * betaorg ^ 2 + 0.00105 * betaorg + 0.343) +_
(0.000000421 * betaorg ^ 3 - 0.0000779 * betaorg ^ 2 + 0.000973 * betaorg + 0.329)) / 2
        ElseIf ComboBox7.SelectedIndex = 2 And direction >= 7.5 And direction < 12.5 Then
            Projectedareafactor = ((0.00000032 * betaorg ^ 3 - 0.000074 * betaorg ^ 2 + 0.00105 * betaorg + 0.343) +_
(0.000000339 * betaorg ^ 3 - 0.000076 * betaorg ^ 2 + 0.0011 * betaorg + 0.341) + (0.000000421 * betaorg ^ 3 - 0.0000779 * betaorg
^ 2 + 0.000973 * betaorg + 0.329) + (0.000000368 * betaorg ^ 3 - 0.0000704 * betaorg ^ 2 + 0.00082 * betaorg + 0.321)) / 4
        ElseIf ComboBox7.SelectedIndex = 2 And direction >= 12.5 And direction < 17.5 Then
            Projectedareafactor = (0.000000339 * betaorg ^ 3 - 0.000076 * betaorg ^ 2 + 0.0011 * betaorg + 0.341 +_
0.000000368 * betaorg ^ 3 - 0.0000704 * betaorg ^ 2 + 0.00082 * betaorg + 0.321) / 2
        ElseIf ComboBox7.SelectedIndex = 2 And direction >= 17.5 And direction < 22.5 Then
            Projectedareafactor = ((0.000000339 * betaorg ^ 3 - 0.000076 * betaorg ^ 2 + 0.0011 * betaorg + 0.341) +_
(0.000000367 * betaorg ^ 3 - 0.0000784 * betaorg ^ 2 + 0.00114 * betaorg + 0.336) + (0.000000368 * betaorg ^ 3 - 0.0000704 *
betaorg ^ 2 + 0.00082 * betaorg + 0.321) + (0.000000404 * betaorg ^ 3 - 0.000074 * betaorg ^ 2 + 0.000931 * betaorg + 0.315)) / 4
        ElseIf ComboBox7.SelectedIndex = 2 And direction >= 22.5 And direction < 27.5 Then
            Projectedareafactor = (0.000000367 * betaorg ^ 3 - 0.0000784 * betaorg ^ 2 + 0.00114 * betaorg + 0.336 +_
0.000000404 * betaorg ^ 3 - 0.000074 * betaorg ^ 2 + 0.000931 * betaorg + 0.315) / 2
        ElseIf ComboBox7.SelectedIndex = 2 And direction >= 27.5 And direction < 32.5 Then
            Projectedareafactor = ((0.000000367 * betaorg ^ 3 - 0.0000784 * betaorg ^ 2 + 0.00114 * betaorg + 0.336) +_
(0.000000396 * betaorg ^ 3 - 0.0000802 * betaorg ^ 2 + 0.00119 * betaorg + 0.325) + (0.000000404 * betaorg ^ 3 - 0.000074 *
betaorg ^ 2 + 0.000931 * betaorg + 0.315) + (0.000000408 * betaorg ^ 3 - 0.000074 * betaorg ^ 2 + 0.000977 * betaorg + 0.308)) / 4
        ElseIf ComboBox7.SelectedIndex = 2 And direction >= 32.5 And direction < 37.5 Then
            Projectedareafactor = (0.000000396 * betaorg ^ 3 - 0.0000802 * betaorg ^ 2 + 0.00119 * betaorg + 0.325 +_
0.000000408 * betaorg ^ 3 - 0.000074 * betaorg ^ 2 + 0.000977 * betaorg + 0.308) / 2
        ElseIf ComboBox7.SelectedIndex = 2 And direction >= 37.5 And direction < 42.5 Then
            Projectedareafactor = ((0.000000396 * betaorg ^ 3 - 0.0000802 * betaorg ^ 2 + 0.00119 * betaorg + 0.325) +_
(0.000000431 * betaorg ^ 3 - 0.0000818 * betaorg ^ 2 + 0.00121 * betaorg + 0.311) + (0.000000408 * betaorg ^ 3 - 0.000074 *
betaorg ^ 2 + 0.000977 * betaorg + 0.308) + (0.000000401 * betaorg ^ 3 - 0.0000716 * betaorg ^ 2 + 0.000911 * betaorg + 0.301)) / 4
        ElseIf ComboBox7.SelectedIndex = 2 And direction >= 42.5 And direction < 47.5 Then
            Projectedareafactor = (0.000000431 * betaorg ^ 3 - 0.0000818 * betaorg ^ 2 + 0.00121 * betaorg + 0.311 +_
0.000000401 * betaorg ^ 3 - 0.0000716 * betaorg ^ 2 + 0.000911 * betaorg + 0.301) / 2
        ElseIf ComboBox7.SelectedIndex = 2 And direction >= 47.5 And direction < 52.5 Then
            Projectedareafactor = ((0.000000431 * betaorg ^ 3 - 0.0000818 * betaorg ^ 2 + 0.00121 * betaorg + 0.311) +_
(0.000000469 * betaorg ^ 3 - 0.0000835 * betaorg ^ 2 + 0.00129 * betaorg + 0.293) + (0.000000401 * betaorg ^ 3 - 0.0000716 *
betaorg ^ 2 + 0.000911 * betaorg + 0.301) + (0.000000393 * betaorg ^ 3 - 0.0000695 * betaorg ^ 2 + 0.00089 * betaorg + 0.293)) / 4
        ElseIf ComboBox7.SelectedIndex = 2 And direction >= 52.5 And direction < 57.5 Then
            Projectedareafactor = (0.000000469 * betaorg ^ 3 - 0.0000835 * betaorg ^ 2 + 0.00129 * betaorg + 0.293 +_
0.000000393 * betaorg ^ 3 - 0.0000695 * betaorg ^ 2 + 0.00089 * betaorg + 0.293) / 2
        ElseIf ComboBox7.SelectedIndex = 2 And direction >= 57.5 And direction < 62.5 Then
            Projectedareafactor = ((0.000000469 * betaorg ^ 3 - 0.0000835 * betaorg ^ 2 + 0.00129 * betaorg + 0.293) +_
(0.000000457 * betaorg ^ 3 - 0.0000783 * betaorg ^ 2 + 0.00119 * betaorg + 0.27) + (0.000000393 * betaorg ^ 3 - 0.0000695 *
betaorg ^ 2 + 0.00089 * betaorg + 0.293) + (0.000000368 * betaorg ^ 3 - 0.0000656 * betaorg ^ 2 + 0.000865 * betaorg + 0.282)) / 4
        ElseIf ComboBox7.SelectedIndex = 2 And direction >= 62.5 And direction < 67.5 Then
            Projectedareafactor = (0.000000457 * betaorg ^ 3 - 0.0000783 * betaorg ^ 2 + 0.00119 * betaorg + 0.27 +_
0.000000368 * betaorg ^ 3 - 0.0000656 * betaorg ^ 2 + 0.000865 * betaorg + 0.282) / 2
        ElseIf ComboBox7.SelectedIndex = 2 And direction >= 67.5 And direction < 72.5 Then
            Projectedareafactor = ((0.000000457 * betaorg ^ 3 - 0.0000783 * betaorg ^ 2 + 0.00119 * betaorg + 0.27) +_
(0.000000327 * betaorg ^ 3 - 0.0000592 * betaorg ^ 2 + 0.000796 * betaorg + 0.244) + (0.000000368 * betaorg ^ 3 - 0.0000656 *
betaorg ^ 2 + 0.000865 * betaorg + 0.282) + (0.000000331 * betaorg ^ 3 - 0.0000601 * betaorg ^ 2 + 0.00079 * betaorg + 0.272)) / 4
        ElseIf ComboBox7.SelectedIndex = 2 And direction >= 72.5 And direction < 77.5 Then
            Projectedareafactor = (0.000000327 * betaorg ^ 3 - 0.0000592 * betaorg ^ 2 + 0.000796 * betaorg + 0.244 +_
0.000000331 * betaorg ^ 3 - 0.0000601 * betaorg ^ 2 + 0.00079 * betaorg + 0.272) / 2
        ElseIf ComboBox7.SelectedIndex = 2 And direction >= 77.5 And direction < 82.5 Then
            Projectedareafactor = ((0.000000327 * betaorg ^ 3 - 0.0000592 * betaorg ^ 2 + 0.000796 * betaorg + 0.244) +_
(0.000000215 * betaorg ^ 3 - 0.0000479 * betaorg ^ 2 + 0.000979 * betaorg + 0.214) + (0.000000331 * betaorg ^ 3 - 0.0000601 *
betaorg ^ 2 + 0.00079 * betaorg + 0.272) + (0.000000299 * betaorg ^ 3 - 0.0000559 * betaorg ^ 2 + 0.000799 * betaorg + 0.26)) / 4
        ElseIf ComboBox7.SelectedIndex = 2 And direction >= 82.5 And direction < 87.5 Then
            Projectedareafactor = (0.000000215 * betaorg ^ 3 - 0.0000479 * betaorg ^ 2 + 0.000979 * betaorg + 0.214 +_
0.000000299 * betaorg ^ 3 - 0.0000559 * betaorg ^ 2 + 0.000799 * betaorg + 0.26) / 2
        ElseIf ComboBox7.SelectedIndex = 2 And direction >= 87.5 And direction < 92.5 Then
```

```
                Projectedareafactor = ((0.000000215 * betaorg ^ 3 - 0.0000479 * betaorg ^ 2 + 0.000979 * betaorg + 0.214) +_
(0.000000211 * betaorg ^ 3 - 0.0000504 * betaorg ^ 2 + 0.00124 * betaorg + 0.213) + (0.000000299 * betaorg ^ 3 - 0.0000559 *
betaorg ^ 2 + 0.000799 * betaorg + 0.26) + (0.000000289 * betaorg ^ 3 - 0.0000548 * betaorg ^ 2 + 0.000806 * betaorg + 0.258)) / 4
            ElseIf ComboBox7.SelectedIndex = 2 And direction >= 92.5 And direction < 97.5 Then
                Projectedareafactor = (0.000000211 * betaorg ^ 3 - 0.0000504 * betaorg ^ 2 + 0.00124 * betaorg + 0.213 +_
0.000000289 * betaorg ^ 3 - 0.0000548 * betaorg ^ 2 + 0.000806 * betaorg + 0.258) / 2
            ElseIf ComboBox7.SelectedIndex = 2 And direction >= 97.5 And direction < 102.5 Then
                Projectedareafactor = ((0.000000211 * betaorg ^ 3 - 0.0000504 * betaorg ^ 2 + 0.00124 * betaorg + 0.213) +_
(0.000000194 * betaorg ^ 3 - 0.0000476 * betaorg ^ 2 + 0.000775 * betaorg + 0.242) + (0.000000289 * betaorg ^ 3 - 0.0000548 *
betaorg ^ 2 + 0.000806 * betaorg + 0.258) + (0.00000029 * betaorg ^ 3 - 0.0000546 * betaorg ^ 2 + 0.000678 * betaorg + 0.266)) / 4
            ElseIf ComboBox7.SelectedIndex = 2 And direction >= 102.5 And direction < 107.5 Then
                Projectedareafactor = (0.000000194 * betaorg ^ 3 - 0.0000476 * betaorg ^ 2 + 0.000775 * betaorg + 0.242 +_
0.00000029 * betaorg ^ 3 - 0.0000546 * betaorg ^ 2 + 0.000678 * betaorg + 0.266) / 2
            ElseIf ComboBox7.SelectedIndex = 2 And direction >= 107.5 And direction < 112.5 Then
                Projectedareafactor = ((0.000000194 * betaorg ^ 3 - 0.0000476 * betaorg ^ 2 + 0.000775 * betaorg + 0.242) +_
(0.000000209 * betaorg ^ 3 - 0.0000502 * betaorg ^ 2 + 0.000561 * betaorg + 0.271) + (0.00000029 * betaorg ^ 3 - 0.0000546 *
betaorg ^ 2 + 0.000678 * betaorg + 0.266) + (0.000000305 * betaorg ^ 3 - 0.0000573 * betaorg ^ 2 + 0.000681 * betaorg + 0.276)) / 4
            ElseIf ComboBox7.SelectedIndex = 2 And direction >= 112.5 And direction < 117.5 Then
                Projectedareafactor = (0.000000209 * betaorg ^ 3 - 0.0000502 * betaorg ^ 2 + 0.000561 * betaorg + 0.271 +_
0.000000305 * betaorg ^ 3 - 0.0000573 * betaorg ^ 2 + 0.000681 * betaorg + 0.276) / 2
            ElseIf ComboBox7.SelectedIndex = 2 And direction >= 117.5 And direction < 122.5 Then
                Projectedareafactor = ((0.000000209 * betaorg ^ 3 - 0.0000502 * betaorg ^ 2 + 0.000561 * betaorg + 0.271) +_
(0.000000217 * betaorg ^ 3 - 0.0000525 * betaorg ^ 2 + 0.000431 * betaorg + 0.295) + (0.000000305 * betaorg ^ 3 - 0.0000573 *
betaorg ^ 2 + 0.000681 * betaorg + 0.276) + (0.000000317 * betaorg ^ 3 - 0.0000595 * betaorg ^ 2 + 0.000644 * betaorg + 0.288)) / 4
            ElseIf ComboBox7.SelectedIndex = 2 And direction >= 122.5 And direction < 127.5 Then
                Projectedareafactor = (0.000000217 * betaorg ^ 3 - 0.0000525 * betaorg ^ 2 + 0.000431 * betaorg + 0.295 +_
0.000000317 * betaorg ^ 3 - 0.0000595 * betaorg ^ 2 + 0.000644 * betaorg + 0.288) / 2
            ElseIf ComboBox7.SelectedIndex = 2 And direction >= 127.5 And direction < 132.5 Then
                Projectedareafactor = ((0.000000217 * betaorg ^ 3 - 0.0000525 * betaorg ^ 2 + 0.000431 * betaorg + 0.295) +_
(0.000000208 * betaorg ^ 3 - 0.0000527 * betaorg ^ 2 + 0.000292 * betaorg + 0.315) + (0.000000317 * betaorg ^ 3 - 0.0000595 *
betaorg ^ 2 + 0.000644 * betaorg + 0.288) + (0.000000352 * betaorg ^ 3 - 0.0000651 * betaorg ^ 2 + 0.00075 * betaorg + 0.297)) / 4
            ElseIf ComboBox7.SelectedIndex = 2 And direction >= 132.5 And direction < 137.5 Then
                Projectedareafactor = (0.000000208 * betaorg ^ 3 - 0.0000527 * betaorg ^ 2 + 0.000292 * betaorg + 0.315 +_
0.000000352 * betaorg ^ 3 - 0.0000651 * betaorg ^ 2 + 0.00075 * betaorg + 0.297) / 2
            ElseIf ComboBox7.SelectedIndex = 2 And direction >= 137.5 And direction < 142.5 Then
                Projectedareafactor = ((0.000000208 * betaorg ^ 3 - 0.0000527 * betaorg ^ 2 + 0.000292 * betaorg + 0.315) +_
(0.000000206 * betaorg ^ 3 - 0.0000537 * betaorg ^ 2 + 0.000235 * betaorg + 0.329) + (0.000000352 * betaorg ^ 3 - 0.0000651 *
betaorg ^ 2 + 0.00075 * betaorg + 0.297) + (0.000000372 * betaorg ^ 3 - 0.0000683 * betaorg ^ 2 + 0.000783 * betaorg + 0.306)) / 4
            ElseIf ComboBox7.SelectedIndex = 2 And direction >= 142.5 And direction < 147.5 Then
                Projectedareafactor = (0.000000206 * betaorg ^ 3 - 0.0000537 * betaorg ^ 2 + 0.000235 * betaorg + 0.329 +_
0.000000372 * betaorg ^ 3 - 0.0000683 * betaorg ^ 2 + 0.000783 * betaorg + 0.306) / 2
            ElseIf ComboBox7.SelectedIndex = 2 And direction >= 147.5 And direction < 152.5 Then
                Projectedareafactor = ((0.000000206 * betaorg ^ 3 - 0.0000537 * betaorg ^ 2 + 0.000235 * betaorg + 0.329) +_
(0.00000022 * betaorg ^ 3 - 0.0000561 * betaorg ^ 2 + 0.000233 * betaorg + 0.338) + (0.000000372 * betaorg ^ 3 - 0.0000683 *
betaorg ^ 2 + 0.000783 * betaorg + 0.306) + (0.000000407 * betaorg ^ 3 - 0.000074 * betaorg ^ 2 + 0.000921 * betaorg + 0.314)) / 4
            ElseIf ComboBox7.SelectedIndex = 2 And direction >= 152.5 And direction < 157.5 Then
                Projectedareafactor = (0.00000022 * betaorg ^ 3 - 0.0000561 * betaorg ^ 2 + 0.000233 * betaorg + 0.338 +_
0.000000407 * betaorg ^ 3 - 0.000074 * betaorg ^ 2 + 0.000921 * betaorg + 0.314) / 2
            ElseIf ComboBox7.SelectedIndex = 2 And direction >= 157.5 And direction < 162.5 Then
                Projectedareafactor = ((0.00000022 * betaorg ^ 3 - 0.0000561 * betaorg ^ 2 + 0.000233 * betaorg + 0.338) +_
(0.000000289 * betaorg ^ 3 - 0.0000657 * betaorg ^ 2 + 0.000522 * betaorg + 0.341) + (0.000000407 * betaorg ^ 3 - 0.000074 *
betaorg ^ 2 + 0.000921 * betaorg + 0.314) + (0.00000044 * betaorg ^ 3 - 0.0000795 * betaorg ^ 2 + 0.00104 * betaorg + 0.323)) / 4
            ElseIf ComboBox7.SelectedIndex = 2 And direction >= 162.5 And direction < 167.5 Then
                Projectedareafactor = (0.000000289 * betaorg ^ 3 - 0.0000657 * betaorg ^ 2 + 0.000522 * betaorg + 0.341 +_
0.00000044 * betaorg ^ 3 - 0.0000795 * betaorg ^ 2 + 0.00104 * betaorg + 0.323) / 2
            ElseIf ComboBox7.SelectedIndex = 2 And direction >= 167.5 And direction < 172.5 Then
                Projectedareafactor = ((0.000000289 * betaorg ^ 3 - 0.0000657 * betaorg ^ 2 + 0.000522 * betaorg + 0.341) +_
(0.000000335 * betaorg ^ 3 - 0.0000717 * betaorg ^ 2 + 0.000696 * betaorg + 0.342) + (0.00000044 * betaorg ^ 3 - 0.0000795 *
betaorg ^ 2 + 0.00104 * betaorg + 0.323) + (0.00000044 * betaorg ^ 3 - 0.00008 * betaorg ^ 2 + 0.00102 * betaorg + 0.328)) / 4
            ElseIf ComboBox7.SelectedIndex = 2 And direction >= 172.5 And direction < 177.5 Then
                Projectedareafactor = (0.000000335 * betaorg ^ 3 - 0.0000717 * betaorg ^ 2 + 0.000696 * betaorg + 0.342 +_
0.00000044 * betaorg ^ 3 - 0.00008 * betaorg ^ 2 + 0.00102 * betaorg + 0.328) / 2
            ElseIf ComboBox7.SelectedIndex = 2 And direction >= 177.5 Then
                Projectedareafactor = ((0.00000032 * betaorg ^ 3 - 0.000074 * betaorg ^ 2 + 0.00105 * betaorg + 0.343) +_
(0.000000335 * betaorg ^ 3 - 0.0000717 * betaorg ^ 2 + 0.000696 * betaorg + 0.342) + (0.00000044 * betaorg ^ 3 - 0.00008 * betaorg
^ 2 + 0.00102 * betaorg + 0.328) + (0.000000421 * betaorg ^ 3 - 0.0000779 * betaorg ^ 2 + 0.000973 * betaorg + 0.329)) / 4
            End If
        End Select

        Dim directbeam As Double = Kbst * Projectedareafactor * 0.7 * Effectivefactor
```

```
                Dim diffusebeam As Double = (Kdst + Krst + Krg) * 0.7 * 0.5 * Effectivefactor
                Dim diffuselong As Double = TotalL * 0.97 * 0.5 * Effectivefactor
                Dim Totalradi As Double = directbeam + diffusebeam + diffuselong
                Dim Tmrt As Double = Math.Sqrt(Math.Sqrt(Totalradi / (Effectivefactor * 0.97 * 5.67 *10 ^ -8))) - 273.15

                Dim radiationdata As String = ComboBox4.SelectedIndex + 1 & ":" & ComboBox5.SelectedIndex & " " & x & "," & y &
" SVF: " & SVF.ToString("F3") & " SVF1: " & SVF1.ToString("f3") & " Kb: " & Kbst.ToString("f1") & " Kd: " &
Kdst.ToString("f1") & " Kr: " & Krst.ToString("f1") & " Krg: " & Krg.ToString("f1") & " La: " & Last.ToString("f1") & " Lo: " &
Lo.ToString("f1") & " Lg: " & Lg.ToString("f1") & " Lveg: " & Lveg.ToString("f1") & " Total K: " & TotalK.ToString("f1") & "
Total L: " & TotalL.ToString("f1") & " Total Q: " & TotalQ.ToString("f1") & " fp: " & Projectedareafactor.ToString("f3") & "
Kb_body: " & directbeam.ToString("f1") & " Kd+Kr+Krg: " & diffusebeam.ToString("f1") & " Total L: " &
diffuselong.ToString("f1") & " Total Absorbed Radiation: " & Totalradi.ToString("f1") & " Tmrt: " & Tmrt.ToString("f1") & vbCrLf
                My.Computer.FileSystem.WriteAllText("C:\Radiationresult.txt", radiationdata, True)
                If TotalQ > 255 Then
                    TotalQ = TotalQ / 10
                End If

                Dim urbancolor As Color = Color.FromArgb(CInt(TotalQ), CInt(TotalQ), CInt(TotalQ))
                Urbanmap.SetPixel(x, y, urbancolor)
                If Totalradi > 255 Then
                    Totalradi = Totalradi / 10 + 100
                End If
                Dim humanradi As Color = Color.FromArgb(CInt(Totalradi), CInt(Totalradi), CInt(Totalradi))
                Humanradimap.SetPixel(x, y, humanradi)
                If Tmrt < 0 Then
                    Tmrt = Tmrt * (-1)
                End If
                If Tmrt > 255 Then
                    Tmrt = Tmrt / 10
                End If
                Dim MRT As Color = Color.FromArgb(CInt(Tmrt), CInt(Tmrt), CInt(Tmrt))
                MRTmap.setpixel(x, y, MRT)
            Next

        Next
        PictureBox1.Image = Urbanmap

    Catch ex As ArgumentException
        MessageBox.Show("There was an error in third view analysis.")

    End Try

    ' Set the PictureBox to display the image.
    ' PictureBox1.Load()

    Try
        ' Call the Process.Start method to open the default browser
        ' with a URL:
        Dim SaveFileDialog1 As New SaveFileDialog()
        SaveFileDialog1.Filter = "Bitmap Image|*.bmp"
        SaveFileDialog1.Title = "Save a Urban Radiation Map Image File"
        SaveFileDialog1.ShowDialog()
        ' If the file name is not an empty string open it for saving.
        If SaveFileDialog1.FileName <> "" Then
            ' Saves the Image via a FileStream created by the OpenFile method.
            Dim fs As System.IO.FileStream = CType _
              (SaveFileDialog1.OpenFile(), System.IO.FileStream)
            ' Saves the Image in the appropriate ImageFormat based upon the
            ' file type selected in the dialog box.
            ' NOTE that the FilterIndex property is one-based.
            Select Case SaveFileDialog1.FilterIndex
                Case 1
                    Me.PictureBox1.Image.Save(fs, _
                      System.Drawing.Imaging.ImageFormat.Bmp)
            End Select
            fs.Close()
        End If
    Catch ex As Exception
        ' The error message
        MessageBox.Show("Unable to save the file.")
```

```
End Try

PictureBox1.Image = Humanradimap
Try
   ' Call the Process.Start method to open the default browser
   ' with a URL:
   Dim SaveFileDialog1 As New SaveFileDialog()
   SaveFileDialog1.Filter = "Bitmap Image|*.bmp"
   SaveFileDialog1.Title = "Save a Human Radiation Map image File"
   SaveFileDialog1.ShowDialog()
   ' If the file name is not an empty string open it for saving.
   If SaveFileDialog1.FileName <> "" Then
      ' Saves the Image via a FileStream created by the OpenFile method.
      Dim fs As System.IO.FileStream = CType _
        (SaveFileDialog1.OpenFile(), System.IO.FileStream)
      ' Saves the Image in the appropriate ImageFormat based upon the
      ' file type selected in the dialog box.
      ' NOTE that the FilterIndex property is one-based.
      Select Case SaveFileDialog1.FilterIndex
         Case 1
            Me.PictureBox1.Image.Save(fs, _
              System.Drawing.Imaging.ImageFormat.Bmp)
      End Select
      fs.Close()
   End If
Catch ex As Exception
   ' The error message
   MessageBox.Show("Unable to save the file.")
End Try

PictureBox1.Image = MRTmap
Try
   ' Call the Process.Start method to open the default browser
   ' with a URL:
   Dim SaveFileDialog1 As New SaveFileDialog()
   SaveFileDialog1.Filter = "Bitmap Image|*.bmp"
   SaveFileDialog1.Title = "Save a Mean Radiant Temperature Map image File"
   SaveFileDialog1.ShowDialog()
   ' If the file name is not an empty string open it for saving.
   If SaveFileDialog1.FileName <> "" Then
      ' Saves the Image via a FileStream created by the OpenFile method.
      Dim fs As System.IO.FileStream = CType _
        (SaveFileDialog1.OpenFile(), System.IO.FileStream)
      ' Saves the Image in the appropriate ImageFormat based upon the
      ' file type selected in the dialog box.
      ' NOTE that the FilterIndex property is one-based.
      Select Case SaveFileDialog1.FilterIndex
         Case 1
            Me.PictureBox1.Image.Save(fs, _
              System.Drawing.Imaging.ImageFormat.Bmp)
      End Select
      fs.Close()
   End If
Catch ex As Exception
   ' The error message
   MessageBox.Show("Unable to save the file.")
End Try
MsgBox("View factor analysis is done.")
```

Human thermal sensation model

```
'Combining MRT and Windspeed files
        Try
            Dim o, p, width, height As Integer
            Dim MRT, Windspeed As Bitmap

            If Microsoft.VisualBasic.Right(TextBox13.Text, 3) = "bmp" And Microsoft.VisualBasic.Right(TextBox14.Text, 3) = "bmp"
Then

                ' Retrieve the image.

                MRT = New Bitmap(TextBox13.Text, True)   'mean radiant temperature
                Windspeed = New Bitmap(TextBox14.Text, True)  'wind speed

                Label13.Text = "Pixel # ( x:" & MRT.Width & ", y:" & MRT.Height & ")"
                Label14.Text = "Pixel # ( x:" & Windspeed.Width & ", y:" & Windspeed.Height & ")"

                ' Loop through the images pixels to reset color.
                For p = 0 To MRT.Height - 1
                    For o = 0 To MRT.Width - 1
                        Dim pixelColor1 As Color = MRT.GetPixel(o, p)
                        Dim pixelcolor2 As Color = Windspeed.GetPixel(o, p)

                        Dim nColor As Color = Color.FromArgb(pixelColor1.R, pixelcolor2.R, 0) 'Pixelcolor1.R: mean radiant temperature
data, Pixelcolor2.R: wind speed data

                        MRT.SetPixel(o, p, nColor)

                        Dim Combinedata As String = o & ", " & p & " MRT: " & nColor.R & " Wind speed: " & nColor.G & vbCrLf
                        My.Computer.FileSystem.WriteAllText("C:\CombineMRTWIND.txt", Combinedata, True)

                    Next
                Next

                Dim newmap As Bitmap

                newmap = MRT
                ' Set the PictureBox to display the image.
                PictureBox1.Image = newmap
                MsgBox("Combining the image file data is done.")
            End If

            If Microsoft.VisualBasic.Right(TextBox13.Text, 3) = "txt" And Microsoft.VisualBasic.Right(TextBox14.Text, 3) = "txt" Then

                o = 0
                p = 0
                width = TextBox15.Text
                Height = TextBox16.Text
                Dim Text1 As String() = IO.File.ReadAllLines(TextBox13.Text)
                Dim Text2 As String() = IO.File.ReadAllLines(TextBox14.Text)
                Dim Text3 As String() = IO.File.ReadAllLines(TextBox13.Text)
                Dim text4 As String() = IO.File.ReadAllLines(TextBox14.Text)
                Dim lines1 As String() = Text1
                Dim lines2 As String() = Text2
                Dim lines3 As String() = Text3
                Dim lines4 As String() = text4

                Dim newimage4 As Bitmap = New Bitmap(width, Height, System.Drawing.Imaging.PixelFormat.Format32bppArgb)
                Dim Counter As Integer = 0
                For Each S1 As String In lines1
                    Dim A As Integer
                    For A = 1 To (Width * 2) Step 2
                        ' Get one character.
                        Dim ss1 As String = Microsoft.VisualBasic.Mid(S1, A, 2)
                        Dim i1 As Integer = CInt(Val(ss1))
                        o = Counter Mod Width
                        p = CInt(Int(Counter / Width))
```

```
            Counter += 1
            Dim pixelcolor As Color = Color.FromArgb(0, i1, 0, 0)
            newimage4.SetPixel(o, p, pixelcolor)
        Next
    Next
    Dim pixelcolor1 As Color = newimage4.GetPixel(o, p)
    Counter = 0
    For Each S2 As String In lines2
        Dim A As Integer
        For A = 1 To (Width * 2) Step 2
            'Get one character.
            Dim ss2 As String = Microsoft.VisualBasic.Mid(S2, A, 2)
            Dim i2 As Integer = CInt(Val(ss2))
            o = Counter Mod Width
            p = CInt(Int(Counter / Width))
            Counter += 1
            pixelcolor1 = newimage4.GetPixel(o, p)
            Dim pixelcolor As Color = Color.FromArgb(0, pixelcolor1.R, i2, 0)
            newimage4.SetPixel(o, p, pixelcolor)
        Next
    Next
    Dim pixelcolor2 As Color = newimage4.GetPixel(o, p)
    Counter = 0
    For Each S3 As String In lines3
        Dim A As Integer
        For A = 1 To (Width * 2) Step 2
            'Get one character.
            Dim ss3 As String = Microsoft.VisualBasic.Mid(S3, A, 2)
            Dim i3 As Integer = CInt(Val(ss3))
            o = Counter Mod Width
            p = CInt(Int(Counter / Width))
            Counter += 1
            pixelcolor2 = newimage4.GetPixel(o, p)
            Dim pixelcolor As Color = Color.FromArgb(0, pixelcolor2.R, pixelcolor2.G, i3)
            newimage4.SetPixel(o, p, pixelcolor)
        Next
    Next
    Dim pixelcolor3 As Color = newimage4.GetPixel(o, p)
    Counter = 0
    For Each S4 As String In lines4
        Dim A As Integer
        For A = 1 To (Width * 2) Step 2
            ' Get one character.
            Dim ss4 As String = Microsoft.VisualBasic.Mid(S4, A, 2)
            Dim i4 As Integer = CInt(Val(ss4))          'building azimuth angle is between 0 (north) and 18 (south) through 9 (east).
            o = Counter Mod Width
            p = CInt(Int(Counter / Width))
            Counter += 1

            pixelcolor3 = newimage4.GetPixel(o, p)
            Dim pixelcolor As Color = Color.FromArgb(i4, pixelcolor3.R, pixelcolor3.G, pixelcolor3.B)
            newimage4.SetPixel(o, p, pixelcolor)

            Dim Combinedata As String = o & ", " & p & " MRT: " & pixelcolor.R & " Wind speed: " & pixelcolor.G & vbCrLf
            My.Computer.FileSystem.WriteAllText("C:\CombineMRTWIND.txt", Combinedata, True)

        Next
    Next
    Me.PictureBox1.Image = newimage4
    Label13.Text = "Pixel # ( x:" & newimage4.Width & ", y:" & newimage4.Height & ")"
    Label14.Text = "Pixel # ( x:" & newimage4.Width & ", y:" & newimage4.Height & ")"
  End If
Catch ex As ArgumentException
  MessageBox.Show("There was an error." & "Check the path to the image file or whether the image sizes are same.")
End Try

'Calculating human thermal index

Dim newmap1 As Bitmap = PictureBox1.Image
```

```
    Dim MAPET As Bitmap = New Bitmap(newmap1.Width, newmap1.Height, System.Drawing.Imaging.PixelFormat._
Format32bppArgb)
    Dim MAPTop As Bitmap = New Bitmap(newmap1.Width, newmap1.Height, System.Drawing.Imaging.PixelFormat._
Format32bppArgb)
    Dim MAPPMV As Bitmap = New Bitmap(newmap1.Width, newmap1.Height, System.Drawing.Imaging.PixelFormat._
Format32bppArgb)
    Dim MAPPPD As Bitmap = New Bitmap(newmap1.Width, newmap1.Height, System.Drawing.Imaging.PixelFormat._
Format32bppArgb)
    Dim MAPPMVET As Bitmap = New Bitmap(newmap1.Width, newmap1.Height, System.Drawing.Imaging.PixelFormat._
Format32bppArgb)
    Dim MAPPPDET As Bitmap = New Bitmap(newmap1.Width, newmap1.Height, System.Drawing.Imaging.PixelFormat._
Format32bppArgb)

    Try
      Dim x, y As Integer
      Dim FCL, HCF, Taa, Tmrta, Tcla, P1, P2, P3, P4, P5, XN, XF, EPS, HCN, HC, Tcl, HL1, HL2, HL3, HL4, HL5, HL6, PMV,
PPD, Ts, Top As Double
      Dim N As Integer
      Dim PMVET, PPDET, IM, LR, DRY, Tsk, EFCTC, PSSK, EREQ, EDIF, EFCHE, EMAX, PWET, ET, ETOLD As Double

      For y = 0 To newmap1.Height - 1
        For x = 0 To newmap1.Width - 1
          Dim pixelcolor As Color = newmap1.GetPixel(x, y)

          Dim MET As Double = TextBox1.Text          'metabolic rate
          Dim Ta As Double = TextBox2.Text           'air temperature
          Dim Tmrt As Integer = pixelcolor.R – 100   'mean radiant temperature
          Dim v As Single = (pixelcolor.G) / 10      'wind speed
          Dim RH As Double = TextBox5.Text           'relative humidity
          Dim clo As Double = TextBox6.Text          'clothing

          Dim FNPS As Double = Math.Exp(16.6536 - 4030.183 / (Ta + 235))
          Dim PA As Double = RH / 100 * FNPS
          Dim ICL As Double = 0.155 * clo
          Dim M As Double = MET * 58.15


          If ICL < 0.078 Then
            FCL = 1 + 1.29 * ICL
          Else
            FCL = 1.05 + 0.645 * ICL
          End If

          HCF = 12.1 * v ^ 0.5
          Taa = Ta + 273
          Tmrta = Tmrt + 273.15
          Tsk = 35.7 - 0.028 * M  'Fanger Eq. 29
          Tcla = Taa + (35.5 - Ta) / (3.5 * (6.45 * ICL + 0.1))
          P1 = ICL * FCL
          P2 = P1 * 3.96
          P3 = P1 * 100
          P4 = P1 * Taa
          P5 = 308.7 - 0.028 * M + P2 * (Tmrta / 100) ^ 4
          XN = Tcla / 100
          XF = Tcla / 50
          N = 0
          EPS = 0.00015

          While Math.Abs(XN - XF) > EPS
            XF = (XF + XN) / 2
            HCN = 2.38 * Math.Abs(100 * XF - Taa) ^ 0.25

            If HCF > HCN Then
              HC = HCF
            Else
              HC = HCN
            End If
            XN = (P5 + P4 * HC - P2 * XF ^ 4) / (100 + P3 * HC)
            N = N + 1
          End While
```

```
Tcl = 100 * XN - 273
PSSK = Math.Exp(16.6536 - 4030.183 / (Tsk + 235))   'Saturated water vapor pressure at skin temperature
'Heat loss diff. through skin
'HL1 = 3.05 * 0.001 * (5733 - 6.99 * M - PA)
HL1 = 3.062 * (PSSK - PA)
'Heat loss by sweating (comfort)
If M > 58.15 Then
   HL2 = 0.42 * (M - 58.15)
Else
   HL2 = 0
End If
'Latent respiration heat loss
'HL3 = 1.7 * 0.00001 * M * (5867 - PA)
HL3 = 0.01725 * M * (5.8662 - PA)
'Dry respiration heat loss
HL4 = 0.0014 * M * (34 - Ta)
'Heat loss by radiation
'HL5 = 3.96 * FCL * (XN ^ 4 - (Tmrta / 100) ^ 4)
HL5 = 0.7 * 5.67 * FCL * (XN ^ 4 - (Tmrta / 100) ^ 4)
'Heat loss by convection
HL6 = FCL * HC * (Tcl - Ta)

'Operative temperature
If v < 0.2 Then
   Top = 0.5 * Ta + 0.5 * Tmrt
ElseIf v >= 0.2 And v < 0.6 Then
   Top = 0.6 * Ta + 0.4 * Tmrt
ElseIf v > 0.6 And v <= 1.0 Then
   Top = 0.7 * Ta + 0.3 * Tmrt
Else
   Top = 9999
End If

'ET (Effective Temperature)
IM = 0.45     'Woodcock ratio
LR = 16.5     'Lewis relation
DRY = HL5 + HL6     'Dry heat loss from clothing
EFCTC = DRY / (Tsk - Top)   'Thermal transmittance
EREQ = M - (HL3 + HL4) - DRY    'Required evaporation
EDIF = 3.062 * (PSSK - PA)  'IM' Diff eq. mod. by IM
EFCHE = IM * LR * EFCTC     'Mass txfr coeff
EMAX = EFCHE * (PSSK - PA)    'Max evap power
PWET = EREQ / EMAX      'Skin wettedness
If PWET < (EDIF / EMAX) Then
   PWET = EDIF / EMAX
End If
If PWET > 1 Then    'Assume wcrit=1
   PWET = 1
End If
ET = Ta
ETOLD = ET + 2
While Math.Abs(ET - ETOLD) > 0.01
   ETOLD = ET
   ET = Top + PWET * IM * LR * (PA - 0.5 * Math.Exp(16.6536 - 4030.183 / (ET + 235)))  'New approximated ET
   ET = 0.5 * ET + 0.5 * ETOLD
End While

'Thermal sensation trans. coeff.
Ts = 0.303 * Math.Exp(-0.036 * M) + 0.028
'Predicted mean vote
PMV = Ts * (M - HL1 - HL2 - HL3 - HL4 - HL5 - HL6)
PMVET = Ts * (M - HL1 - HL2 - HL3 - HL4 - EFCTC * (Tsk - ET))
'Predicted percentage dissat.
PPD = 100 - 95 * Math.Exp(-0.03353 * PMV ^ 4 - 0.2179 * PMV ^ 2)
PPDET = 100 - 95 * Math.Exp(-0.03353 * PMVET ^ 4 - 0.2179 * PMVET ^ 2)

        Dim Humanthermalindex As String = x & ", " & y & " Top: " & Top.ToString("f1") & " ET: " & ET.ToString("f1") & "
PMV: " & PMV.ToString("f1") & " PPD: " & PPD.ToString("f1") & " PMV_ET: " & PMVET.ToString("f1") & " PPD_ET: " &
PPDET.ToString("f1") & vbCrLf
        My.Computer.FileSystem.WriteAllText("C:\Humanthermalindex.txt", Humanthermalindex, True)
```

```
        ET = ET + 100   '0 is 100 in ET. This will eliminate the risk of minus values in color values.
        Dim INDEXET As Color = Color.FromArgb(CInt(ET), CInt(ET), CInt(ET))
        Dim INDEXTop As Color = Color.FromArgb(CInt(Top), CInt(Top), CInt(Top))

        PMV = PMV * 20 + 100  '0 is 100 in PMV. 0.5 change is equal to 10.
        PMVET = PMVET * 20 + 100  '0 is 100 in PMVET. 0.5 change is equal to 10.
        Dim INDEXPMV As Color = Color.FromArgb(CInt(PMV), CInt(PMV), CInt(PMV))
        Dim INDEXPPD As Color = Color.FromArgb(CInt(PPD), CInt(PPD), CInt(PPD))
        Dim INDEXPMVET As Color = Color.FromArgb(CInt(PMVET), CInt(PMVET), CInt(PMVET))
        Dim INDEXPPDET As Color = Color.FromArgb(CInt(PPDET), CInt(PPDET), CInt(PPDET))
        MAPET.SetPixel(x, y, INDEXET)
        MAPTop.SetPixel(x, y, INDEXTop)
        MAPPMV.SetPixel(x, y, INDEXPMV)
        MAPPPD.SetPixel(x, y, INDEXPPD)
        MAPPMVET.SetPixel(x, y, INDEXPMVET)
        MAPPPDET.SetPixel(x, y, INDEXPPDET)
    Next
Next
PictureBox1.Image = MAPET

Try
    ' Call the Process.Start method to open the default browser
    ' with a URL:
    Dim SaveFileDialog1 As New SaveFileDialog()
    SaveFileDialog1.Filter = "Bitmap Image|*.bmp"
    SaveFileDialog1.Title = "Save a ET* Map image File"
    SaveFileDialog1.ShowDialog()
    ' If the file name is not an empty string open it for saving.
    If SaveFileDialog1.FileName <> "" Then
        ' Saves the Image via a FileStream created by the OpenFile method.
        Dim fs As System.IO.FileStream = CType _
            (SaveFileDialog1.OpenFile(), System.IO.FileStream)
        ' Saves the Image in the appropriate ImageFormat based upon the
        ' file type selected in the dialog box.
        ' NOTE that the FilterIndex property is one-based.
        Select Case SaveFileDialog1.FilterIndex
            Case 1
                Me.PictureBox1.Image.Save(fs, _
                  System.Drawing.Imaging.ImageFormat.Bmp)
        End Select
        fs.Close()
    End If
Catch ex As Exception
    ' The error message
    MessageBox.Show("Unable to save the file.")
End Try
PictureBox1.Image = Nothing
PictureBox1.Image = MAPTop
Try
    ' Call the Process.Start method to open the default browser
    ' with a URL:
    Dim SaveFileDialog1 As New SaveFileDialog()
    SaveFileDialog1.Filter = "Bitmap Image|*.bmp"
    SaveFileDialog1.Title = "Save a Top Map image File"
    SaveFileDialog1.ShowDialog()
    ' If the file name is not an empty string open it for saving.
    If SaveFileDialog1.FileName <> "" Then
        ' Saves the Image via a FileStream created by the OpenFile method.
        Dim fs As System.IO.FileStream = CType _
            (SaveFileDialog1.OpenFile(), System.IO.FileStream)
        ' Saves the Image in the appropriate ImageFormat based upon the
        ' file type selected in the dialog box.
        ' NOTE that the FilterIndex property is one-based.
        Select Case SaveFileDialog1.FilterIndex
            Case 1
                Me.PictureBox1.Image.Save(fs, _
                  System.Drawing.Imaging.ImageFormat.Bmp)
        End Select
        fs.Close()
```

```
    End If
Catch ex As Exception
    ' The error message
    MessageBox.Show("Unable to save the file.")
End Try
PictureBox1.Image = Nothing
PictureBox1.Image = MAPPMV
Try
    ' Call the Process.Start method to open the default browser
    ' with a URL:
    Dim SaveFileDialog1 As New SaveFileDialog()
    SaveFileDialog1.Filter = "Bitmap Image|*.bmp"
    SaveFileDialog1.Title = "Save a PMV Map image File"
    SaveFileDialog1.ShowDialog()
    ' If the file name is not an empty string open it for saving.
    If SaveFileDialog1.FileName <> "" Then
        ' Saves the Image via a FileStream created by the OpenFile method.
        Dim fs As System.IO.FileStream = CType _
            (SaveFileDialog1.OpenFile(), System.IO.FileStream)
        ' Saves the Image in the appropriate ImageFormat based upon the
        ' file type selected in the dialog box.
        ' NOTE that the FilterIndex property is one-based.
        Select Case SaveFileDialog1.FilterIndex
            Case 1
                Me.PictureBox1.Image.Save(fs, _
                    System.Drawing.Imaging.ImageFormat.Bmp)
        End Select
        fs.Close()
    End If
Catch ex As Exception
    ' The error message
    MessageBox.Show("Unable to save the file.")
End Try
PictureBox1.Image = Nothing
PictureBox1.Image = MAPPPD
Try
    ' Call the Process.Start method to open the default browser
    ' with a URL:
    Dim SaveFileDialog1 As New SaveFileDialog()
    SaveFileDialog1.Filter = "Bitmap Image|*.bmp"
    SaveFileDialog1.Title = "Save a PPD Map image File"
    SaveFileDialog1.ShowDialog()
    ' If the file name is not an empty string open it for saving.
    If SaveFileDialog1.FileName <> "" Then
        ' Saves the Image via a FileStream created by the OpenFile method.
        Dim fs As System.IO.FileStream = CType _
            (SaveFileDialog1.OpenFile(), System.IO.FileStream)
        ' Saves the Image in the appropriate ImageFormat based upon the
        ' file type selected in the dialog box.
        ' NOTE that the FilterIndex property is one-based.
        Select Case SaveFileDialog1.FilterIndex
            Case 1
                Me.PictureBox1.Image.Save(fs, _
                    System.Drawing.Imaging.ImageFormat.Bmp)
        End Select
        fs.Close()
    End If
Catch ex As Exception
    ' The error message
    MessageBox.Show("Unable to save the file.")
End Try
PictureBox1.Image = Nothing
PictureBox1.Image = MAPPMVET
Try
    ' Call the Process.Start method to open the default browser
    ' with a URL:
    Dim SaveFileDialog1 As New SaveFileDialog()
    SaveFileDialog1.Filter = "Bitmap Image|*.bmp"
    SaveFileDialog1.Title = "Save a PMV_ET* Map image File"
    SaveFileDialog1.ShowDialog()
```

```
            ' If the file name is not an empty string open it for saving.
            If SaveFileDialog1.FileName <> "" Then
                ' Saves the Image via a FileStream created by the OpenFile method.
                Dim fs As System.IO.FileStream = CType _
                    (SaveFileDialog1.OpenFile(), System.IO.FileStream)
                ' Saves the Image in the appropriate ImageFormat based upon the
                ' file type selected in the dialog box.
                ' NOTE that the FilterIndex property is one-based.
                Select Case SaveFileDialog1.FilterIndex
                    Case 1
                        Me.PictureBox1.Image.Save(fs, _
                            System.Drawing.Imaging.ImageFormat.Bmp)
                End Select
                fs.Close()
            End If
        Catch ex As Exception
            ' The error message
            MessageBox.Show("Unable to save the file.")
        End Try
        PictureBox1.Image = Nothing
        PictureBox1.Image = MAPPPDET
        Try
            ' Call the Process.Start method to open the default browser
            ' with a URL:
            Dim SaveFileDialog1 As New SaveFileDialog()
            SaveFileDialog1.Filter = "Bitmap Image|*.bmp"
            SaveFileDialog1.Title = "Save a PPD_ET* Map image File"
            SaveFileDialog1.ShowDialog()
            ' If the file name is not an empty string open it for saving.
            If SaveFileDialog1.FileName <> "" Then
                ' Saves the Image via a FileStream created by the OpenFile method.
                Dim fs As System.IO.FileStream = CType _
                    (SaveFileDialog1.OpenFile(), System.IO.FileStream)
                ' Saves the Image in the appropriate ImageFormat based upon the
                ' file type selected in the dialog box.
                ' NOTE that the FilterIndex property is one-based.
                Select Case SaveFileDialog1.FilterIndex
                    Case 1
                        Me.PictureBox1.Image.Save(fs, _
                            System.Drawing.Imaging.ImageFormat.Bmp)
                End Select
                fs.Close()
            End If
        Catch ex As Exception
            ' The error message
            MessageBox.Show("Unable to save the file.")
        End Try
    Catch ex As ArgumentException
        MessageBox.Show("There was an error.")

    End Try
End Sub

Private Sub Button5_Click(ByVal sender As System.Object, ByVal e As System.EventArgs) Handles Button5.Click
    Try
        ' Call the Process.Start method to open the default browser
        ' with a URL:
        Dim SaveFileDialog1 As New SaveFileDialog()
        SaveFileDialog1.Filter = "Bitmap Image|*.bmp"
        SaveFileDialog1.Title = "Save an Image File"
        SaveFileDialog1.ShowDialog()
        ' If the file name is not an empty string open it for saving.
        If SaveFileDialog1.FileName <> "" Then
            ' Saves the Image via a FileStream created by the OpenFile method.
            Dim fs As System.IO.FileStream = CType _
                (SaveFileDialog1.OpenFile(), System.IO.FileStream)
            ' Saves the Image in the appropriate ImageFormat based upon the
            ' file type selected in the dialog box.
            ' NOTE that the FilterIndex property is one-based.
            Select Case SaveFileDialog1.FilterIndex
```

```
            Case 1
                Me.PictureBox1.Image.Save(fs, _
                  System.Drawing.Imaging.ImageFormat.Bmp)
        End Select


        fs.Close()


    End If
Catch ex As Exception
    ' The error message
    MessageBox.Show("Unable to save the file.")
End Try
```

Appendix D: Examples of how the New model can be used for urban/landscape planning/design

During the last two decades, many urban climate studies were conducted and urban climatic maps (UCMs) produced all around the world which are good indications of how urban climatology can be adapted to urban planning (Ren et al. 2010). The UCMs are a useful tool for planners, but the problem is getting them to use the maps or urban climate knowledge in their plans. Recently, the status of how results of urban climate had affected urban planning and design was studied (Eliasson 2000). The study made three key recommendations for overcoming existing constraints: (1) improve awareness of urban climate among planners, (2) improve communication between urban climatologists and urban planners, and (3) develop tools and courses suitable for urban planners. Furthermore, there are spatial scale differences for planning and design (Eliasson 2000, Oke 2006). City-wide local or meso-scale (i.e., the comprehensive planning level) climatic maps use resolutions of several 10's or 100's of meters and work well for analyzing general urban climatic phenomena (i.e., urban heat island, urban air ventilation, urban air quality and bioclimate), whereas micro-scale (i.e. the detailed planning level) climatic maps have a resolution of less than 10 meters and are used in design. Most UCMs are generalized and employ the large resolutions. Micro-scale climatic maps are usually produced for only small urban areas and not for entire cities. These two different scale maps have their own advantages and disadvantages. Local or meso-scale maps can reduce long simulation time, but cannot be used in design because of their larger resolutions. Global change modification starts from micro-scale climate modification (Brown 2011). The modification needs new design, and for the design stage micro-scale urban climatic maps are required. The new human-urban radiation exchange simulation model is a useful tool for micro-scale level analysis and can be used to produce the micro-scale urban (bio)climatic map. The model can help to improve connections between urban climatology and urban planning, and it will help convinced planners to consider human thermal exchange in their work.

Modification of existing thermally unfavourable outdoor environments

The New model can produce results in text files and create the results as maps of sky view factor (Fig. D.1b), total incoming all-wave radiation on the horizontal ground surface (Fig. D.1c), total all-wave radiation absorbed on the human body surface (Fig. D.1d) and mean radiant temperature (Fig. D.1e).

Human thermal sensation (comfort) can be estimated for one specific spot or mapped over a large area. For one spot, perceived mean vote (PMV) and modified PMV by Gagge (1986) from Fountain and Huizenga (1995), physiological equivalent temperature (PET) from the RayMan model (http://www.mif.uni-freiburg.de/rayman/index.htm) and universal thermal climate index (UTCI, http://www.utci.org) from the UTCI calculator (http://utci.nass-staufen.de/utcineu.php) can be estimated using mean radiant temperature results from the New model (C:\Radiationresult.txt), wind speed and humidity data, human metabolic energy [unit: met (metabolic equivalent of task), one met is the resting metabolic rate during sitting, 58 Wm^{-2}] and clothing insulation (unit: clo). Currently, PET and UTCI are only available for a spot calculation. To create a human thermal sensation (comfort) map, a human thermal sensation computer program using Fountain and Huizenga's (1995) computer code was written in Visual Basic (the main window of the program is given in Fig. D.2). Important computer codes of the human thermal sensation computer program are shown in Appendix C. Air temperature and humidity are assumed to be the same in all places. After a wind speed text file is converted to a bitmap file using a 'Save' button (Fig. D.2), a mean radiant temperature map and a wind speed map are used to calculate human thermal sensations.

To modify one of the existing physical environments, the effects of changing albedos and emissivities can be tested. For example, the left image of Fig. D.1e uses 0.3 and 0.15 for sunny building and ground surface albedos, and the right one uses increased albedos, 0.6 and 0.3 for the same surfaces. The PMV results are shown in Fig. D.1f.

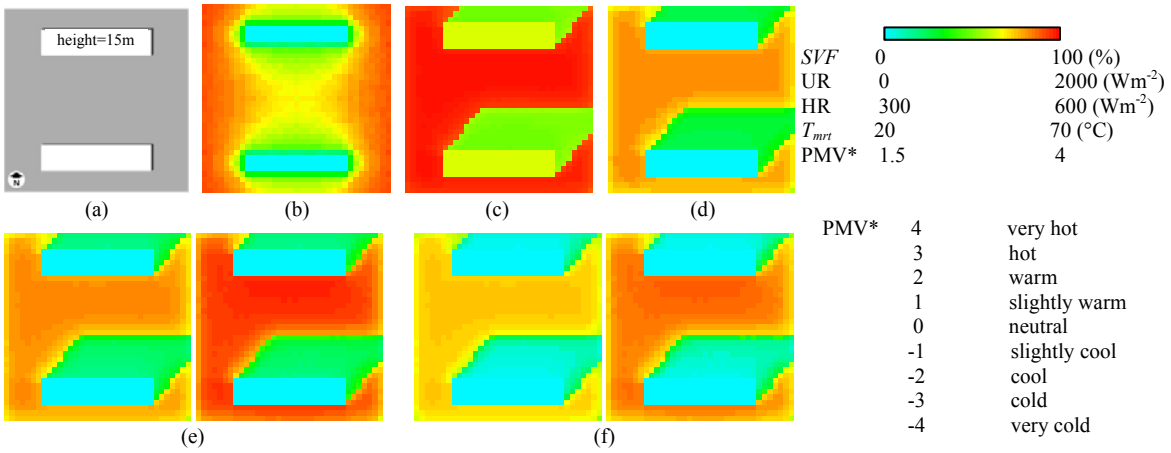

Fig. D.1 Maps created by the New model (the Nanaimo site at 14:00 on July 31, 2009; two 15 meter buildings, 19 meter distance between buildings; air temperature: 30 °C; relative humidity: 50 %; wind speed: 0.3 ms^{-1}; metabolic rate: 1.5 met, the mean of standing and walking activity levels; clothing insulation: 0.55 clo, typical summer clothing): (a) building setting, (b) sky view factor (*SVF*), (c) total incoming all-wave radiation on the horizontal ground surface (UR), (d) total all-wave radiation absorbed on the human body surface (HR), (e) mean radiant temperature (T_{mrt}); left: 0.3 and 0.15 for sunny building and ground surface albedos, right: 0.6 and 0.3 for the same surfaces and (f) perceived mean vote [PMV* modified by Gagge et al. (1986)]; left: from standard albedos, right: from increased albedos. The increased albedos made T_{mrt} increase up to 6 and 3 °C at the sunny and shaded locations, respectively. By the effect of increased T_{mrt}, PMV also increased up to 0.35 and 0.1 at the sunny and shaded locations, respectively

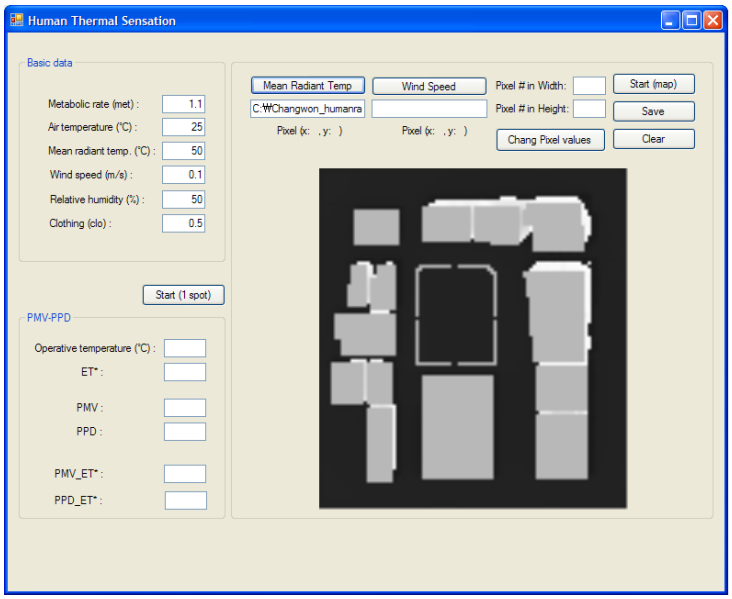

Fig. D.2 Main window of human thermal sensation computer program

Projecting future outdoor environments

The New model can be used to find mean radiant temperatures for unbuilt, future urban settings. A variety of proposed urban settings can be quickly simulated and their effects on the human radiation environment tested. Fig. D.3a–f shows an example of various urban settings. Mean radiant temperature results can be shown as maps (Fig. D.3a-1–f-1). PMV results also can be produced as maps (Fig. D.3a-2–f-2).

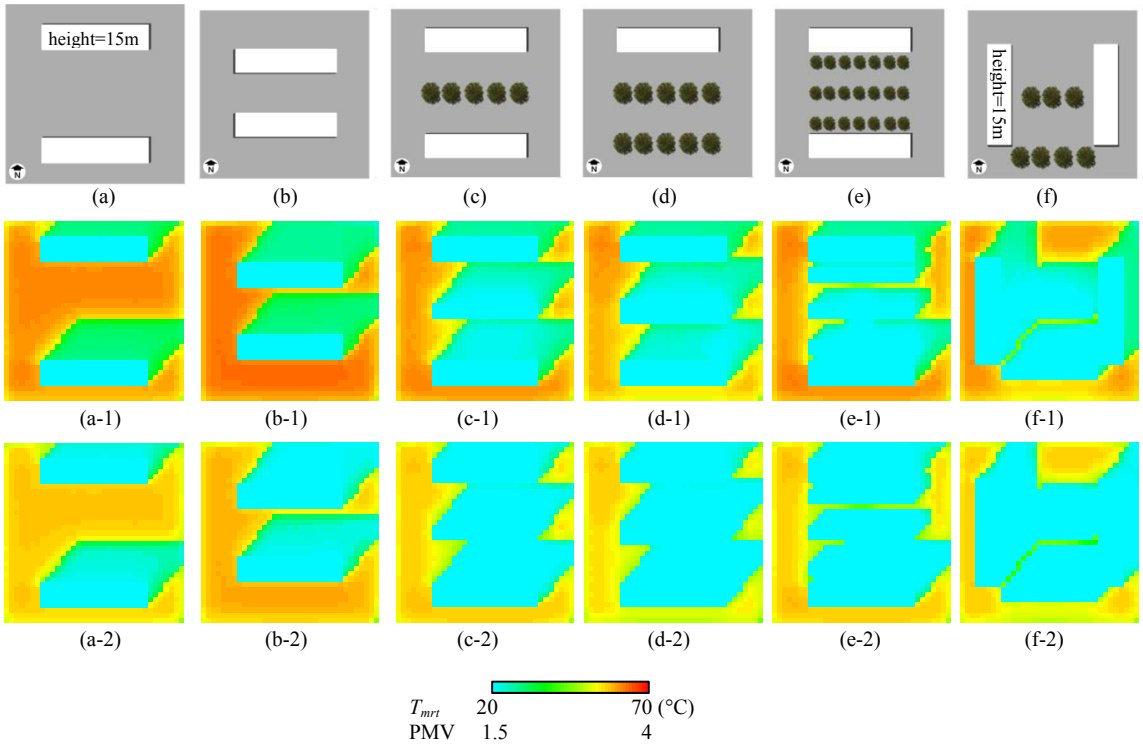

Fig. D.3 Simulating several different options of building and tree arrangements for outdoor thermal comfort (geographic and climatic conditions are the same as Fig. D.1): building and tree settings (a) basic east-west street without tree planting, (b) narrow east-west street, (c) east-west street with central 15 meter high trees, (d) east-west street with two-layer 15 meter high trees, (e) east-west street with three-layer 7 meter high trees and (f) north-south street with two-layer 15 meter high trees. All distances between buildings were 20 meters except (b). (a-1)–(f-1) maps of mean radiant temperature (T_{mrt}), and (a-2)–(f-2) maps of perceived mean vote (PMV). PMV was hot (3.3) at the sunny locations and between slightly warm and warm (1.6) at the shaded locations

As shown in Fig. D.3, urban planners and landscape architects can simulate their own projects using the new model to create better human settlement. They can change spatial variables [building variables (locations, heights, widths, orientation, shape and materials), plant variables (locations, heights, canopy widths and types) and ground variables (heights and materials)], climatic variables (air temperature, wind speed and humidity) and clothing insulation. Also, temporal variables can be considered: specific

hours, daytime, monthly, seasonally or yearly periods. The results will show clearly the effects of various urban settings and give a meaningful solution for comfortable urban outdoor environments. More information can be found in Givoni (1998), Givoni et al. (2003), Brown and Gillespie (1995), Eliasson (2000), Picot (2004), Ali-Toudert and Mayer (2007), Gaitani et al. (2007), Pearlmutter et al. (2007) and Fahmy and Sharples (2009).

References

Ali-Toudert F, Mayer H (2007) Effects of asymmetry, galleries, overhanging facades and vegetation on thermal comfort in urban street canyons. Solar Energy 81: 742-754

Brown RD, Gillespie TJ (1995) Microclimatic Landscape Design: Creating Thermal Comfort and Energy Efficiency. John Wiley & Sons Inc., New York

Brwon RD (2011) Ameliorating the effects of climate change: Modifying microclimates through design. Landscape and Urban Planning, doi:10.1016/j.landurbplan.2011.01.010

Eliasson I (2000) The use of climate knowledge in urban planning. Landscape and Urban Planning 48: 31-44

Fahmy M, Sharples S (2009) On the development of an urban passive thermal comfort system in Cairo, Egypt. Building and Environment 44: 1907-1916

Fountain M, Huizenga C (1995) A Thermal Sensation Model for Use by the Engineering Profession. Environmental Analytics, Piedmont

Gagge AP, Fobelets A, Berglund LG (1986) A standard predictive index of human response to the thermal environment. ASHRAE Transactions 92 (2B): 709-731

Gaitani N, Mihalakakou G, Santamouris M (2007) On the use of bioclimatic architecture principles in order to improve thermal comfort conditions in outdoor spaces. Building and Environment 42: 317-324

Givoni B (1998) Climate Considerations in Building and Urban Design. Van Nostrand Reinhold, New York

Givoni B, Noguchi M, Saaroni H, Pochter O, Yaacov Y, Feller N, Becker S (2003) Outdoor comfort research issues. Energy and Building 35: 77-86

Oke TR (2006) Towards better scientific communication in urban climate. Theoretical and Applied Climatology 84: 179-190

Pearlmutter D, Berliner P, Shaviv E (2007) Integrated modeling of pedestrian energy exchange and thermal comfort in urban street canyons. Building and Environment 42: 2396-2409

Picot X (2004) Thermal comfort in urban spaces: impact of vegetation growth, Case study: Piazza della Scienza, Milan, Italy. Energy and Buildings 36: 329-334

Ren C, Ng EY, Katzschner L (2010) Urban climatic map studies: a review. International Journal of Climatology, doi: 10.1002/joc.2237